EYEC

MONOGRAPH

12 European Young Engineers Conference

GOOD Solution

EYEC Monograph

All papers reviewed by the Scientific Committee

This monograph has been issued for the twelfth edition
of the European Young Engineers Conference which
was held 15 – 17 April 2024 At the Faculty of Chemical
and Process Engineering, Warsaw University of Technology

Warsaw 2024 · Tenth volume
ISBN 978-83-953822-2-2

Contents

Introduction

This is the second stationary edition of the European Young Engineers Conference after CoViD-19 Pandemic. We are delighted that, after two remote editions, our Conference is so popular with young researchers. We are very pleased that among the participants of the 12th edition of our Conference, we can get together with our regular participants as well as many new young scientists taking their first steps in their scientific careers.

Throughout the year of preparation, we have tried, to plan this event even better than in previous years. We warmly encourage you to actively participate in both the formal, scientific part of the Conference as well as the less formal part, which will enable you to network. We hope that in this way, the time of the EYEC Conference will be a time for you to broaden your research horizons, make new scientific connections, which may turn into interesting and innovative scientific research.

We hope that the lectures of the invited Special Guests have enabled you to broaden your existing knowledge or to explore completely new research interests. We are full of hope that we will meet again at next year European Young Engineers Conference to share scientific innovations once again.

This year we are pleased to continue section of our monograph: “From expert’s perspective”. We encourage to read Dr Nikou Hamzehpour’s article as an excellent opportunity to familiarise yourself with a new field of study or to expand your knowledge on a well-known issue. We hope you will find the papers within this book as interesting, as we do.

Here we would like to thank our Special Guests, the Scientific Commission, and all members of the Scientific Committee for your hard work in ensuring the highest level of contributed papers. Your invaluable help and advice are greatly appreciated by all of us, young researchers.

– Organising Committee

1 Special Guests

1.1 Assoc. Prof. Ameya Rege

Ameya Rege*,1,2

1. Institute of Materials Research, German Aerospace Center, Cologne, Germany
2. School of Computing and Mathematics, Keele University, Staffordshire, United Kingdom

e-mail: ameya.rege@dlr.de

Ameya Rege is the head of the research group on Atomistic and Microstructure Simulations at the Department of Aerogels and Aerogel Composites of the Institute of Materials Research at the German Aerospace Center (DLR). He is also a visiting senior lecturer (associate professor) at the School of Computer Science and Mathematics of the Keele University, UK. He completed his Ph.D. in mechanics at the RWTH Aachen University in Germany. Before starting his Ph.D., he studied aerospace engineering at the University of Southern California, U.S.A. He has also been a visiting academic fellow at the Cardiff University, U.K. under the HPC-Europa3 fellowship from the European Commission. He pursues research in multiscale materials modeling of soft materials and high-performance materials simulations.

Abstract: Computational description of porous materials: An aerogel use case

Reconstructing the intricate morphology of nanoporous materials, such as aerogels, poses a formidable challenge when one aspires to attain three-dimensional visual representations of their mesoporous (pore sizes between 2 and 50 nm) nanostructure. The array of available microscopic and tomographic instruments encounters formidable hurdles in penetrating the diverse spectrum of aerogel types, hindering the comprehensive reconstruction of their intricate 3D nanoporous architecture. This is precisely where computational methodologies emerge as a beacon of promise, unveiling their potential to elucidate experimentally observed phenomena and to decipher the intricate interplay between structure and properties.

In pursuit of this objective, the lecture will delve into the realm of computational design of nanoporous materials, with a special emphasis on fascinating aerogels[1]. To this end, the matter of the talk will encompass aerogels derived from inorganic sources, notably silica, as well as those rooted in organic origins, exemplified by phenolic-based variants. In the backdrop of the global quest for sustainable and environmentally responsible solutions, biobased materials, specifically those arising from biowaste, command growing attention. In this context, the meticulous modelling of such aerogels, particularly from polysaccharides such as cellulose and carrageenan, will be illustrated. Furthermore, the seamless integration of these models within a computational framework for the purpose of simulating composites will be discussed.

Finally, as we usher in the era of rapid materials development, the latter part of the discussion will turn its attention towards the harnessing of machine learning approaches. These approaches not only facilitate predictive modelling but also empower the reverse engineering of synthesis parameters, thereby paving the way for the advent of AI-driven, self-learning laboratories.

1.2 Dagmara Chmielewska-Śmietanko, PhD

Dagmara Chmielewska-Śmietanko*,1

1. Institute of Nuclear Chemistry and Technology, Warsaw, Poland

e-mail: d.chmielewska@ichtj.waw.pl

Dagmara Chmielewska-Śmietanko is an assistant professor at the Institute of Nuclear Chemistry and Technology, Warsaw, Poland. She graduated in Chemical and Process Engineering from Warsaw University of Technology, where she also completed her Ph.D. She has been involved in many international and national projects on application of electron beam accelerators in industry, medicine, protection of environment and also in societal application. Principal Investigator in 11 project funded by the Polish Ministry of Science and Higher Education and International Agency of Atomic Energy. Co-author of more than 30 publications and 13 Polish and international patents. Many of the invented solutions were awarded at the international Invention Shows in Brussel, Seoul, Moscow and Warsaw. Board member of the Polish Nuclear Society. Currently, the coordinator of consortium composed of 6 scientific institutions and 3 industrial partners in the Euratom Horizon Europe project RADOV "Radiation harvesting of bioactive peptides from egg proteins and their integration in advanced functional products".

[1] Rege, A., A Perspective on Methods to Computationally Design the Morphology of Aerogels. Advanced Engineering Materials, 2023. 25: p. 2201097

Abstract: Ionizing radiation as a tool for engineering

KEYWORDS: *ionizing radiation, electron beam accelerators, gamma chambers, engineering*

Ionizing radiation is the unique tool having multiple applications. Starting from chemistry and medicine, through nanotechnology and protection of environment, ending with the conservation of cultural heritage objects. Some of these applications were developed many years ago, commercialized and implemented on the industrial scale. Several of them were scaled-up and demonstrated in the pilot plants. Nevertheless, this area is still developing and many new promising ideas for application of ionizing radiation are presently under development.

This work includes the state of art in the field and presents review on the most interesting applications of ionizing radiation. Radiation sterilization of medical products and tissue grafts is the flagship example of the application of the ionizing radiation. Second area were ionizing radiation is applied commercially is polymer processing. Electron beam accelerators are used for the cross-linking of cable insulators or pre-crosslinking the rubber sheet before the vulcanization process in order to avoid the tyre's defects during processing. Food hygenisation with ionizing radiation can prevent pests from developing in stored products, inhibit sprouting and also replace the use of some preservatives or pesticides. Sterile Insect Technique involving ionizing radiation is the control method of insects which are vectors of human diseases and their populations. Several applications of ionizing radiation for protection of environment as NO_x and SO_2 removal from flue gas, sewage sludge disinfection for the use as the fertilizer or ballast water disinfection have been developed, Even protection of cultural heritage involves some methods based on the ionizing radiation that can be used for artefacts disinfection, consolidation or cleaning. Recently, huge interest in application of ionizing radiation for the modification of biomaterials in order to develop plant growth promoters or to obtain bioactive peptides has been demonstrated. Moreover, ionizing radiation is a very powerful tool to be used for the synthesis and modification of different materials including nanomaterials.

This overview will enable to introduce different possibilities of ionizing radiation application in engineering to develop a new beneficial products and technologies

Acknowledgements

This work is funded from the European Union's Horizon 2020 Research and Innovation programme under Grant Agreement No 101004730 and from the European Union's Euratom Research and Training Programme (EURATOM) Horizon Europe under Grant Agreement No 101061694.The work published as part of an international project co-financed by the program of the Minister of Science and Higher Education entitled "PMW" in the years 2021–2025; contract no.5180/H2020/2021/2.

1.3 Francisco M. Fernandes, PhD

Francisco M. Fernandes*,1

1. PARIS CONDENSED MATTER CHEMISTRY LABORATORY, SORBONNE UNIVERSITY, PARIS, FRANCE

e-mail: francisco.fernandes@sorbonne-universite.fr

Francisco M. Fernandes obtained a degree in Applied Chemistry and a MSc in Environmental Sciences from the University of Minho in Braga, Portugal. He has then joined Prof. Ruiz-Hitzky's group at the Materials Science Institute of Madrid (CSIC) to pursue a PhD in Applied Physical Chemistry, focusing on the interface between biopolymers and clay minerals in bionanocomposite materials. In 2011, he integrated the Laboratory of Condensed Matter Chemistry (LCMCP) at Sorbonne Université as a post-doctoral fellow, under the guidance of Dr. N. Nassif, where he developed collagen-based materials by spray drying.

Dr. Fernandes was appointed assistant professor in 2013 Sorbonne Université (Materials & Biology team at the LCMC), and passed his *Habilitation à Diriger des Recherches* in 2022. In 2016 he held a position of Visiting Lecturer at the Department of Physics at King's College London. His current research interests revolve around the transformation of "classical" materials fabrication techniques into biofabrication techniques. In particular, he has developed a recognized expertise on ice templating applied to biological entities—from biomolecules up to living cells. Dr. Fernandes has authored of 47 research papers, 8 book chapters and is the co-inventor of 7 international patents. In 2023 he became editorial board member of Advanced Biology. He leads the Materials and Biology research group at Sorbonne since January 2024.

Abstract: Engineering the local environment surrounding biological entities during freezing

KEYWORDS: *ice templating, phase diagram, cryobiology, biomimetics, collagen*

Freezing is ubiquitous in nature. In oceans, rivers, soils, and in the atmosphere, ice is formed under radically different environmental conditions that depend on hydration, temperature and pressure. In most of these conditions freezing threatens the integrity and the viability of biological entities. Paradoxically, cryopreservation (*i.e.* freezing biological entities under strictly controlled conditions) is the only solution to extend the lifespan of living cells, and to preserve biomolecules. In this lecture we will focus on the interaction between biological matter (from biopolymers up to living mammalian cells) with a controlled freezing front[2].

During freezing, ice growth induces a phase separation between pure ice crystals, and the remaining solutes and suspended particles. These freezing events impose compositional, thermal and osmotic gradients that can be potentially deleterious to the integrity of the constitutive biological entities. Despite their apparent simplicity, these gradients have remained elusive for decades. We will discuss some of our recent results in decrypting the evolving physicochemical environment of cells during freezing. Using an original coupling of techniques—spanning from calorimetry, *in situ* cryoconfocal microscopy and SAXS diffraction—we will explore the relevance of directional freezing in the elaboration of living materials from model organisms like yeast[3] and bacteria, as well as in the cryopreservation of mammalian cells in the absence of toxic cryoprotectants.

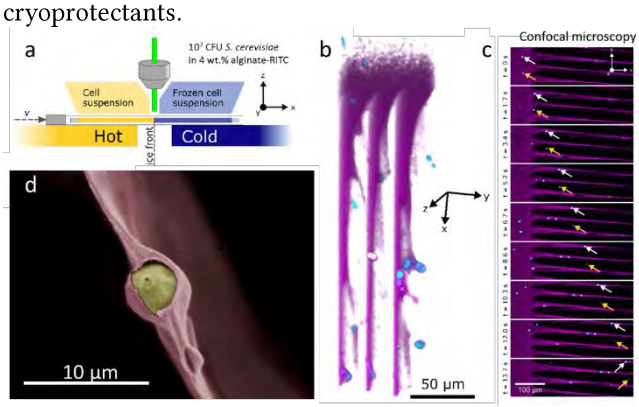

Figure 1.3.1. Studying the physicochemical conditions formed during directional freezing of model *S. cerevisiae cells*. a) Cryoconfocal microscopy system setup. b) 3D reconstruction of the freezing front interacting with suspended cells. c) Time-series of the interaction of the freezing front with suspended cells. White arrows point to cells encapsulated in the biopolymer fraction and yellow arrows point to cells directly embedded in ice. d) *S. cerevisiae* cell encapsulated in polysaccharide matrix.

[2] Qin, K., Parisi, C. & Fernandes, F. M. Recent advances in ice templating: From biomimetic composites to cell culture scaffolds and tissue engineering. J. Mater. Chem. B 9, 889–907 (2021)

1.4 Alvaro Garcia Cruz, PhD

Alvaro Garcia Cruz*,1

1. SAAT HEALTHCARE LTD., UNITED KINGDOM

e-mail: alvaro.garcia.consulting@gmail.com

Dr. Alvaro Garcia Cruz is a scientist, technologist, and entrepreneur. He obtained his bachelor's degree in chemistry from the Universidad of Guanajuato, Mexico, in 2008, and his master's degree in Catalysis and Physical Chemistry from the University Claude Bernard Lyon in France in 2010. His diverse research experiences include projects in the synthesis of antibiotics at the University of Dallas (USA), biopolymers, and bio detergents at the University of Avignon (France), and core-shell nanostructures for catalysis applications at the Institute of Catalysis and Surface Chemistry in Cracow (Poland).

He completed his Ph.D. in Nano and Biotechnology at the University Claude Bernard Lyon in France, sponsored by CONACYT, with an Academic Excellence Scholarship in 2015. Subsequently, he worked as an Assistant Professor at the Institute of Catalysis and Physical Chemistry in Warsaw (Poland), focusing on electrochemical sensors and polymers in 2016. From 2017 to 2023, he served as a Senior Scientist at the University of Leicester, making significant contributions to industrial research projects and leading initiatives related to sensor technology for medical applications, detection of explosives and drugs, Microplate assay, and drug delivery, including participation in several Horizon program European and NATO projects.

In 2020, he co-founded Gamanity Health and Cosmetics, a start-up emphasizing sustainable, organic skincare, and health products, and currently serves as the UK Business Manager there. Since 2023, he has been working as a Scientific Officer at SAAT Healthcare Ltd in the UK, leading commercial expertise in Biotechnology and Medical Devices, with a focus on R&D management, compliance, and fostering strategic collaborations for innovative product development. His areas of expertise include In Vitro Diagnostics (IVD), quality management, and business development.

His research and technological endeavours focus on the development of Medical Diagnostic tools employing Optical and Electrochemical sensors, Wearable and Wireless sensors, Conducting polymers, Bioelectronics,

[3] Qin, K. et al. Unveiling Cells' Local Environment during Cryopreservation by Correlative In Situ Spatial and Thermal Analyses. J. Phys. Chem. Lett. 11, 7730–7738 (2020)

Microplate assays, Nanoactuators, Drug delivery, Epitope mapping, and Nanozymes. With a prolific academic record, he has published over 45 peer-reviewed articles and holds 5 patents, two of which are licensed to the Biotech industry. He is a distinguished member of both the French Chemical Society and the Mexican Chemical Society.

Abstract: Entrepreneurship and Innovation

Embarking on the journey of entrepreneurship is a thrilling adventure that not only sharpens your skills but also empowers you to tackle challenges and shape the future of your community.

This oral presentation is designed for individuals who are enthusiastic about exploring entrepreneurship and mastering the art of innovation management. Innovation and entrepreneurship thrive on creativity, resilience, and a collective vision of building a better world. Drawing from my own entrepreneurial experiences, I aim to share practical insights, offering invaluable guidance on navigating obstacles, seizing opportunities, and cultivating a mindset essential for success. Whether you're an engineer, scientist, or simply someone with a curious mind eager to unleash your entrepreneurial potential, this presentation serves as a wellspring of inspiration.

It arms you with the indispensable guidance and tools necessary to embark on your entrepreneurial journey with confidence and unwavering determination.

1.5 Grzegorz Izydorczyk, PhD

Grzegorz Izydorczyk*,1

1. Department of Advanced Material Technologies, Faculty of Chemistry, Wroclaw University of Science and Technology, Wroclaw, Poland

e-mail: grzegorz.izydorczyk@pwr.edu.pl

Dr. Eng. Grzegorz Izydorczyk - an assistant professor in the Department of Advanced Materials Technology at Wroclaw University of Science and Technology and Technical Head at the PCA and ILAC-MRA accredited Chemical Laboratory for Multielement Analysis. His scientific activities include the development of agrochemical technologies for sustainable agriculture, e.g., by exploiting the phenomenon of allelopathy or by valorising biowaste, and the evaluation of the effects of new agrochemicals on plant stress and soil health. Specialist in instrumental analysis using ICP-OES, AAS, IC, TCD techniques. Co-author of 48 scientific publications, 5 patents and 5 patent applications.

Abstract: Engineering vs. sustainable agriculture and food production

Keywords: *agriculture; food production; soil health, fertilizer, plant protection products*

With the constant growth of the world's population, the need for engineering innovations in agriculture has arisen, with the aim of providing sufficient, high-quality food. A number of solutions are available on the market to improve crop yields, improve nutritional properties of crops, e.g. through biofortification with micronutrients, season-independence, or to increase the efficiency of livestock production, while maintaining the welfare of livestock. However, the intensification of plant cultivation and animal husbandry is associated with a number of negative effects, such as soil depletion and health disturbances, excessive chemicalization of the environment causing water eutrophication, accumulation of pesticide residues in plant tissues, or greenhouse gas or light pollution. This phenomenon is further intensified by the wastage of a significant amount of food produced, most often through the imbalance of supply chains, failures, or excessive buying and non-consumption of products by households.

Such a situation is forcing scientists to look for new solutions to reduce the negative effects of both intensive agriculture and excessive consumptionism. The latest trends in the agroengineering sector include the valorization of waste for fertilizer purposes, the use of natural plant defense mechanisms such as allelopathy to reduce the use of plant protection products, improving the digestibility of feedstuffs and increasing their assimilability, or striving to increase the application of biofertilizers, organic or organic-mineral fertilizers and biostimulants for plant growth to improve the health and fertility of soils. These activities are carried out in accordance with the guidelines of the European Union derived from the idea of sustainable development, the Green Deal and constantly changing legal regulations. As a result, high quality food is ensured while maintaining the welfare of crops and livestock, as well as demonstrating actions to reduce the negative impact of agriculture on the environment.

Acknowledgements

This work was financed by European Union's Horizon 2020 Research & Innovation Programme under grant agreement No 696356 and from the Executive Agency for Higher Education, Research, Development and Innovation Funding - UEFISCDI (Romania), the National Centre for Research and Development - NCBR (Poland), Agenda Estatal de Inves-Tigacion - AEI (Spain), and the Ministry of Agriculture and Forestry - MMM (Finland).

2 Scientific Commission

2.1 Assoc. Prof. Nadia Shardt

Department of Chemical Engineering, Norwegian University of Science and Technology, Norway

Nadia Shardt is an Associate Professor at the Norwegian University of Science and Technology (NTNU). She completed her PhD in Chemical Engineering at the University of Alberta in Canada and carried out postdoctoral research at the Institute for Atmospheric and Climate Science (ETH Zurich). She has expertise in microfluidics and interfacial thermodynamics (surface tension, phase equilibrium, and contact angles) and is interested in applications including water treatment, foams and emulsions, and cloud microphysics.

2.2 Grzegorz Cieślak, PhD

Łukasiewicz Research Network – Warsaw Institute of Technology, Warsaw, Poland

Grzegorz Cieślak, PhD Eng., works in Centre of Electroplating Technology, Łukasiewicz Research Network – Warsaw Institute of Technology. Since the beginning of his professional career, he has been involved in issues related to the production and research of coatings deposited by chemical and electrochemical reduction methods. He has worked on new types of materials in the form of metallic coatings, including alloy and composite coatings.

His scientific achievements include co-authorship in about 40 publications, presentations at 20 conferences, 3 patents, numerous awards at invention exhibitions and participation as a contractor in several R&D projects. In his doctoral thesis defended at the Faculty of Materials Science and Engineering, Warsaw University of Technology, he dealt with the influence of graphene on the structure and selected properties of Ni/graphene composite coatings.

2.3 Zuzanna Bojarska, PhD

Faculty of Chemical and Process Engineering, Warsaw University of Technology, Warsaw, Poland

Dr. Zuzanna Bojarska holds the position of Assistant Professor at the Faculty of Chemical and Process Engineering at Warsaw University of Technology (WUT). In the current year, she successfully defended her doctoral dissertation in the discipline of chemical engineering at WUT. Her research pursuits primarily lie in the synthesis, characterization, and application of hybrid nanomaterials. Presently, her focus is dedicated to advancing hydrogen production processes for sustainable energy innovation. Dr. Bojarska has co-authored 12 publications, contributed to 1 patent, and 4 patent applications. She has worked in 8 scientific projects and is the manager of one of them.

2.4 Grzegorz Izydorczyk, PhD

Department of Advanced Material Technologies, Faculty of Chemistry, Wroclaw University of Science and Technology, Wroclaw, Poland

Dr. Eng. Grzegorz Izydorczyk - an assistant professor in the Department of Advanced Materials Technology at Wroclaw University of Science and Technology and Technical Head at the PCA and ILAC-MRA accredited Chemical Laboratory for Multielement Analysis. His scientific activities include the development of agrochemical technologies for sustainable agriculture, e.g., by exploiting the phenomenon of allelopathy or by valorising biowaste, and the evaluation of the effects of new agrochemicals on plant stress and soil health. Specialist in instrumental analysis using ICP-OES, AAS, IC, TCD techniques. Co-author of 48 scientific publications, 5 patents and 5 patent applications.

2.5 Rasa Keruckienė, PhD

Department of Polymer Chemistry and Technology, Faculty of Chemical Technology, Kaunas University of Technology, Kuanas, Lithuania

Dr. Rasa Keruckienė is a researcher at Kaunas University of Technology, Department of Polymer Chemistry and Technology. She defended her doctoral dissertation in the field of Materials Science at KTU in 2017. She has won the Best research work of Young Researcher in the field of Chemistry, Physics and Mathematics awarded by Lithuanian Academy of Sciences in 2018. Her research interests and experience are in the field of the design, synthesis, characterization of organic electroactive compounds by experimental and theoretical methods as well as their thermal, electrochemical and photophysical properties investigation.

2.6 Bartosz Nowak, PhD

Faculty of Chemical and Process Engineering, Warsaw University of Technology, Warsaw, Poland

Bartosz Nowak, PhD Eng., works at the Faculty of Chemical and Process Engineering, Warsaw University of Technology. His primary focus is functionalising and modifying porous materials, nanotechnology, and sol-gel chemistry. Bartosz's research focuses on adapting organosilica-based aerogels to meet specific process application requirements. He strives to understand the process and develop tailor-made materials with matched morphology, wettability, and chemical structure, ultimately defining the final parameters and functionalities.

Bartosz's expertise lies in producing aerogels and aerogel-based hybrid materials for diverse engineering applications. These range from customising air filters, delivering substrates for transgenic root cultures, and providing supportive matrices for phase-change materials stabilisation or thermophotocatalysis. His work encompasses practical and theoretical aspects of aerogel synthesis, utilising the sol-gel technique to achieve tailored product specifications.

2.7 Paulina Trzaskowska, PhD

Centre for Advanced Materials and Technologies CEZAMAT, Warsaw University of Technology, Warsaw, Poland

Paulina Trzaskowska, PhD Eng. is a biomaterial engineer working as an assistant professor in Centre for Advanced Materials and Technologies CEZAMAT, Warsaw University of Technology. After doctoral defence at Faculty of Chemical and Process Engineering in 2018, she continued her work on obtaining and enhancing biomaterials intented to function with living cells and tissues. Her expertise lays in studying biointerfaces with specials regards to cell-biomaterial interaction. She has developed several well-functioning biocompagtible and hemocompatible coatings on polymers and metals. These coatings, obtained in situ directly on the biomaterials surface, has been proven to be robust and performing very well towards cells and blood, significantly reducing blood clotting. Dr Trzaskowska also holds experience in stem cells dufferentiation in contact with bioactive implants. Recently she has been working on rapid endothelialization on metallic biomaterials in collaboration with University Hospital Erlangen. She has more than 30 published works.

2.8 Karol Ulatowski, PhD

Faculty of Chemical and Process Engineering, Warsaw University of Technology, Warsaw, Poland

Karol Ulatowski, PhD. Eng., is an employee of the Faculty of Chemical and Process Engineering, Warsaw University of Technology. He focuses his research on the bioprocesses involving the gas phase. His expertise lies in the investigation of nanobubble generation and stability mechanisms as well as their applications in life sciences. Karol is developing ways of supplying nanobubbles to the cultures of animal and plant cells, as well as microorganisms. His main goal is to be able to intensify the growth and metabolic activity of given cell cultures or microorganisms using tailored nanobubbles, which will have appropriate number, size, composition, and surface stabilizers. Such nanobubbles can then be implemented in various branches of biotechnology and the general life science industry, including food additives and drug manufacturing, medicine, agriculture as well as animal culture.

3 Scientific Committee

Assoc. prof. Robert Cherbański	Warsaw University of Technology, Poland
Assoc prof. Andrzej Krasiński	Warsaw University of Technology, Poland
Beata Butruk-Raszeja, PhD	Warsaw University of Technology Poland
Karol Ćwieka, PhD	Warsaw University of Technology, Poland
Katarzyna Dąbkowska-Susfał, PhD	Warsaw University of Technology, Poland
Paulina Trzaskowska, PhD	Centre for Advanced Materials and Technologies CEZAMAT, WUT, Poland
Michał Wojasiński, PhD	Warsaw University of Technology Poland
Krzysztof Wojtas, PhD	Warsaw University of Technology, Poland

4 Organising Committee

The twelfth edition of the European Young Engineers Conference has been organised by the following members of the Scientific Club of Chemical and Process Engineering "Venturi", students and researchers of the Faculty of Chemical and Process Engineering:

Grzegorz Bernacki, BSc
Jan Ciołkowski
Rafał Czajka, BSc
Krzysztof Czyżewski
Nikodem Dąbrowski, BSc
Laura Derwiszyńska
Mateusz Dygas
Julia Gdesz
Izabela Kazimierczak
Monika Klimek, BSc
Iga Komar, BSc
Radosław Krzosa, MSc
Zuzanna Kupniewska
Jakub Lewandowski, BSc
Hanna Ławrynowicz
Adrian Malinowski
Maria Marecka
Kajetan Masiak
Kamila Matysiak, BSc
Ignacy Michalski
Mateusz Młynek, MSc
Martyna Musiatowicz
Natalia Nowak
Gabriela Plona
Maria Rewolińska
Aleksandra Sawczuk
Józef Siwkowski
Bartosz Sobolewski
Michał Stor, MSc
Kamil Pruchniak, BSc
Adam Romanowicz
Miłosz Włodarczyk

5 Coordinators of the 12th EYEC

Monika Klimek, BSc

Main Coordinator, Coordinator of the Graphics Section,
Member of the Scientific Club of Chemical and Process Engineering "Venturi"

Rafał Czajka, BSc

Coordinator of the Logistics Section,
Board Member of the Scientific Club of Chemical
and Process Engineering "Venturi"

Mateusz Dygas

Coordinator of the Contact Section,
Member of the Scientific Club of Chemical
and Process Engineering "Venturi"

Grzegorz Bernacki, BSc

Coordinator of the Monograph Section,
Chairman of the Scientific Club of Chemical
and Process Engineering "Venturi"

Michał Stor, MSc

Coordinator of the Monograph Section,
PhD candidate at the Faculty of Chemical
and Process Engineering, WUT

Nikodem Dąbrowski, BSc

Coordinator of the Social Media Section,
Board Member of the Scientific Club of Chemical
and Process Engineering "Venturi"

Kamil Pruchniak, BSc

Coordinator of the Sponsorship Section,
Member of the Scientific Club of Chemical
and Process Engineering "Venturi"

6 From expert's perspective

6.1 How to combat dust sources? Lessons learned from the nature and laboratory simulations of soil crusts

Nikou Hamzehpour*,1
1. Soil science and Engineering Department, Faculty of Agriculture, University of Maragheh, Maragheh, Iran
e-mail: nhamzehpour@maragheh.ac.ir

KEYWORDS: *aerosols, lake Urmia, sodium chloride, clay minerals*

About the author

Dr. Nikou Hamzehpour studied soil paedology at the University of Tarbiat Modares, Tehran, Iran, where she obtained a PhD in soil science in 2012. Since then, she teaches at the University of Maragheh, Iran. Her research has focused on different aspects of Lake Urmia (Hyper-saline salt lake in the northwest of Iran) including soil salinization, saline soils' pedogenesis, lake Urmia playa formation and evolution and the environmental consequences of its drying. She has accomplished several national projects on this topic. During past few years, her focus was on the study of the dust hot spots' characteristics, their physico-chemical stabilization and aerosol properties. In 2020 and during a one-year sabbatical, hosted by Atmospheric Chemistry group at ETH University in Switzerland, she started to work on the role of soil-dust from Lake Urmia playa on ice nucleation and the role of soil minerals as well as soil physico-chemical characteristics on heterogeneous freezing temperature.

Abstract

Newly formed playas, due to global warming and climate change, have become one of the major dust sources worldwide. Lake Urmia (LU), which has lost up to 90% of its surface area, is no exception. In these regions, areas with the absent stable surface crusts, can be the source of airborne dust causing health and environmental issues due to their high salt content and the presence of toxic elements. While in some places due to the surface crusts, playa surfaces are highly stable against wind, in some other parts, they have become the major dust sources in the region, putting at risk the life of millions of people living nearby. At the present work, we summarise the main factors protecting the soil surface against wind under natural condition and factors determining their stability against wind force and then the results from the application of soil cementing agents as a case are given. Results showed that crust samples from highly stable regions against wind force possessed the most stable crusts with an average thickness of 2.1 cm and maximum pressure resistance between 6000 and 7500 kPa, while the least stable lands had weak and limited crust development. Correlation coefficients (CC) between soil crust physicochemical properties and crust stability parameters revealed that clay, silt, and organic matter improved crust resilience and decrease soil erodible fraction by improving the crust thickness, while salt content and electrical conductivity increased the strength of the developed crusts. SEM images and elemental mapping revealed that NaCl is the main cementing agent of the developed soil crusts on LU playa surfaces. NaCl along with phyllosilicates has increased the crust stability against wind erosion while in highly erodible regions, low content of clay minerals along with the prevalence of geologic carbonates and lower NaCl content, limited crust formation and stability. Learning from the nature, the application of super-saturated salt solution extracted from LU, along with the sodium alginate (SA) and sodium silicate (SS) solutions, led to the induction of the stable surface crusts. In SA treatments, SA created a contentious mask over soil particles, while SS increased the size of the aggregates. These results showed that super saturated brine with high NaCl concentration as well as SA with 0.5-1% and SS with 3-5%, can improve the soil resilience of highly erodible playa surfaces against wind speeds up to 20 $m \cdot s^{-1}$.

Introduction

Long-term climate change especially when it is influenced by human activity, is one of the main global causes of aridity and desertification, where new and dangerous sources of dust may be created (Kok et al., 2021; Brahney et al., 2015; D'Odorico et al., 2013). In Iran, meteorological data over the past few decades have shown that precipitation and its pattern are affected by climate change (Ahmadi et al., 2022; Pour et al., 2020; Asakereh, 2020; Daneshvar et al., 2019). The coincidence of this global phenomenon with local changes (population growth and uneven abstraction of underground water sources) has exposed Iran's environment to numerous risks, as well as desiccation of several lakes such as Urmia, Hamoon, Jazmurian, Bakhtegan and Parshan, and drying up of many seasonal rivers and wetlands, leading to new dust sources all over the country (Rad et al., 2022; Abadi et al., 2022; Jowkar et al., 2021; Soleimani et al., 2021; Schulz et al., 2020).

Generally, arid lands of the world, which make up more than 40% of the earth's surface, can be an important source of dust (Middleton and Goudie, 2001). Almost 30% of the global dust emission is from dried salty playa lakes (Farebrother et al., 2017; Varga et al., 2014). In fact, playas can be a significant source of dust storms when the lake's water level changes frequently due to the variations in rainfall and wind patterns. Dust emission from playa surfaces is largely composed of salt minerals and its amount varies widely depending on the soil moisture content, surface roughness, strength of surface deposits or salt crusts, and type of existing salt minerals (Papi et al., 2022; Sweeney et al., 2016).

Lake Urmia (LU), in the northwest of Iran, is among the largest salt lakes in the world, with an average salt content of 220-380 $g \cdot L^{-1}$, ≈350 $mm \cdot y^{-1}$ annual precipitation and

>1000 mm·y^{-1} evaporation (Sharifi et al., 2018). By 2023, the lake has drastically lost ~90% of its water body. As a result, much of the historical lake bed has been exposed and subjected to the formation and evolution of various playa surfaces (Hamzehpour et al., 2022a; Motaghi et al., 2020; Schultz et al., 2020; Hamzehpour et al., 2018). As a consequence of the gradual shrinking of LU and LU playa (LUP) formation, several playa surfaces such as clay flat (CF), clay flat-salt crust (CF-SC); puffy ground (PG); sandy-salt crust (Sa-SC); sand sheet (Sa-sheet) and salt crust (SC) have evolved (Hamzehpour et al., 2022a; Taghizadeh et al., 2021; Motaghi et al., 2020). Among which, PG, Sa-sheet, and Sa-SC surfaces are highly susceptible to wind erosion, due to the fluctuation of the groundwater level and large fraction of silt and sand sized particles (Hamzehpour et al., 2022a).

Various methods have been invented and applied to stabilize erodible surfaces including building windbreaks, adding clay, sodium silicate or mulch (Asl et al., 2019; Neeladharan et al., 2018). More recently synthesizing and application of polymeric materials to increase soil resilience to wind have become more popular (Lee et al., 2020; Wang et al., 2019; Movahedan et al., 2012). However, on large-scales, most of these additives could be either expensive or not environmentally friendly.

There have been limited studies on developed crusts on LUP (Kheirfam, 2022; Motaghi et al., 2020). Therefore, at the present work, a detailed study was conducted on the study of physicochemical and mineralogical properties of soil crusts as well as determining the main factors contributing to their stability in order to combat dust sources in the future.

Materials and Methods

Soil sampling

Lake Urmia (LU) is located in the northwestern Iran between 36°45′ to 38°20′ N and 44°50′ to 46°10 E. The historical surface area and depth of the lake was almost 5200 km^2 and 16 m, which has reduced to less than 1000 km^2 and few mm in summer 2023, leading to the vast exposure of the lake bed as well as salt crust deposition at the margins and bottom layer of the lake brine.

In the previous studies, all lands from the recession of LU in the western and eastern parts have been studied and along with the study of the evolved playa surfaces, their physicochemical properties and resilience to wind erosion are also determined (Hamzehpour and Marcolli, 2024; Hamzehpour et al., 2022; Taghizadeh et al., 2021; Motaghi et al., 2020; Alkhayer et al., 2019) (Figure 6.1.1.). Based on these studies, Sa-sheets and Sa-SCs in the western LU (Figure 6.1.**1**. a and b); abandoned agricultural lands and Sa-SCs in the southeast (Figure 6.1.1 d and e) and puffy grounds in the east and south of LU (Figure 6.1.1.c) are the most prone areas to wind erosion and aerosol release.

The study area includes most of the western lands of LU playa (LUP) with an extension of 378 km^2 (Figure 6.1.1. a). It is located between 45°06′ to 45°13′ E and 37°19′ to 37°53′ N. the study area was previously studied from 2018 to 2020 for its major playa surfaces (Figure 6.1.1.b), their physicochemical properties, and susceptibility to wind erosion (Taghizadeh-Mehrjardi et al., 2021) and the contribution of the susceptible playa surfaces to wind erosion was determined using the correlation between soil and dust samples (Hamzehpour et al., 2022a).

Soli crust analysis

Soil crust thickness was measured using a Vernier Caliper with a 0.1 mm precision. To determine the surface strength of the natural crusts, an automatic micro penetrometer (model MP11, Iran) was used to measure maximum and mean pressure values with a needle to penetrate into the crust samples at a rate of 0.3 mm·s^{-1} to a depth of 30 mm with an applied maximum pressure of 12000 kPa. Based on the criteria proposed by Schoeneberger et al. (2012) for penetration resistance classes, values less than 100 kPa are very low (VL), between 100–1000 kPa, low (L), 1000–2000 kPa, moderate (M) and higher than 2000 kPa are considered as high (H) resistance.

Crust erodible fraction (EF) was determined in dry state using a rotary sieve with a 0.84 mm grid. To determine the physicochemical properties of the crust samples, a part of the collected crust samples was crushed and then passed through a 2 mm sieve. Soil electrical conductivity (EC), acidity (pH) and soluble Na^+ and K^+ were measured in 1:2.5 soil-to-water extracts using a Jenwey conductivity meter (model 4510), a VWR Symphony SB70P pH meter, and a Sherwood Flame photometer (model 410), respectively. Total (Ca^{2+}+Mg^{2+}) was determined using titration with EDTA. Soil organic carbon (OC) was measured by wet oxidation (Nelson and Sommers, 1996); and soil calcium carbonate equivalent (CCE) was determined using back titration of the remaining HCl (Sparks et al., 2020). A hydrometer method was used to determine soil textural classes (Gee and Or, 2002).

X-ray diffraction measurements were made using a PANalytical diffractometer, X'PERT Model: X'Pert MPD with a cobalt anode and Cu–Kα (40 kV, 40 mA). The powder samples were step-scanned at room temperature from 10° to 70° 2theta (step width 0.05°2Theta, counting time 1 s per step). Qualitative analysis of X-ray diffractograms for common minerals is done with the X'Pert High Score Plus identification software on the ICDD database. For scanning electron microscopy (SEM) analysis, A 1×1 cm crust sample was placed on a stopper and kept in a vacuum for 10 min before being coated with a thin layer of gold to prevent the specimen from charging under the electron beam during imaging. The structure of the crust was characterized to a depth of 2 mm using a field-emission scanning electron microscope (FEI QUANTA 200) equipped with energy-dispersive X-ray spectroscopy (EDX).

Laboratory soil crust simulations

Soil samples from highly erodible surfaces with less resilience to wind erosion were taken. Based on the knowledge of the factors affecting soil crust stability, different solutions of super-saturated salt by using Lake Urmia salt, sodium alginate with varying concentrations (0.5 -2%) and sodium silicate (1-5%) were sprayed on the samples and left to be solar evaporated. After crust formation, crust thickness, compressive strength was determined (see section *Soil sampling*) and their wind edibility were determined in a wind tunnel.

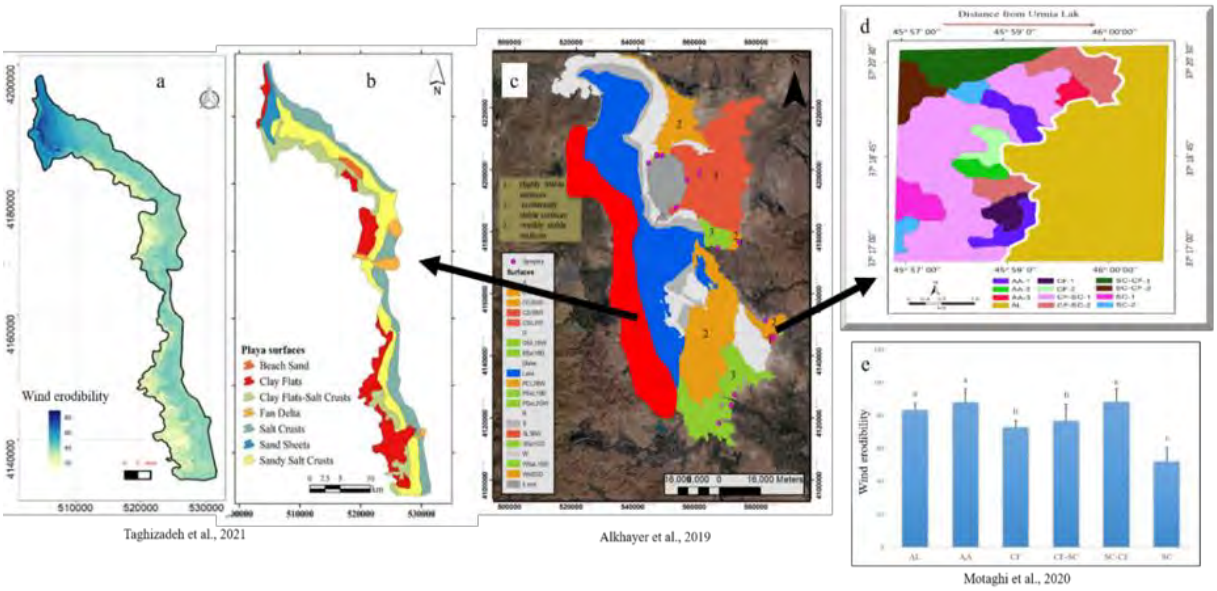

Figure 6.1.1. The studied playa surfaces (PS) of Lake Urmia Playa (LUP) and their wind erodibility (WE). (a) and (b) WE and PS of the western ULP; c: WE and PS of the northeast to the south of ULP; d and e: WE and PS of the eastern ULP shown in red polygon in part c. SC: salt crust; CF: clay flats; AA: abandoned agricultural lands. Maps are adopted from Taghizadeh et al. (2021); Motaghi et al. (2020) and Alkhayer et al. (2019).

Results

Soli properties affecting its resilience to wind erosion

By using Pearson correlation coefficients (CC) the important properties affecting crust stability were determined among studied soil crust. Based on the results obtained, positive CC were observed between soil erodible fraction and sand content while a strong negative CC between EF and both crust thickness and compressive strength were observed. On the other hand, clay, silt and OC showed positive CC with crust thickness which indicates their importance in improving soil crust resilience against wind force (CC > 0.5). Conversely, high EC, Ca, and Na content of the crusts do not improve crust thickness, however, they enhance the compressive strength of the soils (CC = 0.47–0.53). Although calcium carbonates are known as a cementing agents in soils, they are negatively correlated with crust thickness (CC = -0.58) and compressive strength. Overall, crust thickness and compressive strength are able to decrease soil erodible fraction and eventually lead to land susceptibility to wind erosion.

Mineralogical composition of soil crusts

In the previous section, we have shown that by decreasing crust thickness and compressive strength, their erodibility by wind increases. The mineralogical analysis of the some of the studied soil crusts revealed that quartz was the prevailing mineral in all of the samples and calcite, halite, and sodium carbonate were existed in almost all of the crust samples (Figure 6.1.2). Aragonite, dolomite, and gypsum were also detected in some of the studied crust samples. In crust samples taken from playa surfaces with high resilience to wind erosion (e.g. clay flats) with strong compressive strength (> 9000 kPa), the NaCl existed in high concentrations in comparison to crusts with less resilience.

In a crust sample taken from sandy salt crust playa surface (Sa-SC) with 1.71 cm thickness and maximum compressive strength of almost 10000 kPa, the halite peak was sharper and more intense than those with less stability. Based on these observations, it seems that Na^+ improves crust stability by increasing crust compressive strength. In sediments of LU playa, Na^+ is dominant in as halite (Hamzehpour et al., 2018; Motaghi et al., 2020; Hamzehpour et al., 2022). Therefore, it plays a major role in crust stability in the western LU playa. This could be due to crystallization of NaCl through and within soil particle agglomerates and thus tightly binding them together (Warrence et al., 2002). This is backed up by the absence of halite in least stable playa surfaces (Sa-sheets) where crust development was very limited and they were too fragile to be collected (Figure 6.1.2 b).

Aragonite was observed in high amount in the least stable playa surfaces such as Sa-sheets. however, it was almost absent in highly stable playa surfaces (e.g. CFs). Previous studies have also confirmed that aragonite as well as dolomite ad calcite are the main constituents of the aerosols in western LUP (Hamzehpour et al., 2022a and b).

Elemental analysis

The SEM images of two crust samples, one from the highly stable playa surfaces (Figure 6.1.3) and one from dust sources (Figure 6.1.4) show that Na and Cl exist in every spot in the samples (Figure 6.1.3 and Figure 6.1.4 b and c). however, they concentrations are higher in CF in comparison to Sa-sheets. Elemental maps also showed that paedogenic carbonates (calcite), do not distribute uniformly in the soil matrix of CF, but they have accumulated in pore spaces or around sand particles (Figure 6.1.3 f). while in Sa-sheet sample, it has uniformly distributed in the soil matrix revealing its geologic origin rather than paedogenic (Figure 6.1.4 f).

Based on the results from this section, we conclude that pedogenic carbonates can act as cementing agents along with NaCl intergrowth between and on the surfaces of the coarse particles (Sirjani et al., 2019; Motaghi et al., 2020), both increasing the surface crust thickness and stability. In the Sa-sheet, on the other hand, the dominance of larger aragonite particles of geologic origin with less interaction between particles prevents crust formation and stabilization.

Lab simulation of the stable crust

The application of super-saturated salt solution (dominated by NaCl) improved soil resilience to wind erosion. for example, soil crust thickness increased from 2.55 mm in untreated sample to 15.05 mm; compressive strength increased from 433.4 kPa to 2099.6 kPa while soil loss reduced from 47.3% to less than 3%. In case of the sodium alginate application, induced soil crusts and compressive strength were 15.3 mm and 1813.0 kPa and soil loss was less than 1%. To a great surprise, while sodium silicate increased crust compressive strength to 2128.1 kPa, induced crusts were 6.5 mm and soil loss during wind tunnel only reduced to 28.72% which was less effective than salt solution and sodium alginate. SEM imaged of the induced crusts are given in Figure 6.1.5. In crusts induced by super-saturated salt solution, salt crystallization has coved soil aggregates, leading to increased soil compressive strength and soil resilience against wind erosion. In SA treatments, SA created a contentious mask over soil particles, while SS increased the size of the aggregates. In all of these three cases, similar to what happens under natural condition, soil aggregate size and the coherence within soil particles increased leading to reduced soil susceptibility against wind.

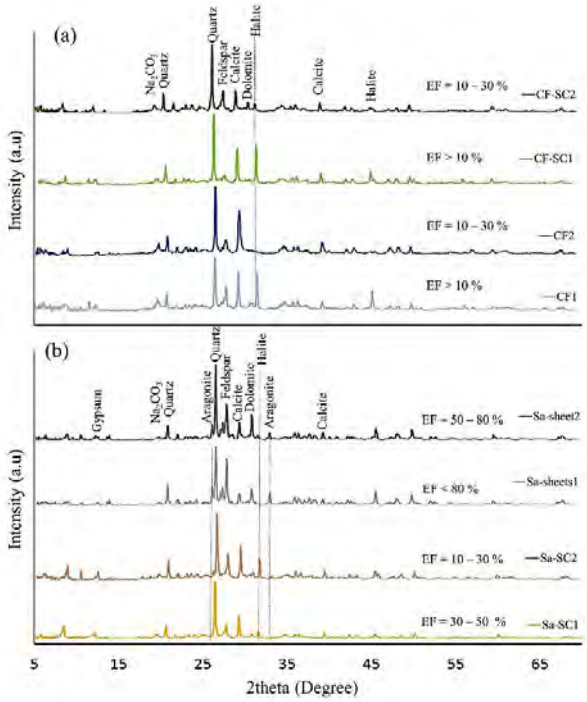

Figure 6.1.2. X-ray diffractograms of the soil crust samples of the western Lake Urmia playa with mineral assignments. a: clay flats (CF) and clay flats-salt crusts (CF-SC) b: sandy salt crusts (Sa-SC) and sand sheets (Sa-sheets). Samples with an erodible fraction (EF) less than 10% and 10–30% had the most stable crusts. Qualitative analysis of X-ray diffractograms for common minerals is done by XPert High Score Plus identification software on the ICDD database. Note that minor shares of other minerals cannot be detected with this setup.

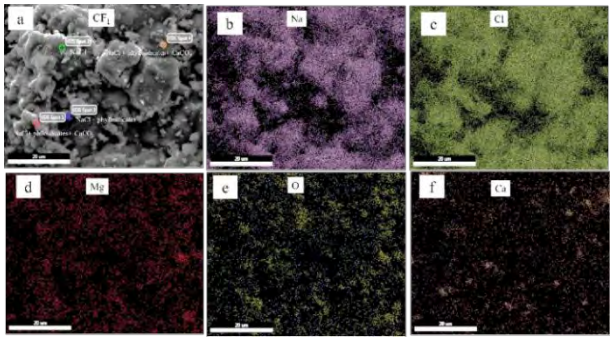

Figure 6.1.3. SEM image of the CF in 5000x magnification Na: sodium; Cl: Chlorine; Mg: Magnesium; O: Oxygen; Ca: Calcium.

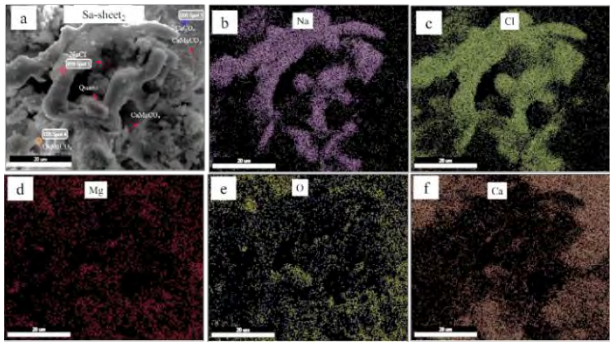

Figure 6.1.4. SEM image of the Sa-sheet in 5000x magnification. Na: sodium; Cl: Chlorine; Mg: Magnesium; O: Oxygen; Ca: Calcium.

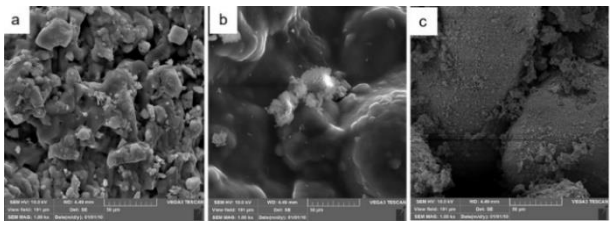

Figure 6.1.5. SEM images of induced crusts by (a) super-saturated salt; (b) sodium alginate; (c) sodium silicate.

Summary and conclusion

The present study showed that clay and silt size particles as well as organic compounds and Na^+ concentration are the major soil properties improving soil crust stability and compressive strength, while geologic carbonates and sand correlated negatively with crust stability against wind. The presence of organic compounds accompanied with the prevalence of phyllosilicates and NaCl are the major reasons for stable crust formation, conversely, silt size fraction, NaCl, and pedogenic carbonates (calcite) increase crust stability by clogging pore spaces. In crust samples from Sa-sheets, the negative effect on crust formation of carbonates present in the sand fraction in the form of aragonite could not be counterbalanced by carbonates present as calcite as cementing agents, which explains the negative correlation of CCE with crust stability. Moreover, the NaCl content proved to be insufficient to connect skeleton grains of geologic carbonates by building bridges between them.

This study showed that intrinsic physicochemical properties of the emerged playa surfaces control crust stability. Pedogenic carbonate formation together with NaCl dissolution and re-precipitation within pore spaces and ped surfaces can lead to physicochemical crust formation over LU playa surfaces when biological crust development is insufficient.

References

Abadi, A. R. S., Hamzeh, N. H., Shukurov, K., Opp, C., & Dumka, U. C. (2022). Long-term investigation of aerosols in the Urmia Lake region in the Middle East by ground-based and satellite data in 2000–2021. Remote Sensing, 14(15), 3827.

Ahmadi, F., Nazeri Tahroudi, M., Mirabbasi, R., & Kumar, R. (2022). Spatiotemporal analysis of precipitation and temperature concentration using PCI and TCI: a case study of Khuzestan Province, Iran. Theoretical and Applied Climatology, 149(1-2), 743-760.

Alkhayer, M., Eghbal, M. K., & Hamzehpour, N. (2019). Geomorphic surfaces of eastern lake Urmia Playa and their influence on dust storms. Journal of Applied Sciences and Environmental Management, 23(8), 1511-1520.

Alkhayer, M., Eghbal, M. K., & Hamzehpour, N. (2019). Geomorphic surfaces of eastern lake Urmia Playa and their influence on dust storms. Journal of Applied Sciences and Environmental Management, 23(8), 1511-1520.

Alkhayer, M., Eghbal, M. K., & Hamzehpour, N. (2023). Brine geochemical changes and salt crust evolution of Lake Urmia in Iran. CATENA, 231, 107310.

Asakereh, H. (2020). Decadal variation in precipitation regime in northwest of Iran. Theoretical and Applied Climatology, 139, 461-471.

Asl, F. N., Asgari, H. R., Emami, H., & Jafari, M. (2019). Combined effect of micro silica with clay, and gypsum as mulches on shear strength and wind erosion rate of sands. International Soil and Water Conservation Research, 7(4), 388-394.

Brahney, J., Ballantyne, A. P., Kociolek, P., Leavitt, P. R., Farmer, G. L., & Neff, J. C. (2015). Ecological changes in two contrasting lakes associated with human activity and dust transport in western Wyoming. Limnology and Oceanography, 60(2), 678-695.

D'Odorico, P., Bhattachan, A., Davis, K. F., Ravi, S., & Runyan, C. W. (2013). Global desertification: Drivers and feedbacks. Advances in water resources, 51, 326-344.

Mansouri Daneshvar, M. R., Ebrahimi, M., & Nejadsoleymani, H. (2019). An overview of climate change in Iran: facts and statistics. Environmental Systems Research, 8(1), 1-10.

Farebrother, W., Hesse, P. P., Chang, H. C., & Jones, C. (2017). Dry lake beds as sources of dust in Australia during the Late Quaternary: A volumetric approach based on lake bed and deflated dune volumes. Quaternary Science Reviews, 161, 81-98.

Hamzehpour, N. & Marcolli, C. (2024). Soil crust development on different playa surfaces of Lake Urmia and its controlling factors-an insight to combat dust sources. Catena, accepted for publication.

Hamzehpour, N., Eghbal, M. K., Abasiyan, S. M. A., & Dill, H. G. (2018). Pedogenic evidence of Urmia Lake's maximum expansion in the late Quaternary. Catena, 171, 398-415.

Hamzehpour, N., Marcolli, C., Pashai, S., Klumpp, K., & Peter, T. (2022a). The Urmia Playa as source of airborne dust and ice nucleating particles–Part 1: Correlation between soils and airborne samples. Atmospheric Chemistry and Physics, 22, 14905-14930.

Hamzehpour, N., Marcolli, C., Klumpp, K., Thöny, D., & Peter, T. (2022b). The Urmia Playa as source of airborne dust and ice nucleating particles–Part 2: Unravelling the relationship between soil dust composition and ice-nucleation activity. Atmospheric Chemistry and Physics, 22, 14931-14956.

Jowkar, L., Panahi, F., Sadatinejad, S. J., & Shakiba, A. (2021). The Spatio-Temporal Variability of Extreme Temperature Using Gridded AgMERRA Dataset over the Bakhtegan-Maharloo Basin, Iran. ECOPERSIA, 9(3), 179-189.

Kheirfam, H. (2022). Spatial prioritization of wind-erosion-prone areas in the dried-up beds of Lake Urmia; using field sampling and in-vitro measurement. CATENA, 217, 106507.

Kok, J. F., Adebiyi, A. A., Albani, S., Balkanski, Y., Checa-Garcia, R., Chin, M., ... & Wan, J. S. (2021). Contribution of the world's main dust source regions to the global cycle of desert dust. Atmospheric Chemistry and Physics, 21(10), 8169-8193.

Marcolli, C., Calzaferri, G. (1997). Vibrational structure of monosubstituted octahydrosilasesquioxanes. J. Phys. Chem. B, 101, 4925–4933.

Middleton, N. J., & Goudie, A. S. (2001). Saharan dust: sources and trajectories. Transactions of the Institute of British Geographers, 26(2), 165-181.

Motaghi, F. A., Hamzehpour, N., Abasiyan, S. M. A., & Rahmati, M. (2020). The wind erodibility in the newly emerged surfaces of Urmia Playa Lake and adjacent agricultural lands and its determining factors. Catena, 194, 104675.

Neeladharan, C., Sathish, P., Nandhini, A., Priya, R., Fathima, I. S., Srimathi, J., & Melvisharam, V. (2018). Stabilization of soil by using marble dust with sodium silicate as binder. International Journal of Advanced Research Trends in Engineering and Technology, 5(5), 45-49.

Papi, R., Attarchi, S., Darvishi Boloorani, A., & Neysani Samany, N. (2022). Characterization of hydrologic sand and dust storm sources in the Middle East. Sustainability, 14(22).

Pour, S. H., Wahab, A. K. A., & Shahid, S. (2020). Spatiotemporal changes in precipitation indicators related to bioclimate in Iran. Theoretical and Applied Climatology, 141, 99-115.

Rad, A. M., Kreitler, J., Abatzoglou, J. T., Fallon, K., Roche, K. R., & Sadegh, M. (2022). Anthropogenic stressors compound climate impacts on inland lake dynamics: The case of Hamun Lakes. Science of The Total Environment, 829, 154419.

Schoeneberger, P.J., Wysocki, D.A. Benham, Soil Survey Staff, 2012. Field book for describing and sampling soils. Version 3.0. Natural Resource Conservation Service, National Soil Survey Center, Lincoln.

Schulz, S., Darehshouri, S., Hassanzadeh, E., Tajrishy, M., & Schüth, C. (2020). Climate change or irrigated agriculture–what drives the water level decline of Lake Urmia. Scientific Reports, 10(1), 236

Sharifi, A., Shah-Hosseini, M., Pourmand, A., Esfahaninejad, M., & Haeri-Ardakani, O. (2018). The vanishing of Urmia lake: a geolimnological perspective on the hydrological imbalance of the world's second largest hypersaline lake.

Sirjani, E., Sameni, A., Moosavi, A. A., Mahmoodabadi, M., & Laurent, B. (2019). Portable wind tunnel experiments to study soil erosion by wind and its link to soil properties in the Fars province, Iran. Geoderma, 333, 69-80.

Soleimani Sardoo, F., Karami, S., & Hoseinhamzeh, N. (2021). Determining and analysing the temporal and spatial trend of dust and its effect on vegetation and precipitation (Case study of Jazmourian Basin). Environmental Erosion Research Journal, 11(3), 64-81.

Sweeney, M. R., Zlotnik, V. A., Joeckel, R. M., & Stout, J. E. (2016). Geomorphic and hydrologic controls of dust emissions during drought from Yellow Lake playa, West Texas, USA. Journal of Arid Environments, 133, 37-46.

Taghizadeh-Mehrjardi, R., Hamzehpour, N., Hassanzadeh, M., Heung, B., Goydaragh, M. G., Schmidt, K., & Scholten, T. (2021). Enhancing the accuracy of machine learning models using the super learner technique in digital soil mapping. Geoderma, 399, 115108.

Vaculíková, L., Plevová, E. (2005). Identification of clay minerals and micas in sedimentary rocks, Acta Geodyn. Geomater, 2(2), 167-175.

Varga, G., Újvári, G., & Kovács, J. (2014). Spatiotemporal patterns of Saharan dust outbreaks in the Mediterranean Basin. Aeolian Research, 15, 151-160.

Volkov, D. S., Rogova, O. B., Proskurnin, M. A. (2021). Organic matter and mineral composition of silicate soils: FTIR comparison study by photoacoustic, diffuse reflectance, and attenuated total reflection modalities. Agronomy, 11, 1879.

Warrence, N. J., Bauder, J. W., & Pearson, K. E. (2002). Basics of salinity and sodicity effects on soil physical properties. Department of Land Resources and Environmental Sciences, Montana State University-Bozeman, MT, 129, 1-29.

7 Monographic articles

7.1 Hydrodynamics of filtration drying of food industry secondary raw materials

Oleksandr Ivashchuk[1], Volodymyr Atamanyuk[1], Roman Chyzhovych*[,1], Serhii Barabakh[1]

1. Department of Chemical Engineering, Lviv Polytechnic National University, Lviv, Ukraine
e-mail: roman.a.chyzhovych@lpnu.ua

KEYWORDS: biomass, brewer's spent grain, filtration drying, hydrodynamics, CFD

Abstract

The paper presents the results of computer modeling regarding the hydrodynamics of thermal agent movement through a stationary layer of dried barley brewer's spent grain. The modeling involved determining the characteristics of the porous zone, such as the values of the viscous $1/\alpha$ and inertial C_2 resistance coefficients. The simulation was conducted using the *k-ω SST* turbulence model in the *ANSYS Fluent 2022 R2* software package. The investigation focused on the heights of the dried brewer's spent grain layer within the range of H = 90÷110 mm and thermal agent flow velocities of w_0 = 0.84÷1.78 m/s. The average modeling error across all experimental points, based on the experimental data of the layer's hydraulic resistance, was determined to be 2,91%.

Introduction

Exploring additional applications for plant biomass stands out as a crucial focus of research, aiming not just to discover novel utilization possibilities but also to enhance and streamline existing ones. Employing a rational approach to environmental conservation will diminish the volume of plant waste accumulation in industrial settings, contributing to the amelioration of the overall environmental conditions (Zeko-Pivač et al., 2022).

A notable plant-based waste product deserving attention is barley brewer's spent grain, a by-product originating from industrial beer production (Hassan et al., 2020, Mussatto et al., 2006). The considerable residual moisture content in brewer's spent grain (~70%$_{wt.}$) post the technological process hinders its potential for secondary use (Eliopoulos et al., 2022, Ikram et al., 2017). This high moisture level results in quick spoilage of the by-product within approximately 2 to 3 days (Ivashchuk et al., 2022).

Considering the mentioned factors, the current applications for the secondary use of barley brewer's spent grain involve the need for partial or complete drying. These applications include food additives for bakery products (Mussatto et al., 2006, Ktenioudaki et al., 2012), fertilizing agricultural land (Aboukila et al., 2013), using as raw materials for biogas production (Mussatto et al., 2006, Mussatto et al., 2014), and manufacturing solid fuel briquettes (Ivashchuk et al., 2022), among others.

To dry barley brewer's spent grain, a highly efficient filtration drying method is suggested due to its benefits (Kobeyeva et al., 2022), especially when dealing with drying dispersed plant materials in a stationary layer.

An initial examination of the fluid dynamics of the thermal agent's flow through the stationary layer of the material under study will help in identifying its hydraulic resistance. This information is crucial for designing and calculating drying equipment to estimate the energy requirements for generating a pressure difference during the drying of dispersed materials. Analyzing the experimental data on the hydrodynamics of the thermal agent's movement will enable computer modeling of the process to predict the hydraulic resistance at various heights of the barley brewere's spent grain stationary layer.

Experimental

Experimental investigations of the thermal flow dynamics through a stationary layer of dispersed material were conducted using barley brewer's spent grain obtained from the production line of the "Kumpel" brewery in Lviv, Ukraine.

Before subjecting the initial plant material, barley brewer's spent grain, to further processes, excess moisture was removed by employing filtration drying in an experimental laboratory setup (Ivashchuk et al., 2021).

The study focused on the hydrodynamics of the thermal agent's flow through the layer of dried barley brewer's spent grain to assess how the fictitious velocity w_0 of the thermal agent influences the hydraulic resistance ΔP of the stationary layer of the material under investigation. In addition to determining the material's stationary layer resistance, the study also involved assessing the resistance of the perforated baffle in the cylindrical container (Figure 7.1.1) of the laboratory filtration drying setup (Ivashchuk et al., 2021). The hydraulic resistance of the dried barley brewer's spent grain layer was then calculated by finding the difference between the experimentally obtained value and the value derived from the polynomial equation for each studied air flow rate (Figure 7.1.2).

To regulate the layer height of the dispersed material in the cylindrical container, the bulk density of barley brewer's grain was established using the methodology outlined in Ivashchuk et al. (2024), resulting in a value of 175.2 kg·m^{-3}. Additionally, the layer porosity was experimentally determined using an equation:

$$\varepsilon = 1 - \frac{V_p}{V} \qquad (7.1.1.)$$

where ε is the porosity of the material layer, m^3/m^3; V_p is the pore volume, m^3; V is the total volume, m^3, following the procedures outlined in Ivashchuk et al. (2024), yielding a value of 0.32 m^3/m^3 for the dried raw material. The average moisture content of the material was measured to be 12.69%$_{wt}$.

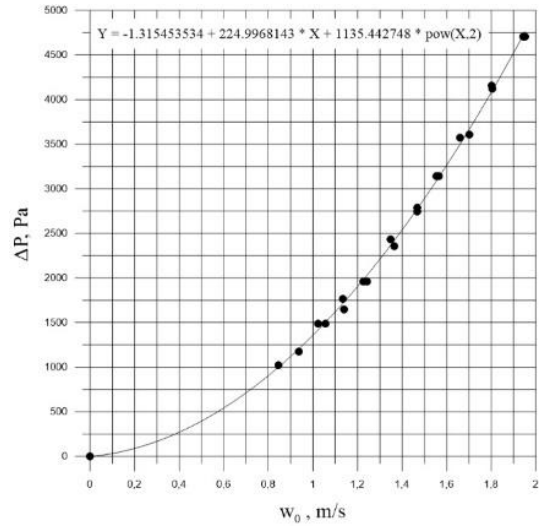

Figure 7.1.1 Change in the hydraulic resistance of a cylindrical container's perforated baffle depending on the velocity of the thermal agent.

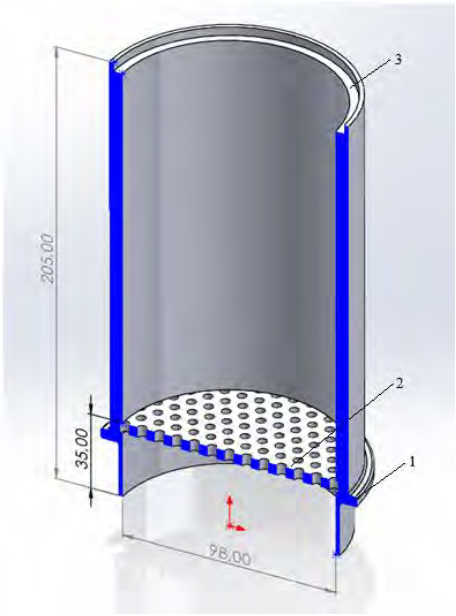

Figure 7.1.2 Cross-section of the 3D container model: 1 – container body, 2 – perforated baffle, 3 – thermal insulation insert.

To calculate the pressure drop as air flows through a porous layer of the material being studied, practical application often involves utilizing the relationship referred to as the Darcy-Weisbach equation:

$$\Delta P = \lambda \cdot \frac{H}{d_e} \cdot \frac{\rho \cdot w^2}{2} \qquad (7.1.2.)$$

where ΔP is the hydraulic resistance of the material layer, Pa; λ is the layer resistance coefficient; H is the height of the material layer, m; d_e is the equivalent diameter, m; ρ is the gas or liquid flow density, kg·m^{-3}; w is the actual velocity of gas or liquid flow, m·s^{-1}.

$$\frac{\Delta P}{H \cdot w_0} = A \cdot \frac{\mu \cdot a^2}{32 \cdot \varepsilon^3} + B \cdot \frac{\rho \cdot a}{8 \cdot \varepsilon^3} \cdot w_0 \qquad (7.1.3)$$

After making transformations, described in detail in Ivashchuk et al. (2024), the modified Darcy-Weisbach equation or the Ergan equation is obtained:

To simplify equation (7.1.3), let us make substitutions for values A^* and B^* that depend on the structure of the material under study and the parameters of the thermal agent, which makes it possible to determine them experimentally.

$$\frac{\Delta P}{H \cdot w_0} = A^* + B^* \cdot w_0 \qquad (7.1.4)$$

Results and discussion

Following the guidance provided in Ansys Fluent User's Guide (2013), the porous media method within the ANSYS Fluent software package was used for computer simulation, specifically modelling the thermal agent's flow through the dispersed layer of the research material. The simulation was based on the system of Navier-Stokes differential equations and the flow continuity equation, incorporating the Darcy equation to ascertain the value of the layer hydraulic resistance ΔP (Ansys Fluent User's Guide, 2013, Wang et al., 2010).

The optimal layer height for drying in industrial conditions is about 100 mm, which varies depending on the operating process requirements. Taking into account the results of previous computer simulations of the movement of a thermal agent through layers of dispersed materials of plant origin (Ivashchuk et al., 2023), as well as the conclusions drawn from these studies, which recommend reducing the step size of the heights of the material layers to improve accuracy, the simulation of thermal flow through layers of dried barley brewer's spent grain was carried out with a smaller interval for the studied heights.

The hydrodynamics study of the thermal agent movement through a stationary layer of dried brewer's spent grain provides experimental data in the form of a graphical representation depicting the impact of the fictitious flow rate w_0 on the variation in hydraulic resistance ΔP of the studied material layer (Figure 7.1.3).

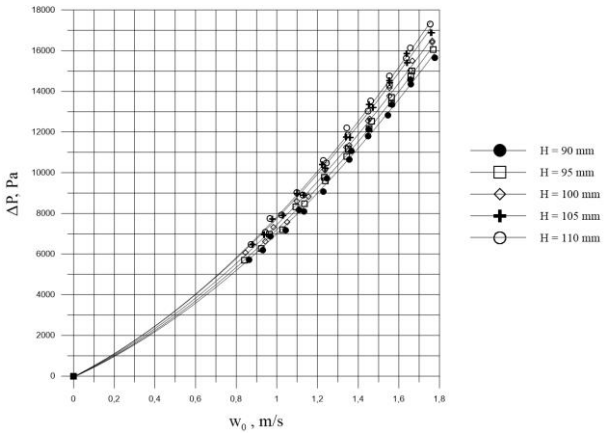

Figure 7.1.3 Variations in hydraulic resistance within the dried brewer's spent grain layer in relation to the fictitious speed of the thermal agent at different layer heights (T=17 °C, H=90÷110 mm, w_0=0.84÷1.78 m·s^{-1}).

Table 7.1.1 Relative errors in computer modeling for the analyzed heights of the dried brewer's spent grain layer, ranging from H=90 to 110 mm.

Material layer height, mm	90	95	100	105	110	The average value:
Average modeling error, %	3.91	1.82	1.64	2.15	5.03	2.91

Based on the experimental data of the hydrodynamics of the movement of the heat agent through the layer of the material under study, a graphical representation was constructed (Figure 7.1.4) using the linear equation derived from the Darcy-Weisbach equation (Kowalczuk et al., 2022):

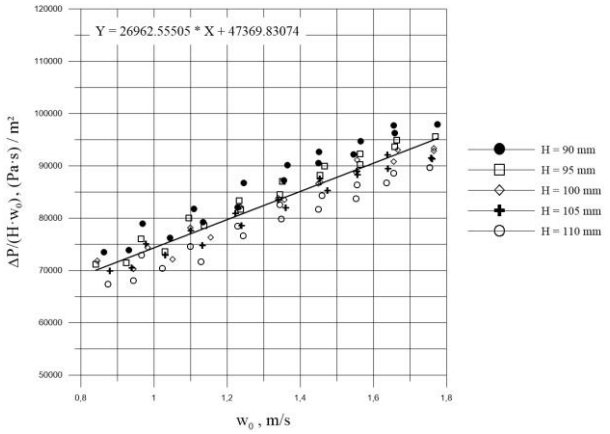

Figure 7.1.4 Graphical representation of $\Delta P/(H \cdot w_0) = f(w_0)$ for the investigated layer heights (T = 17 °C, H = 90÷110 mm, w_0 = 0.84÷1.78 m·s^{-1}).

The coefficients in the equation of the graphical dependence shown in Figure 7.1.4 correspond to the values A^* and B^*, and equation (7.1.4) will take the following form:

$$\frac{\Delta P}{H \cdot w_0} = 47369.83 + 26962.55 \cdot w_0 \qquad (7.1.5)$$

Computer simulations of thermal flow movement through a dispersed material layer were performed using the *ANSYS Fluent 2022 R2* software and the *k-ω SST* turbulence model, following the guidelines (Ivashchuk et al., 2024, Zaïdi et al., 2010). The porous modeling zone characteristics were defined by the porosity value ε and the viscous $1/\alpha$ and inertial C_2 resistance coefficients of the dried brewer's grains layer, which were determined as 2.65·10^9 m^{-2} and 44309 m^{-1}, respectively.

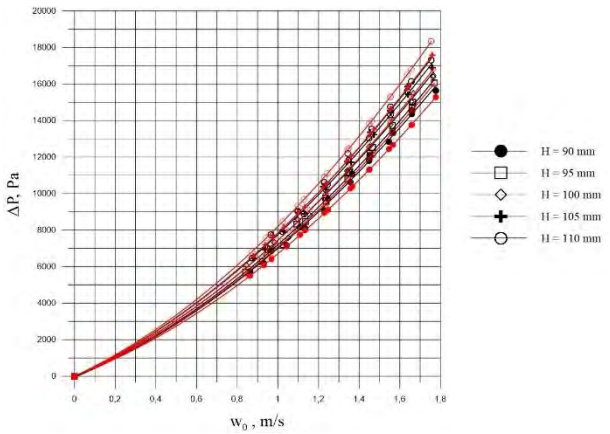

Figure 7.1.5 Visual representation comparing the modeled hydraulic resistance values (––– red lines) with the experimental values (––– black lines) (T=17 °C, H=90÷110 mm, w_0=0.84÷1.78 m·s^{-1}).

The modeling results (Figure 7.1.5) align well with the experimental findings. The use of experimental data for smaller pitch heights of the dispersed material is justified because it allows for an increase in the accuracy of computer modeling of the process hydrodynamics.

The results obtained validate the initial conclusions outlined in Ivashchuk et al. (2024), emphasizing the importance of narrowing the range of studied heights for enhanced modeling accuracy. A reduced height interval in the studied layer provides more intricate and precise data, influencing modeling outcomes positively and enhancing the precision of predicting the process's hydrodynamics.

The calculated relative modeling errors are less than those for larger range and are presented in Table 7.1.1. The average relative error across all experimental points in the study is 2.91%. The highest average error, 5.03%, corresponds to the layer height H=110 mm.

To illustrate the pattern of the thermal agent's flow through the stationary layer of the investigated material, the simulation outcomes were presented in the form of a static pressure field distribution (Figure 7.1.6 a) and a vector velocity field (Figure 7.1.6 b) in the cross-sectional plane of the computational domain.

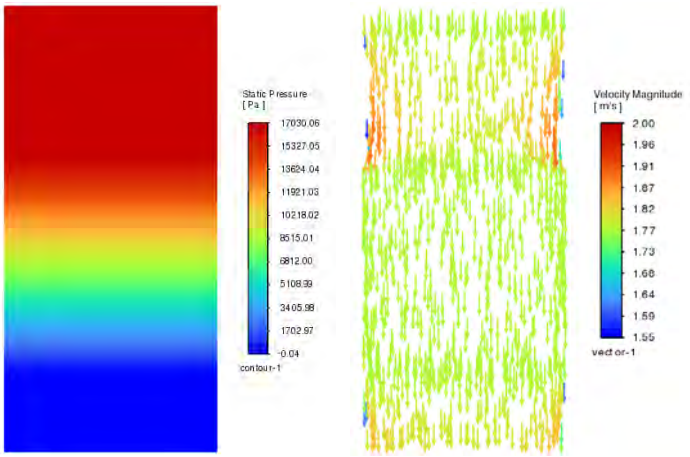

(a) **(b)**

Figure 7.1.6 An instance illustrating the distribution of the static pressure field (a) and the vector velocity field (b) in the cross-sectional plane of the simulation area for H = 100 mm, w_0 = 1.78 m·s^{-1}.

Visual representations of the static pressure field distribution and the vector velocity field in the cross-section plane of the modelling area are simulated. The analysis focuses on understanding the variations in static pressure and velocity along the airflow path. Examining the presentation of the static pressure field distribution (Figure 7.1.6 a), we note a progressive reduction in static pressure along the trajectory of the thermal agent's flow through the simulated area, maintaining a constant value in the zones above and below the material layer. Simultaneously, the vector representation of the velocity field (Figure **7.1.6**, b) illustrates the linear movement pattern of the thermal agent throughout

the simulated area. Additionally, a decrease is evident near the walls of the simulated area and at the entrance to the porous zone.

Conclusions

The hydrodynamics of the thermal agent's flow through a stationary layer of dried barley brewer's spent grain was simulated using the *ANSYS Fluent 2022 R2* software package. The investigation involved a variety of heights for the dried barley brewer's spent grain layer H = 90÷110 mm and thermal agent velocities w_0=0.84÷1.78 m·s^{-1}.

Within the investigated height range of H = 90÷110 mm, the average relative modeling error is determined to be 2.91%. The data from the modeling results support the earlier conclusions about the rationale for narrowing down the range of examined parameters.

The computer modeling of the studied process enables the prediction of the hydraulic resistance value for the dried barley brewer's spent grain layer within the specified height limits. This prediction is essential for designing and calculating drying equipment to anticipate the energy expenses associated with generating a pressure difference during the drying of dispersed material.

Acknowledgment

Authors are expressing their gratitude to CADFEM UA LLC, the official distributor of Ansys Inc. in Ukraine, for help with the software licensing.

Author contributions

Oleksandr Ivashchuk – experimental plan, preparation and conduct of experimental study, analysis and processing of results, writing of the article, general supervision of the work; Volodymyr Atamanyuk – experimental plan, analysis and processing of results, writing of the article; Roman Chyzhovych – preparation and conduct of experimental study, analysis and processing of results, writing of the article; Serhii Barabakh – preparation and conduct of experimental study.

References

Aboukila, E. F., Nassar, I. N., Rashad, M., Hafez, M., & Norton, J. B. (2013). Reclamation of calcareous soil and improvement of squash growth using brewers' spent grain and compost. *J. Saudi Soc. Agric. Sci.*, 17(4), 390–397. https://doi.org/10.1016/j.jssas.2016.09.005

Ansys Fluent User's Guide (15th ed.) (2013). ANSYS, Inc. URL: www.ansys.com

Eliopoulos, C., Arapoglou, D., Chorianopoulos, N., Markou, G., & Haroutounian, S. (2022). Conversion of brewers' spent grain into proteinaceous animal feed using solid state fermentation. *Environ. Sci. Pollut. Res.*, 29, 29562–29569. https://doi.org/10.1007/s11356-021-15495-w

Hassan, S. S., Ravindran, R., Jaiswal, S., Tiwari, B. K., Williams, G. A., & Jaiswal, A. K. (2020). An evaluation of sonication pretreatment for enhancing saccharification of brewers' spent grain. *Waste Manage.*, 105, 240–247. https://doi.org/10.1016/j.wasman.2020.02.012

Ikram, S., Huang, L., Zhang, H., Wang, J., & Yin., M. (2017). Composition and Nutrient Value Proposition of Brewers Spent Grain. *J. Food Sci.*, 82(10), 2232–2242. https://doi.org/10.1111/1750-3841.13794

Ivashchuk, O. S., Atamanyuk, V. M., Chyzhovych, R. A., Kiiaieva, S. S., Duleba, V. P., & Sobechko, I. B. (2022). Research of solid fuel briquettes obtaining from brewer's spent grain. *Journal of Chemistry and Technologies*, 30(2), 216-221. https://doi.org/10.15421/jchemtech.v30i2.256749

Ivashchuk, O. S., Atamanyuk, V. M., Gnativ, Z. Ya., Chyzhovych, R. A., & Zherebetskyi, R. R. (2021). Research into kinetics of filtration drying of alcohol distillery stillage. *Vopr. Khim. Khim. Tekhnol.*, 4, 58–65. https://doi.org/10.32434/0321-4095-2021-137-4-58-65

Ivashchuk, O., Chyzhovych, R., & Atamanyuk, V. (2023). CFD-modeling of thermal agent flow through a layer of Barley Brewer's spent grain. *2023 4th International Scientific Conference "Chemical Technology and Engineering". Proceedings*, 31-37. https://doi.org/10.23939/cte2023.031

Ivashchuk, O., Chyzhovych, R., & Atamanyuk, V. (2024). Simulation of the thermal agent movement hydrodynamics through the stationary layer of the Alcohol Distillery Stillage. *Case Studies in Chemical and Environmental Engineering*, *9*, 100566. https://doi.org/10.1016/j.cscee.2023.100566

Kobeyeva, Z., Khussanov, A., Atamanyuk, V., Hnativ, Z., Kaldybayeva, B., Janabayev, D., & Gnylianska, L. (2022). Analyzing the kinetics in the filtration drying of crushed cotton stalks. *East.-Eur. J. Enterp. Technol.*, 1 (8(115), 55–66. https://doi.org/10.15587/1729-4061.2022.252352

Kowalczuk, Z., & Tatara, M. S. (2020). Improved model of isothermal and incompressible fluid flow in pipelines versus the Darcy–Weisbach equation and the issue of friction factor. *J. Fluid Mech.*, *891*. https://doi.org/10.1017/jfm.2020.131

Ktenioudaki, A., Chaurin, V., Reis, S., & Gallagher, E. (2012). Brewer's spent grain as a functional ingredient for breadsticks. *Int. J. Food Sci. Technol.*, 47(8), 1765–1771. https://doi.org/10.1111/j.1365-2621.2012.03032.x

Mussatto, S. I. (2014). Brewer's spent grain: a valuable feedstock for industrial applications. *J. Sci. Food Agric.*, 94(7), 1264–1275. https://doi.org/10.1002/jsfa.6486

Mussatto, S. I., Dragone, G., & Roberto, I. C. (2006). Brewers' spent grain: generation, characteristics and potential applications. *J. Cereal Sci.*, 43(1), 1–14. https://doi.org/10.1016/j.jcs.2005.06.001

Wang, Y., Brannock, M., Cox, S., & Leslie, G. (2010). CFD simulations of membrane filtration zone in a submerged hollow fibre membrane bioreactor using a porous media approach. *J. Membr. Sci.*, 363(1-2), 57–66. https://doi.org/10.1016/j.memsci.2010.07.008

Zaïdi, H., Fohanno, S., Taïar, R., & Polidori, G. (2010). Turbulence model choice for the calculation of drag forces when using the CFD method. *J. Biomech.*, *43*(3), 405–411. https://doi.org/10.1016/j.jbiomech.2009.10.010

Zeko-Pivač, A., Tišma, M., Žnidaršič-Plazl, P., Kulisic, B., Sakellaris, G., Hao, J., & Planinić, M. (2022). The potential of Brewer's spent grain in the circular bioeconomy: State of the art and future perspectives. *Frontiers in Bioengineering and Biotechnology*, *10*. https://doi.org/10.3389/fbioe.2022.870744

7.2 Mechanism studies of new initiating systems for 3D printing of dental crowns and bridges

Małgorzata Noworyta[1], Monika Topa-Skwarczyńska[1], Katarzyna Starzak[1], Jakub Pietraszewski[1], Martyna Sitko[1], Andrzej Świeży[1,2], Filip Petko[1,2], Joanna Ortyl*[,1,2,3]

1. Faculty of Chemical Engineering and Technology, Cracow University of Technology, Cracow, Poland
2. Photo HiTech Ltd., Cracow, Poland
3. Photo4Chem Ltd., Cracow, Poland

email: jortyl@pk.edu.pl

KEYWORDS: photopolymerization, dentistry, 3D printing, polymer materials, photoinitiators

Abstract

Lighting used polymerisation is also currently used particularly in dentistry, for the 3D printing of dentures or dental braces ideally suited to the palate of the individual consumer, as well as for obtaining bone fillings and in dentistry for curing dental fillings directly in the patient's mouth with light from the visible range. The photopolymerization aspect of the dental industry is extremely important and evolving, as there is a constant search for suitable initiator systems adapted to new monomers and patient needs. It is important to ensure the safety of the systems used and eliminate potential risks in terms of, for example, mutagenicity or cytotoxicity. Accurate printing is also desirable in this type of industry, as it ensures patient comfort. Therefore, spectroscopic analyses and extensive studies of the kinetics of photopolymerization processes using novel initiating systems dedicated to obtaining polymeric dental materials 3D printing techniques were conducted. Photoinitiating systems were used for cationic polymerization of vinyl monomer which is a novelty in the production of 3D polymeric materials in dentistry.

Introduction

Photopolymerization, due to its advantages, such as the fact that it occurres at room temperature, which entails energy savings due to the lack of need to heat the reaction system, is used in many industries (Jerzy Pączkowski 2003). This type of process is used in the coatings, furniture manufacturing, 3D printing and cosmetics which are just some of countless examples of industrial applications of photopolymerization processes to obtain light-curedmaterials (Jankowska et al. 2024). Three-dimensional (3D) printing is an ever-growing revolution in the field of manufacturing, enabling the precise and individualized creation of objects with complex structures with a high accuracy of dimensional mapping against the designed object created using the CAD (Computer-Aided Design) environment (Prasad & Smyth 2016; Randazzo et al. 2016; Stansbury & Idacavage 2016; Yan et al. 2018). Dentistry, as a beneficiary of technological advances, is increasingly taking advantage of this modern technology, and this includes printing techniques such as FDM (Fused Deposition Modeling), SLA (Stereolithography), DLP (Digital Light Processing) or SLS (Selective Laser Sintering), among others (Lin et al. 2019; Kim et al. 2020; Meglioli et al. 2020; Khonsari et al. 2021; Tian et al. 2021; Zeller et al. 2021). These techniques are used especially in the context of manufacturing dental crowns and bridges. Modern 3D printing technologies not only expand the possibilities of shaping structures, but also pose challenges for researchers and practicing dentists to improve initiation processes. The composition of prepared formulations and, in particular, the initiator system used, the monomers and admixtures used play a key role in defining the parameters of the 3D printing process, directly influencing the precision and mechanical and aesthetic properties of the final products (Dawood et al. 2015; dos Santos et al. 2021; Aati et al. 2022; Topa-Skwarczyńska et al. 2022; de Campos et al. 2023; Noworyta et al. 2023).

In this study, a basic spectroscopic study of the photoinitiators used in the systems and the chain conveyor additive was conducted. The polymerization kinetics of the produced compositions were investigated, including determination of the final conversions and induction times of studied compositions. The disappearance of the vibration bands characteristic of the specific bonds present in the used monomer was monitored directly during the real-time measurement. In the present study, new systems were proposed to initiate the photopolymerization process in combination with vinyl monomer that have not yet been used in dentistry and commonly used methacrylate monomers which allows to exclude ones such as Bis-GMA with potentially harmful effects on the human body. The paper presents an attempt to obtain materials by the 3D printing method using systems that polymerize according to the radical mechanism and also the cationic one.

Methods

Materials

Two radical photoinitiators TPO-L and 39-134 and two cationic photoinitiators SYLANTO - 7MP and EDOT - were used in the study. The monomers undergoing photopolymerization according to the radical mechanism were urethane dimethacrylate (UDMA) and triethylene glycol dimethacrylate (TEGDMA) whereas in a cationic manner reacts the applied trifunctional vinyl monomer tris [4-(vinyloxy)butyl]trimelliate (VBT). The formulas of the various substances are presented on Figure 7.2.1 and Figure 7.2.**2** and Fig. 2. In the study, a chain conveyor – ethyl 2-(p-tolyl-sulfonyloxy)prop-2-enoate (AFCT) was used, the pattern of which is presented on the Figure 7.2.1 and acetonitrile was used as the solvent in the spectroscopic studies.

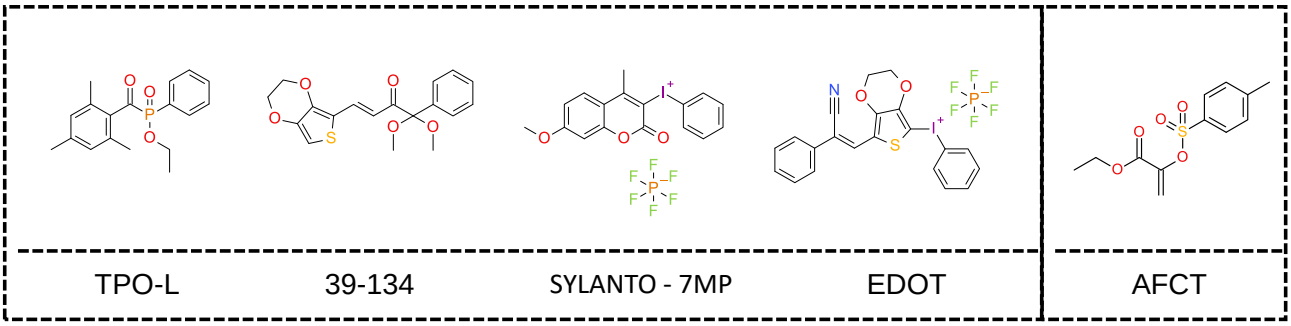

Figure 7.2.1 Photoinitiators and chain transfer used in research.

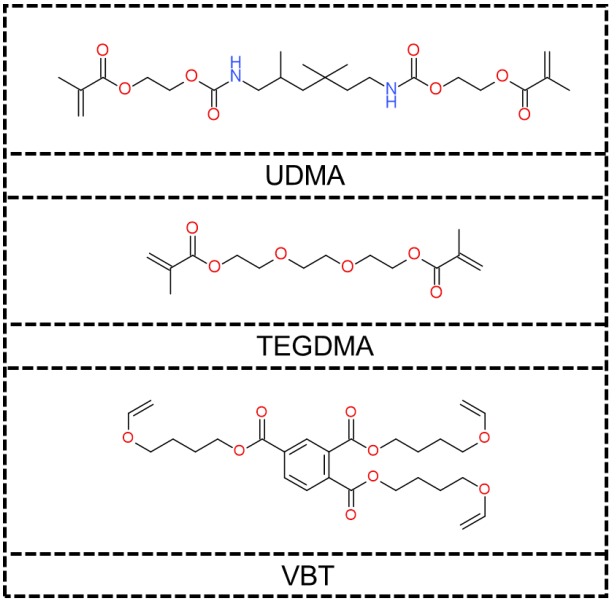

Figure 7.2.2 Monomers used in research.

Absorbance Measurement

A SilverNova spectrometer and a wide-band, tungsten-deuterium lamp were used to perform spectrophotometric studies, which acted as a UV-Vis light source. Both pieces of equipment are manufactured by StellarNet Inc. Absorbance spectra of solutions placed in a quartz cuvette with an optical path of exactly 1 centimeter were recorded. TPO-L photoinitiator solution of $6.33 \cdot 10^{-4}$ mol·dm^3, 39-134 photoinitiator solution of $2.89 \cdot 10^{-5}$ mol·dm^3 were used to conduct the experiments, Sylanto - 7MP photoinitiator solution with a concentration of $3.72 \cdot 10^{-5}$ mol·dm^{-3}, and Edot photoinitiator solution with a concentration of $3.24 \cdot 10^{-5}$ mol·dm^{-3}. The solution of the chain transfer in acetonitrile had a concentration of $1.83 \cdot 10^{-3}$ mol·dm^{-3}. To study the effect of AFCT on the absorbance of photoinitiators, the results were examined for solutions containing 5 µL, 10 µL, 15 µL and 30 µL each due to the fact that higher concentrations of the chain conveyor caused measurement disturbances in the form of saturated and overlapping absorption bands.

Photostability Measurement

Photodecomposition studies of the otherwise photostability of the photoinitiators used were carried out using a SilverNova spectrometer and a broadband deuterium-tungsten UV-Vis lamp by StellarNet Inc. A M405L4 Vis-LED from Thorlabs Inc. was used to expose the prepared solutions. Measurements were carried out in a quartz cuvette with four transparent walls with an optical path of exactly 1 centimeter containing 3 mL of the analysed solution and using a Vis-LED 405 nm with the light intensity at the sample of 10 mW·cm^{-2}, for 30 minutes and for an integration time of 10 seconds. A DC2200 device from Thorlabs Inc. was used as the power supply for the above-mentioned diode. The solutions used in the study were analogous to the absorbance study but using appropriate dilutions. For the photodecomposition measurement for the samples containing AFCT, the solutions were mixed at a volume ratio of 1:1. The initial AFCT solution in acetonitrile had a concentration of $7.41 \cdot 10^{-5}$ mol·dm^{-3}.

Real-Time FT-IR Photopolymerization Measurements

The kinetics and final conversion steps of the polymer compositions were measured in real time using Fourier-transform infrared spectroscopy. The equipment used to conduct the process was a *i10 Nicole*^{TM} spectrometer from Thermo Scientific, which has a special horizontal attachment that makes it possible to conduct the measurements of kinetics of photopolymerization process online. To irradiate the samples during the measurements, a M405L4 Vis-LED from Thorlabs Inc. was used, the power of the light beam used was 20 mW·cm^{-2}. An optical fiber with a length of 1.2 m and a diameter of 0.5 cm was responsible for delivering the light radiation to the sample. Illumination of the test compositions was started 10 seconds after the start of measurement data recording. OMNIC software was used to record measurement data. The compositions consisted of 1%$_{w/w}$ photoinitiator and 32%$_{w/w}$ and 26%$_{w/w}$ for the radical and cationic reacting composition, respectively. For the radical composition, a blend of two monomers UDMA and TEGDMA was used in a weight ratio of 7:3. The test samples had a film thickness of 1.4 mm. Conversion rates were calculated from equation (7.2.1) where A is the area of the monitored band, and A_0 is the initial value of the area of the monitored band. The bandwidth monitored in the systems is 6164 cm^{-1}.

$$Conversion\ [\%] = \left(1 - \frac{A}{A_0}\right) * 100\% \qquad (7.2.1)$$

3D Printing

A Lumen X+^{TM} printer provided by CELLINK was used to carry out DLP test printing. Printing was carried out on a special plate coated with polydimethylsiloxane (PDMS). The height of a single layer was set at 50 µm the irradiation time for the first layers was 150 seconds and each subsequent layer was 30 seconds using the maximum power of the printer.

Table 7.2.1 Absorbance characteristics of photoinitiators with the addition of AFCT

Acronym / Amount of AFCT	Extinction at the longest wave band ($dm^3 \cdot mol^{-1} \cdot cm^{-1}$)				λ_{max-ab} at the longest wave band (nm)			
	TPO-L	39-134	Sylanto-7MP	EDOT	TPO-L	39-134	Sylanto-7MP	EDOT
-	243	22802	18198	31405	373	356	353	380
5 µL	491	22698	37279	31597	372	356	355	380
10 µL	540	22823	37552	31926	371	356	351	380
15 µL	547	23290	38104	32364	371	356	351	379
30 µL	610	23902	39346	33050	368	356	351	378

Results and Discussion

Spectroscopic Measurements – Absorbance

Absorbance studies of individual photoinitiators and AFCT agent were performed. TPO-L and SYLANTO-7MP were used as commercial references for the new photoinitiators 39-134 and EDOT. It was observed that all photoinitiators tested absorb within visible light including at 405 nm, while the AFCT agent at a given concentration exhibits no absorption above 280 nm. The cationic photoinitiator EDOT has the highest molar extinction coefficient (Figure 7.2.3).

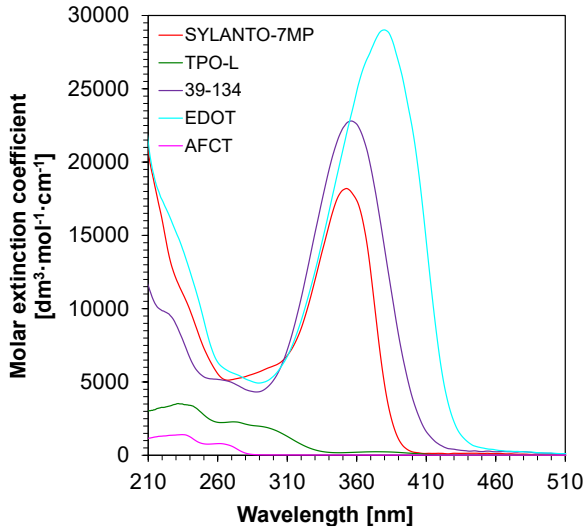

Figure 7.2.3 Absorption spectrum of photoinitiators and chain transfer used.

To investigate the effect of AFCT agent addition on the absorption of the photoinitiators tested, measurements were carried out for solutions of each photoinitiator containing the addition of 5 µL, 10 µL, 15 µL and 30 µL of chain conveyor. The results are presented in Table 7.2.1. It was observed that, in each case, the molar extinction coefficient increased with a maximum for the longest band after the addition of the AFCT agent portion (Figure 7.2.4-7). There was also a slight shift in the maximum of the analysed bands with the omission of the radical photoinitiator 39-134.

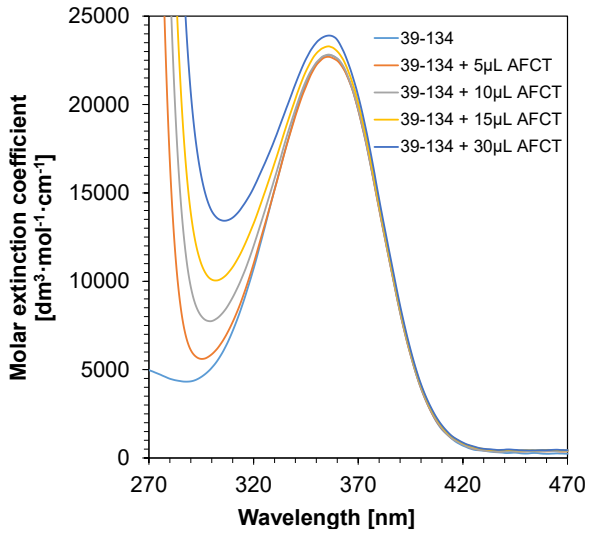

Figure 7.2.4 Absorption spectrum of 39-134 with AFCT.

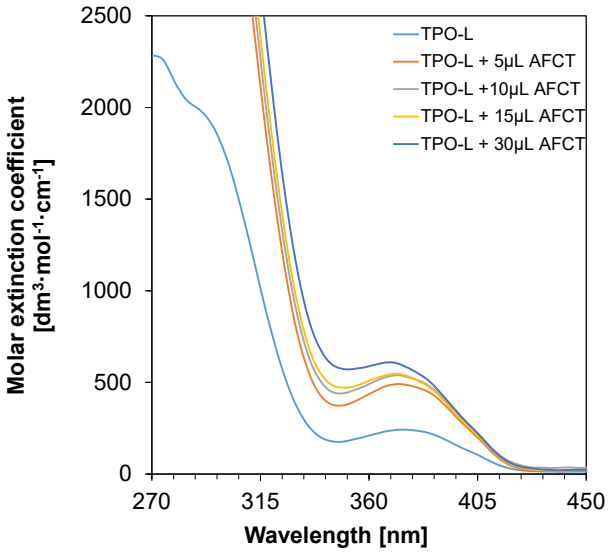

Figure 7.2.5 Absorption spectrum of TPO-L with AFCT.

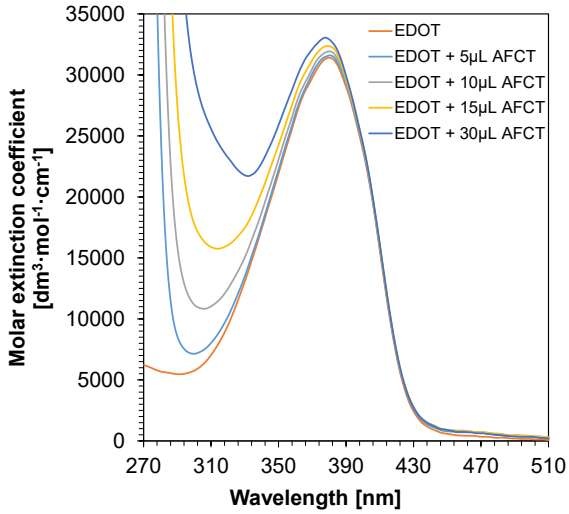

Figure 7.2.6 Absorption spectrum of EDOT with AFCT.

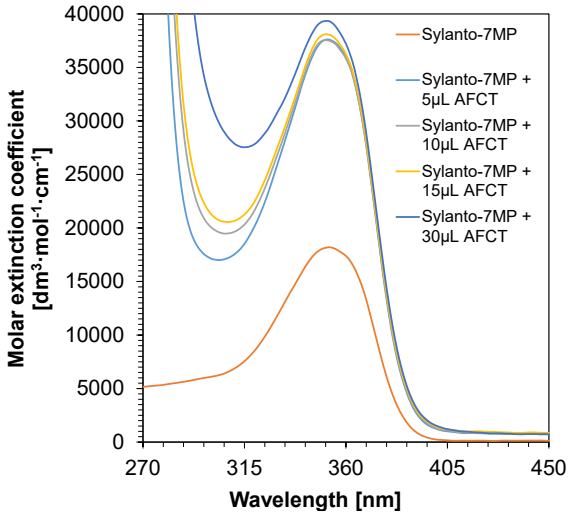

Figure 7.2.7 Absorption spectrum of SYLANTO-7MP with AFCT.

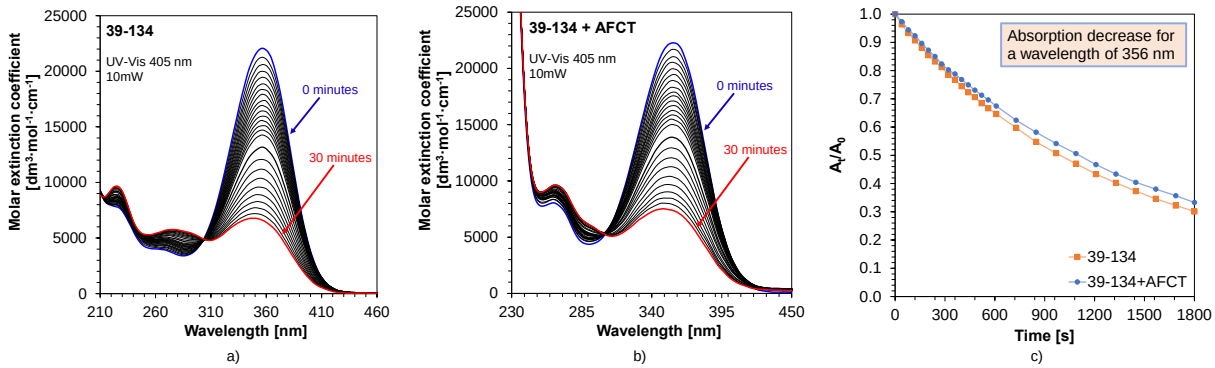

Figure 7.2.8 a) Photolysis of photoinitiator 39-134, **b)** effect of AFCT addition to the irradiated solution, **c)** correlation of changes in normalized absorbance over time for the band maximum at 356 nm for compound 39-134 and the tested photoinitiator with AFCT addition under 405 nm diode irradiation and 10 mW incident beam power for 30 min.

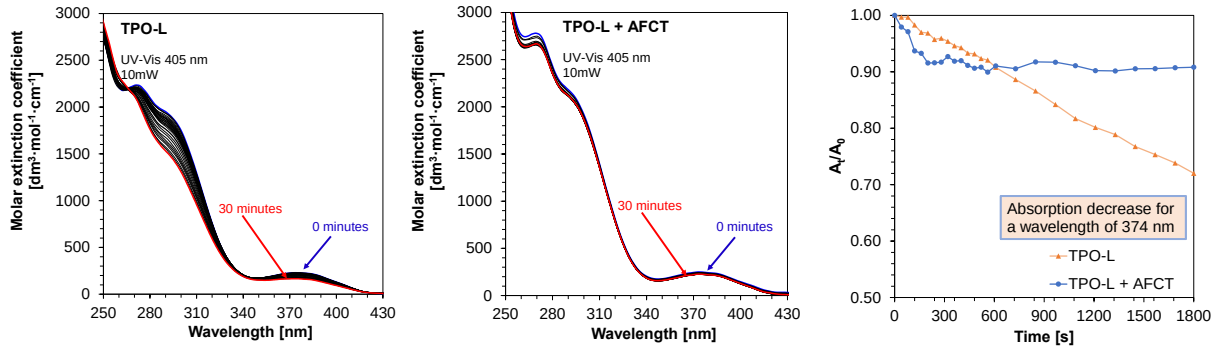

Figure 7.2.9 a) Photolysis of photoinitiator TPO-L, **b)** effect of AFCT addition to the irradiated solution, **c)** correlation of changes in normalized absorbance over time for the band maximum at 374 nm for compound TPO-L and the tested photoinitiator with AFCT addition under 405 nm diode irradiation and 10 mW incident beam power for 30 min.

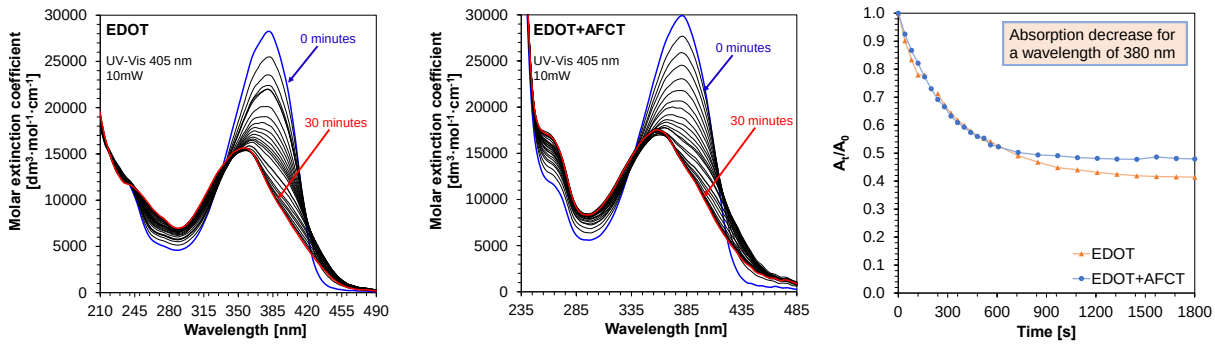

Figure 7.2.10 a) Photolysis of photoinitiator EDOT, **b)** effect of AFCT addition to the irradiated solution, **c)** correlation of changes in normalized absorbance over time for the band maximum at 380 nm for compound EDOT and the tested photoinitiator with AFCT addition under 405 nm diode irradiation and 10 mW incident beam power for 30 min.

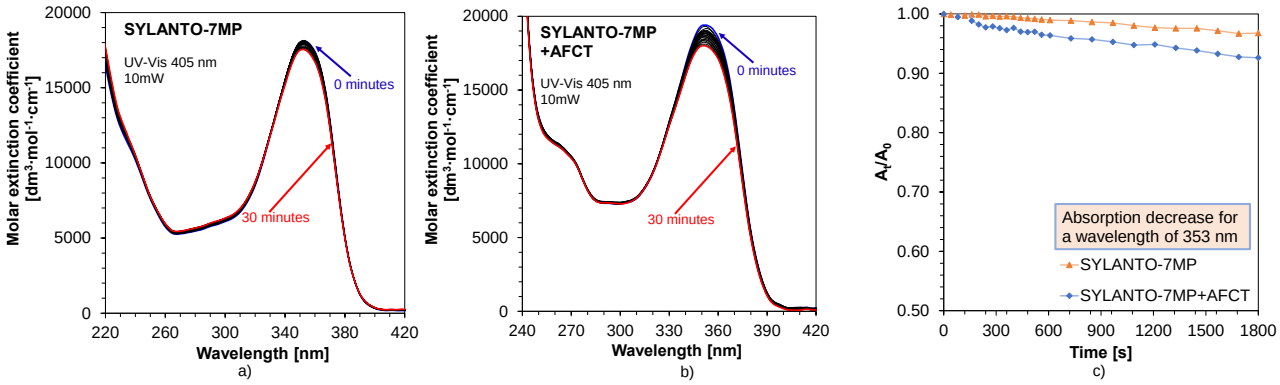

Figure 7.2.11 a) Photolysis of photoinitiator SYLANTO-7MP, **b)** effect of AFCT addition to the irradiated solution, **c)** correlation of changes in normalized absorbance over time for the band maximum at 353 nm for compound SYLANTO-7MP and the tested photoinitiator with AFCT addition under 405 nm diode irradiation and 10 mW incident beam power for 30 min.

Spectroscopic Measurements – Photolysis

Photostability tests were carried out on photoinitiators and systems containing a photoinitiator solution and an AFCT chain conveyor solution. For this purpose, one-dilute photoinitiator solutions and one-dilute AFCT agent solution were prepared and used for absorbance tests. The individual solutions of the photoinitiator compounds and the chain conveyor were mixed in a quartz cuvette at a volume ratio of 1:1. In the case of the radical photoinitiator 39-134 and the cationic photoinitiators, there is a slight change in the final degree of decomposition of the test substances after the addition of AFCT agent (Figure 7.2.8 c),Figure 7.2.10 c), Figure 7.2.11 c)) for the EDOT photoinitiator there was a slight decrease in decomposition efficiency. For the commercial radical photoinitiator TPO-L, there was a large decrease in photolysis efficiency after the addition of the AFCT agent.

Real-Time FT-IR

In order to verify the suitability of the proposed radical (39-134+UDMA/TEGDMA 7:3, 39-134+AFCT+UDMA/ /TEGDMA 7:3), cationic (EDOT+VBT, EDOT+AFCT+VBT) and hybrid (39-134+UDMA/TEGDMA 7:3+EDOT+VBT, 39-134+UDMA/TEGDMA 7:3+EDOT+ VBT+AFCT) photopolymerization was measured using Fourier-transform infrared spectroscopy. The degree of over-reactivity of the reactive groups in the polymer was calculated by monitoring the fading of the 6164 cm^{-1} band surface corresponding to the vibrations of the corresponding bonds in the system (Figure 7.2.12). The systems were irradiated for 900 seconds with a 405 nm diode. Light of this length is commonly used in 3D printers using photopolymerisation methods. In the case of radical compositions, the addition of a chain conveyor to the system resulted in a decrease in the final conversion rate of the composition (Table 7.2.2), while the resulting kinetic curve changed uniformly and no sudden, uncontrolled conversion of monomer to polymer was observed (Figure 7.2.13). The colour of the samples changed from cloudy to yellow due to the addition of AFCT agent.

The addition of the AFCT reagent to the cationic polymerizing system resulted in a significant increase in the final conversion rate of the tested composition as shown in Figure 7.2.14. It can be seen that from about 200 seconds onwards, there was a gradual but faster increase in the monomer conversion rate than for the composition without the carrier.

An attempt was made to obtain a polymer produced by a hybrid method. A composition containing a monomer polymerising according to the cationic mechanism and monomers polymerising according to the radical mechanism was added. A chain conveyor was added to this system, which did not significantly affect either the final conversion rate, which was 14% for the sample without the conveyor, or the photopolymerisation process itself (Figure 7.2.**15**).

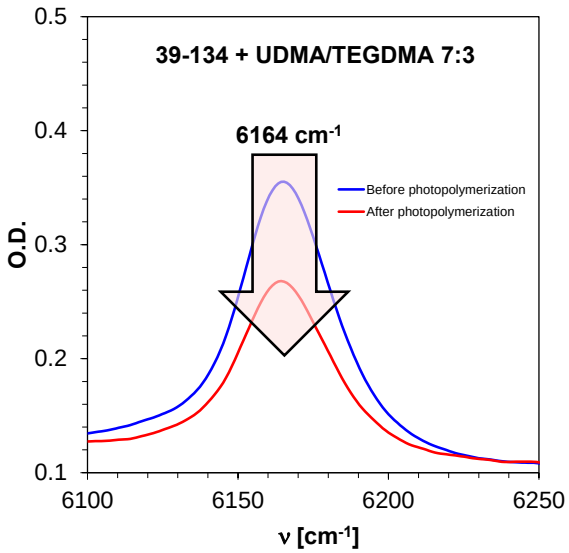

Figure 7.2.12 The decay of the 6164 cm^{-1} band monitored in the system, equivalent to the degree of conversion of the composition.

Table 7.2.2 Final conversion rates of the tested compositions determined by the FT-IR Real-Time method.

Composition	Conversion (%)
39-134 + UDMA/TEGDMA 7:3	38
39-134 + UDMA/TEGDMA 7:3+ AFCT	19
EDOT+VBT	19
EDOT+VBT+AFCT	50
39-134+UDMA/TEGDMA 7:3+EDOT+VBT	14
39-134+UDMA/TEGDMA 7:3+EDOT+VBT+AFCT	11

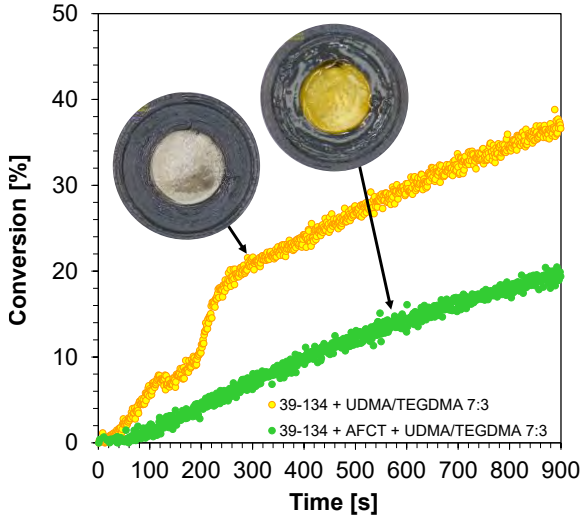

Figure 7.2.13 Kinetic profiles showing the course of photopolymerization of radical reactive compositions and the effect of AFCT on the reactivity of the system. A 1.4 mm thick sample exposed to a 20 mW·cm^{-2} light beam at 405 nm for 900 seconds.

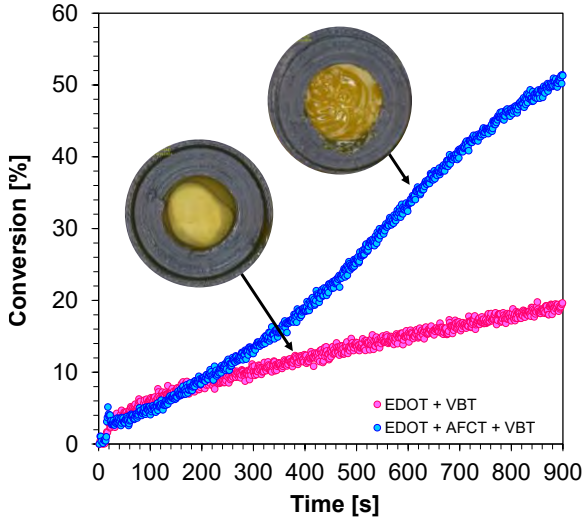

Figure 7.2.14 Kinetic profiles showing the course of photopolymerization of cationically reactive compositions and the effect of AFCT on the reactivity of the system. A 1.4 mm thick sample exposed to a 20 mW·cm^{-2} light beam at 405 nm for 900 seconds.

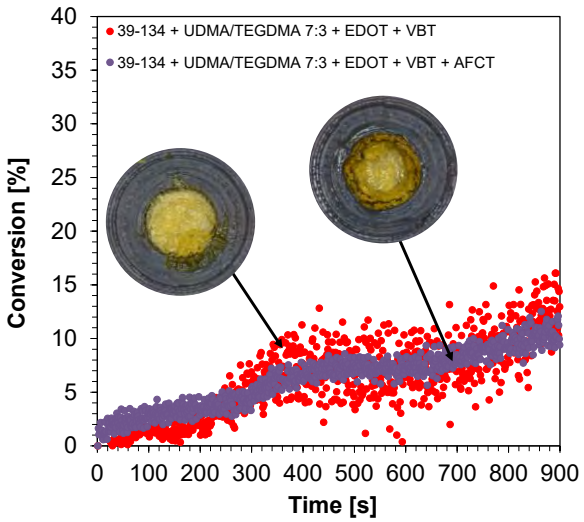

Figure 7.2.15 Kinetic profiles showing the photopolymerization process of combinatorially reactive compositions and the effect of AFCT on the reactivity of the system. A 1.4 mm thick sample exposed to a 20 mW·cm^{-2} light beam at 405 nm for 900 seconds.

Applications – 3D Printing

The 3D printing of a composition containing the commercial initiator TPO-L and mixtures of UDMA/TEGDMA monomers in a 7:3 weight ratio and the AFCT reagent was also attempted. High resolution printing with good reproduction was then achieved (Figure 7.2.16).

Therefore, an attempt was also made to use polymerizing compositions according to the cationic mechanism of EDOT+VBT and EDOT+VBT+AFCT for 3D printing. 3D printing was performed using a Lumen printer. In each case, a printed polymer slice of approximately 1 mm thickness was obtained. Therefore, these compositions have potential in high-resolution 3D printing in the dental industry, among others, after optimization of the composition and printing parameters (Figure 7.2.17).

Conclusion

The presented studies demonstrate that the newly proposed photoinitiators and photoinitiating systems are capable of initiating the light-induced polymerization processes of both free-radical and cationic mechanism upon the use of a 405 nm diode irradiation which was supported by the results obtained from photodegradation studies and FT-IR analyses. The effectiveness of the new photoinitiator as a single-component initiating system can be established for all compositions tested. However, the addition of a chain conveyor to the composition significantly affects the final conversion when a vinyl monomer is used in the photopolymerization process occurring according to the cationic mechanism. An important aspect that should be emphasized is the fact that the investigated initiating systems can be used in the case of using very low intensities of light at the sample, which is important in the case of creating materials dedicated for medical applications such as dentistry, because it allows to carry out the in situ photopolymerization process in a much safer way. Therefore, they can act as efficient photoinitiators in various dental applications. Due to their absorption characteristics extending into the visible light region, they can potentially be used in a wide range of light-based 3D printing techniques. to the individual composition. However, it should be noted that given the results obtained, especially from FT-IR analyses, it is potentially possible to use the described compositions in 3D printing, but after undertaking a careful testing to determine the appropriate printing parameters for each individual composition. In order to obtain precise DLP-based 3D prints using the presented compositions based on a newly synthesized photoinitiator, printing parameters such as the thickness of a single layer, its exposure time and light intensity must be adjusted.

Acknowledgements

The research was funded by National Centre for Research and Development in Poland under the Lider Program, grant number LIDER13/0156/2022. Moreover the synthesis of AFCT reagent was funded by the National Science Centre (NCN, Poland), PRELUDIUM 17, project no: 2019/33/N/ST5/03015.

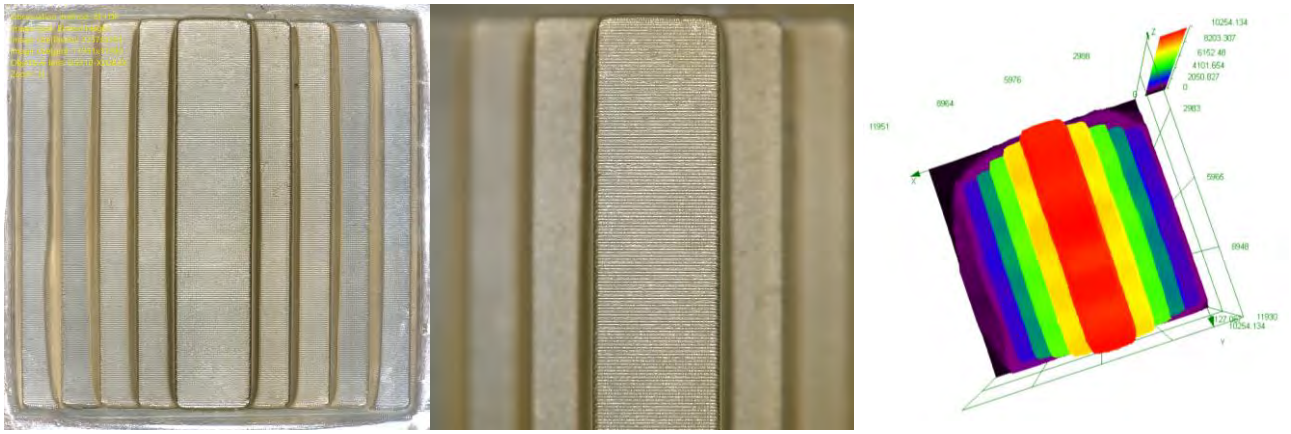

Figure 7.2.16 3D printing from a composition TPO-L + UDMA/TEGDMA 7:3 + AFCT

a) b)

Figure 7.2.17 a) The slice obtained from the composition of EDOT+VBT+AFCT, **b)** the slice obtained from the composition of EDOT+VBT.

References

Aati, Sultan, Aneja, Seerat, Kassar, Michael, Leung, Ryan, Nguyen, Anh, Tran, Susan, Shrestha, Barsha & Fawzy, Amr. (2022) 'Silver-loaded mesoporous silica nanoparticles enhanced the mechanical and antimicrobial properties of 3D printed denture base resin'. *Journal of the Mechanical Behavior of Biomedical Materials*, 134, 105421.

Campos, Murilo Rodrigues de, Botelho, André Luis & Reis, Andréa Cândido dos. (2023) 'Antimicrobial incorporation on 3D-printed polymers used as potential dental materials and biomaterials: a systematic review of the state of the art'. *Polymer Bulletin*, 80, 7313–7340.

Dawood, A., Marti, B. Marti, Sauret-Jackson, V. & Darwood, A. (2015) '3D printing in dentistry'. *British Dental Journal*, 219, 521–529.

Jankowska, Magdalena, Lepcio, Petr, Chachaj-Brekiesz, Anna, Galek, Mariusz, Petko, Filip, Vozárik, Andrej & Ortyl, Joanna. (2024) 'High-efficiency pentafluorostilbene-based photocatalysts dedicated to preparing fluorescent 3D printed polymer nanocomposites'. *Virtual and Physical Prototyping*, 19, 1–25.

Jerzy Pączkowski. (2003) *Fotochemia polimerów. Teoria i zastosowanie.* . Toruń: Wydawnictwo Uniwersytetu Mikołaja Kopernika .

Khonsari, Roman Hossein, Adam, Jeremy, Benassarou, Mourad, Bertin, Hélios, Billotet, Benjamin, Bouaoud, Jebrane, Bouletreau, Pierre, Garmi, Rachid, Gellée, Timothée, Haen, Pierre, Ketoff, Serge, Lescaille, Géraldine, Louvrier, Aurélien, Lutz, Jean Christophe, Makaremi, Masrour, Nicot, Romain, Pham-Dang, Nathalie, Praud, Morgan, Saint-Pierre, Françoise, Schouman, Thomas, Sicard, Ludovic, Simon, François, Wojcik, Thomas & Meyer, Christophe. (2021) 'In-house 3D printing: Why, when, and how? Overview of the national French good practice guidelines for in-house 3D-printing in maxillo-facial surgery, stomatology, and oral surgery'. *Journal of Stomatology, Oral and Maxillofacial Surgery*, 122, 458–461.

Kim, Taehun, Lee, Sangwook, Kim, Guk Bae, Hong, Dayeong, Kwon, Jinhee, Park, Jae Woo & Kim, Namkug. (2020) 'Accuracy of a simplified 3D-printed implant surgical guide'. *Journal of Prosthetic Dentistry*, 124, 195-201.e2.

Lin, Liwei, Fang, Yingfeng, Liao, Yuxuan, Chen, Gang, Gao, Chunxia & Zhu, Peizhi. (2019) '3D Printing and Digital Processing Techniques in Dentistry: A Review of Literature'. *Advanced Engineering Materials*, 21, 1801013.

Meglioli, Matteo, Naveau, Adrien, Macaluso, Guido Maria & Catros, Sylvain. (2020) '3D printed bone models in oral and cranio-maxillofacial surgery: a systematic review'. *3D Printing in Medicine 2020 6:1*, 6, 1–19.

Noworyta, Małgorzata, Topa-Skwarczyńska, Monika, Jamróz, Paweł, Oksiuta, Dawid, Tyszka-Czochara, Małgorzata, Trembecka-Wójciga, Klaudia & Ortyl, Joanna. (2023) 'Influence of the Type of Nanofillers on the Properties of Composites Used in Dentistry and 3D Printing'. *International Journal of Molecular Sciences*, 24.

Prasad, Leena Kumari & Smyth, Hugh. (2016) '3D Printing technologies for drug delivery: a review'. *Drug Development and Industrial Pharmacy*, 42, 1019–1031.

Randazzo, Michael, Pisapia, Jared, Singh, Nickpreet & Thawani, Jayesh. (2016) '3D printing in neurosurgery: A systematic review'. *Surgical Neurology International*, 7, S801.

Santos, Juliana dos, Oliveira, Rafaela S de, Oliveira, Thayse V de, Velho, Maiara C, Konrad, Martina V, Silva, Guilherme S da, Deon, Monique, R Beck, Ruy C, Santos, J dos, Oliveira, R S de, Oliveira, T V de, Velho, M C, Deon, M, R Beck, R C, Konrad, M V & Silva, G S da. (2021) '3D Printing and Nanotechnology: A Multiscale Alliance in Personalized Medicine'. *Advanced Functional Materials*, 31, 2009691.

Stansbury, Jeffrey W. & Idacavage, Mike J. (2016) '3D printing with polymers: Challenges among expanding options and opportunities'. *Dental Materials*, 32, 54–64.

Tian, Yueyi, Chen, Chun Xu, Xu, Xiaotong, Wang, Jiayin, Hou, Xingyu, Li, Kelun, Lu, Xinyue, Shi, Hao Yu, Lee, Eui Seok & Jiang, Heng Bo. (2021) 'A Review of 3D Printing in Dentistry: Technologies, Affecting Factors, and Applications'. *Scanning*, 2021.

Topa-Skwarczyńska, Monika, Noworyta, Małgorzata & Ortyl, Joanna. (2022) 'Badania kinetyczne i reologiczne kompozytów stomatologicznych nowej generacji'.

Yan, Qian, Dong, Hanhua, Su, Jin, Han, Jianhua, Song, Bo, Wei, Qingsong & Shi, Yusheng. (2018) 'A Review of 3D Printing Technology for Medical Applications'. *Engineering*, 4, 729–742.

Zeller, Alexander N., Neuhaus, Michael Tobias, Fresenborg, Sina, Zimmerer, Rüdiger M., Jehn, Philipp, Spalthoff, Simon, Gellrich, Nils Claudius & Dittmann, Jan Alfred. (2021) 'Accurate and cost-effective mandibular biomodels: a standardized evaluation of 3D-Printing via fused layer deposition modeling on soluble support structures'. *Journal of Stomatology, Oral and Maxillofacial Surgery*, 122, 355–360.

7.3 Bioinks and bioprinting. A short review.

Agnieszka Piontek*,1, Jadwiga Laska2

1. Faculty of Electrical Engineering, Automatics, Computer Science and Biomedical Engineering, AGH University of Krakow, Krakow, Poland
2. Faculty of Materials Engineering and Ceramics, AGH University of Krakow, Krakow, Poland

e-mail: piontek@student.agh.edu.pl

KEYWORDS: bioink, 3D bioprinting, tissue engineering

Abstract

This short review article presents the current state of knowledge in the field of bioprinting and bioinks. Bioprinting technology enables obtaining three-dimensional cell-laden construct that faithfully imitates natural tissue. Produced in this way tissue or entire organ is ready for implantation in the organism or for testing purposes in laboratory. Currently, intensive research is underway in this area. The most important challenges are to provide living cells with an environment for survival and proliferation under the conditions of the printing process and to obtain a complex, hierarchical and vascularized construct that can imitate the origin tissue and be fully functional. Bioprinting techniques as well as currently investigated materials for bioinks fabrication has been discussed.

Introduction

The simultaneous development of medicine and technology allows us to develop modern solutions that can become a rescue for patients struggling with various ailments. Dynamic progress is observed in the field of tissue engineering, which uses the knowledge of, among others, in the field of medicine, biochemistry and materials science in order to produce biomimetic tissue structures. One of the innovative techniques in this area is 3D bioprinting, enabling quick and precise mapping of computer-designed constructs. An increasing number of publications on the use of various 3D bioprinting methods and discussing innovative strategies for the production of hybrid inks give the prospect that this technology may prove to be a breakthrough solution in modern therapies.

The biggest challenge in bioprinting is matching the printing method and the properties of the ink base material in order to ensure the viability of the cells that are a component of the bioink. For this reason, numerous studies are conducted on the possibility of using various biocompatible materials that enable a controlled, repeatable and effective process of printing 3D tissue constructs and ensuring full functionality of a given substitute after implantation of the model in vivo (Hong et al., 2018; Szymoniuk et al., 2023).

Reasons for the development of tissue engineering

The development of civilization increases the quality of life of millions of people, but with it the demand for implantation materials and organs increases, which is caused by, among others, increasing life expectancy and lifestyle diseases. Modern transplantology faces many problems, the most important of which is the shortage of organs suitable for transplantation. For many years, the greatest demand has been recorded for kidneys, but due to the fact that it is a paired organ, a living donor transplant is possible In the case of heart or pancreas transplantation is possible only from a deceased donor, and the demand for organs is many times greater than the number of transplants performed (*Organ Donation Statistics | organdonor.gov*, b.d.).

An important condition for successful transplantation is adequate protection and fast transport of allogeneic organs (Saidi & Hejazii Kenari, 2014). The transport time should be as short as possible from the moment of obtaining the organ to the moment of transplantation. This time may be slightly longer for organs with less blood supply (such as blood vessels), but it is still limited to a few hours. The complexity and difficulty of the transplantation procedure is also a big challenge for doctors. In addition, there is a risk of transplant rejection and the emerging immune response makes it necessary for the patient to take immunosuppressive drugs for life.

Xenogeneic, i.e. zoonotic, transplants may be the answer to some of the above-mentioned problems. An example is pork or fish skin xenotransplantation, designed to stabilize the wound environment until autologous transplantation (Kohlhauser et al., 2021). The limitations of this method are genetic differences between humans and animals, the possibility of transmitting zoonotic diseases and ethical issues. Research is underway on the use of organs, in particular kidneys, liver, heart and islets of Langerhans, derived from transgenic pigs in which MHC molecules are deactivated or immunosuppressive transgenes are expressed in a given tissue (Fischer & Schnieke, 2022).

The gold standard for skin grafts are full-thickness or partial-thickness autografts, which are most often taken from the thighs, back and buttocks. Unfortunately, their use is limited in the case of extensive cavities. An alternative is to use biobanked, prepared sheets of biologically nonviable donor skin. This is a temporary solution that allows you to protect the wound for the time needed to obtain a proper graft. In allogeneic transplantation, matching the major histocompatibility complex (MHC) molecules of the donor and recipient, which are similar in related individuals, is a major challenge (Schlottmann et al., 2021).

The development of tissue engineering is an alternative to organ transplantation (Kianian et al., 2023; Shinkar & Rhode, 2022). Its aim is to restore the structure and functionality of the organ by using porous scaffolds and cells characteristic of a given organ. The main task of the scaffolding is to give the structure the right shape. The structure of the scaffold allows for the reconstruction of the structure of natural tissue, which allows it to maintain its mechanical and physical parameters, diffusion of nutrients and enable cell adhesion and migration. A properly designed scaffold supported by additional factors, such as growth factors, enables cell proliferation and high survival, and ultimately the creation of tissue suitable for implantation. The classic approach to the production of the proper structures assumes the production of a scaffold, e.g. by means of electrospinning, self-assembly of fibers or foaming with gas, and then deposition of cells on the scaffold. Another practice assumes that a scaffold is made of a material containing cells embedded in it. This solution enables precise control of structural properties and better integration of cells with the material and their even distribution throughout the structure (Manita et al., 2021). The latter includes the 3D tissue bioprinting method.

3D bioprinting is an innovative technique that uses Rapid Prototyping methods to produce spatial models that

reflect the structure of natural tissue. The idea of bioprinting is to apply successive layers of bioink until the expected shape of the construct is obtained. This technology is used in the development of drug delivery systems as well as in the printing of organ-on-chip and lab-on-chip systems (Arrigoni et al., 2017; Chliara et al., 2022; Krakos et al., 2023). However, there are particularly high hopes for its use in tissue engineering. This technique enables to control the properties of the material in time and space, to ensure the precise location of various cells and to take into account the anatomical features of the tissue, such as the pore system and the network of blood vessels (Manita et al., 2021).

3D Bioprinting process

Bioprinting consists of several stages, each of which is extremely important and affects the final effect. Initially, the purpose of producing a given tissue should be considered, because biomimetic structures can have different purposes (Mendoza-Cerezo et al., 2023). The produced tissues can replace a part of the human body, but also be intended for testing drugs and cosmetics or imitate, for example, cancer tissues, which in turn are used for modeling diseases, diagnostics and testing various methods of treatment (Gao et al., 2021; Mao et al., 2020; Shukla et al., 2022). The purpose of the construct will depend on the choice of the printing method, materials and cells intended for bioink, and the conditions in which both the printing process and the subsequent incubation of the tissue will take place. The detailed bioprinting process, on the example of skin bioprinting, is shown in Figure 7.3.1 (Fulden, 2021).

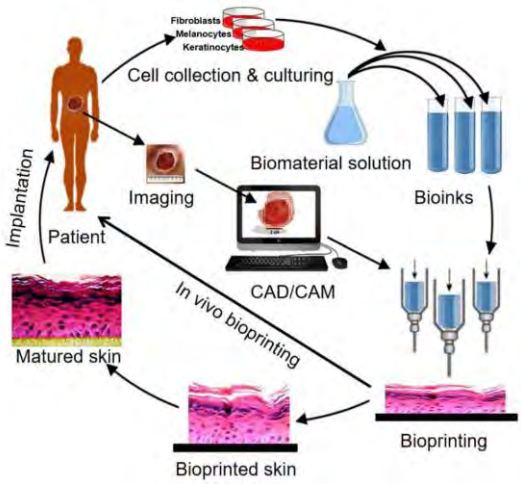

Figure 7.3.1 Stages of the bioprinting process on the example of skin bioprinting. Reprinted from (Ulucan-Karnak F., 2021); https://doi.org/10.17352/gjbbs.000015; CC License 3.0.

The first stage of bioprinting focuses on imaging the natural tissue in order to obtain information about its basic anatomical properties. Methods such as X-ray imaging, ultrasonography, magnetic resonance imaging and computed tomography are used for this. The two-dimensional images obtained in this way are segmented using appropriate algorithms in order to isolate the anatomical regions present in the model. This process makes it possible to combine all the information obtained from 2D images and create a 3D model, which in turn is represented as a triangulated surface in the STL format, which makes it possible to read the file on a 3D printer (Beski et al., 2015). In the next stage, using Slicer software, the model is divided into layers and each of them is described by an instruction contained in the G code, which is the programming language of, e.g., 3D printers. Thanks to the 3D reconstruction in CAD software, the model can be modified manually by inserting, deleting or changing individual fragments. The internal anatomy of the imaged tissue and pore structure are also verified. The details are determined by adjusting the dimensions of the voxels in the rendered 3D model (Saini et al., 2021). Designing 3D models is facilitated by numerical methods and simulations, e.g., finite element analysis and computational fluid dynamics, which allow to determine the mechanical properties of the construct, optimize the parameters of the microstructure and examine the permeability of the tissue model before it is printed (Vijayavenkataraman et al., 2018).

In the next step, bioink is prepared, which consists of a biomaterial designed to reproduce the extracellular matrix and its properties, cells obtained directly from the patient or from cell lines, and growth factors (Groll et al., 2018). The vast majority of bioinks are made of hydrogels, therefore the key to the bioprinting process is to provide a cross-linking agent responsible for the sol-gel transformation (Gungor-Ozkerim et al., 2018). During cross-linking, the structure of the hydrogel stabilizes, providing the construct with enhanced mechanical properties (Parak et al., 2019). The cross-linking agent can be provided by the environment in which the bioprinting process takes place (e.g. temperature change), but sometimes it requires adding an initiator to the bioink that causes the crosslinking process under certain conditions (e.g. photoinitiator) (Rajabi et al., 2021). Bioprinting using bioink consisting of exogenous biomaterial is currently the most popular method, but there is also a technique in which cells can be printed without the use of a scaffolding material (Ozbolat, 2017). This method uses aggregates of cells that are formed into tissues in the shape of spheroids or fibers, and then deposited according to a specific pattern. In subsequent stages, the tissues fuse and mature to form a functional construct. This approach also requires the use of biomaterials, but they function as a cell-free substrate or supports that are removed after cell fusion (Khademhosseini & Camci-Unal, 2018).

After preparing the bioink, the proper bioprinting process begins, which should be carried out in sterility and in conditions that allow cross-linking of the hydrogel. Description of the most commonly used manufacturing methods is presented in section *3D Bioprinting Methods*. It is important to select the appropriate printing method for the prepared bioink, as factors specific to various methods, e.g., shear forces or UV radiation, occurring during the process, can significantly reduce the survival of cells. Regardless of the method used, the device used for tissue bioprinting should ensure high resolution and accuracy in placing the material, be characterized by high speed and a high degree of freedom of movement, and enable the application of several types of bioink (Ozbolat, 2017). Full automation of the process as well as ease of use and sterilization of the bioprinter are also desirable. In order to ensure the dynamic development of this field, the devices should also be universal and affordable.

After the bioprinting process is completed, the fabricated construct should be placed in a bioreactor to ensure conditions for further growth, differentiation and maturation of the tissue. The newly formed tissue is supplied with nutrients and chemically and physically stimulated. Among

the devices used, there are static bioreactors, perfusion bioreactors and rotating vessels, which differ primarily in the way they deliver nutrients. The advantage of dynamic bioreactors over static ones is the ability to control such factors as pH, temperature, oxygen saturation or flow rate (Zhang et al., 2021). The choice of bioreactor depends on the type of tissue produced and its resistance to mechanical stress and pressure caused by the flow of supplied components. After a certain incubation time, the mature tissue or organ is placed in the patient's body or used for further research, depending on its intended use. In a few applications, the construct can be placed in situ in the human body, which in this case acts as a bioreactor (Saini et al.., 2021).

3D Bioprinting methods

The most commonly used methods are based on microextrusion, which use mechanical (piston, screw) or pneumatic (air pump) systems to form continuous, cylindrical streams of bioink arranged in layers (Ravanbakhsh et al., 2021; Tarassoli et al., 2021). Individual methods are presented in Figure 7.3.2. The continuity of the extruded material affects the structural integrity of the produced tissue, which in turn makes it the most convenient way to print porous cellular structures (Ozbolat, 2017). The bioinks used in this technique are characterized by a wide range of viscosity, which facilitates the creation of large tissue constructs. The advantages of the extrusion method also include low cost of production, affordability and the possibility of using bioinks with high cell density. However, compared to other methods, the resolution of the discussed technique is very low and the process itself is long. Moreover, mechanical stress occurring at the time of extrusion of bioink through the nozzle significantly reduces cell survival (Cho et al., 2019). When using this technology, special attention should be paid to the interactions between the bioink and the substrate as well as the appropriate configuration of the nozzle, which depends on the method of biomaterial cross-linking (Dell et al., 2022). Incorrect selection of bioink and nozzle parameters may lead to clogging.

Figure 7.3.2 Methods of extrusion bioprinting using: A. piston, B. air pump, C. screw (Ravanbakhsh et al.., 2021). Reprinted with permission John Wiley & Sons, Inc., License Number 5710810354269.

The second group of solutions is based on inkjet bioprinting (or droplet bioprinting), which is derived from traditional 2D inkjet printers and consists in non-contact application of bioink droplets to the substrate (Gudapati et al., 2016). Due to the method of producing drops, we can distinguish inkjet bioprinting, electrohydrodynamic spraying, acoustic bioprinting and microvalve (Ozbolat, 2017). The oldest and most developed method is inkjet bioprinting, in which drops are generated using gravity, atmospheric pressure and the fluid mechanics of the bioink solution. Droplet size can be controlled by thermal and piezoelectric activators as well as electrostatic or electromagnetic forces, which ensures very good resolution and accuracy of bioink deposition (Lee et al., 2023). The described approaches are presented in Figure 7.3.3. The advantages of inkjet bioprinting also include high printing speed, low cost and versatility of using this technology (Saini et al., 2021). Moreover, the method allows the creation of constructs composed of a variety of components, which allows the formation of complex heterocellular tissue. The main disadvantage is the limited choice of bioink, which must have a low viscosity to avoid nozzle clogging. Liquid bioink requires rapid cross-linking, often using chemical modifications or UV radiation, which reduces cell viability. In addition, the number of cells in the bioink is limited, because their too high density and the possibility of their gravitational deposition also leads to clogging of the nozzle (Cho et al., 2019).

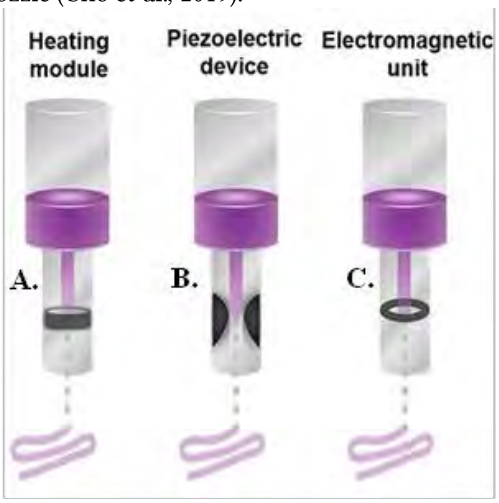

Figure 7.3.3 Examples of approaches in inkjet bioprinting to control the droplet size using A. thermal, B. piezoelectric, C. electromagnetic activators (Ravanbakhsh et al., 2021). Reprinted with permission John Wiley & Sons, Inc. License Number 5710810354269.

The last group of methods is based on the use of laser technologies, which, due to the mechanism of operation, can be divided into processes involving photopolymerization and methods based on cell transfer (Ozbolat, 2017; Saini et al., 2021). The first group includes stereolithography, which consists in the selective polymerization of photocurable biomaterial by the action of UV radiation, on a porous substrate placed at the surface of the bioink. After the first layer is produced, the substrate is moved up or down, depending on the approach, to a distance equal to the thickness of the layer, and the polymerization process is repeated according to the pattern defined by CAD software. In the methods based on cell transfer, the mechanism of transferring cells contained in the

culture medium or in the hydrogel is used, using continuous or pulsed, monochromatic laser energy. The transferred portion of bioink is placed on a receiving substrate and crosslinked. Figure 7.3.4 schematically illustrates both approaches. Laser methods avoid direct contact of the bioink with the dispenser, which ensures high resolution and speed of bioprinting and high cell survival (no mechanical stress). It is also possible to use bioinks with a high cell density. However, prolonged exposure to laser energy or UV radiation significantly reduces cell viability. The disadvantage is also the high price of the technology and its inability to use many materials, which makes it impossible to produce complex constructs. In addition, stereolithography uses photoinitiators that have cytotoxic properties (Kumar & Kim, 2020).

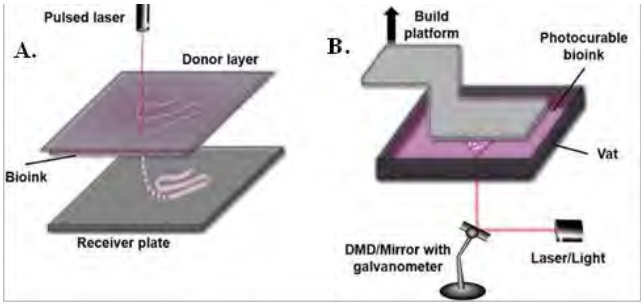

Figure 7.3.4 Laser-assisted bioprinting methods. A. Cell transfer approach, B. Stereolithography (Ravanbakhsh et al., 2021). Reprinted with permission John Wiley & Sons, Inc. License Number 5710810354269.

None of the methods is without drawbacks, which is why numerous attempts are made to combine various bioprinting strategies and integrate conventional tissue engineering methods with bioprinting techniques in order to achieve the best results (Fazal et al., 2021; Koch et al., 2021; Liu et al., 2022; Nandakumar et al., 2023). Increasingly, modern bioprinters allow the use of two or three techniques during one printing process. For example, the Cellink BioX6 device allows the use of both extrusion heads (pneumatic, syringe) and an electromagnetic inkjet printing head (Jesperlindahl, b.d.). What's more, the bioprinter is also equipped with a nozzle designed for classic printing of synthetic polymers, which can be used to produce scaffolds that provide additional stability to the constructs.

Materials used on bioinks

The bioprinting process often requires the use of several types of inks, which, depending on their function, can be divided into supportive, temporary, structural and functional (Groll et al., 2018). Due to the dynamic development of the field of bioprinting, the definition of bioink is constantly changing. Initially, the term referred to the cells themselves, which were applied to a hydrogel, called bioapaper. In subsequent years, this term was used to describe all the inks used in the bioprinting process. However, with the development of this technology, it became necessary to divide the materials used into bioinks, i.e. substances containing living cells in their composition, and biomaterial inks, i.e. not containing living cells.

Bioink plays the role of an artificial extracellular matrix and enables biomimetic reproduction of natural tissue and protection of the cells contained in it during the bioprinting process. In its composition, it may contain growth factors that are designed to support the growth and proliferation of cells in the manufactured construct (Matai et al., 2020). The most commonly used materials are hydrogels, which, due to the ability to bind a large amount of water in their structure, well imitate the natural environment of the tissue (L. G. Zhang et al., 2015). In addition, their structure can be modified (e.g. with ligands) to ensure better cell adhesion. In order to prepare bioink, a precursor of a given hydrogel is usually used, which is crosslinked during or after the printing process to form a hydrogel (Groll et al., 2018). Some approaches use pre-crosslinking of the precursor solutions to achieve a higher viscosity of the material.

Currently used bioinks are based primarily on natural polymers (biopolymers) of plant, animal or derived from microorganisms. These are substances that occur naturally in living organisms, which is why they are characterized by very good biocompatibility and negligible toxicity to cells (X. Wang et al., 2017). Natural hydrogels can be divided into two main groups, polysaccharides and polypeptides (Rashid et al., 2019). The first group includes chitosan and alginate, and the second collagen and its derivative - gelatin. Not all biopolymers show properties that support cell growth and development, but at the same time they may have better mechanical properties than other biopolymers, enabling printing of the construct (Dell et al., 2022). This approach, however, does not allow to overcome the main disadvantage of natural polymers, which is their poor mechanical strength and brittleness, which, combined with a long crosslinking time, effectively hinder obtaining a stable construct. Most natural polymers are cheap and readily available, but due to being sourced from natural sources, their properties may vary between batches of samples.

An innovative approach in the creation of bioink is the use of decellularized extracellular matrix (dECM), which is mainly obtained from pig organs (Sahranavard et al., 2022; Yang et al., 2023). The process of decellularization and preparation of the material is long and involves mechanical, chemical and enzymatic methods (Cho et al., 2019). The successful procedure allows to remove about 98% of the cellular content and the final product is a low-viscosity gel-like bioink (Ozbolat, 2017; Z. Wang et al., 2021). Components such as collagen, fibronectin, elastin, laminin, growth factors, cytokines and enzymes are present in dECM and have not been removed in the preparation process. Thanks to their presence, dECM-based bioinks enable a close reflection of the tissue microenvironment and ensure constant access to diverse nutrients. These features make it the best imitation of natural tissue. However, in addition to the long-term preparation process mentioned above, the use of dECM is also limited by the low availability of relevant tissues (Z. Wang et al., 2021). Moreover, in order to obtain a relatively small volume of bioink, it is necessary to process a large amount of the original tissue, which results in a high cost. In addition, dECM is characterized by poor mechanical properties and a long cross-linking time, and residues of chemical reagents used in the decellularization process can cause toxicity of the material. Synthetic polymer frameworks could be printed to maintain shape stability of the scaffold and also to enhance good deposition of the bioink. The comparison of different approaches to bioprinting with dECM bioink is presented on Figure 7.3.5 (Pati et al., 2014).

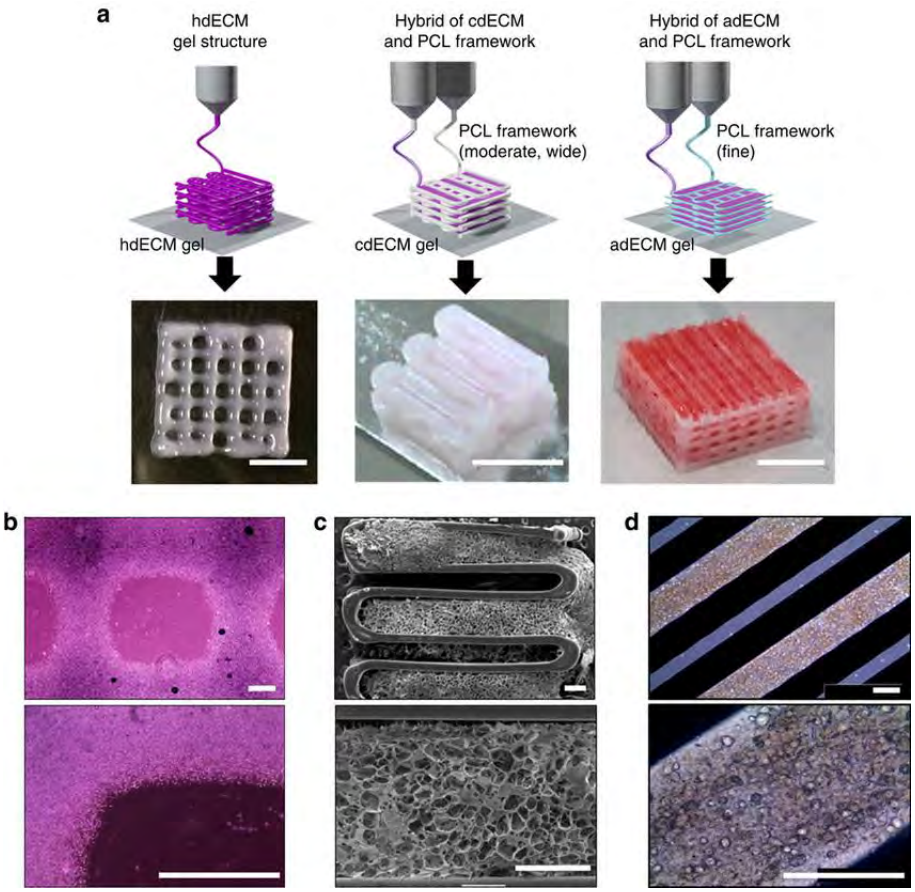

Figure 7.3.5 Comparison of bioprinting approaches for producing scaffolds using dECM bioinks. (a) comparison of techniques and final prints; (b, c, d) SEM images of final scaffolds. Reprinted from (Pati et al., 2014); https://doi.org/10.1038/ncomms4935; CC License 3.0.

Synthetic polymers are characterized by significantly better mechanical properties than natural polymers and the extracellular matrix devoid of cells. Their properties, such as porosity and elasticity, can be easily controlled, making it easy to match the material to the characteristics of the natural tissue (Cho et al., 2019). However, cell integration, growth and proliferation is hampered due to the low biocompatibility of the material. For this reason, synthetic polymers are mainly used as sacrificial materials to improve the strength and stiffness of printed constructs. One of the most commonly used synthetic polymers are polycaprolactone (PCL), poly(lactic acid) (PLA) and poly(ethylene glycol) (PEG). The various properties of natural and synthetic polymers are combined in hybrid approaches, in which biopolymers are designed to support cell growth, while synthetic polymers act as a scaffold that maintains the shape and stability of the printed tissue until the natural polymer is fully cross-linked (Ashammakhi et al., 2019). Moreover, the materials used can interact with each other. For example, modification of PEG with reactive groups makes it a cross-linking agent for natural polymers, e.g. for gelatin (Gungor-Ozkerim et al., 2018).

Bioinks must meet a number of requirements, the most important of which are biocompatibility and lack of cytotoxic and immunogenic properties (Cho et al., 2019) . In addition, the material used should ensure the stability and mechanical integrity of the printed tissue, its biomimetic reproduction and the possibility of even distribution of properly concentrated cells in the bioink. The biodegradability of the substance should be matched to the rate of tissue regeneration. Another important feature of bioink is its, so-called, bioprintability, i.e. compatibility of the material used with the selected printing process. This term therefore covers a set of features that enable the production of a tissue construct from bioink using the selected method (Ozbolat, 2017). In the case of inkjet bioprinting, the important features of the bioink will be, among others, low viscosity, non-fibrous nature and the ability to quickly crosslink. The viscosity of the material is not of key importance in the extrusion method, although it is not without significance, while when selecting the bioink, special attention should be paid to the shear thinning property. The use of stereolithography requires careful selection of a non-toxic photoinitiator. Regardless of the method, the material should be appropriately selected for the type of cells used. It should be remembered that any physical influences occurring during the printing process (temperature, UV radiation, pressure) can significantly reduce cell survival. Depending on the needs, the biomaterial should allow the addition of drugs or growth factors. The ink used should also be cheap and easily available, and its preparation should be uncomplicated.

Properly matched crosslinking conditions of bioink play a significant role in creating a functional construct. There are three crosslinking methods: chemical, physical and enzymatic (Ozbolat, 2017; L. G. Zhang et al., 2015). Chemical crosslinking is permanent and consists of a covalent bonds between polymer chains. In turn, physical crosslinking is in most cases reversible and is based on ionic bonds, hydrogen bonds, hydrophobic forces and molecular entanglements (Khademhosseini & Camci-Unal, 2018).

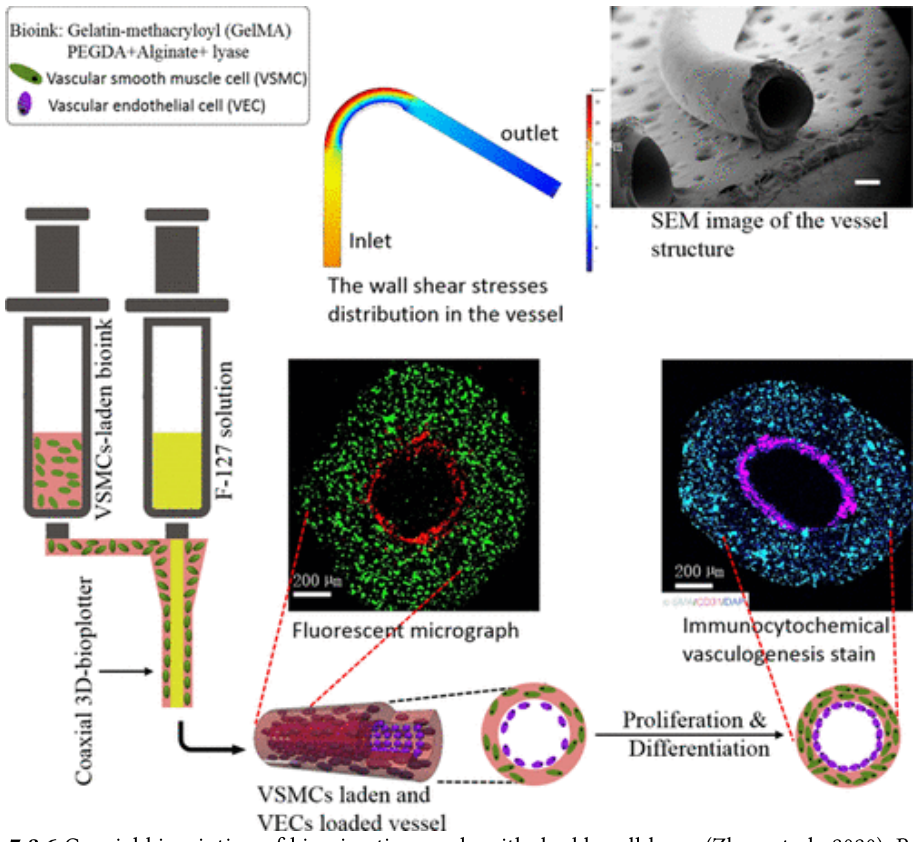

Figure 7.3.6 Coaxial bioprinting of biomimetic vessels with double cell layer (Zhou et al., 2020). Reprinted with permission from ACS Appl. Mater. Interfaces 2020, 12, 41, 45904–45915. Copyright 2020 American Chemical Society

Enzymatic cross-linking is based on enzymatic reactions between the hydrogel and an enzyme, e.g. bacterial. Bioinks can also be formed by a combination of crosslinking methods. Depending on the method, the speed and degree of crosslinking may be affected by the concentration of the crosslinking agent or the intensity of its impact. The degree of crosslinking, in turn, affects the stiffness, viscosity, melting point and strength of the material. The fabrication scheme of the tissue construct is also of key importance, especially in inkjet and extrusion bioprinting (Ozbolat, 2017). Depending on the hydrogel used and its crosslinking mechanism, the crosslinking agent can be printed alternately with bioink, sprayed on individual layers of the material or exposed to UV radiation. Another method involves bioprinting the ink into a cross-linking agent solution.

The future and the challenges of bioprinting technology

The most serious challenge faced by the bioprinting technology is the creation of a developed and hierarchical vascular system in the newly formed tissue, which would provide cells with access to nutrients. Oxygen diffusion, possible in a layer with a maximum thickness of 100-200 μm, significantly reduces the thickness of currently printed constructs (Dwivedi & Mehrotra, 2020). Various vascularization strategies have been developed to address this problem (Rajabi et al., 2021; Turner et al., 2020). Bioinks are enriched with angiogenic factors, which are designed to stimulate the growth and development of blood vessels in the patient's body (Y. Zhang et al., 2021). Another approach is to produce vascular networks of synthetic or natural origin, which are then printed with bioink to create the actual tissue. After printing the construct, these networks are dissolved and the tissue is perfused. Empty spaces in the tissue are overgrown with endothelium, thus creating a network of vessels. An interesting approach is the use of magnetic nanoparticles to obtain capillaries (Aljohani et al., 2018). This method also makes it possible to control the position of the vessels in the tissue. Coaxial bioprinting also allows to produce tubular scaffolds, which can successfully mimic natural vessels. The process of printing and its results are presented on Figure 7.3.6 (Zhou et al., 2020).

The selection of appropriate biomaterials for the production of ink is crucial for the success of the process, hence the dynamic development in this field. An innovative solution is the use of intelligent materials, mainly hydrogels sensitive to external stimuli, such as temperature, humidity, pH, magnetic field, electric field or radiation (Rahimnejad et al., 2023). The use of this type of bioink allows the development of the so-called 4D bioprinting, the main advantage of which is the ability to control the shape and properties of the printed tissue (Vijayavenkataraman et al., 2018). The idea of 4D bioprinting and factors that can stimulate material are presented on

Figure 7.3.7 (Faber et al., 2024). Research is also conducted on the use of ceramic-based bioinks for bone tissue regeneration (Dwivedi & Mehrotra, 2020).

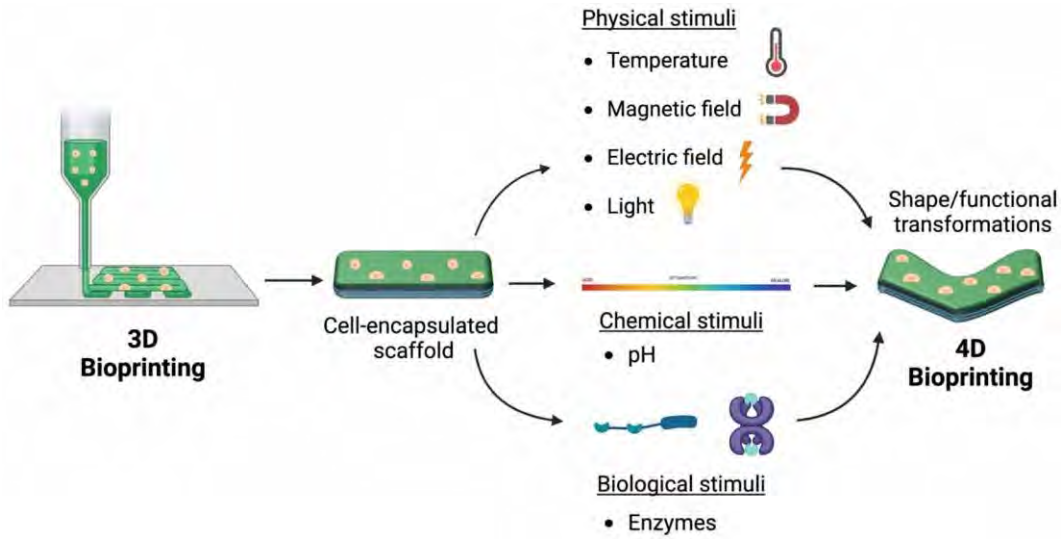

Figure 7.3.7 The idea of 4D bioprinting. Reprinted without any changes from (Faber et al., 2024). CC License 4.0. https://doi.org/10.1088/1758-5090/acfdd0.

Manufacturing methods require improvement of parameters, which is achieved by using hybrid methods of bioprinting (Cho et al., 2019). In addition to combining techniques, multi-nozzle systems with different nozzle diameters are also used to increase print resolution and speed. This approach could help generate complex, heterocellular tissues and enable the reconstruction of the hierarchical structure of blood vessels. The development of bioprinting technology can also contribute to the optimization of other technologies, e.g. organ-on-chip or drug delivery systems. The precision obtained in the printing process can in the future be used to distribute active biomolecules and drugs in the tissue, which will certainly accelerate the healing process.

Conclusion

The integration of medicine and technology has propelled the field of tissue engineering within which 3D bioprinting could be a promising breakthrough. The dynamic development of this field may contribute to solving the problem of low availability of organs for transplantation. Applying hybrid materials, combining bioprinting techniques as well as different conventional manufacturing methods, could be useful to obtain complex and functional structures that will imitate natural tissue in details. Moreover, the use of bioprinted tissues for testing drugs and cosmetics may be an excellent alternative to animal tests, and the possibility of modelling cancer diseases could accelerate the development of new therapies and contribute to understanding the processes underlying these diseases.

The careful choice of appropriate printing methods, bioink materials, and post-printing incubation conditions is crucial to the success of manufacturing scaffolds. All of those factors must be compatible with applied cells, which is a serious challenge nowadays and will be the goal of further research in this field. Moreover, to obtain functional tissue, extensive and hierarchical vascular network is needed, what has not been yet successfully achieved. Finally, the repeatability of the process and enhancing its parameters is needed to implement 3D bioprinting in a large scale.

Acknowledgements

We are grateful for financial support from the Faculty of Electrical Engineering, Automatics, Computer Science and Biomedical Engineering of the AGH University of Kraków, grant No. 16.16.120.773.

References

Aljohani, W., Ullah, M. W., Zhang, X., & Yang, G. (2018). Bioprinting and its applications in tissue engineering and regenerative medicine. *International Journal of Biological Macromolecules*, *107*, 261–275. https://doi.org/10.1016/j.ijbiomac.2017.08.171

Arrigoni, C., Gilardi, M., Bersini, S., Candrian, C., & Moretti, M. (2017). Bioprinting and Organ-on-Chip Applications Towards Personalized Medicine for Bone Diseases. *Stem Cell Reviews and Reports*, *13*(3), 407–417. https://doi.org/10.1007/s12015-017-9741-5

Ashammakhi, N., Ahadian, S., Xu, C., Montazerian, H., Ko, H., Nasiri, R., Barros, N., & Khademhosseini, A. (2019). Bioinks and bioprinting technologies to make heterogeneous and biomimetic tissue constructs. *Materials Today. Bio*, *1*, 100008. https://doi.org/10.1016/j.mtbio.2019.100008

Beski, D., Dufour, T., Gelaude, F., Ilankovan, A., Kvasnytsia, M., Lawrenchuk, M., Lukyanenko, I., Mir, M., Neumann, L., Nguyen, A., Soares, A., Sauvage, E., Vanderperren, K., & Vangeneugden, D. (2015). Software for Biofabrication. W *Essentials of 3D Biofabrication and Translation* (s. 19–41). Elsevier. https://doi.org/10.1016/B978-0-12-800972-7.00002-5

Chliara, M. A., Elezoglou, S., & Zergioti, I. (2022). Bioprinting on Organ-on-Chip: Development and Applications. *Biosensors*, *12*(12), 1135. https://doi.org/10.3390/bios12121135

Cho, D.-W., Kim, B. S., Jang, J., Gao, G., Han, W., & Singh, N. K. (2019). *3D bioprinting: Modeling In vitro tissues and organs using tissue-specific bioinks*. Springer.

Dell, A. C., Wagner, G., Own, J., & Geibel, J. P. (2022). 3D Bioprinting Using Hydrogels: Cell Inks and Tissue Engineering Applications. *Pharmaceutics*, *14*(12), 2596. https://doi.org/10.3390/pharmaceutics14122596

Dwivedi, R., & Mehrotra, D. (2020). 3D bioprinting and craniofacial regeneration. *Journal of Oral Biology and Craniofacial Research*, *10*(4), 650–659. https://doi.org/10.1016/j.jobcr.2020.08.011

Faber, L., Yau, A., & Chen, Y. (2024). Translational biomaterials of four-dimensional bioprinting for tissue regeneration. *Biofabrication*, *16*(1), 012001. https://doi.org/10.1088/1758-5090/acfdd0

Fazal, F., Diaz Sanchez, F. J., Waqas, M., Koutsos, V., Callanan, A., & Radacsi, N. (2021). A modified 3D printer as a hybrid bioprinting-electrospinning system for use in vascular tissue engineering applications. *Medical Engineering & Physics*, *94*, 52–60. https://doi.org/10.1016/j.medengphy.2021.06.005

Fischer, K., & Schnieke, A. (2022). Xenotransplantation becoming reality. *Transgenic Research*, *31*(3), 391–398. https://doi.org/10.1007/s11248-022-00306-w

Fulden, U.-K. (2021). 3D Bioprinting in Medicine. *Global Journal of Biotechnology and Biomaterial Science*, 001–005. https://doi.org/10.17352/gjbbs.000015

Gao, C., Lu, C., Jian, Z., Zhang, T., Chen, Z., Zhu, Q., Tai, Z., & Liu, Y. (2021). 3D bioprinting for fabricating artificial skin tissue. *Colloids and Surfaces B: Biointerfaces*, *208*, 112041. https://doi.org/10.1016/j.colsurfb.2021.112041

Groll, J., Burdick, J. A., Cho, D.-W., Derby, B., Gelinsky, M., Heilshorn, S. C., Jüngst, T., Malda, J., Mironov, V. A., Nakayama, K., Ovsianikov, A., Sun, W., Takeuchi, S., Yoo, J. J., & Woodfield, T. B. F. (2018). A definition of bioinks and their distinction from biomaterial inks. *Biofabrication*, *11*(1), 013001. https://doi.org/10.1088/1758-5090/aaec52

Gudapati, H., Dey, M., & Ozbolat, I. (2016). A comprehensive review on droplet-based bioprinting: Past, present and future. *Biomaterials*, *102*, 20–42. https://doi.org/10.1016/j.biomaterials.2016.06.012

Gungor-Ozkerim, P. S., Inci, I., Zhang, Y. S., Khademhosseini, A., & Dokmeci, M. R. (2018). Bioinks for 3D bioprinting: An overview. *Biomaterials Science*, *6*(5), 915–946. https://doi.org/10.1039/C7BM00765E

Hong, N., Yang, G., Lee, J., & Kim, G. (2018). 3D bioprinting and its *in vivo* applications. *Journal of Biomedical Materials Research Part B: Applied Biomaterials*, *106*(1), 444–459. https://doi.org/10.1002/jbm.b.33826

jesperlindahl. (b.d.). BIO X6™—3D bioprinter. *CELLINK*. Pobrano 19 wrzesień 2022, z ttps://www.cellink.com/bioprinting/bio-x6-3d-bioprinter/

Khademhosseini, A., & Camci-Unal, G. (Red.). (2018). *3D bioprinting in regenerative engineering: Principles and applications*. Taylor & Francis.

Kianian, S., Zhao, K., Kaur, J., Lu, K. W., Rathi, S., Ghosh, K., Rogoff, H., Hays, T. R., Park, J., Rafailovich, M., Simon, M., Bui, D. T., Khan, S. U., Dagum, A. B., & Singh, G. (2023). Autologous Skin Grafts, versus Tissue-engineered Skin Constructs: A Systematic Review and Meta-analysis. *Plastic and Reconstructive Surgery. Global Open*, *11*(6), e5100. https://doi.org/10.1097/GOX.0000000000005100

Koch, F., Thaden, O., Tröndle, K., Zengerle, R., Zimmermann, S., & Koltay, P. (2021). Open-source hybrid 3D-bioprinter for simultaneous printing of thermoplastics and hydrogels. *HardwareX*, *10*, e00230. https://doi.org/10.1016/j.ohx.2021.e00230

Kohlhauser, M., Luze, H., Nischwitz, S. P., & Kamolz, L. P. (2021). Historical Evolution of Skin Grafting—A Journey through Time. *Medicina*, *57*(4), 348. https://doi.org/10.3390/medicina57040348

Krakos, A., Cieślak, A., Hartel, E., Łabowska, M. B., Kulbacka, J., & Detyna, J. (2023). 3D bio-printed hydrogel inks promoting lung cancer cell growth in a lab-on-chip culturing platform. *Microchimica Acta*, *190*(9), 349. https://doi.org/10.1007/s00604-023-05931-8

Kumar, H., & Kim, K. (2020). Stereolithography 3D Bioprinting. W J. M. Crook (Red.), *3D Bioprinting* (T. 2140, s. 93–108). Springer US. https://doi.org/10.1007/978-1-0716-0520-2_6

Lee, J. M., Huang, X., Goh, G. L., Tran, T., & Yeong, W. Y. (2023). Understanding droplet jetting on varying substrate for biological applications. *International Journal of Bioprinting*, *9*(5), 758. https://doi.org/10.18063/ijb.758

Liu, F., Quan, R., Vyas, C., & Aslan, E. (2022). Hybrid biomanufacturing systems applied in tissue regeneration. *International Journal of Bioprinting*, *9*(1), 646. https://doi.org/10.18063/ijb.v9i1.646

Manita, P. G., Garcia-Orue, I., Santos-Vizcaino, E., Hernandez, R. M., & Igartua, M. (2021). 3D Bioprinting of Functional Skin Substitutes: From Current Achievements to Future Goals. *Pharmaceuticals*, *14*(4), 362. https://doi.org/10.3390/ph14040362

Mao, S., Pang, Y., Liu, T., Shao, Y., He, J., Yang, H., Mao, Y., & Sun, W. (2020). Bioprinting of *in vitro* tumor models for personalized cancer treatment: A review. *Biofabrication*, *12*(4), 042001. https://doi.org/10.1088/1758-5090/ab97c0

Matai, I., Kaur, G., Seyedsalehi, A., McClinton, A., & Laurencin, C. T. (2020). Progress in 3D bioprinting technology for tissue/organ regenerative engineering. *Biomaterials*, *226*, 119536. https://doi.org/10.1016/j.biomaterials.2019.119536

Mendoza-Cerezo, L., M. Rodríguez-Rego, J., Macías-García, A., C. Marcos-Romero, A., & Díaz-Parralejo, A. (2023). Evolution of bioprinting and current applications. *International Journal of Bioprinting*, *9*(4), 0. https://doi.org/10.18063/ijb.742

Nandakumar, N., Iyyer, S., Mohan, T., Nair, S. V., & Sathy, B. N. (2023). Smart Design for Hybrid Bioprinting of Scalable and Viable Tissue Constructs. *Tissue Engineering Part A*, ten.tea.2023.0188. https://doi.org/10.1089/ten.tea.2023.0188

Organ Donation Statistics | organdonor.gov. (b.d.). Pobrano 17 sierpień 2022, z https://www.organdonor.gov/learn/organ-donation-statistics

Ozbolat, I. T. (2017). *3D Bioprinting: Fundamentals, principles and applications*. Academic Press.

Parak, A., Pradeep, P., Du Toit, L. C., Kumar, P., Choonara, Y. E., & Pillay, V. (2019). Functionalizing bioinks for 3D bioprinting applications. *Drug Discovery Today*, *24*(1), 198–205. https://doi.org/10.1016/j.drudis.2018.09.012

Pati, F., Jang, J., Ha, D.-H., Won Kim, S., Rhie, J.-W., Shim, J.-H., Kim, D.-H., & Cho, D.-W. (2014). Printing three-dimensional tissue analogues with decellularized extracellular matrix bioink. *Nature Communications*, *5*(1), 3935. https://doi.org/10.1038/ncomms4935

Rahimnejad, M., Jahangiri, S., Zirak Hassan Kiadeh, S., Rezvaninejad, S., Ahmadi, Z., Ahmadi, S., Safarkhani, M., & Rabiee, N. (2023). Stimuli-responsive

biomaterials: Smart avenue toward 4D bioprinting. *Critical Reviews in Biotechnology*, 1–32. https://doi.org/10.1080/07388551.2023.2213398

Rajabi, N., Rezaei, A., Kharaziha, M., Bakhsheshi-Rad, H. R., Luo, H., RamaKrishna, S., & Berto, F. (2021). Recent Advances on Bioprinted Gelatin Methacrylate-Based Hydrogels for Tissue Repair. *Tissue Engineering Part A*, *27*(11–12), 679–702. https://doi.org/10.1089/ten.tea.2020.0350

Rashid, T. U., Sharmeen, S., Biswas, S., Ahmed, T., Mallik, A. K., Shahruzzaman, Md., Sakib, Md. N., Haque, P., & Rahman, M. M. (2019). Gelatin-Based Hydrogels. W Md. I. H. Mondal (Red.), *Cellulose-Based Superabsorbent Hydrogels* (s. 1601–1641). Springer International Publishing. https://doi.org/10.1007/978-3-319-77830-3_53

Ravanbakhsh, H., Karamzadeh, V., Bao, G., Mongeau, L., Juncker, D., & Zhang, Y. S. (2021). Emerging Technologies in Multi-Material Bioprinting. *Advanced Materials*, *33*(49), 2104730. https://doi.org/10.1002/adma.202104730

Sahranavard, M., Sarkari, S., Safavi, S., & Ghorbani, F. (2022). Three-dimensional bio-printing of decellularized extracellular matrix-based bio-inks for cartilage regeneration: A systematic review. *Biomaterials Translational*, *3*(2), 105–115. https://doi.org/10.12336/biomatertransl.2022.02.004

Saidi, R. F., & Hejazii Kenari, S. K. (2014). Challenges of organ shortage for transplantation: Solutions and opportunities. *International Journal of Organ Transplantation Medicine*, *5*(3), 87–96.

Saini, G., Segaran, N., Mayer, J., Saini, A., Albadawi, H., & Oklu, R. (2021). Applications of 3D Bioprinting in Tissue Engineering and Regenerative Medicine. *Journal of Clinical Medicine*, *10*(21), 4966. https://doi.org/10.3390/jcm10214966

Schlottmann, F., Bucan, V., Vogt, P. M., & Krezdorn, N. (2021). A Short History of Skin Grafting in Burns: From the Gold Standard of Autologous Skin Grafting to the Possibilities of Allogeneic Skin Grafting with Immunomodulatory Approaches. *Medicina*, *57*(3), 225. https://doi.org/10.3390/medicina57030225

Shinkar, K., & Rhode, K. (2022). Could 3D extrusion bioprinting serve to be a real alternative to organ transplantation in the future? *Annals of 3D Printed Medicine*, *7*, 100066. https://doi.org/10.1016/j.stlm.2022.100066

Shukla, P., Yeleswarapu, S., Heinrich, M. A., Prakash, J., & Pati, F. (2022). Mimicking tumor microenvironment by 3D bioprinting: 3D cancer modeling. *Biofabrication*, *14*(3), 032002. https://doi.org/10.1088/1758-5090/ac6d11

Szymoniuk, M., Mazurek, M., Dryla, A., & Kamieniak, P. (2023). The application of 3D-bioprinted scaffolds for neuronal regeneration after traumatic spinal cord injury – A systematic review of preclinical in vivo studies. *Experimental Neurology*, *363*, 114366. https://doi.org/10.1016/j.expneurol.2023.114366

Tarassoli, S. P., Jessop, Z. M., Jovic, T., Hawkins, K., & Whitaker, I. S. (2021). Candidate Bioinks for Extrusion 3D Bioprinting—A Systematic Review of the Literature. *Frontiers in Bioengineering and Biotechnology*, *9*, 616753. https://doi.org/10.3389/fbioe.2021.616753

Turner, P. R., Murray, E., McAdam, C. J., McConnell, M. A., & Cabral, J. D. (2020). Peptide Chitosan/Dextran Core/Shell Vascularized 3D Constructs for Wound Healing. *ACS Applied Materials & Interfaces*, *12*(29), 32328–32339. https://doi.org/10.1021/acsami.0c07212

Vijayavenkataraman, S., Yan, W.-C., Lu, W. F., Wang, C.-H., & Fuh, J. Y. H. (2018). 3D bioprinting of tissues and organs for regenerative medicine. *Advanced Drug Delivery Reviews*, *132*, 296–332. https://doi.org/10.1016/j.addr.2018.07.004

Wang, X., Ao, Q., Tian, X., Fan, J., Tong, H., Hou, W., & Bai, S. (2017). Gelatin-Based Hydrogels for Organ 3D Bioprinting. *Polymers*, *9*(12), 401. https://doi.org/10.3390/polym9090401

Wang, Z., Kapadia, W., Li, C., Lin, F., Pereira, R. F., Granja, P. L., Sarmento, B., & Cui, W. (2021). Tissue-specific engineering: 3D bioprinting in regenerative medicine. *Journal of Controlled Release*, *329*, 237–256. https://doi.org/10.1016/j.jconrel.2020.11.044

Yang, X., Ma, Y., Wang, X., Yuan, S., Huo, F., Yi, G., Zhang, J., Yang, B., & Tian, W. (2023). A 3D-Bioprinted Functional Module Based on Decellularized Extracellular Matrix Bioink for Periodontal Regeneration. *Advanced Science*, *10*(5), 2205041. https://doi.org/10.1002/advs.202205041

Zhang, J., Wehrle, E., Rubert, M., & Müller, R. (2021). 3D Bioprinting of Human Tissues: Biofabrication, Bioinks, and Bioreactors. *International Journal of Molecular Sciences*, *22*(8), 3971. https://doi.org/10.3390/ijms22083971

Zhang, L. G., Fisher, J. P., & Leong, K. W. (2015). *3D bioprinting and nanotechnology in tissue engineering and regenerative medicine*. Academic Press is an imprint of Elsevier.

Zhang, Y., Kumar, P., Lv, S., Xiong, D., Zhao, H., Cai, Z., & Zhao, X. (2021). Recent advances in 3D bioprinting of vascularized tissues. *Materials & Design*, *199*, 109398. https://doi.org/10.1016/j.matdes.2020.109398

Zhou, X., Nowicki, M., Sun, H., Hann, S. Y., Cui, H., Esworthy, T., Lee, J. D., Plesniak, M., & Zhang, L. G. (2020). 3D Bioprinting-Tunable Small-Diameter Blood Vessels with Biomimetic Biphasic Cell Layers. *ACS Applied Materials & Interfaces*, *12*(41), 45904–45915. https://doi.org/10.1021/acsami.0c14871

8 Scientific articles

8.1 The effect of 1,4-butanediol on the efficiency of CO_2 absorption and inhibition of NH_3 escape during the mineral carbonation of gypsum

Temesgen Abeto Amibo*[,1,2], Donata Konopacka-Łyskawa[1]

1. Gdansk University of Technology, Gdansk, Poland
2. Jimma University, Jimma, Ethiopia

e-mail: temesgen.amibo@pg.edu.pl

KEYWORDS: *mineral carbonation, butanediol, CO_2 capture, gypsum, ammonia desorption*

Abstract

Effectively and affordably advancing methodology for selectively capturing and storing CO_2 from diverse sources is one of the central challenges in addressing climate change. Ammonia solutions, highly valued for advantages like improved absorption efficiency and reduced regeneration energy needs, face a problem due to ammonia's high volatility, causing desorption during gas flow. Nevertheless, ammonia solutions as the CO_2 absorption solvent are proposed for reasons of cost-effectiveness, high capacity, and versatility. Various studies employ inorganic, organic, and nanoparticles as additives to tackle this issue. In this particular study, different concentrations of 1,4-butanediol were utilized to counteract ammonia escape and enhance CO_2 absorption.

This study explored the optimal concentration of 1,4-butanediol for maximizing CO_2 absorption and minimizing ammonia desorption. Mineral carbonation of gypsum slurry was carried out in a bubble reactor with a magnetic stirrer maintaining constant speed for 1 hour. The gas introduced to the reactor was a mixture of CO_2 and air. The gas flow was controlled by the mass controllers. Gas sensors were used to determine the concentration of CO_2 and NH_3 in the outlet gas. The initial and final pH values were measured. The liquid phase was ammonia solutions at a concentration of 1.69 mol·dm^{-3} with the addition of varying concentrations of 1,4-butanediol (ranging from 0.1 to 0.5 mol·dm^{-3}). The ratio of gypsum to liquid phase was maintained as 1:14 (kg·dm^{-3}). Based on measured CO_2 and NH_3 concentrations, the efficiency of carbon dioxide absorption and the efficiency of ammonia escape inhibition were calculated.

Results demonstrated a direct correlation between increased additive weight, enhanced CO_2 absorption, and effective inhibition of ammonia escape. The addition of 1,4-butanediol enhances CO_2 dispersion within the solution, expanding the gas-solvent contact area and promoting a more effective absorption process. Therefore, it effectively inhibits the escape of ammonia during reactions by temporarily binding free ammonia in the solution. The application of 1,4-butanediol emerges as a promising strategy for optimizing the overall efficiency and performance of the studied processes.

Introduction

CO_2, recognized as a heat-trapping and greenhouse gas, experiences a notable increase in concentration primarily attributed to the extraction and combustion of fossil fuels such as coal, natural gas, and oil (Soeder, 2021). Over the span from the first industrial revolution in the 18th century to the present day, the concentration of CO_2 has surged by 50% (Simmer et al., 2023). According to the 2022 Our World in Data Report, the primary contributor to atmospheric CO_2 concentration, illustrated in (Figure 8.1.1 (a)), is presently the Asian continent, particularly China and India, collectively accounting for approximately 53% of total emissions. The United States contributes 18% to the total emissions released into the atmosphere, while the European Union (EU) contributes 17%, Africa, with a focus on South Africa, South America, Brazil, and other unlisted regions each contributes 4% to the total emissions(Hannah Ritchie, 2023). As depicted in (Figure 8.1.1(b)). When expressed as a percentage of the total cumulative emissions starting from 1750 to 2022, the United States accounts for approximately 25%, the EU for around 22%, China for about 18%, the United Kingdom (UK) for 8%, India for 6% and other countries collectively contributing a smaller share compared to the mentioned nations. The increasing CO_2 concentration in the atmosphere can cause climate change, ocean acidification that impacts living things (i.e. plants and animals), drought, etc (Hunter, 2007). Therefore, exploring different methods of permanently capturing CO2 from the atmosphere is necessary to sequester the huge amount of CO_2 released by human activities.

There are different methods and techniques are employed to capture CO_2 from the gas mixture such as absorption, adsorption, and membrane methods. In absorption amine-based solvents, ammonia, and others are used. Adsorption utilizes solid sorbent and liquid sorbent. Membrane uses different materials as a membrane to separate it from other components (Wu et al., 2020). These are also the well-known methods to capture CO_2 from the atmosphere, flue, and waste gases like biological processes, mineral carbonation and cryogenic processes (Bui et al., 2018; Castro-Muñoz et al., 2022; Cheng et al., 2023; Galina et al., 2023; Goli et al., 2016; Kim et al., 2023; Zajac et al., 2023). Gypsum is utilized in the mineral carbonation process to capture CO2 from its source. It is the process where divalent metal ions react chemically with carbon dioxide,

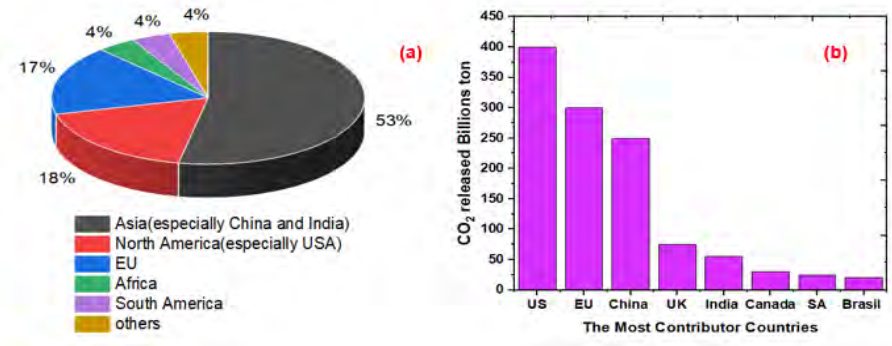

Figure 8.1.1 (a) World CO_2 concentration emission: (b) cumulative CO2 emission. Source: Global Carbon Project (2022) published on: Our World in Data

forming carbonates. The mineral carbonation can be categorized into direct and indirect forms. Indirect mineral carbonation involves a sequential extraction and carbonation process to produce metal carbonate products. On the other hand, direct mineral carbonation consists of a single step of carbonation to yield carbonated products.

For the CO_2 absorption process, different solvents such as monoethanolamine (MEA), diethanolamine (DEA), methyl diethanolamine (MDEA), and ammonia are particularly effective for absorbing carbon dioxide due to their cost-efficiency, and stability. It is established that monoethanolamine (MEA) and diethanolamine (DEA) exhibit optimal performance at lower temperatures compared to methyl diethanolamine (MDEA) (de Ávila et al., 2015).

Currently, ammonia attracts attention over other amine-based solvents due to its affordable, having a high CO_2 capture capability, and not degrading in the presence of O_2 and SO_2 (Amibo & Konopacka-Łyskawa, 2024). Aqueous ammonia solutions also have the potential to absorb other acid gases than carbon dioxide, such as NO_x and SO_x found in exhaust gases. Additionally, processes that use NH_3 solutions have a low demand for energy (Liu et al., 2009; Wang et al., 2018). The main problem employing ammonia during CO_2 absorption is NH_3 desorption during the gas flow. To prevent the escape of ammonia, varying amounts of organic additives are used.

Various studies have shown the positive effect of various organic additives to increase the efficiency of CO_2 absorption and reduce NH_3 desorption. Seo et al.(Seo et al., 2012) found that the inhibition of ammonia escaping in the absorption system by the addition of organic additives such as glycine, ethylene glycol, and glycerol was 5.1%, 38.4%, and 59.91%, respectively. In addition to this, another study reported that glycerine and isoamyl alcohol has a high capacity to inhibit ammonia escaping by 46.38% and 42.87%, respectively (Shuangchen et al., 2013). In the study presented by Czaplicka et al. (Czaplicka et al., 2022), the effects of organic additives on CO_2 absorption and $CaCO_3$ precipitation during mineral carbonation were presented. In this investigation, neopentyl glycol (NPG) had a greater tendency to inhibit ammonia escaping in both the absorption and the precipitation system. Improvement of CO_2 capture was 39.1%, and 83.1% was for NH_3 desorption. The experimental finding reports remarkable results that wereobtained by using NPG as an organic additive, and the high amounts of CO_2 absorbed in both absorption and precipitation systems were 85.4% and 86.1%, respectively.

Carbon dioxide can be efficiently captured and managed through the incorporation of gypsum in the presence of a CO_2-absorbing solvent like ammonia and organic additives. In this research gypsum ($CaSO_4 \cdot 2H_2O$) was used as a source of divalent metal ions (Ca^{2+} ions). The introduced CO_2 reacted with calcium ions and formed calcium carbonate whereas ammonia reacted with sulfate ions and formed ammonium sulfate, which is a valuable fertilizer. In this work, the gypsum carbonation process was performed in the presence of an organic additive 1,4-butanediol. The main objective of this research was to determine the influence of 1,4-butanediol on CO_2 absorption efficiency in the aqueous gypsum suspension containing ammonia. The second objective was to determine the effects of the organic additive on ammonia desorption during the carbonation process.

Methods

During the experiments, the following chemicals were utilized: ammonia solution of 25% (≥96.0%; POCH, Poland), gypsum ($CaSO_4 \cdot 2H_2O$) ((Chempur, Poland)), 1,4-butanediol (99.0%, Acros-Organics, Taiwan), water from reversed osmosis, CO_2 (Oxygen s.c., Poland), hydrochloric acid (35-38%, POCH, Poland), and sodium hydroxide (POCH, Poland).

In this research, a liquid-gas carbonation method was employed. The glass bubble reactor with capacity of 0.5 dm^3 equipped with the fritted glass as a gas distributor and the magnetic stirrer was used for the batch carbonation experiments. The reactor was filled with gypsum, ammonia solution, and organic additives. The mass of gypsum was 7% wt./wt. of the solution, the concentration of ammonia used was 1.68 $mol \cdot dm^{-3}$, and 1,4-butanediol having the concentration of 0.1 $mol \cdot dm^{-3}$ to 0.5 $mol \cdot dm^{-3}$ were utilized. The total volume of liquid was 0.3 dm^3. Before and after the reaction of carbonation the pH of the solution was measured. The inlet gas was a mixture of air and CO_2 and its flow was regulated at constant flow rates by employing a mass flow controller. The air and CO_2 flow rates were maintained at 0.007083 $dm^3 \cdot s^{-1}$ and 0.00125 $dm^3 \cdot s^{-1}$, respectively, to obtain the volume fraction of CO_2 in the air mixture 15%. The air from the source was passed through the adsorption column with NaOH to remove the air humidity. A magnetic stirrer was adjusted at 300 rpm. The outlet gas was diluted with the air controlled by the mass controller and the unreacted CO_2 and ammonia were analysed by the specific sensors. The detailed scheme of used experimental setup was described by Czaplicka et al. (Czaplicka et al., 2022). The reaction was performed at room temperature and atmospheric pressure for 1 hour. After the carbonation process, the suspension was filtered using a vacuum filter and the obtained precipitate was dried overnight at a temperature of 105 °C.

Results and Discussion

pH of the reaction mixtures

As shown in (Table 8.1.1), the initial pH values before the carbonation of gypsum slurry containing ammonia and organic additive varied from 12.28 for the control process (without 1,4-butanediol) to 11.71 for the highest tested concentration of the used diol. After carbonation the pH value of the reaction mixture decreased and the recorded values were from a range of 9.31 to 9.98. The other study on mineral carbonation supports that the pH of the solution decreased after the carbonation experiment (Huang et al., 2022; Mattila & Zevenhoven, 2015). The reason for lowering the pH is the absorption of CO_2 and the subsequent formation of carbonic acid in the solution. When hydrolysed, increases the concentration of hydrogen ions and increases the dissociation of ammonia. Moreover, during the precipitation of calcium carbonate in the solution, the concentration of sulfate ions increases, which also contributes to lowering the pH.

Table 8.1.1 pH values of reaction mixture before and after the carbonation experiment

Additive concentration, mol·dm^{-3}	Initial pH	Final pH
0.0	12.28	9.98
0.1	12.24	9.89
0.2	11.99	9.49
0.3	11.89	9.42
0.4	11.87	9.42
0.5	11.71	9.31

Carbon dioxide absorption

During the carbonation of gypsum slurry containing ammonia, several reactions corresponding to the Mersburg process occur (Avşar et al., 2022). The first reaction described by Equation (8.1.1.) shows the conversion of ammonia into ammonium hydroxide. The NH_4OH formation makes the solution alkaline medium. Equation (8.1.2.) implies CO_2 introduced reacted with ammonium hydroxide and then form ammonium carbonate. Equation (8.1.3.) is an overall reaction between the gypsum and ammonium carbonate and forms $CaCO_3$, $(NH_4)_2SO_4$, and H_2O. Unreacted CO_2 and desorbed NH_3 leave the solution in the outlet gas stream.

$$NH_{3(g)} + H_2O_{(g)} \rightarrow NH_4OH_{(aq)} \quad (8.1.1.)$$

$$2NH_4OH_{(aq)} + CO_{2(g)} \rightarrow (NH_4)_2CO_{3(aq)} + H_2O_{(l)} \quad (8.1.2.)$$

$$CaSO_4 \cdot 2H_2O_{(S)} + (NH_4)_2CO_{3(aq)} \rightarrow \rightarrow CaCO_{3(S)} + (NH_4)_2SO_{4(aq)} + 2H_2O_{(l)} \quad (8.1.3.)$$

The concentration of carbon dioxide in the exhaust gas is recorded in percent of volume fraction. (Figure 8.1.2(a)) shows changes in CO_2 concentration in the exhaust gas over time for randomly selected experiments. When the concentration of organic additive 1,4-butanediol increased the outlet percentage volume fraction of CO_2 was decreased. In the case of the control experiment *(without organic additive)*, the volume fraction of CO_2 ranged between 6-8% means from the total introduced CO_2 from the source more than 42% left the reactor without reaction. However, when 0.5 M concentration of 1,4-bunatne diol was added, a percentage volume fraction of CO_2 with a maximum of 4% was recorded and unreacted CO_2 left the reactor at an average of around 12%. The percentage volume fraction of CO_2 vs. time diagrams are similar in shape and they have four main stages such as in stage I, stage II, stage III, and stage IV. Stage I shows the complete consumption of introduced CO_2 within the reactor due to the high alkalinity solution favoring the consumption of CO_2. Next in stage II, the outlet CO_2 concentration sharply rises until it reaches to stable point. This substantial increase makes a high amount of CO_2 released from the solution. Stage III is an almost stable stage but the CO_2 concentration slightly fluctuates and its near-constant values. This stage continues for a long time from around 500 to 2500. In stage IV, a slight increase in outlet percentage volume fraction of CO_2. Based on the recorded CO_2 concentration in the inlet and outlet gas, the number of moles of carbon dioxide captured during the process was calculated, and the results are presented in (Figure 8.1.2**Błąd! Nie można odnaleźć źródła odwołania.** (b)). It can be seen, that the number of moles consumed increased when the concentration of additives increased. Previous results also indicated that an organic compound could promote CO_2 absorption, but the effect of additive concentration was not investigated (Czaplicka et al., 2022; Konopacka-Łyskawa, Amibo, et al., 2023).

Ammonia escaping

In the percent volume fraction of ammonia recorded over the time of reaction is presented. Generally, the course of ammonia desorption can be divided into four stages. In stage I, there is no recorded ammonia at outlet streams but as time goes a small amount of ammonia escape from the reactor this stage is termed stage II. In stage II, the ammonia concentration initiates an upward trend and reaches the maximum point.

Then, the ammonia concentration starts to decline. Beginning from this spot until it becomes stable this stage is termed stage III. Next, the final stage is in a quasi-stable state, i.e., stable with small changes and it starts around 3000 to the end of the reaction. Based on the results of the NH_3 concentration in the exhaust gas, the total number of moles of desorbed ammonia was calculated and is shown in (Figure 8.1.3 (b)). It can be seen that the amount of escaped ammonia significant decrease when the concentration of additives increase.

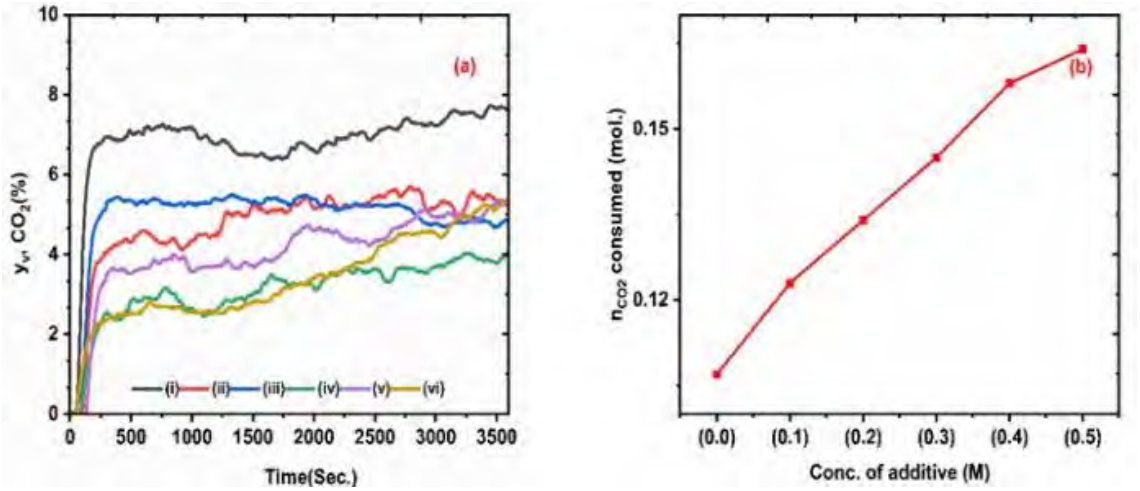

Figure 8.1.2 (a) Percent volume fraction of CO2 (i) control; (ii) Concentration of 0.1 M additive; (iii) Concentration of 0.2 M additive; (iv) Concentration of 0.3 M additive; (v) Concentration of 0.4 M additive and (vi) Concentration of 0.5 M additive; (b) the amount of average mole CO2 consumed at different additive concentration.

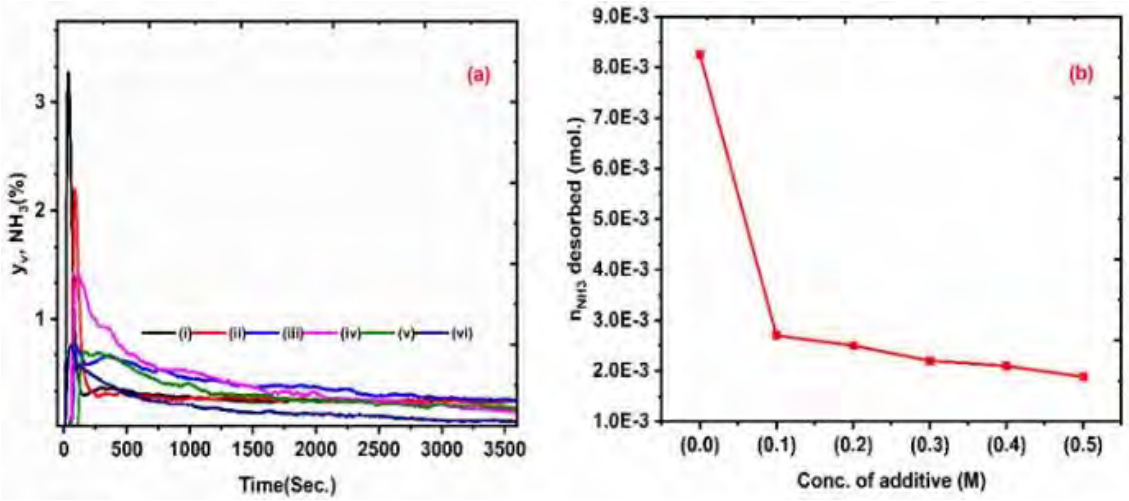

Figure 8.1.3 (a) Percent volume fraction of NH3 (i) control; (ii) Concentration of 0.1 M additive; (iii) Concentration of 0.2M additive; (iv) Concentration of 0.3M additive; (v) Concentration of 0.4M additive and (vi) Concentration of 0.5 M additive; (b) the amount of average mole NH3 escaped from the reactor at different additive concentration.

CO_2 absorption efficiency

The efficiency of CO_2 absorption was calculated using Equation (8.1.4.):

$$\eta_{CO_2} = \frac{n_{Con.}}{n_{in.}} \cdot 100\ \% \qquad (8.1.4.)$$

where η_{CO_2} denotes the efficiency of CO_2 absorbed during the mineral carbonation process, $n_{Cons.}$ and $n_{init.}$ denotes the mole of CO_2 consumed and the initial mole of CO_2, respectively.

The mole CO_2 introduced into the system was calculated. The known values of CO_2 flow rate , the time of the reaction, and the amount of CO_2 consumed was calculated based on the CO_2 concentration in the outlet gas stream. From Figure 8.1.4, small amounts of additive enhance CO_2 absorption. As illustrated in the diagram, the efficiency for control CO_2 absorption was 57.47%, for 0.1 M, 0.2 M, 0.3 M, 0.4 M, and 0.5 M were 65.87%, 71.91%, 77.56%, 84.27%, and 87.65% respectively. From the study findings of Czaplicka et al. (Czaplicka et al., 2022), various organic additives such as glycerol, ethylene glycol, methanol, isopropanol, pentaerythritol, and neopentyl glycol were utilized. The calcium carbonate precipitation process with organic additives showed greater capability to absorb CO_2. In this study, the highest CO_2 absorption efficiency was 86.1% by employing neopentyl glycol, and this result is comparable with the current finding of CO_2 absorption efficiency of gypsum carbonation.

NH_3 escaping inhibition

Due to its high vapor pressure, ammonia is volatile, evaporates, and escapes from the solution even at lower temperatures (Ma et al., 2016; Valera-Medina et al., 2021). In a similar manner, ammonia has a great tendency to escape from the solution during mineral carbonation. This makes it difficult to utilize ammonia during the CO_2 absorption process in the large-scale CO_2 absorption and mineral carbonation process. The amount of ammonia escape inhibited during mineral carbonation reaction can be calculated by using Equation (8.1.5.).

$$\alpha_{NH_3} = \frac{n_C - n_A}{n_C} \cdot 100\% \qquad (8.1.5.)$$

where α_{NH_3}, n_C, and n_A denotes for ammonia escaping inhibition, mole of ammonia escape inhibited without organic additive *(Control)* and mole of ammonia escape inhibited with different concentrations of 1,4-butanediol.

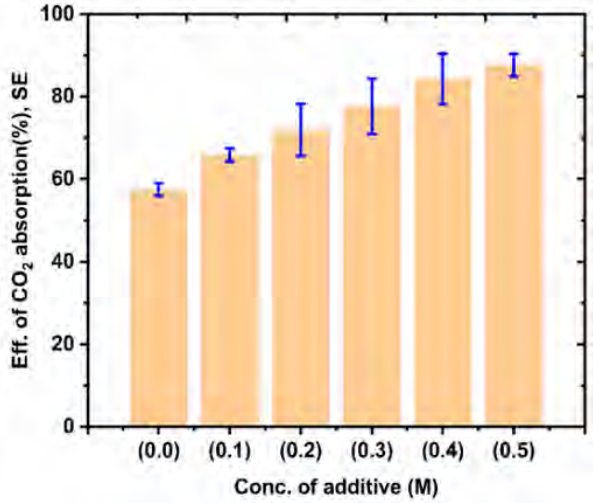

Figure 8.1.4 Efficiency of CO2 absorption with standard error.

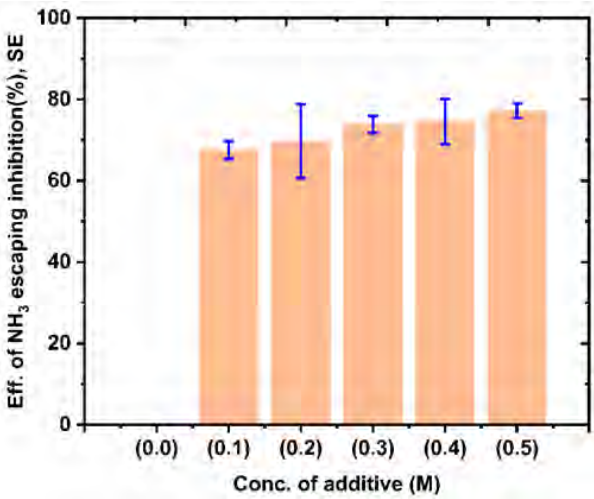

Figure 8.1.5 Efficiency of ammonia escaping inhibition with standard error.

In Figure 8.1.4, the efficiency of ammonia escaping inhibition and efficiency of ammonia escaping inhibition with standard error demonstrated. When the concentration of

organic additive increases the ammonia desorption decreases. At different concentrations of 1,4-butanediol i.e., 0.1 M, 0.2 M, 0.3 M, 0.4 M, and 0.5 M the ammonia escaping inhibition was 65.57%, 69.69%, 73.89%, 74.54, and 77.27% respectively. The highest amount of ammonia escaping inhibition was attained at a concentration of 0.5M of 1,4-butanediol. The organic additive reduces ammonia escape due to the ability of organic additive to make temporary bonds with ammonia and inhibit evaporation of ammonia during mineral carbonation reaction. Most organic additives have reactive functional groups like -OH and $–NH_2$ boosting their capacity to inhibit the evaporation through its bond (Czaplicka et al., 2020).

Conclusion

This work presents the effect of 1,4-butanediol on CO_2 absorption and ammonia desorption during carbonation of a gypsum suspension in the presence of ammonia. It has been shown that even a small amount of diol (0.1M, i.e. 0.9% by weight) causes significant improvements in CO_2 capture and limits the escape of ammonia from the reaction mixture. The increase in the concentration of the organic additive both increased the amount of CO_2 absorbed in the mineral carbonation process and reduced the amount of desorbed ammonia. Therefore, the best results were obtained for the highest tested concentration of 1,4-butanediol, with the CO_2 absorption efficiency of 87.65% and the effectiveness of inhibiting ammonia escape of 77.27%. In conclusion, the addition of 1,4-butanediol into the reactive mixture during mineral carbonation of gypsum is an encouraging approach for optimizing CO_2 uptake capacity and minimizing ammonia desorption in this process.

References

Amibo, T. A., & Konopacka-Łyskawa, D. (2024). The influence of α,ω-diols and SiO2 particles on CO2 absorption and NH3 escaping during carbon dioxide capture in ammonia solutions. *Journal of CO2 Utilization*, *80*, 102698. https://doi.org/10.1016/j.jcou.2024.102698

Avşar, C., Tümük, D., Ertunç, S., & Gezerman, A. O. (2022). A Review on Ammono-Carbonation Reactions: Focusing on the Merseburg Process. *Chemical Review and Letters*, *5*(1), 83–91. https://doi.org/10.22034/CRL.2022.329067.1154

Bui, M., Adjiman, C. S., Bardow, A., Anthony, E. J., Boston, A., Brown, S., Fennell, P. S., Fuss, S., Galindo, A., Hackett, L. A., Hallett, J. P., Herzog, H. J., Jackson, G., Kemper, J., Krevor, S., Maitland, G. C., Matuszewski, M., Metcalfe, I. S., Petit, C., … Mac Dowell, N. (2018). Carbon capture and storage (CCS): the way forward. *Energy & Environmental Science*, *11*(5), 1062–1176. https://doi.org/10.1039/C7EE02342A

Castro-Muñoz, R., Zamidi Ahmad, M., Malankowska, M., & Coronas, J. (2022). A new relevant membrane application: CO2 direct air capture (DAC). *Chemical Engineering Journal*, *446*, 137047. https://doi.org/10.1016/j.cej.2022.137047

Cheng, H., Fan, Y., Tarlet, D., Luo, L., & Fan, Z. (2023). Microfluidic-based chemical absorption technology for CO2 capture: Mass transfer dynamics, operating factors and performance intensification. *Renewable and Sustainable Energy Reviews*, *181*, 113357. https://doi.org/10.1016/j.rser.2023.113357

Czaplicka, N., Dobrzyniewski, D., Dudziak, S., Jiang, C., & Konopacka-Łyskawa, D. (2022). Improvement of CO2 absorption and inhibition of NH3 escape during CaCO3 precipitation in the presence of selected alcohols and polyols. *Journal of CO2 Utilization*, *62*,102085. https://doi.org/10.1016/j.jcou.2022.102085

Czaplicka, N., Konopacka-Łyskawa, D., Kościelska, B., & Łapiński, M. (2020). Effect of selected ammonia escape inhibitors on carbon dioxide capture and utilization via calcium carbonate precipitation. *Journal of CO2 Utilization*, *42*, 101298. https://doi.org/10.1016/j.jcou.2020.101298

de Ávila, S. G., Logli, M. A., & Matos, J. R. (2015). Kinetic study of the thermal decomposition of monoethanolamine (MEA), diethanolamine (DEA), triethanolamine (TEA) and methyldiethanolamine (MDEA). *International Journal of Greenhouse Gas Control*, *42*, 666–671. https://doi.org/10.1016/j.ijggc.2015.10.001

Galina, N. R., Arce, G. L. A. F., Maroto-Valer, M., & Ávila, I. (2023). Experimental Study on Mineral Dissolution and Carbonation Efficiency Applied to pH-Swing Mineral Carbonation for Improved CO2 Sequestration. *Energies*, *16*(5), 2449. https://doi.org/10.3390/en16052449

Goli, A., Shamiri, A., Talaiekhozani, A., Eshtiaghi, N., Aghamohammadi, N., & Aroua, M. K. (2016). An overview of biological processes and their potential for CO 2 capture. *Journal of Environmental Management*, *183*, 41–58. https://doi.org/10.1016/j.jenvman.2016.08.054

Hannah Ritchie, P. R. and M. R. (2023). *CO_2 and Greenhouse Gas Emissions*. https://ourworldindata.org/contributed-most-global-co2

Huang, Y., Zheng, X., Wei, Y., He, Q., Yan, S., & Ji, L. (2022). Protonated amines mediated CO2 mineralization of coal fly ash and polymorph selection of CaCO3. *Chemical Engineering Journal*, *450*, 138121. https://doi.org/10.1016/j.cej.2022.138121

Hunter, P. (2007). The impact of CO 2. *EMBO Reports*, *8*(12), 1104–1106. https://doi.org/10.1038/sj.embor.7401130

Kim, S., Shin, H., & Kang, J. S. (2023). Electrochemical reduction of captured CO2: A route toward the integrated carbon capture and utilization. *Current Opinion in Electrochemistry*, *40*, 101321. https://doi.org/10.1016/j.coelec.2023.101321

Konopacka-Łyskawa, D., Abeto Amibo, T., Dobrzyniewski, D., & Łapiński, M. (2023). Improving carbon dioxide capture in aqueous ammonia solutions by fine SiO 2 particles. *Chemical and Process Engineering: New Frontiers*, 16–16. https://doi.org/10.24425/cpe.2023.146718

Liu, J., Wang, S., Zhao, B., Tong, H., & Chen, C. (2009). Absorption of carbon dioxide in aqueous ammonia. *Energy Procedia*, *1*(1), 933–940. https://doi.org/10.1016/j.egypro.2009.01.124

Ma, S., Chen, G., Gao, R., Wen, J., & Ma, L. (2016). Experimental research of ammonia escape in CO_2 absorption using ammonia solution in wetted-wall column. *International Journal of Greenhouse Gas Control*, *51*, 254–259. https://doi.org/10.1016/j.ijggc.2016.05.022

Mattila, H. P., & Zevenhoven, R. (2015). Mineral carbonation of phosphogypsum waste for production of useful carbonate and sulfate salts. *Frontiers in Energy Research*, *3*(NOV), 1–8. https://doi.org/10.3389/fenrg.2015.00048

Seo, J.-B., Jeon, S.-B., Kim, J.-Y., Lee, G.-W., Jung, J.-H., & Oh, K.-J. (2012). Vaporization reduction characteristics of aqueous ammonia solutions by the addition of

ethylene glycol, glycerol and glycine to the CO2 absorption process. *Journal of Environmental Sciences*, *24*(3), 494–498. https://doi.org/10.1016/S1001-0742(11)60797-3

Shuangchen, M., Huihui, S., Bin, Z., & Gongda, C. (2013). Experimental study on additives inhibiting ammonia escape in carbon capture process using ammonia method. *Chemical Engineering Research and Design*, *91*(12), 2775–2781. https://doi.org/10.1016/j.cherd.2013.05.015

Simmer, R. A., Jansen, E. J., Patterson, K. J., & Schnoor, J. L. (2023). Climate Change and the Sea: A Major Disruption in Steady State and the Master Variables. *ACS Environmental Au*, *3*(4), 195–208. https://doi.org/10.1021/acsenvironau.2c00061

Soeder, D. J. (2021). Greenhouse gas sources and mitigation strategies from a geosciences perspective. *Advances in Geo-Energy Research*, *5*(3), 274–285. https://doi.org/10.46690/ager.2021.03.04

Valera-Medina, A., Amer-Hatem, F., Azad, A. K., Dedoussi, I. C., de Joannon, M., Fernandes, R. X., Glarborg, P., Hashemi, H., He, X., Mashruk, S., McGowan, J., Mounaim-Rouselle, C., Ortiz-Prado, A., Ortiz-Valera, A., Rossetti, I., Shu, B., Yehia, M., Xiao, H., & Costa, M. (2021). Review on Ammonia as a Potential Fuel: From Synthesis to Economics. *Energy & Fuels*, *35*(9), 6964–7029. https://doi.org/10.1021/acs.energyfuels.0c03685

Wang, F., Zhao, J., Miao, H., Zhao, J., Zhang, H., Yuan, J., & Yan, J. (2018). Current status and challenges of the ammonia escape inhibition technologies in ammonia-based CO2 capture process. *Applied Energy*, *230*, 734–749. https://doi.org/10.1016/j.apenergy.2018.08.116

Wu, Y., Xu, J., Mumford, K., Stevens, G. W., Fei, W., & Wang, Y. (2020). Recent advances in carbon dioxide capture and utilization with amines and ionic liquids. *Green Chemical Engineering*, *1*(1), 16–32. https://doi.org/10.1016/j.gce.2020.09.005

Zajac, M., Maruyama, I., Iizuka, A., & Skibsted, J. (2023). Enforced carbonation of cementitious materials. *Cement and Concrete Research*, *174*, 107285. https://doi.org/10.1016/j.cemconres.2023.107285

8.2 Study on quality characteristics of black chokeberry processing by-products using the fermentation process

Sylwia Sady[1], Patrycja Kawałek[*,2], Adam Konopelski[2], Zuzanna Płaczek[2], Nikola Dłużniewska[2], Karolina Pakuła[2], Aleksandra Kaczmarek[3]

1. Department of Natural Science and Quality Assurance, Institute of Quality Science, Poznan University of Economics and Business, Poznan, Poland
2. Student Scientific Association NEXUS, Department of Natural Science and Quality Assurance, Institute of Quality Science, Poznan University of Economics and Business, Poznan, Poland
3. WSB Merito University, Poznan, Poland

e-mail: patkowa012@gmail.com

KEYWORDS: *chokeberry, by-products, sustainable fermented product, food design*

Abstract

In recent years, there has been an increase in interest in fruit processing by-products, which include seeds, pulp remains and peel, due to the high content of nutritionally valuable ingredients. In the food industry, black chokeberry pomace can be a valuable secondary raw material due to its use in the production of, among others, innovative additives enriching food products or ingredients of dietary supplements. The market is seeing an increasing popularity of fermented products, especially those based on vegetables or fruits. Many studies have confirmed that the fermentation process can increase the antioxidant activity of plant extracts. It is suggested that metabolic hydrolysis influences the growth of phenolic compounds. Moreover, during the fermentation process, plant cell walls decompose, resulting in the release or synthesis of biologically active compounds, including those with antioxidant activity.

The aim of the study was to evaluate the microbiological quality and antioxidant potential of fermented black chokeberry pomace in terms of its potential use as an alternative source of valuable ingredients for the design of new food products. Fermented black chokeberry pomace may encourage a circular bioeconomy and constitute a potentially new direction for the valorization of black chokeberry processing by-products in the food industry. The scope of the research included the assessment of microbiological quality, total content of phenolic compounds, reducing power and antiradical activity. The content of polyphenolic compounds and antioxidant activity varied depending on the type of microorganism mixture used. The most intense growth was observed in black chokeberry pomace samples inoculated with yeast.

Introduction

The use of pomace poses a major challenge in the agrifruit industry (Iqbal et al., 2021). Despite its high nutritional value, a significant portion of pomace serves as animal feed or is treated as waste (subjected to incineration or composting). The reprocessing of pomace, including its utilization as a component in functional food, medical nutrition, dietary supplements, and cosmetics, aligns with the objective of combating food waste within the framework of a closed-loop economy strategy (European Commission et al., 2020; Venskutonis et al., 2020). Additionally, it contributes to the economic benefits of companies (May and Guenther et al., 2020).

In recent years, numerous studies have been conducted to examine the antioxidant properties of black chokeberry pomace (Sady et al., 2023; Andrade et al., 2021; Babaoğlu et al., 2022; Dulf et al., 2018; Rodríguez-Werner et al., 2019). Black chokeberry is valued for its high content of various nutrients, including dietary fibre, vitamins, minerals, and a significant amount of polyphenols (Andrade et al., 2021). However, due to the tart taste of black chokeberry berries, it is not popular with consumers. Processing black chokeberry allows for the concealment of its undesirable organoleptic characteristics. To mitigate these undesirable traits, black chokeberry is often processed and combined with other berries or fruits (e.g., blueberries and apples). Due to its intense colour, black chokeberry is used as a food dye in beverages, yogurts, jellies, syrups, and juices. It is also a primary ingredient in jams, teas, syrups, and juices (Grunovaitė et al., 2016; Sidor et al., 2019; Y. Zhang et al., 2021).

One of the processes that can alter the organoleptic qualities of berry-based products and black chokeberry pomace is fermentation (Markkinen et al., 2019). Fermentation involves the use of microorganisms such as lactic acid bacteria and yeasts, whose products exhibit new organoleptic properties and potentially higher nutritional value (Duan et al., 2023; Žuntar et al., 2020). Fermentation offers the opportunity to modify the organoleptic characteristics of the fermented product, influencing aspects such as taste, aroma, consistency, acidity, and food color (Duan et al., 2023; Klewicka and Lipińska et al., 2016; L. Zhang et al., 2021). In the case of black chokeberry pomace, the change in organoleptic characteristics occurs through the reduction of components such as proanthocyanidins, responsible for undesirable sensory traits like bitterness and acidity (Markkinen et al., 2019). Fermentation allows for increased economic benefits by enabling the processing of agricultural waste and extending the shelf life of fermented products. However, drawbacks of fermentation include the lack of standardization of the ferment due to the use of diverse raw materials (L. Zhang et al., 2021). Additionally, the use of different strains in fermentation implies varied effects on the organism (Chugh and Kamal-Eldin et al., 2020; Žuntar et al., 2020).

The aim of this study was to assess the microbiological quality and antioxidant potential of fermented black chokeberry pomace in terms of its potential use as an alternative source of valuable ingredients for designing new food products. Fermented black chokeberry pomace could encourage closed-loop biorefinery practices and potentially represent a new direction in the valorization of by-products from black chokeberry processing in the food industry.

Methods

Research Material

The research material consisted of commercially available dried black chokeberry pomace. Until the fermentation process was conducted, the pomace was stored in the absence of light at room temperature.

Fermentation of Black Chokeberry Pomace

In the experiment, fermentation of black chokeberry pomace was conducted in two variants: (I) black chokeberry pomace was inoculated with *Lactobacillus* and *Lactococcus* bacteria (sample PFL), and (II) with Saccharomyces yeast (sample PFS). Fermentation of black chokeberry pomace was carried out using reference strains of lactic acid bacteria from the American Type Culture Collection (ATCC): *Lactobacillus acidophilus* ATCC 4356, *Lactobacillus rhamnosus* ATCC 7496, and *Lactoccocus lactis subsp. lactis* ATCC 11454, as well as yeast strains of *Saccharomyces cerevisiae* ATCC 4098 and *Saccharomyces cerevisiae* ATCC 9763. Depending on the direction of the experiment, general and selective microbiological media were used: Plate Count Agar (PCA) for general bacterial cultivation, Malt Extract Agar (MEA) for yeast and mould cultivation, MRS (de Man, Rogosa, and Sharpe) Agar to determine the number of lactic acid bacteria, Baird-Parker agar to detect the presence of Staphylococcus aureus bacteria, and Violet Red Bile Glucose (VRBG) agar to detect the presence of Enterobacteriaceae bacteria. Black chokeberry pomace samples were collected immediately after introducing microorganisms (sample PK), as well as after two days of fermentation, and then lyophilised.

Microbiological Analysis

Microbiological quality of black chokeberry pomace before and after the fermentation process was assessed using a cultivation method. A 1 mL sample was taken from a mixture prepared with black chokeberry pomace, and a series of tenfold dilutions were made in sterile physiological saline. Dilutions and the original sample were plated on general and selective microbiological media. Plates with PCA and MEA were incubated at 30°C for 24 to 72 hours, while other media were incubated at 37°C for 24-48 hours. Colonies of microorganisms were then counted on the plates using an automatic colony counter, EasyCount 2, with statistical correction, and the colony-forming units (cfu)·mL^{-1} of the reaction mixture were determined.

Phenolic Content Analysis using QUENCHER - Folin-Ciocalteu Method

The method was adapted from the test developed by Del Pino-García et al (2015). A 0.7 M sodium carbonate solution was prepared by dissolving Na_2CO_3 in distilled water using an ultrasonic bath (Polonic) for 3 minutes. The solution was filtered to obtain a clear mixture. Subsequently, a reaction mixture was prepared taking 10 mg of a mixture of microcrystalline cellulose and black chokeberry pomace (in a 9:1 ratio) in a 10 mL volumetric flask, adding 0.2 mL distilled water, and 0.2 mL of Folin-Ciocalteu reagent. After 5 minutes of incubation in the dark at room temperature, 4 mL of 0.7 M filtered Na_2CO_3 solution was added, and the volume was adjusted with distilled water. The sample was shaken in the dark at room temperature using a laboratory shaker (GFL 3006) at 250 revolutions for 60 minutes. The sample was then transferred to a cuvette, and absorbance was measured at a wavelength of 750 nm using a UV/VIS spectrophotometer, Jasco V-770. The reference was the above reaction mixture with distilled water instead of the sample. A standard curve was prepared similarly to the sample. The results were expressed as gallic acid equivalents, in (μmol GAE)/(g of black chokeberry pomace).

Reducing Power Analysis using QUENCHER – FRAP Test

The reducing power of black chokeberry pomace tested was evaluated using the FRAP (Ferric Reducing Antioxidant Power) test based on the methodology of Del Pino-García et al. (2015). A FRAP working solution was prepared containing a solution of 10 mmol of TPTZ (2,4,6-tripyridyl-S-triazine) in 40 mmol of HCl, 20 mmol $FeCl_3 \cdot 6H_2O$, and 300 mmol of acetic acid buffer at pH=3.6 (diluted with distilled water in a volume ratio). Then, a reaction mixture was prepared by taking 10 mg of a mixture of microcrystalline cellulose and black chokeberry pomace (in a 9:1 ratio) in a flask and adding 10 mL of the FRAP working solution. The sample was shaken in the dark at room temperature using a laboratory shaker (GFL 3006) at 250 revolutions for 30 minutes. Absorbance was measured at a wavelength of 593 nm using a UV/VIS spectrophotometer, Jasco V-770. The reference was the FRAP working solution with distilled water instead of the sample. All measurements were performed at least in triplicate. A standard curve was prepared similarly to the sample. The results were expressed as trolox equivalents, in (μmol Tx)/(g of black chokeberry pomace).

Antioxidant Properties Analysis using QUENCHER - DPPH Test

Antioxidant properties were measured according to Del Pino-García et al. (2015). A 0.06 mM working solution of DPPH radical (2,2-diphenyl-1-picrylhydrazyl) was prepared by dissolving DPPH in 100% methanol using an ultrasonic bath (Polsonic) for 3 minutes. The stability of the DPPH radical was measured at a wavelength of 517 nm using a UV/VIS spectrophotometer, Jasco V-770. Then, a reaction mixture was prepared by taking 10 mg of a mixture of microcrystalline cellulose and black chokeberry pomace (in a 9:1 ratio) in a flask and adding 10 mL of the DPPH working solution. The sample was shaken in the dark at room temperature using a laboratory shaker (GFL 3006) at 250 revolutions for 30 minutes. Absorbance was measured, and the reference was the DPPH working solution with distilled water instead of the sample. A standard curve was prepared similarly to the sample. The results were expressed as trolox equivalents, in (μmol Tx)/(g of black chokeberry pomace).

Statistical Analysis

The presented results of microbiological analysis, total phenolic compound content, and antioxidant potential of black chokeberry pomace are the arithmetic mean of at least three parallel determinations. Results are presented as mean ± standard deviation. Calculations were performed using TIBCO Statistica 13.3 software.

Table 8.2.1 Microbiological Quality of Fermented Black Chokeberry Pomace Using Reference Strains of *Lactobacillus* and *Lactococcus* Bacteria and *Saccharomyces* Yeast;

Sample	Number of microorganisms (log CFU·mL^{-1})					
	PK		PFL		BFS	
	Beginning of the fermentation	2nd day	Beginning of the fermentation	2nd day	Beginning of the fermentation	2nd day
Total microbial count	n.d.	n.d.	$2.67 \cdot 10^5$	$6.14 \cdot 10^4$	n.d.	n.d.
Lactic acid bacteria	n.d.	n.d.	$0.92 \cdot 10^6$	$5.41 \cdot 10^4$	n.d.	n.d.
Yeast	n.d.	n.d.	n.d.	n.d.	$5.28 \cdot 10^4$	$7.89 \cdot 10^6$
Staphylococcus aureus	n.d.	n.d.	n.d.	n.d.	n.d.	n.d.
Enterobacteriaceae	n.d.	n.d.	n.d.	n.d.	n.d.	d.

n.d. – not detected; d. – detected; Source: own study

Results and Discussion

The microbiological quality of black chokeberry pomace samples before and after fermentation was determined based on inoculations carried out in both general and selective media. The test results are presented in Table 8.2.1.

The results of the study indicated that at the beginning of fermentation in the control sample (PK), no microorganisms were observed in any of the culture medium tested. Lyophilised black chokeberry particles were present in all samples. In samples inoculated with a mixture of *Lactobacillus* and *Lactococcus* bacteria (PFL), the total microbial count was $2.67 \cdot 10^5$ cfu·mL^{-1} of the reaction mixture, while the count of lactic acid bacteria was $0.92 \cdot 10^6$ cfu·mL^{-1}. On the contrary, in samples inoculated with a mixture of *Saccharomyces cerevisiae* yeast (BFS), the yeast count was $5.28 \cdot 10^4$ cfu·mL^{-1}. No bacteria of the Staphylococcus genus or Enterobacteriaceae family were observed in the samples examined. The obtained results are comparable with existing literature data. The intense growth of the starter culture, especially lactic acid bacteria, hinders the growth of undesirable microorganisms such as staphylococci or *Enterobacteriaceae*. These bacteria typically thrive in the initial stage of fermentation, but their growth is impeded by the increasing number of microorganism cells used as starter cultures and the metabolites produced, such as organic acids (Wuyts et al., 2018).

After two days of fermentation in the control sample (PK), no presence of microorganisms was observed on any of the tested culture media. In samples inoculated with a mixture of *Lactobacillus* and *Lactococcus* bacteria (PFL), the total microbial count was $6.14 \cdot 10^4$ cfu·mL^{-1}, while the count of lactic acid bacteria was $5.41 \cdot 10^4$ cfu·mL^{-1}. On the other hand, in samples inoculated with a mixture of Saccharomyces cerevisiae yeast (PFS), the yeast count was $7.89 \cdot 10^6$ cfu·mL^{-1}. Moreover, an increase in yeast count was observed on the MRS medium, which is specific for lactic acid bacteria. It can be assumed that yeast can adapt to less favourable conditions, simultaneously using available nutrients and stimulating their own reproduction. The presence of nutrients in black chokeberry, coupled with its high polyphenol content, may have facilitated the growth and reproduction of yeast, contributing to the observed results. Limited occurrence of bacteria from the *Enterobacteriaceae* family was observed on the second day of fermentation of black chokeberry pomace inoculated with yeast.

By-products of black chokeberry processing serve as a source of substances with antioxidant properties, including radical-scavenging abilities. In the study, the QUENCHER technique was used to evaluate the overall content of phenolic compounds, reducing power and antioxidant activity of fermented black chokeberry pomace. In the direct QUENCHER technique, the assessment of antioxidant properties is not preceded by an extraction procedure, as absorbance measurement is carried out directly after mixing the sample with the radical. The advantages of the QUENCHER technique include time efficiency, minimal use of solvents (due to the absence of an extraction procedure), and its relative simplicity (Henrion et al., 2018).

Table 8.2.2 presents the results of the overall content of phenolic compounds, reducing power, and radical-scavenging activity of fermented black chokeberry pomace using reference strains of *Lactobacillus* and *Lactococcus* bacteria (PFL) and *Saccharomyces* yeast (PFS) at the start time (PK) and after 48 hours of fermentation. The content of polyphenols, reducing power, and radical-scavenging activity depended on the applied starter culture. Before fermentation processes, the QUENCHER-TPC value of black chokeberry pomace was 321.1±33.9 (µmol GAE)/(1 g of pomace), QUENCHER-FRAP was 98.5±3.5 (µmol Tx)/(1 g of pomace), and QUENCHER-DPPH was 232.9±7.9 (µmol Tx)/(1 g of pomace).

In the initial fermentation period of black chokeberry pomace (PK) using a mixture of bacteria from the *Lactobacillus* and *Lactococcus* genera, as well as yeast from the *Saccharomyces* genus, total content of phenolic compounds was at the level of 261.1 µmol GAE/1 g pomace, reducing power was 80.1 µmol Tx/1 g pomace, while the antioxidant activity oscillated at 189.3 µmol Tx/1 g pomace. Total phenolic content obtained was higher than in the study conducted by Del Pino-García et al. (2015), where non-fermented grape pomace showed an overall phenolic content of 78.3±2.37 (µmol GAE)/(1 g of pomace). This difference indicates the high polyphenol content of black chokeberry pomace, which is associated with the antioxidant properties of black chokeberry, as often confirmed in the literature (Denev et al., 2019; X. Z. Liu et al., 2021).

Table 8.2.2. Overall Content of Phenolic Compounds (QUENCHER - TPC), Reducing Power (QUENCHER - FRAP), and Antioxidant Activity (QUENCHER - DPPH) of Fermented Black Chokeberry Pomace Using Reference Strains of *Lactobacillus* and *Lactococcus* Bacteria and *Saccharomyces* Yeast;

Sample	Fermentation time	QUENCHER - TPC (µmol GE/1 g pomace)	QUENCHER - FRAP (µmol Tx/1 g pomace)	QUENCHER - DPPH (µmol Tx/1 g pomace)
PK	0 day	261.1±20.4	80.1±7.6	189.3±10.4
PFL	2nd day	274.4[b]±11.5	84.2±5.9	199.1±6.8
PFS	2nd day	291.9[a]±27.8	108.3±3.9	231.7±12.1

Results presented as mean ± standard deviation.; Source: author's own work.

After two days of fermentation of black chokeberry pomace inoculated with a mixture of bacteria from the *Lactobacillus* and *Lactococcus* genera (PFL), the content of phenolic compounds, reducing power, and antioxidant activity slightly increased to 274.4 (µmol GAE)/(1 g of pomace), 84.2 (µmol Tx)/(1 g of pomace), 199.1 (µmol Tx)/(1 g of pomace), respectively. The highest increase in polyphenols and antioxidant activity was observed in samples fermented with yeast (291.9 (µmol GAE)/(1 g of pomace), 108.3 (µmol Tx)/(1 g of pomace), 231.7 (µmol Tx)/(1 g of pomace)). The results obtained are consistent with some data from the literature, where an increase in polyphenol levels was also observed through fermentation by lactic acid bacteria and yeast (Escudero-López et al., 2013). According to data from the literature, changes in antioxidant activity may depend on the composition of polyphenolic compounds. Some hydroxycinnamic acids, such as gallic acid or caffeic acid, can combine or bind to other components, such as sugars or amino acids, and therefore are potentially more stable (Queiroz et al., 2011).

Conclusions

The presented study focuses on the possibility of fermenting by-products of black chokeberry processing using microorganisms such as lactic acid bacteria and yeast. The research results indicate that fermentation conditions influence the microbiological quality, polyphenol content, and antioxidant properties of black chokeberry pomace. Fermented black chokeberry pomace, due to its potential health benefits, may find application in various food products, contributing to greater utilisation of by-products and creating a more sustainable closed-loop economy. Therefore, further research is necessary to better understand the impact of fermentation on the antioxidant activity of black chokeberry and determine the optimal conditions to obtain high-quality post-fermentation products.

Acknowledgements

This publication was written as part of the project entitled: 'TEAcycle - innovative functional teas based on fruit by-products', financed from the state budget funds allocated by the Minister of Education and Science as part of the programme 'Student Scientific Circles Create Innovations', contract no. SKN/SP/569242/2023.

References

Iqbal, A., Schulz, P., & Rizvi, S. S. H. (2021). Valorization of bioactive compounds in fruit pomace from agro-fruit industries: Present Insights and future challenges. Food Bioscience, 44, 101384. https://doi.org/10.1016/j.fbio.2021.101384

European Commission. (2020). A new Circular Economy Action Plan for a cleaner and more competitive Europe. Downloaded on 16 March 2023 from: https://eur-lex.europa.eu/legal-content/EN/TXT/?qid=1583933814386&uri=COM:2020:98:FIN

Venskutonis, P. R. (2020). Berries. W: Ch. M. Galanakis (red.), Valorization of Fruit Processing By-Products. Academic Press, 95–125. https://doi.org/10.1016/b978-0-12-817106-6.00005-8

May, N., & Guenther, E. (2020). Shared benefit by Material Flow Cost Accounting in the food supply chain – The case of berry pomace as upcycled by-product of a black currant juice production. Journal of Cleaner Production, 245. https://doi.org/10.1016/j.jclepro.2019.118946

Sady, S. (2023). Wytłoki aronii jako komponent innowacyjnych osłonek jadalnych. 1st ed. Wydawnictwo Uniwersytetu Ekonomicznego w Poznaniu. https://doi.org/10.18559/978-83-8211-172-9

Andrade, T. A., Hamerski, F., López Fetzer, D. E., Roda-Serrat, M. C., Corazza, M. L., Norddahl, B., & Errico, M. (2021). Ultrasound-assisted pressurized liquid extraction of anthocyanins from Aronia melanocarpa pomace. Separation and Purification Technology, 276. https://doi.org/10.1016/j.seppur.2021.119290

Babaoğlu, A. S., Unal, K., Dilek, N. M., Poçan, H. B., & Karakaya, M. (2022). Antioxidant and antimicrobial effects of blackberry, black black chokeberry, blueberry, and red currant pomace extracts on beef patties subject to refrigerated storage. Meat Science, 187. https://doi.org/10.1016/j.meatsci.2022.108765

Dulf, F. V., Vodnar, D. C., Dulf, E.-H., Diaconeasa, Z., & Socaciu, C. (2018). Liberation and recovery of phenolic antioxidants and lipids in black chokeberry (Aronia melanocarpa) pomace by solid-state bioprocessing using Aspergillus niger and Rhizopus oligosporus strains. LWT - Food Science and Technology, 87, 241–249. https://doi.org/10.1016/j.lwt.2017.08.084

Rodríguez-Werner, M., Winterhalter, P., & Esatbeyoglu, T. (2019). Phenolic Composition, Radical Scavenging Activity and an Approach for Authentication of Aronia melanocarpa Berries, Juice, and Pomace. Journal of Food Science. https://doi.org/10.1111/1750-3841.14660

Grunovaitė, L., Pukalskienė, M., Pukalskas, A., & Venskutonis, P. R. (2016). Fractionation of black black chokeberry pomace into functional ingredients using high pressure extraction methods and evaluation of their antioxidant capacity and chemical composition. Journal of Functional Foods, 24, 85–96. https://doi.org/10.1016/j.jff.2016.03.018

Sidor, A., Drożdżyńska, A., & Gramza-Michałowska, A. (2019). Black black chokeberry (Aronia melanocarpa) and its products as potential health-promoting factors - An overview. Trends in Food Science & Technology, 89, 45–60. https://doi.org/10.1016/j.tifs.2019.05.006

Zhang, Y., Zhao, Y., Liu, X., Chen, X., Ding, C., Dong, L., Jimping, Z., Shuwen, S., Ding, Q., Khatoom, S., Zhiqiang, C., Wencong, L., Shen, L., & Xiao, F. (2021). Chokeberry (Aronia melanocarpa) as a new functional food relationship with health: An overview. Journal of Future Foods, 1, 168–178. https://doi.org/10.1016/j.jfutfo.2022.01.006

Markkinen, N., Laaksonen, O., Nahku, R., Kuldjärv, R., & Yang, B. (2019). Impact of lactic acid fermentation on acids, sugars, and phenolic compounds in black black chokeberry and sea buckthorn juices. Food Chemistry, 286, 204–215. https://doi.org/10.1016/j.foodchem.2019.01.189

Duan, W., Guan, G., Zhang, H.-L., Wang, F.-Z., Lu, R., Li, D.-M., Geng, Y., & Xu, Z.-H. (2023). Improving flavor, bioactivity, and changing metabolic profiles of goji juice by selected lactic acid bacteria fermentation. Food Chemistry, 408, 135155. https://doi.org/10.1016/j.foodchem.2022.135155

Žuntar, I., Petric, Z., Kovačević, D. B., & Putnik, P. (2020). Safety of Probiotics: Functional Fruit Beverages and Nutraceuticals. Foods, 9(7), 947. https://doi.org/10.3390/foods9070947

Klewicka, E., & Lipińska, L. (2016). Aktywność przeciwgrzybowa bakterii fermentacji mlekowej z rodzaju Lactobacillus. ŻYWNOŚĆ. Nauka. Technologia. Jakość, 2016, 1(104), 17–31. https://doi.org/10.15193/zntj/2016/104/098

Zhang, L., Zhang, M., & Mujumdar, A. S. (2021). New technology to overcome defects in production of fermented plant products- a review. Trends in Food Science & Technology, 116, 829–841. https://doi.org/10.1016/j.tifs.2021.08.014

Chugh, B., & Kamal-Eldin, A. (2020). Bioactive compounds produced by probiotics in food products. Current Opinion in Food Science, 32, 76–82. https://doi.org/10.1016/j.cofs.2020.02.003

Del Pino-García, R., García-Lomillo, J., Rivero-Pérez, M. D., González-SanJosé, M. L., & Muñiz, P. (2015). Adaptation and Validation of QUick, Easy, New, CHEap, and Reproducible (QUENCHER) Antioxidant Capacity Assays in Model Products Obtained from Residual Wine Pomace. Journal of Agricultural and Food Chemistry, 63(31), 6922–6931. https://doi.org/10.1021/acs.jafc.5b01644

Wuyts S., Van Beeck W., Oerlemans E.F., Wittouck S., Claes I.J., De Boeck I., Weckx S., Lievens B., De Vuyst L., Lebeer, S. (2018) Carrot juice fermentations as man-made microbial ecosystems dominated by lactic acid bacteria. Applied and Environmental Microbiology, 84 (12). https://doi.org/10.1128/AEM.00134-18

Henrion, M., Servaes, M., Thielecke, F., & Fogliano, V. (2018). Application of the QUENCHER methodology to the food industry. Food Chemistry, 240, 951–958. https://doi.org/10.1016/j.foodchem.2017.07.119

Liu, X. Z., Ju, Y., Bao, N., Luo, Y. L., Huang, L. L., Cao, N. X., Liu, M. Z., Bo, J. N., Zhang, S., & Yan, Y. (2021). Effects of polyphenol-rich Aronia melanocarpa pomace feeding on growth performance, biochemical profile, and meat quality in pigs at weaned and finishing stages. Livestock Science, 252, 104674. https://doi.org/10.1016/j.livsci.2021.104674

Escudero-López B., Cerrillo I., Herrero-Martín G., Hornero-MéndezD., Gil-Izquierdo A., Medina S., Ferreres F., Berná G., Martín F., Fernández-Pachón M.S. (2013) Fermented orange juice: source of higher carotenoid and flavanone contents. Journal of Agricultural and Food Chemistry, 61, 8773-8782. https://doi.org/10.1021/jf401240p

Queiroz C., Lopes M.L.M., Fialho E., Valente-Mesquita V.L. (2011) Changes in bioactive compounds and antioxidant capacity of fresh-cut cashew apple. Food Research International, 44, 1459-1462. https://doi.org/10.1016/j.foodres.2011.03.021

8.3 Polydopamine as a possible binding agent for antithrombotic coating for small-diameter artificial vascular grafts

Jakub Knap-Kowalski*,1, Beata Butruk-Raszeja1

1. Faculty of Chemical and Process Engineering, Warsaw University of Technology, Warsaw, Poland
e-mail: jakubkarolkowalski@gmail.com

KEYWORDS: p*olydopamine,* polyurethane vascular grafts, platelet adhesion, *surface modification*

Abstract

One of the main issues limiting the wide-spread application of vascular implants is a high risk of thrombosis, which can lead to failure of whole medical procedure. One of currently used methods of improving vascular implants hemocompatibility is introduction of coatings with antithrombotic agents. However, oftentimes the adhesion of agent to modified surface is not strong enough to be effective in long-term implantation. Application of polydopamine (PDA), thanks to its unique properties, is a topic of an increasing number of biomedical studies. This work examines examine PDA coating as a potential binding layer for further introduction of bioactive agents. We decided to use albumin as an agent that could decrease adhesion.

This work describe protocol for two-step modification with PDA and albumin. Next, we analysed the influence of selected process parameters (modification time, solution pH) on surface wettability and platelets adhesion. Properties of PDA- and albumin-coated surfaces have been compared to uncoated surfaces and samples coated with antithrombotic agents without application of PDA layer. For assessing the wettability of potential grafts, the contact angle of water droplet was measured. Antithrombotic effect of applied coatings was analysed in a closed loop filled with whole human blood.

PDA coating highly increases the wettability of polyurethane surfaces and increases the adhesion of platelets, comparing to unmodified samples. However, application of second layer (albumin) resulted in reduction of platelet adhesion for both examined variant.

Surfaces modified with PDA and albumin presented the lowest platelets adhesion of all proposed modification procedures. Percentage of platelet-occupied surface for samples coated with PDA and albumin was significantly lower compared to samples coated with albumin without application of PDA layer. This suggest that PDA is a viable candidate for further studies on binding agents for multi-layered antithrombotic coatings.

Introduction

Polydopamine is formed by autooxidation of dopamine (Liu et al., 2014). The first publication describing its use to modify surfaces in order to alter their properties dates to 2007. This study aimed to artificially imitate the way in which mussels are able to adhere to selected surfaces (Haeshin et al., 2007).

Subsequent studies have shown that PDA is able to significantly increase the hydrophilicity of previously hydrophobic materials. When polymerised from a dopamine solution directly onto a modified surface, it forms a layer that adapts to the structure of the material, allowing PDA to be used on a wide range of substrates. Furthermore, the presence of PDA allows further modification of the surface, allowing for further specialisation (Davidsen et al., 2021). These features have led to increased interest in PDA in the scientific world and the search for applications for it. For example, PDA has found applications in bone tissue engineering. It could be used as a key ingredient in pastes for 3D printing of biomimicking and biodegradable scaffolds for bone tissue regeneration (Chen et al., 2020).

The possibility of adapting PDA for tissue engineering applications is a frequent subject of research. It has been shown that surfaces coated with PDA have significantly higher cell adhesion and proliferation(Pacelli et al., 2020).

The current dominant cause of death worldwide is cardiovascular disease. In 2019, an estimated 17.9 million people worldwide died as a result of the development of cardiovascular disease – summing up to 32% of the total number of deaths(World Health Organization, 2021).

Currently, there are several options for performing life-saving transplants for treatment of cardiovascular diseases: Allotransplantation – receiving a transplant from a human donor; xenotransplantation – receiving tissue from a non-human donor. Both have the disadvantage of limited size match between donor and recipient as well as the high risk of transplant rejection (Buján et al., 2004).

A third option, addressing the problems of the previous ones, is autotransplantation. Receiving transplant form recipient tissue. This highly lowers the possibility of inflammation. This method, in some cases, can also allow the grafts to be sized to specific requirements (Lee et al., 2007).

Another way is to use synthetic prostheses. This solution is used when other methods of transplantation are ill advised. Synthetic prostheses, especially when replacing small-diameter blood vessels, are unfortunately characterised by poor hemocompatibility, leading to a higher risk of thrombosis, which can lead to blockages of lumen of the grafts. Various materials are used to make prostheses. One of the longest-established polymers used for this purpose is Dacron®, whose applications are limited due to its high risk of thrombosis. The high coagulability of blood flowing through this type of prosthesis is particularly noticeable in the case of small-diameter prostheses (<6 mm), while the antithrombotic coatings used are often washed off the prosthesis surface after implantation, leading to unfavourable thrombus formation even after initial acceptance of the implant by the recipient(Gupta & Mandal, 2021).
Research into the use of other polymers for the construction of small-diameter blood vessel prostheses is ongoing. Polymeric materials that could be used as prostheses have to fulfil several requirements that are difficult to achieve simultaneously. One of the approaches is trying to mitigate mentioned problems by mimicking the design of naturally occurring vessels in the human body. It is imperative that the prostheses do not significantly increase the coagulability of the blood with which they come into contact. Further important aspects for successful transplantation are the absence of immune response and low protein adhesion to the surface of the prosthesis (Zhuang et al., 2021).

Table 8.3.1 Material variants analysed in the study.

Modification symbol	1st step - Incubation time [h]	1st step - dopamine concentration [mg/ml]	2nd step - Incubation time [h]	2nd step –albumin concentration [mg/ml]	2nd step – solution pH
IF	-	-	-	-	-
1PDA	1	2	-	-	-
2PDA	2	2	-	-	-
4PDA	4	2	-	-	-
24PDA	24	2	-	-	-
3ALB7.5	-	-	3	10	7.5
1PDA_3ALB7.5	1	2	3	1	7.5
1PDA_3ALB7.5x10	1	2	3	10	7.5
1PDA_3ALB9.5x10	1	2	3	10	9.5
1PDA_3ALB9.5	1	2	3	1	9.5

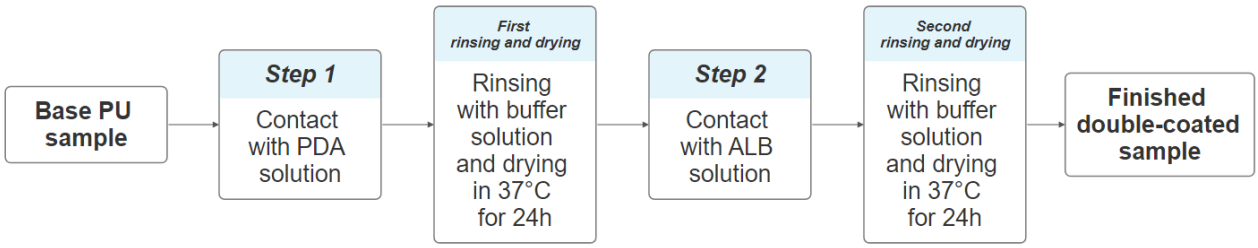

Figure 8.3.1 Scheme of two-step modification

One of the polymers on which research is ongoing is polyurethane. The samples of potential vascular prostheses considered in this article were obtained using the phase inversion method. This technique is based on the difference in solubility of the polymer in solvents and its non-solvents. When the non-solvent is added to the polymer and solvent solution, a process is induced leading to the formation of two phases that differ in polymer content. Through diffusion processes striving towards an interfacial equilibrium state, the polymer precipitates out of solution. The resulting polymer has a porous structure. The process of obtaining prostheses has been previously described (Kuźmińska et al., 2021).

The aim of the presented research was to analyse the possibility of modifying polyurethanes using PDA coating and bioactive agents reducing platelet adhesion. Adhesion of platelets on the surface of vascular implants is an undesirable phenomenon, leading to the formation of clots and occlusion of the vessel lumen. Albumin was analysed as bioactive agent.

Methods

Materials

PDA was obtained by spontaneous polymerisation of dopamine using its hydrochloride. Dopamine hydrochloride, human albumin and N,N-dimethylacetamide (HMDS) were obtained from Sigma-Aldrich. The ethanol used during the study was sourced from POCH. Ultrapure water was used to prepare the solutions.

The polyurethane used for the cylindrical prostheses is ChronoFlex C75A sourced in granulated form from AdvanSource Biomaterial.

Surface modification protocol

Cylindrical polyurethane prostheses (inner diameter in a 6-7 mm range) were prepared using solvent-induced phase inversion method described in previous paper (Kuźmińska et al., 2021). Next prostheses were subjected to surface modifications. Solutions used to prepare different material variant are presented in Table 8.3.1.

In brief, analyzed samples were immersed in first solution (PDA in given concentration and pH) and second solution with solutions containing bioactive agent (albumin). After each modification step samples were washed with phosphate buffer (pH=7.4). Finally, samples were dried for 24 h at 37°C.

Simplified scheme of two-step modification is pictured on Table 8.3.1.

Wettability

Measurements were carried out using an automatic KRÜSS optical goniometer connected to a computer. Cylindrical specimens were cut open alongside its length and glued on standard laboratory glass slides with double-sided tape to allow access to the inner surface of the specimen. Each variant was tested in triplicate. At least 3 different, randomly selected spots per each material variant were analysed. The volume of each droplet was 5 µL. The automatic ability to detect the angle between the tangent to the droplet and the test surface was used - for this purpose, the visible droplet deposited on the sample was assumed to be part of a circle. The line defining the surface of the test specimen (baseline) was set manually based on the observation of the surface by the integrated camera of the goniometer.

Platelet adhesion

It was decided that whole blood would be used in the study. Whole blood is an acceptable source material for platelet adhesion study in flow systems as reported by others (Mangin et al., 2020). Blood was collected from a woman with no known blood clotting disorders. Blood was collected using a BD Vacutainer® vacuum blood collection system into test tubes containing trisodium citrate buffer solution. The first portion of blood was discarded. The collected blood was then introduced into a system shown in

Figure 8.3.2. The contact time between the blood and each sample was 1 h. The blood was then removed from the system. The prosthesis was rinsed with 0.9% sodium chloride solution after contact. After rinsing, the samples were subjected to a chemical preservation and drying procedure for microscope observation.

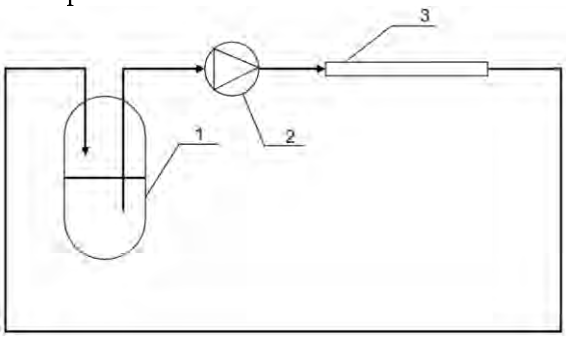

Figure 8.3.2. Flow system used for of platelet adhesion analysis; 1 – Vessel with blood; 2 – peristaltic pump; 3 – polyurethane graft

Preparation of specimen for observation under scanning electron microscope

The samples were dehydrated in ethanol solutions of increasing concentrations: 50%, 60%, 70%, 80%, 90% and 96% (10 minutes in each solution) After dehydration, the samples were placed in a solution of N,N-dimethylacetamide (HMDS) and ethanol (1:2) for 20 minutes. After this time, the samples were placed in an HMDS and ethanol solution (2:1) for 20 minutes. The samples were then placed in pure HMDS under fume hoof until the solution evaporated. It was decided to use HMDS as it improves the preservation of biological objects and is suggested as an effective replacement for critical point drying (Shively & Miller, 2009).

Once the samples were dry, their internal surfaces were coated with a layer of carbon using a vacuum sputtering machine, which allowed observation with a scanning electron microscope (SEM). Photographs of the internal surfaces were taken to estimate the area occupied by adhered platelets. ImageJ software was used to measure the surface area occupied by the adhered platelets to the modified surface (Schneider et al., 2012). The surface area of the platelets was automatically measured by the programme. Example of analysed mask highlighting the area measured on top of base image (1PDA_3ALB7.5) is depicted on Figure 8.3.**3**. Base image is presented on the left side for comparison.

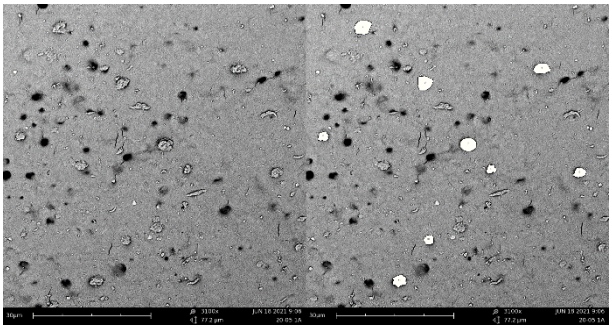

Figure 8.3.3. From left to right: SEM image of a sample (1PDA 3ALB7.5) and the same image with highlighted area of adhered platelets

With knowledge of the scale of the image shown in the information bar, it was possible to determine the area occupied by the observed platelets. Fifteen images per modification variant were taken, meaning that 96,000 μm^2 of each modification variant were examined. The percentage of platelet-occupied surface (%PLT) were calculated according to the formula:

$$PLT[\%] = \frac{\text{surface area of adhered platelets } [\mu m^2]}{96{,}000\ [\mu m^2]} \cdot 100\% \quad (8.3.1.)$$

Results and discussion

Wettability

The averaged results of the measurements are summarised in

Table 8.3.**2**. Graphs represented by Figure 8.3.3 andFigure 8.3.**4** are based on the collected data. All calculations were performed in OriginPro 2021 software under an educational licence.

A significant decrease in mean wettability angle was observed for almost every modification. The exceptions appeared to be two-step modifications completed by contacting the albumin solution at a higher concentration (40 mg·mL^{-1}). It should be noted that samples treated only with albumin at a concentration of 10 mg·mL^{-1} show a wide range of measured wettability angles with a sizable proportion of measurements close in value to the unmodified polyurethane surface.

The averaged results suggest that the longer the PDA modification lasts, the less effect it has on the change in wettability angle. No significant change in the average wetting angle value was observed when comparing samples modified with PDA at 4 h with those in contact with the modifying solution for 24 h. However, it was noted that the maximum value of the recorded wetting angle decreased after an additional 20 h of modification.

All surfaces modified according to the scheme: "PDA+albumin" were characterised by a significant increase in the minimum, maximum and mean wetting angle values compared to surfaces modified with PDA alone.

Changing the pH level of albumin solution affected the average values of wetting angle. For each concentration considered, surfaces modified with albumin solution in PBS showed a lower wetting angle than surfaces modified with albumin solution in carbonate buffer. This difference is particularly apparent for the higher concentration of albumin (10 mg·mL^{-1}).

Table 8.3.2 Wettability of the samples.

Modification symbol	Minimum wetting angle [°]	Maximum wetting angle value [°]	Average wetting angle [°]
IF	78	84	81
1PDA	22	50	33
2PDA	36	64	53
4PDA	18	53	30
24PDA	18	36	29
3ALB7.5	58	80	65
1PDA_3ALB7.5	45	56	50
1PDA_3ALB7.5x10	34	52	43
1PDA_3ALB9.5x10	51	75	63
1PDA_3ALB9.5	46	65	57

Table 8.3.3 Platelet- occupied area and wettability of analysed materials

Modification symbol	area occupied by platelets [µm²]	wettability [°]	PLT [%]
IF	1844	81	1.92%
1PDA	3238	33	3.37%
3ALB7.5	3236	65	3.37%
1PDA_3ALB7.5	1003	50	1.05%
1PDA_3ALB7.5x10	1479	43	1.54%
1PDA_3ALB9.5x10	831	63	0.87%
1PDA_3ALB9.5	331	57	0.35%

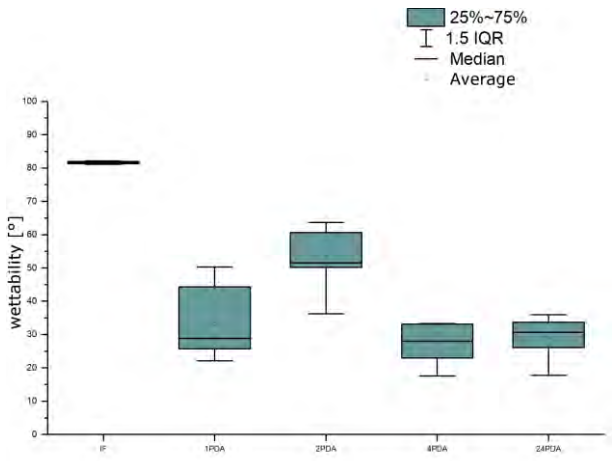

Figure 8.3.4. Effect of PDA solution incubation time on surface wettability.

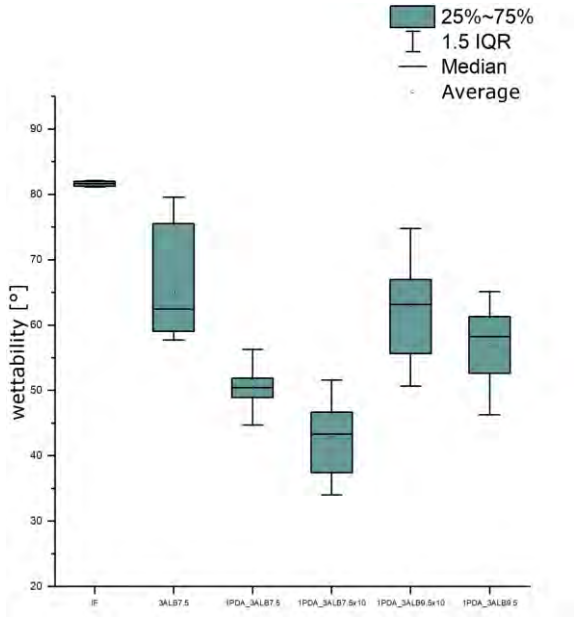

Figure 8.3.5. Effect of concentration and pH of modifying solutions on surface wettability.

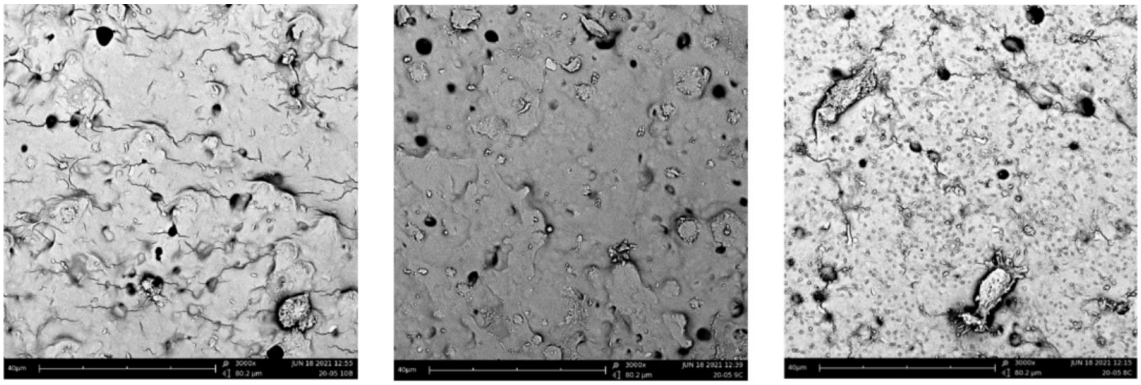

Figure 8.3.6 Example of surfaces examined under microscope. From left to right: IF, 1PDA, 3ALB7.5

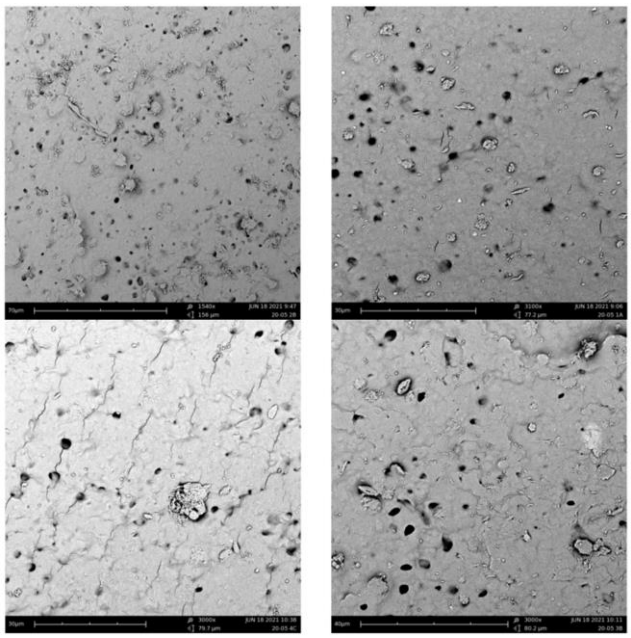

Figure 8.3.7 Example of surfaces examined under microscope; Top row from left to right: 1PDA_3ALB9.5, 1PDA_3ALB7.5, bottom row from left to right: 1PDA_3ALB9.5x10, 1PDA_3ALB7.5x10.

The results of the measurements and calculations are summarised in Table 8.3.3. Figure 8.3.7 was drawn based on Table 8.3.3. Every variant of surface modification highly influenced the measured values of wettability and PLT. One step modification with only PDA or ALB greatly increased platelet adhesion. Those variants had the highest observed platelet adhesion during this study, even greater than unmodified PU which suggest that surface exposed to one step modifications with PLA or ALB via simple dip method don't possess antithrombotic properties.

Samples modified with two step method possessed different properties than samples modified with only one solution. All samples exposed to both solutions had lower platelet adhesion than unmodified PU which suggest that simple dip method could be utilised for antithrombotic coatings as long as the method includes a binder compound in its first stage.

All considered modifications did increase the hydrophilicity of polyurethane samples.

Conclusions

The study shows that PDA has a significant effect on the adhesion of platelets to surfaces modified with it.

The presence of PDA in the modifying solution also affects the hydrophilicity of the sample.

From the data collected and calculations performed, it was noted that the platelet adhesion is highly dependent on the presence of other modification steps. Which may suggest that PDA acts as binding agent between modified surface and chosen antithrombotic coating (albumin). Samples modified with PDA alone showed higher adhesion than pure polyurethane samples, with an increase of more than 75% in the area occupied by platelets. This observation strengthens the assumption that PDA coating have glue-like properties. This view is further enforced by observation of a decrease in platelet affinity to the sample surface after exposing them to a second modification solution containing albumin.

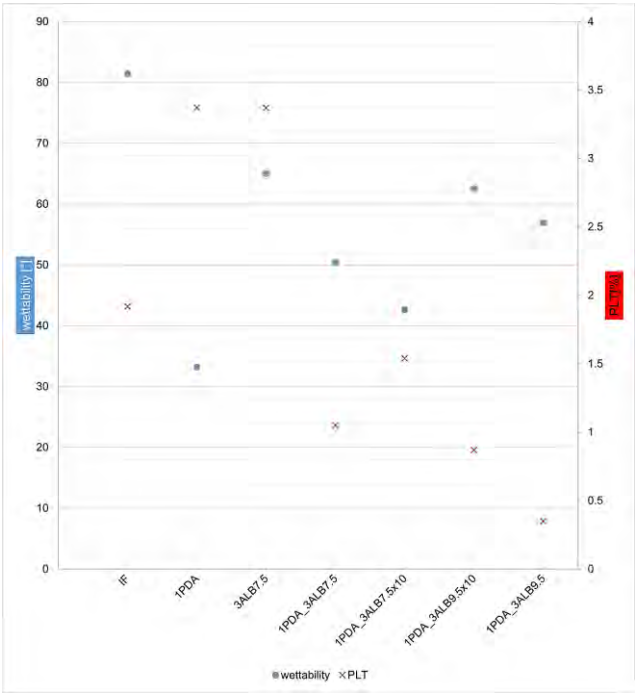

Figure 8.3.8 Platelet-occupied area and wettability of analysed materials.

An important observation is the increase in platelet adhesion for samples modified with strong albumin solution alone relative to unmodified grafts. When this step was combined with the PDA modification into a two-step modification, the area occupied by platelets decreased by 46% relative to the area modified by albumin alone. This could suggest that albumin, without prior modification with PDA, did not fully coat the modified area. Hence impact of modification based solely on albumin on platelet adhesion was opposite to expected. Albumin, because of its size, could not be visible on SEM images obtained during this study (Jantakee et al., 2021). To validate the statement that albumin coating was not fully effective additional tests should be conducted, such as FTIR-ATR surface analysis. However, investigating in greater detail the impact of albumin solutions on polyurethane surfaces is outside the scope of this article.

The results of carried out experiments could indicate the possibility of using PDA solutions as one of the steps in the modification of polyurethane surfaces for the production of synthetic vascular grafts for strengthening the connection between antithrombotic agent and the material of prosthesis.

Acknowledgements

This work was supported by The National Science Centre, Poland, grant number: UMO-2020/39/I/ST5/01131.

References

Buján, J., García-Honduvilla, N., & Bellón, J. M. (2004). Engineering conduits to resemble natural vascular tissue. *Biotechnology and Applied Biochemistry*, *39*(1), 17–27. https://doi.org/10.1042/ba20030111

Chen, T., Zou, Q., Du, C., Wang, C., Li, Y., & Fu, B. (2020). Biodegradable 3D printed HA/CMCS/PDA scaffold for repairing lacunar bone defect. *Materials Science and Engineering C*, *116*(May), 111148. https://doi.org/10.1016/j.msec.2020.111148

Davidsen, M. B., Teixeira, J. F. L., Dehli, J., Karlsson, C., Kraft, D., Souza, P. P. C., & Foss, M. (2021). Post-treatments of polydopamine coatings influence cellular response. *Colloids and Surfaces B: Biointerfaces*, *207*(July), 111972. https://doi.org/10.1016/j.colsurfb.2021.111972

Gupta, P., & Mandal, B. B. (2021). Tissue-Engineered Vascular Grafts: Emerging Trends and Technologies. *Advanced Functional Materials*, *31*(33), 1–28. https://doi.org/10.1002/adfm.202100027

Haeshin, L., Shara M, D., William, M. M., & Phillip B, M. (2007). Mussel-Inspired Surface Chemistry for Multifunctional Coatings. *Science*, *318*(5849), 426–430.

Jantakee, K., Prapan, A., Chaiwaree, S., Suwannasom, N., Kaewprayoon, W., Georgieva, R., Tragoolpua, Y., & Bäumler, H. (2021). Fabrication and characterization of human serum albumin particles loaded with non-sericin extract obtained from silk cocoon as a carrier system for hydrophobic substances. *Polymers*, *13*(3), 1–17. https://doi.org/10.3390/polym13030334

Kuźmińska, A., Kwarta, D., Ciach, T., & Butruk-Raszeja, B. A. (2021). Cylindrical polyurethane scaffold fabricated using the phase inversion method: Influence of process parameters on scaffolds' morphology and mechanical properties. *Materials*, *14*(11). https://doi.org/10.3390/ma14112977

Lee, S. J., Yoo, J. J., Lim, G. J., Atala, A., & Stitzel, J. (2007). In vitro evaluation of electrospun nanofiber scaffolds for vascular graft application. *Journal of Biomedical Materials Research Part A*, *83A*(4), 999–1008.

Liu, Y., Ai, K., & Lu, L. (2014). Polydopamine and its derivative materials: Synthesis and promising applications in energy, environmental, and biomedical fields. *Chemical Reviews*, *114*(9), 5057–5115. https://doi.org/10.1021/cr400407a

Mangin, P. H., Gardiner, E. E., Nesbitt, W. S., Kerrigan, S. W., Korin, N., Lam, W. A., & Panteleev, M. A. (2020). In vitro flow based systems to study platelet function and thrombus formation: Recommendations for standardization: Communication from the SSC on Biorheology of the ISTH. *Journal of Thrombosis and Haemostasis*, *18*(3), 748–752. https://doi.org/10.1111/jth.14717

Pacelli, S., Paolicelli, P., Petralito, S., Subham, S., Gilmore, D., Varani, G., Yang, G., Lin, D., Casadei, M. A., & Paul, A. (2020). Investigating the Role of Polydopamine to Modulate Stem Cell Adhesion and Proliferation on Gellan Gum-Based Hydrogels. *ACS Applied Bio Materials*, *3*(2), 945–951. https://doi.org/10.1021/acsabm.9b00989

Schneider, C. A., Rasband, W. S., & Eliceiri, K. W. (2012). NIH Image to ImageJ: 25 years of image analysis. *Nature Methods*, *9*(7), 671–675. https://doi.org/10.1038/nmeth.2089

Shively, S., & Miller, W. R. (2009). The use of HMDS (hexamethyldisilazane) to Replace Critical Point Drying (CPD) in the Preparation of Tardigrades for SEM (Scanning Electron Microscope) Imaging. *Transactions of the Kansas Academy of Science*, *112*(3–4), 198–200. https://doi.org/10.1660/062.112.0407

World Health Organization. (2021). *Cardiovascular diseases (CVDs) key facts*. World Health Organization. https://www.who.int/news-room/fact-sheets/detail/cardiovascular-diseases-(cvds)

Zhuang, Y., Zhang, C., Cheng, M., Huang, J., Liu, Q., Yuan, G., Lin, K., & Yu, H. (2021). Challenges and strategies for in situ endothelialization and long-term lumen patency of vascular grafts. *Bioactive Materials*, *6*(6), 1791–1809. https://doi.org/10.1016/j.bioactmat.2020.11.028

8.4 The impact of proton radiation on osteoblasts

Magdalena Król*,[1], Barbara Zagrajczuk[2], Zuzanna Piątek[3], Elżbieta Menaszek[3], Renata Szymańska[1]

1. Department of Applied Nuclear Physics, Faculty of Physics and Applied Computer Science, AGH University of Cracow, Cracow, Poland
2. Department of Silicate Chemistry and Macromolecular Compounds, Faculty of Materials Science and Ceramics, AGH University of Krakow, Krakow, Poland
3. Department of Cytobiology, Faculty of Pharmacy, Jagiellonian University, Cracow, Poland

e-mail: krolmagda@student.agh.edu.pl

KEYWORDS: *radiation, osteoblasts, proton beam, tumor osteoblast-like cells, molecular biology*

Introduction

Tumor treatment heavily relies on high-dose radiation, a potent tool in eliminating pathological cells. However, this approach presents challenges, particularly adverse effects on bones, such as osteopenia and osteoporosis. Cancer patients undergoing radiotherapy often experience complications like radiation-induced bone necrosis and frequent fractures. This concern extends beyond terrestrial treatments; it reaches into space travel, where astronauts face bone mass loss due to both cosmic radiation exposure and prolonged microgravity conditions.

Methods

In the pursuit of understanding the intricate effects of high-energy proton radiation on cellular systems, this research focused on two cell types, NHOst (Normal Human osteoblast) and MG63 (human osteoblast-like cells derived from bone tumor). A 225 MeV proton accelerator was utilized, employing an entrance dose that contributed to a reduction in uncertainties associated with the delivered dose. Varied doses of radiation were used: 0.5 Gy, 2 Gy and 10 Gy. The experiment aimed to investigate the immediate and lasting impacts of radiation, exploring viability, repair mechanisms, and potential functional implications. In addition to standard viability assessments, complementary assays were conducted to gain a comprehensive understanding of the cellular responses. The PrestoBlue test was used to assess cell viability and metabolic activity and the ToxiLight assay was instrumental in evaluating the toxicity levels associated with the experimental conditions. Furthermore, the incorporation of Enzyme-Linked Immunosorbent Assay (ELISA) for GADD45 expanded the investigation into the molecular realm.

NHOst cells exhibited an immediate decline in viability, correlating with increasing radiation doses. The initial measurement highlighted immediate radiation effects on cell viability. Extended incubation revealed a significant increase in cell activity associated with repair attempts after radiation exposure. This observation suggested that cells initiate complex repair mechanisms in response to radiation-induced stress. Despite initial impact, irradiated cells tended to return to values comparable to control cells over time, indicating efficient repair mechanisms mitigating prolonged damage.

In MG63 cells, a 10 Gy dose led to a substantial viability decrease, confirming a lasting impact on cell survival. Unlike previous cell lines showing some improvement in viability, cells exposed to a 10 Gy dose maintained low viability even two days post-irradiation, suggesting sustained and lasting effects, involving significant damage or disruption of repair processes hindering cell regeneration.

Results

Cell Viability Assessment Using the PrestoBlue™ Test

Cell viability assessment was conducted at five different time points to evaluate the impact of radiation on the metabolic activity of NHOst and MG63 cells over time.

NHOst

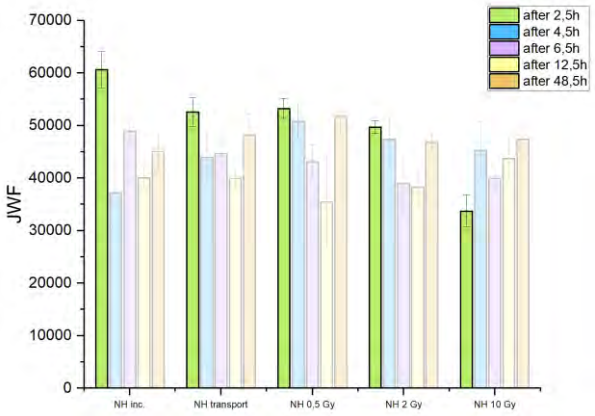

Figure 8.4.1 Viability of NHOst Cells with Specific Reference to the First Measurement Time Point

At 2.5 hours post-irradiation, corresponding to the initial measurement time point, a distinct decline in the metabolic activity of NHOst cells was observed, concomitant with an increase in the radiation dose. The radiation exhibited an immediate and visible impact on the viability of NHOst cells.

A significant difference was noted when comparing two control groups: one that remained in the incubator and another that was present during the transportation of plates to the irradiation site. Results indicate that transportation had a negative effect on the viability of cells in the control group. This may suggest that transport conditions, such as vibrations and temperature fluctuations, could adversely affect their well-being.

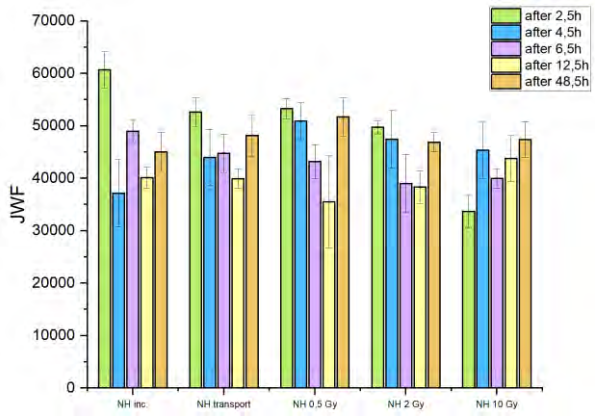

Figure 8.4.2 Viability of NHOst Cells with Detailed Measurement Time Points

Following an extended period after irradiation, a significant increase in the metabolic activity of NHOst cells was observed compared to the values obtained 2.5 hours post-irradiation. This increase may be attributed to the cells' attempt to repair damage caused by the earlier radiation exposure. Furthermore, it was observed that over a longer period post-irradiation (up to 48 hours), NHOst cells exhibited a substantial improvement in viability, reaching levels comparable to those before irradiation.

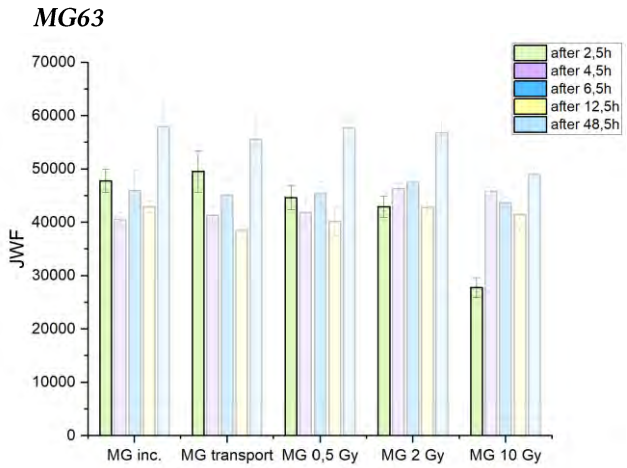

Figure 8.4.3 Results of the viability test for MG63 cells with emphasis on the first measurement point, JWF - relative units of fluorescence.

Similar to NHOst cells, a significant decrease in the viability of cells exposed to a dose of 10 Gy was observed. This confirms the substantial and lasting impact of this specific radiation dose on the ability of cells to survive.

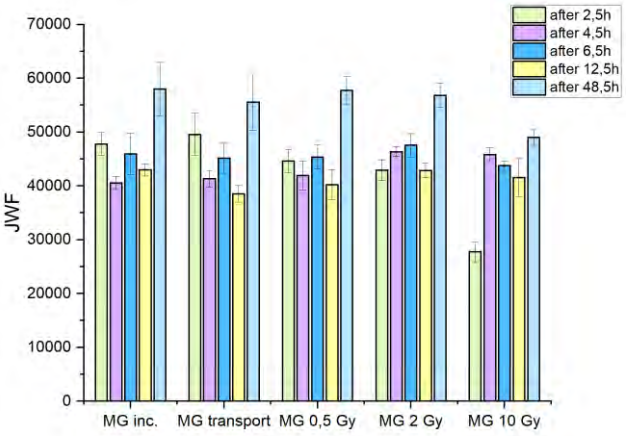

Figure 8.4.4 Viability Test Results for MG63 Cells with all Measurement Points Visible

The particularly intriguing observation is that, unlike the previous cell line which showed some improvement in viability in subsequent measurements, cells exposed to a dose of 10 Gy maintain low viability even two days post-irradiation. This suggests that this radiation dose had a prolonged impact on the cells, potentially involving severe damage or disruption of repair processes hindering cell regeneration.

For lower doses, no significant differences in cell viability were observed, even after extended incubation. It can be hypothesized that these radiation doses did not have a significant effect on cell viability.

Cytotoxicity and Cell Proliferation Assessment - ToxiLight Test

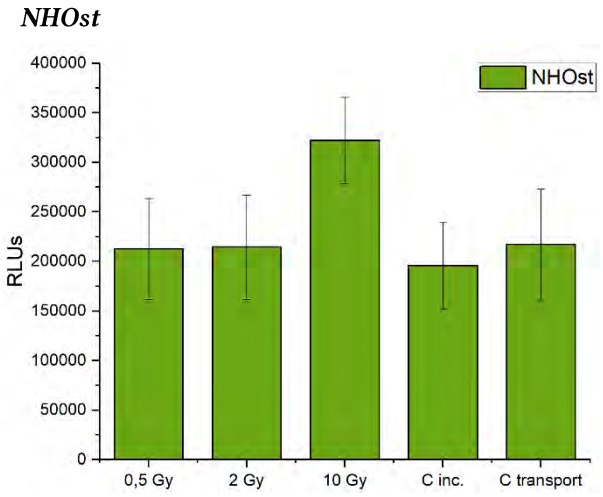

(a) Cytotoxicity

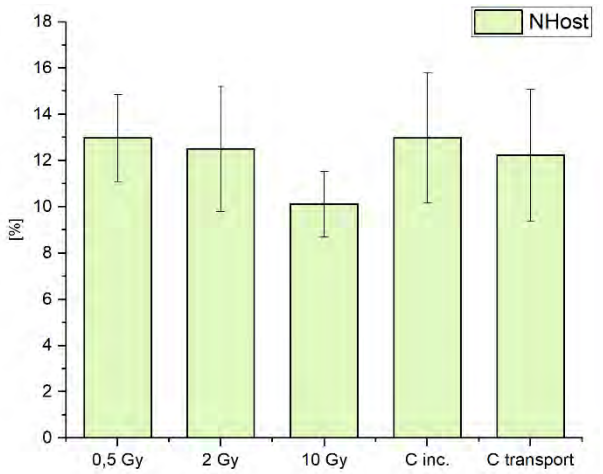

(b) Proliferation

Figure 8.4.5 Cytotoxicity and Proliferation Values of NHOst Cells for Different Radiation Doses and Controls at 48 Hours Post-Irradiation.

In the case of cytotoxicity for NHOst cells at 48 hours, no significant differences were observed either between individual doses of applied radiation, irradiated cells and controls, or among the control groups. On the other hand, regarding the proliferation of NHOst cells at 48 hours, a significant increase was noted for cells exposed to a radiation dose of 10 Gy compared to cells subjected to lower radiation doses and controls. No significant differences in proliferation values were observed between NHOst cells irradiated with 0.5 Gy, 2 Gy, and the control group. The lack of significant differences in cytotoxicity among samples likely stemmed from the assessment conducted relatively long after irradiation, during which, as indicated by viability assessment results, cells exhibited partial improvement in well-being compared to the period immediately post-irradiation.

MG63

In the case of MG63 cells no significant differences were observed in both cytotoxicity and proliferation at 48 hours among individual radiation doses, irradiated cells, and control groups. The presence of relatively large standard errors might contribute to the lack of discernible distinctions, suggesting a need for cautious interpretation of the results.

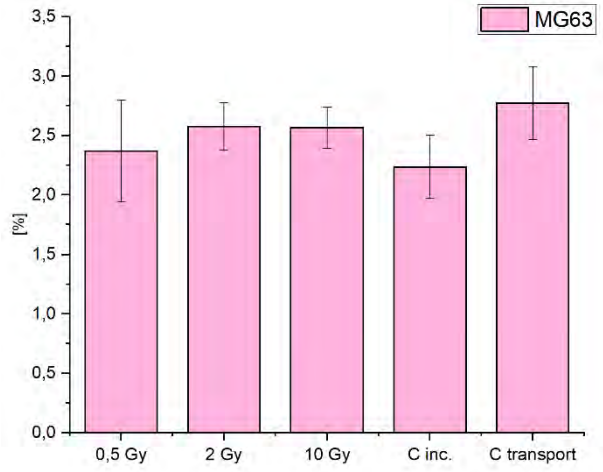

(a) Cytotoxicity

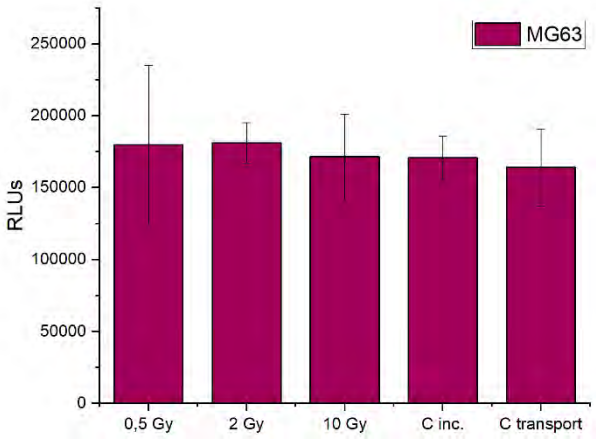

(b) Proliferation

Figure 8.4.6 Cytotoxicity and Proliferation Values of MG63 Cells for Different Radiation Doses and Controls at 48 Hours Post-Irradiation.

Enzyme-Linked Immunosorbent Assay (ELISA)

In the initial phase, a standard curve was established to convert optical results (absorbance) into quantitative results, such as protein concentration.

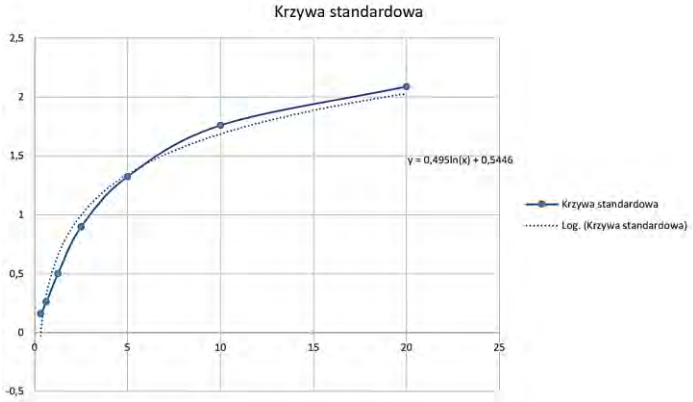

Figure 8.4.7 Standard Curve.

NHOst

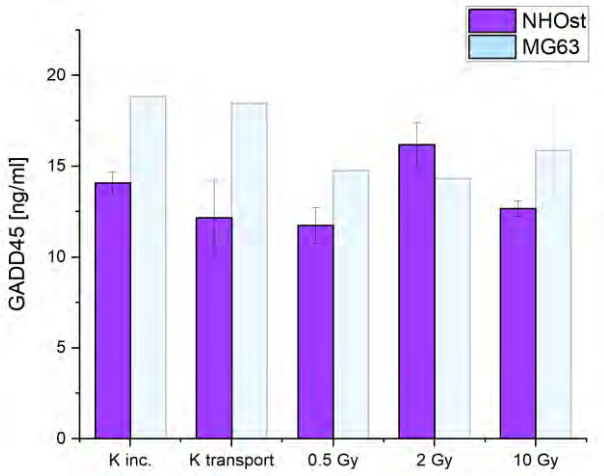

Figure 8.4.8 Results of the enzyme-linked immunosorbent assay (ELISA) for NHOst cells.

The levels of GADD protein under field conditions (12.15 ng·ml^{-1}) are slightly lower than under control conditions in the incubator. This decrease may suggest that environmental changes induce some adaptive cellular response, but the stress is not intense enough to result in a significant increase in GADD protein.

After exposing cells to a dose of 0.5 Gy, GADD protein levels (11.73 ng·ml^{-1}) are lower than under control conditions, indicating an initial stage of cellular response to low-intensity stress, possibly related to DNA repair.

Following exposure to a dose of 2 Gy, a significant increase in GADD protein levels (16.18 ng·ml^{-1}) is observed. This increase can be interpreted as an intensification of the cellular response to substantial DNA damage. Activation of robust repair mechanisms occurs, and GADD protein expression is upregulated for effective damage repair. GADD protein levels for a dose of 10 Gy (12.66 ng·ml^{-1}) suggest that cells are experiencing intense stress but may be in a phase where there are limitations in complete repair, resulting in cellular adaptation to stress or only partial repair.

MG63

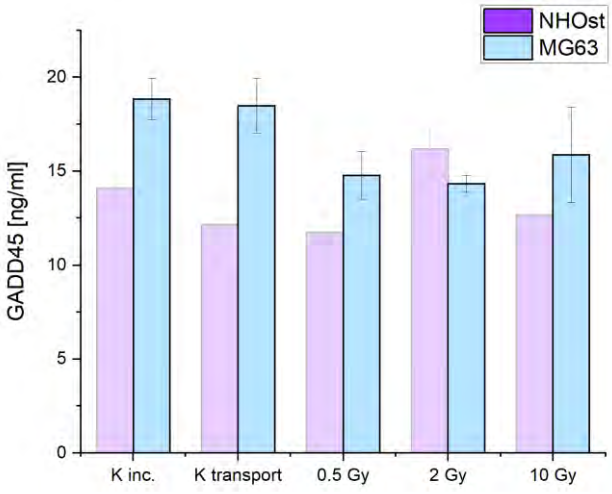

Figure 8.4.9 Results of the enzyme-linked immunosorbent assay (ELISA) for MG63 cells.

The change in control conditions slightly affects the reduction in the GADD protein level. After exposure to a

dose of 0.5 Gy, a lower GADD protein level (14.77 ng·ml^{-1}) is observed compared to the control, suggesting that MG63 cells activate compensatory control mechanisms leading to a decrease in protein levels.

In the case of a 2 Gy dose, protein levels are similar to 0.5 Gy. This may indicate that MG63 cells may already be intensively responding to lower radiation doses. The highest level of GADD protein (15.87 ng·ml^{-1}) observed for a dose of 10 Gy may indicate a strong response of MG63 cells to substantial DNA damage, yet they still maintain a relative ability to respond to this stressor.

Conclusion

NHOst cells, subject to radiation, experienced an initial viability dip swiftly succeeded by a surge in metabolic activity—an indicative effort at cellular repair. Over time, these cells demonstrated a remarkable return to vitality, showcasing adept repair mechanisms. In contrast, MG63 cells experienced a sustained impact following exposure to a radiation dose of 10 Gy, manifesting a significant and enduring reduction in viability persisting even after a two-day period. This observation suggests substantial damage that impedes the cellular regenerative capacity.

Within the domain of NHOst cells, the 48-hour post-irradiation assessment did not reveal substantial cytotoxic variations across administered doses. Nevertheless, a discernible increase in proliferation was observed specifically at the 10 Gy dose, suggesting a potential manifestation of an adaptive cellular response. Contrastingly, in the case of MG63 cells, no significant alterations were discerned in cytotoxicity at lower doses, thus not providing clear indications of cellular damage.

NHOst cells exhibited a subtle decrease in response under field conditions. The observed elevation in GADD levels following a 2 Gy dose indicated a robust DNA damage response. Conversely, MG63 cells displayed a reduction in GADD protein levels post-0.5 Gy, suggestive of compensatory mechanisms, while heightened levels at 10 Gy underscored a robust response to significant DNA damage.

In essence, this study transcends the immediate impacts, offering a comprehensive understanding of cellular resilience and vulnerability. It highlights the intricate interplay between damage and repair, providing insights into the adaptability of cells under stress. The acknowledgment of the influence of transport conditions on initial viability underscores the necessity for meticulous experimental consideration

Acknowledgements

I would like to express my sincere gratitude to Prof. Justyna Miszczyk for her invaluable assistance in irradiating cells and coordinating the entire undertaking at CCB IFJ. I appreciate the unwavering support and dedication throughout the process.

The project was financed by AGH University of Science and Technology as part of a grant obtained through the activities of the scientific club SKNF Bozon.

8.5 The influence of Hydrothermal Carbonization process on reduction of Heavy Metals and Polycyclic Aromatic Hydrocarbons from sewage sludge – a short review

Zuzanna Prus*[,1], Katarzyna Styszko[2], Małgorzata Wilk[1]

1. Department of Heat Engineering & Environment Protection, Faculty of Metals Engineering and Industrial Computer Science, AGH University of Krakow, Department of Cracow, Poland
2. Department of Coal Chemistry and Environmental Sciences, Faculty of Energy and Fuels, AGH University of Krakow, Krakow, Poland

e-mail: zprus@agh.edu.pl

KEYWORDS: *hydrothermal carbonization, sewage sludge, heavy metals, polycyclic aromatic hydrocarbons*

Introduction

The growth of the world's population, dynamic urbanization, and increasing industrial activity lead to a higher amount of wastewater being generated. Consequently, effective wastewater management, especially sewage sludge (the main by-product) is necessary and crucial for environmental care. Proper handling of sewage waste poses an economic, social, and environmental concern (Tasca et al., 2022). The type of wastewater flowing into the wastewater treatment plant (WWTP) determines the physical and chemical composition of the sludge. Sewage sludge (SS) is a complex, heterogeneous mixture of dissolved and undissolved substances, contains organic and inorganic matter, nutrients, microorganisms, and many chemicals, resulting from various mechanical, biological, and chemical processes within WWTPs. Some compounds such as nutrients should be recycled, but some toxic chemicals should be disposed of in order not to cause an environmental threat. Conventional wastewater and SS treatment technologies applied in WWTPs have been devised to directly minimize sludge production from biological treatments but have not been designed to effectively remove micropollutants. Many researchers indicate the presence of unwanted and potentially dangerous substances in SS such as heavy metals (HMs) (Huang & Yuan, 2016; Liu et al., 2018a; Peng et al., 2017; Tasca et al., 2022; Y. jie Wang et al., 2022; Zhang et al., 2021), polycyclic aromatic hydrocarbons (PAHs) (Gondek et al., 2016; Lang et al., 2019; Peng et al., 2017; Sundqvist, 2021), pharmaceuticals (Alipour et al., 2022; Charlson, 2017; Sundqvist, 2021), polychlorinated biphenyls (PCBs) (Alipour et al., 2022; Brookman et al., 2018; Tasca et al., 2022), pesticides (Ponce-Robles et al., 2017; Sánchez et al., 2004; Tasca et al., 2022), and pathogens. Because of the possible applications of this biomass, it is necessary to maintain its environmental neutrality.

SS can generally be used for agricultural, land, or energy production purposes. The most popular direction of sludge management in Europe and the United States is composting and use in agriculture as fertilizer - more than 50% (Nizetto et al., 2016), and in Ireland more than 80% (Singh & Agrawal, 2008). In Europe, SS management, disposal, and recycling procedures are governed by both national legislation and directives from the European Union (EU). These directives outline specific guidelines and limitations concerning the handling of SS. Directive 99/31/EC prohibits its disposal in landfills, while directive 86/278/EEC imposes restrictions on applying SS to soil due to its HM content. Within the last few years, thermochemical treatments of SS have been increasingly used and are more frequently preferred than biological procedures because of their reduced processing time and superior conversion efficiencies. Incineration and co-incineration methods are strictly regulated by the Directive 2010/75/EU. Directive 2008/98/EC focuses on promoting reuse, recycling and encouraging the extraction of energy from waste materials (Tasca et al., 2022).

One of the promising technologies for the SS management is hydrothermal carbonization (HTC). This thermochemical process has gained significant attention in recent years because of its promising potential in transforming various types of biomass into a valuable resource of energy. The HTC process, shown in Figure 8.5.1, offers a sustainable approach to address the challenges posed by the SS to convert this organic-rich material into a carbonaceous product known as hydrochar (HC). It involves the transformation of organic materials at high temperature and high-pressure conditions in the presence of water. It is usually carried out in a stainless steel autoclave in a temperature range 180–250 °C under high autogenous pressure for about 0.5-8 h in an inert atmosphere, and in an aqueous environment (Ahmad et al., 2018). The main advantage is that no drying of the feedstock is required, which significantly reduces the energy consumption during the preparation. Longer reaction times allow for more extensive degradation, while optimal pressure and moisture levels contribute to the efficiency of the process. When certain feedstock is heated, the composition and physical properties of both organic and inorganic contaminants is changed.

Inorganic contaminants including HMs, minerals, and salts undergo several transformations and reactions affected by the high-temperature conditions. For example, HMs can undergo changes in their speciation or chemical forms due to complexation, precipitation, or sorption onto the carbonaceous material formed during HTC (Kalderis et al., 2014; Pan, 2023; Tasca et al., 2022). These alterations in speciation can affect the mobility and bioavailability of HMs, potentially reducing their environmental impact (Huang & Yuan, 2016). Organic compounds present in feedstocks such as PAHs, pharmaceuticals and hormones also undergo decomposition or breakdown due to elevated temperature and high-pressure conditions (Iñiguez et al., 2019; Tasca et al., 2022). The primary determinant affecting the elimination and breakdown of organic matter with notably high thermal stability compared to other compounds, is the temperature applied along with the high pressure. These promote chemical reactions such as hydrolysis, dehydration, decarboxylation, and others that lead to the degradation of complex organic molecules. It results in the breakdown of larger organic molecules into simpler and more stable compounds, such as water, carbon dioxide, methane, and organic acids (Jun C., Na W., Dongsheng W., 2023; Turcanu et al., 2022). High temperatures facilitate the breakdown of chemical bonds, altering the molecular structures of contaminants, and reducing their concentrations in the final product (Morais et al., 2018).

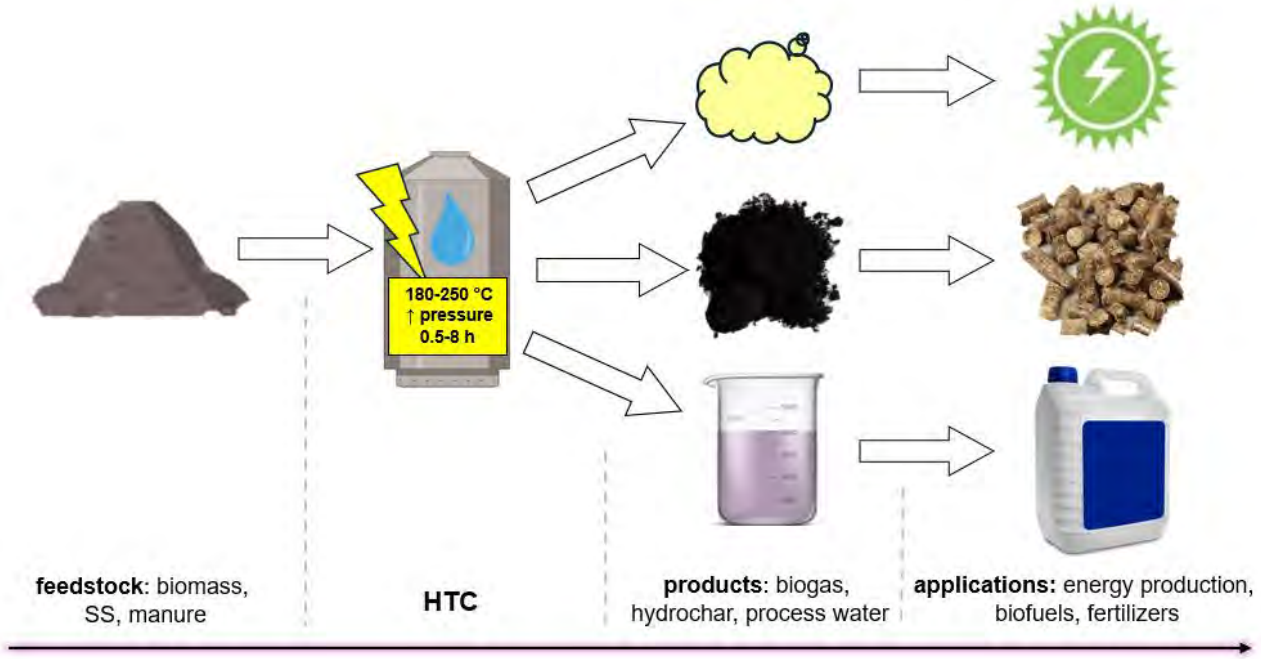

Figure 8.5.1 General scheme of the HTC process

HC derived from SS might be used as a fertilizer and soil conditioner if it does not contain harmful substances. Therefore, it is crucial to produce HC with a limited amount of organic contaminants. There are some research studies confirming the positive effect of HTC on the reducing HM and degradation of PAHs in biomass and organic waste. In this study, the short review of the degradation of inorganic and organic contaminants present in the SS was taken into account, with special attention focused on HMs and PAHs.

Removal of HMs

The mechanism of HMs transformation during HTC of the SS was thoroughly reviewed by Pan (2023). The prevailing consensus is that the accessibility and environmental toxicity of HMs are primarily based on their specific chemical forms or speciation. Their primary chemical forms determine the distribution and mobility within thermal reactions such as HTC. Generally, HTC could decrease the presence of HMs from raw SS initially stabilizing (Pan, 2023). This effect has also been confirmed by Huang & Yuan (2016), who outlined the techniques used to assess the degree of HMs contamination or risk. They examined the migration and alteration patterns of HMs due to the various thermal reactions. This investigation encompassed several facets, e.g. the influence of reaction temperature, the impact of additives, and the significance of reaction time. The conclusion is that elevating the reaction temperature and time results in a rise in the overall HM content within the HC. Some research indicates that Zn, Cd, Cu, and Pb degrade at high temperatures and go into the gas phase, when Cr, Ni, and Fe are less volatile and more thermally stable, and therefore the ashes were enriched with them as the process temperature increased (Zajac et al., 2019). Shi et al. (2013) also noted that the majority of HMs in SS remain in HC after HTC. Liu et al. (2018) investigated Mn, Ni, Cr, Pb, Zn Cu and Hg derived from the SS from municipal WWTP in Shandong Province, China. The sludge contained 81% moisture and underwent no additional pretreatment except drying at 105 °C for 24 h and subsequent crushing in mortar. The HTC parameters were: the temperature of 200 °C, the residence time of 30 min and the reaction was carried out in the nitrogen, which was fed to the system. Identification of various types of HMs and their leaching ability in the SS/HC were accomplished through the BCR & TCLP methods.

The BCR (formerly known as the European Community Bureau of Reference, now the Institute for Reference Materials and Measurements) method for HM content analysis refers to a sequential extraction procedure designed to assess the chemical forms or fractions of HMs in solid samples, particularly soil and sediment. It helps to determine their potential mobility, bioavailability, and environmental risk. It involves a series of chemical extractions in a step-by-step process that targets different fractions of HMs bound to specific components of the sample. These fractions are often categorized as: exchangeable, acid-soluble, reducible, oxidizable, and residual (Huang & Yuan, 2016). The Toxicity Characteristic Leaching Procedure (TCLP) is a laboratory method used in the United States to determine the mobility of both organic and inorganic contaminants present in waste materials. It specifically assesses whether these contaminants would leach out of the waste under simulated landfill conditions and potentially pose a risk to the environment if the waste were disposed of in a landfill. The procedure involves mixing a representative sample of the waste material with an acidic solution (acetic acid at a controlled pH) and then subjecting it to agitation or tumbling for a specified time. This process simulates the conditions found in a landfill where the waste may come in contact with an acidic rainwater or other solutions, potentially causing the leaching of contaminants (Sorini & Jackson, 1988).

HMs were extracted, and their concentrations were quantified by Inductively Coupled Plasma Optical Emission spectroscopy (ICP-OES) and Cold Vapor Atomic Fluorescence Spectrometry (CVAFS). After HTC, most HMs were redistributed to the HC (about 70-90%) and their solid content was higher in HC than in corresponding SS as presented in Table 8.5.1.

Table 8.5.1 Values of HMs and TLCP concentrations in HCs within different HTC processes

HM	*Mn*	*Cr*	*Ni*	*Cu*	*Zn*	*Pb*	*Cd*	*Hg*	*T-t*	*Reference*
c increase in HC, %	36.3	11.9	17.0	22.0	24.1	34.4	23.9	25.8	200-3	Liu et al. (2018b)
leach reduction%	21.5	50.0	68.3	77.4	50.4	9.6	62.5	66.7		
c increase in HC, %	*x*	17.2-31.5	3.8-13.7	17.9-33.6	17.0-62.0	18.1-34.9	10.3-21.2	*x*	160-0.5 180-0.5 200-0.5 220-0.5	Wang et al. (2016)
leach reduction%		80.6-94.4	31.6-54.8	14.9-87.9	30.3-87.9	*increase*	44.1-67.6			
c increase in HC, %	4.6-15.8	15.4-28.2	*nd*	33.0-80.6	2.0-9.5	*nd*	*nd*	*nd*	180-3 200-0.5 220-0.5 240-3	Zhang et al. (2021)
leach reduction%	*increase*	38.4-74.7	*nd*	74.2-90.2	20.2-47.5	*nd*	*nd*	*nd*		

where c stands for concentration, T – temperature, °C; t – time, h; x – not tested, nd – not detected

The researchers also conducted a pyrolysis process of the SS/HC within the temperature range 350-950 °C. It was observed that the content of Cd, Mn, Zn, and Pb in the corresponding chars firstly increased, and then decreased substantially when the temperature exceeded 650, 800 and 950 °C, respectively. Cr, Cu, and Ni generally increased with temperature. HMs extracted by the TCLP test could directly threaten the health of plants with the introduction of chars into the soil. For the HC, the average released HMs levels were lower compared to the SS sample (Table 8.5.1). Studies showed that higher temperatures are required to effectively remove HMs from the SS e.g. during pyrolysis. The HTC process generally did not reduce the content of such HMs in the SS, but it did reduce their leachable fractions becoming less mobile, minimizing environmental risks during agricultural or land use (Liu et al., 2018b). Similar effects on HMs were examined by Wang et al. (2016) who studied the immobilization and the risk assessment of HMs in SS during HTC and pyrolysis, also. Selected compounds such as Cu, Zn, Cr, and Ni were chosen as representatives of the HMs group by the first stage of HTC. The SS samples with a moisture content of 82.3% were collected from WWTP in Xiamen, China, dried at 105 °C for 24 h and then crushed in the mortar and mixed with the deionized water. HTC processes at 160, 180, 200 and 220 °C and 0.5 h were carried out under oxygen-free conditions achieved by the inflow of pure argon. In this study, a BCR and TCLP procedures were applied to identify such HMs and also evaluate their leaching potential. The post-extraction concentrations of each HM were analyzed using Inductively Coupled Plasma Mass Spectrometry (ICP-MS). After HTC, all selected HMs were redistributed and their concentrations in the HC were significantly higher than in liquid products, as well as in the corresponding SS samples. The HM concentrations in HCs and their leaching values increased mainly according to increasing process temperature, what is shown in Table 8.5.1. The amount of leached Pb was higher than in the SS sample. Combining the BCR with the TCLP method confirmed that most of the HMs in SS can migrate from bioavailable to more stable fractions due to HTC, causing accumulation and immobilization in HCs. Zhang et al. (2021) also traced the changes in HM forms due to HTC and have also come to a conclusion about their immobilization and accumulation in HC. Dewatered SS samples were collected from a textile WWTP (Zhejiang, China) and then mixed directly with deionized water. The temperatures for the HTC process were 180, 200, 220 and 240 °C with a reaction time of 0.5 or 3 h, and the nitrogen was supplied to replace air in the reactor. In this research, the BCR and the TCLP methods were also applied. Cu, Cr, Mn, and Zn were extracted from the SS and the HC, and then analyzed with Inductively Coupled Plasma Atomic Emission Spectroscopy (ICP-AES) technique. In general, the HTC resulted in elevated levels of HMs present in the HC samples, with the most significant change observed in the case of Cu. The reduction of other HMs was also observed (Table 8.5.1). Additional HTC reactions were performed at a temperature of 220 °C with longer residence time (4 h and 5 h). Generally, as the temperature and duration of the HTC increased, there was an initial upward trend followed by a subsequent decline in the levels of HM found in the solid product. These fluctuations depended largely on the specific HTC conditions.

Removal of PAHs

Some studies have verified that PAHs tend to concentrate in HCs, rather than in process water (with about 9:1 ratio), while the anticipated gaseous yields are projected to be very low (Jiang et al., 2022, Liu et al., 2021). However, the formation and dispersion of PAHs during HTC were highly intricate and closely associated with both the feedstock utilized and the specific conditions applied (Lang et al., 2019). Overall, the temperature increases the decomposition of organic compounds in feedstock to promote PAH precursors e.g. benzene and phenol, and finally their generation. Furthermore, a migration of PAHs with comparatively lower boiling points into the gaseous by-product is observed, potentially leading to a reduction in the overall concentration of PAHs found in HCs and process water (Gong et al., 2016). Therefore, their concentration in final solid, liquid, and gaseous products is determined by the balance between their rates of synthesis and decomposition, primarily influenced by the temperature of the process (Lang et al., 2019). Selected results of the study of PAHs concentration in thermally carbonized SS are shown in Table 8.5.2.

Table 8.5.2 Values of PAH concentrations in HCs within different HTC processes

PAH	Nap	Acy	Ace	Flu	Phe	Ant	Fla
c increase in HC, %	decrease/nd	nd	decrease/nd	decrease/nd	83.3-decrease/nd	>7.4-decrease/nd	1000-23.9
c increase in HC, %	36.4-118.0	12.6-74.2	9.2-44.2	20.1-37.9	40.7-decrease	0.1-66.8	53.0-150.2
c increase in HC, %	x	x	x	x	25.0	99.2	52.9

PAH	Pyr	BaP	Chr	Total content	T-t	Reference
c increase in HC, %	94.6-decrease	77.3-decrease	86.8-decrease	x	220-1.4	Tasca et al., 2022
c increase in HC, %	46.5-decrease	42.6-166.0	12.9-decrease	50.5-decrease	180-10 200-10 220-10	Lang et al., 2019
c increase in HC, %	28.4	40.4	44.7	45.2	180-1	Alipour et al., 2022

where c stands for concentration, T - temperature, °C; t - time, h; x – not tested, nd – not detected

The exact relationship between temperature and PAH abundance is still inconsistent (Alipour et al., 2022). Tasca et al. (2022) studied various chemical compounds, including PAHs and HMs, too. As a result of the limited literature data on these compound contents in SS and HCs, they performed experiments to characterize them in this regard. Twenty three PAHs were chosen, including anthracene (Ant), fluorene (Flu), phenanthrene (Phe), benzo-[a]pyrene (BaP), acenaphthylene (Acy), acenaphthene (Ace), naphthalene (Nap), and pyrene (Pyr). Digested SS samples were collected from six different WWTPs of Tuscany (Italy), where five out of the six plants have implemented biological nitrogen removal technology. Half of them were stabilized anaerobically and the other half in aerobic conditions. The HTC process of each sample, diluted with distilled water to 15% by weight percentage of solid content, was carried out at 220 °C for 85 min. After that, particular compounds were extracted by the ultrasonic technique, and then determined using High Performance Liquid Chromatography (HPLC) coupled with a programmable fluorescent detector. Such PAHs as anthracene and perylene were detected only in two SS samples, both at a concentration of <0.04 $mg \cdot kg^{-1}$. Naphthalene was detected only in one sample at 0.030 $mg \cdot kg^{-1}$, and the presence of pyrene was the most significant at concentration >0.1 $mg \cdot kg^{-1}$. The total PAH content in the HCs was generally lower up to 50.5% compared to raw SS samples, and the concentration of many of the compounds was the detection limit of the instrument (<0.005 $mg \cdot kg^{-1}$) marked as not detected in Table 8.5.1. The concentration of a few compounds such as Acy, Ace, and Ant increased slightly, but not above 12.6%, 9,2%, and 0.1%, respectively. It can be assumed that the HTC process successfully reduced the content of PAHs from SS. As mentioned before, the key factors influencing the elimination of PAHs are mainly their volatility and susceptibility to thermal degradation (Wu et al., 2017, Dai et al., 2014). Alipour et al. (2022) investigated the fate of selected organic pollutants in SS from two different sources during two main thermal methods: the pyrolysis and the HTC. Ten of the most common forms of PAHs like Ant, BaP, Chr, Pyr, Fla, Phe etc. were analyzed in SS and HC samples. Stabilized SS samples after an extended aeration process were obtained from WWTPs from southern Tehran and Ekbatan (Iran), dried at 105 °C for 24 h, and then 0.5-2.0 mm particle size were separated for experiments. HC was produced from SS sample and deionized water in a 1:1 ratio, at a temperature of 180 °C for 1 h with the nitrogen supplied to the reactor. The slurry was then filtrated and dried again under the same conditions as the raw material. After extraction from the array, the selected PAHs were analyzed using Gas Chromatography coupled with Mass Spectrometry (GC-MS). After HTC, every PAH content was significantly reduced (25.0-99%), and their total concentration in solid product lowered by approximately 45.2%. This study revealed that HTC could significantly reduce PAHs content from SS considerably due to thermal decomposition.

Conclusions

In conclusion, HTC might be a potential method for mitigating the presence of HMs and PAHs in SS by converting it into a more stable and potentially reusable material. The review of available studies proves that the HTC process can significantly immobilize and reduce leaching of HMs as well as reduce the concentrations of PAHs in SS, within the solid matrix of HC, depending on the conditions applied. However, before its agricultural, land, or energy production application, it's crucial to ensure that the HC meets regulatory standards regarding other contaminant levels. More research and field studies are necessary to optimize the process, assess its long-term effectiveness, and ensure the safety and environmental sustainability of using HC derived from SS. Future perspectives of HC materials should consider the possibilities of scaling up and obtain the optimal parameters of the HTC process to produce HCs with the best properties depending on destination.

Acknowledgements

The research was funded by the Ministry of Science and Higher Education [AGH University grant no. 16.16.110.663 and no. 16.16.210.476].

References

Ahmad, F., Silva, E. L., & Varesche, M. B. A. (2018). Hydrothermal processing of biomass for anaerobic digestion – A review. *Renewable and Sustainable Energy Reviews*, *98*, 108–124. https://doi.org/10.1016/J.RSER.2018.09.008

Alipour, M., Asadi, H., Chen, C., & Besalatpour, A. A. (2022). Fate of organic pollutants in sewage sludge during thermal treatments: Elimination of PCBs, PAHs, and PPCPs. *Fuel*, *319*, 123864. https://doi.org/10.1016/j.fuel.2022.123864

Brookman, H., Gievers, F., Zelinski, V., Ohlert, J., & Loewen, A. (2018). Influence of hydrothermal carbonization on composition, formation and elimination of biphenyls, dioxins and furans in sewage sludge. *Energies*, *11*, 1582. https://doi.org/10.3390/en11061582

Charlson, A. (2017). *Removal of pharmaceuticalcontainingwastewater by bioandhydrochar adsorbents: Adsorption capacity and surface functionalities.* https://www.diva-portal.org/smash/get/diva2:1113675/FULLTEXT01.pdf

Dai, Q., Jiang, X., Jiang, Y., Jin, Y., Wang, F., Chi, Y., & Yan, J. (2014). Formation of PAHs during the pyrolysis of dry sewage sludge. *Fuel*, *130*, 92–99. https://doi.org/10.1016/j.fuel.2014.04.017

Gondek, K., Mierzwa-Hersztek, M., Smreczak, B., Baran, A., Kopeć, M., Mróz, T., Janowski, P., Bajda, T., & Tomczyk, A. (2016). Content of PAHs, activities of γ-radionuclides and ecotoxicological assessment in biochars. *Polish Journal of Chemical Technology*, *18*(4), 27–35. https://doi.org/10.1515/pjct-2016-0067

Gong, M., Zhu, W., Zhang, H., Su, Y., & Fan, Y. (2016). Polycyclic aromatic hydrocarbon formation from gasification of sewage sludge in supercritical water: The concentration distribution and effect of sludge properties. *Journal of Supercritical Fluids*, *113*, 112–118. https://doi.org/10.1016/j.supflu.2016.03.021

Huang, H. J., & Yuan, X. Z. (2016). The migration and transformation behaviors of heavy metals during the hydrothermal treatment of sewage sludge. *Bioresource Technology*, *200*, 991–998. https://doi.org/10.1016/j.biortech.2015.10.099

Iñiguez, M. E., Conesa, J. A., & Fullana, A. (2019). Hydrothermal carbonization (HTC) of marine plastic debris. *Fuel*, *257*, 116033. https://doi.org/10.1016/j.fuel.2019.116033

Jiang, C., Chen, Z., Lu, B., Li, Z., Zhang, S., Liu, Y., & Luo, G. (2022). Hydrothermal pretreatment reduced microplastics in sewage sludge as revealed by the combined micro-Fourier transform infrared (FTIR) and Raman imaging analysis. *Chemical Engineering Journal*, *450*(2), 138163. https://doi.org/10.1016/j.cej.2022.138163

Jun C., Na W., Dongsheng W., W. Z. (2023). Molecular properties and biotoxicity of dissolved organic matter leached from microplastic (MP-DOM) during typical hydrothermal treatment of sewage sludge. *Science of The Total Environment*, *892*, 164548. https://doi.org/10.1016/j.scitotenv.2023.164548

Kalderis, D., Kotti, M. S., Méndez, A., & Gascó, G. (2014). Characterization of hydrochars produced by hydrothermal carbonization of rice husk. *Solid Earth*, *5*(1), 477–483. https://doi.org/10.5194/se-5-477-2014

Lang, Q., Zhang, B., Li, Y., Liu, Z., & Jiao, W. (2019). Formation and toxicity of polycyclic aromatic hydrocarbons during CaO assisted hydrothermal carbonization of swine manure. *Waste Management*, *100*, 84–90. https://doi.org/10.1016/j.wasman.2019.09.010

Liu, T., Liu, Z., Zheng, Q., Lang, Q., Xia, Y., Peng, N., & Gai, C. (2018a). Effect of hydrothermal carbonization on migration and environmental risk of heavy metals in sewage sludge during pyrolysis. *Bioresource Technology*, *247*, 282–290. https://doi.org/10.1016/j.biortech.2017.09.090

Liu, T., Tian, L., Liu, Z., He, J., Fu, H., Huang, Q., Xue, H., & Huang, Z. (2021). Distribution and toxicity of polycyclic aromatic hydrocarbons during CaO-assisted hydrothermal carbonization of sewage sludge. *Waste Management*, *120*, 616–625. https://doi.org/10.1016/j.wasman.2020.10.025

Morais, R. L., Santiago, M. F., Zang, J. W., Fonseca-Zang, W. A., & Schimidt, F. (2018). Removal of synthetic sex hormones by hydrothermal carbonization. *Anais Da Academia Brasileira de Ciencias*, *90*(2), 1327–1336. https://doi.org/10.1590/0001-3765201820170176

Nizetto, L., Bussi, G., Futter, M. N., Butterfield, D., & Whitehead, P. G. (2016). A theoretical assessment of microplastic transport in river catchments and their retention by soils and river sediments. *Environmental Science: Processes & Impacts*, *18*(8), 1050–1059. https://doi.org/https://doi.org/10.1039/c6em00206d

Pan, R. (2023). The Heavy Metals Transformation During The Pyrolysis And Hydrothermal Carbonation of Municipal Sewage Sludge. *E3S Web of Conferences*, *393*, 03001. https://doi.org/10.1051/e3sconf/202339303001

Peng, N., Li, Y., Liu, T., Lang, Q., Gai, C., & Liu, Z. (2017). Polycyclic Aromatic Hydrocarbons and Toxic Heavy Metals in Municipal Solid Waste and Corresponding Hydrochars. *Energy and Fuels*, *31*(2), 1665–1671. https://doi.org/10.1021/acs.energyfuels.6b02964

Ponce-Robles, L., Rivas, G., Esteban, B., Oller, I., Malato, S., & Agüera, A. (2017). Determination of pesticides in sewage sludge from an agro-food industry using QuEChERS extraction followed by analysis with liquid chromatography-tandem mass spectrometry. *Analytical and Bioanalytical Chemistry*, *409*(26), 6181–6193. https://doi.org/10.1007/s00216-017-0558-5

Sánchez, M. E., Estrada, I. B., Martínez, O., Martín-Villacorta, J., Aller, A., & Morán, A. (2004). Influence of the application of sewage sludge on the degradation of pesticides in the soil. *Chemosphere*, *57*(7), 673–679. https://doi.org/10.1016/j.chemosphere.2004.07.023

Shi, W., Liu, C., Shu, Y., Feng, C., Lei, Z., & Zhang, Z. (2013). Synergistic effect of rice husk addition on hydrothermal treatment of sewage sludge: Fate and environmental risk of heavy metals. *Bioresource Technology*, *149*, 496–502. https://doi.org/10.1016/j.biortech.2013.09.114

Singh, R. P., & Agrawal, M. (2008). Potential Benefits and Risks of Land Application of Sewage Sludge. *Waste Manage*, *28*, 346–358. https://doi.org/https://doi.org/10.1016//j.wasman.2006.12.010

Sorini, S., & Jackson, L. (1988). Evaluation of the Toxicity Characteristic (TCLP) on Utility Wastes. *Nuclear and Chemical Waste Management*, *8*, 217–223. https://doi.org/https://doi.org/10.1016/0191-815X(88)90029-0

Sundqvist, B. (2021). *Polyaromatic Hydrocarbons in Hydrochars : Hydrothermal Carbonization of Sewage Sludge.* https://www.diva-portal.org/smash/get/diva2:1575602//FULLTEXT01.pdf

Tasca, A. L., Vitolo, S., Gori, R., Mannarino, G., Raspolli Galletti, A. M., & Puccini, M. (2022). Hydrothermal carbonization of digested sewage sludge: The fate of heavy metals, PAHs, PCBs, dioxins and pesticides. *Chemosphere*, *307*, 135997. https://doi.org/10.1016/j.chemosphere.2022.135997

Ţurcanu, A. A., Matei, E., Râpă, M., Predescu, A. M., Coman, G., & Predescu, C. (2022). Biowaste Valorization Using Hydrothermal Carbonization for Potential Wastewater Treatment Applications. *Water*, *14*, 2344. https://doi.org/10.3390/w14152344

Wang, X., Li, C., Zhang, B., Lin, J., Chi, Q., & Wang, Y. (2016). Migration and risk assessment of heavy metals in sewage sludge during hydrothermal treatment combined with pyrolysis. *Bioresource Technology*, *221*, 560–567. https://doi.org/10.1016/j.biortech.2016.09.069

Wang, Y. jie, Yu, Y., Huang, H. jun, Yu, C. long, Fang, H. sun, Zhou, C. huo, Yin, X., Chen, W. hua, & Guo, X. chun. (2022). Efficient conversion of sewage sludge into hydrochar by microwave-assisted hydrothermal carbonization. *Science of the Total Environment*, *803*, 149864. https://doi.org/10.1016/j.scitotenv.2021.149874

Wu, Q., Yu, S., Hao, N., Wells, T., Meng, X., Li, M., Pu, Y., Liu, S., & Ragauskas, A. J. (2017). Characterization of products from hydrothermal carbonization of pine. *Bioresource Technology*, *244*, 78–83. https://doi.org/10.1016/j.biortech.2017.07.138

Zajac, G., Szyszlak-Bargłowicz, J., & Szczepanik, M. (2019). Influence of biomass incineration temperature on the content of selected heavy metals in the ash used for fertilizing purposes. *Applied Sciences*, *9*, 1790. https://doi.org/10.3390/app9091790

Zhang, X., Zhou, J., Xu, Z., Zhu, P., & Liu, J. (2021). Characterization of heavy metals in textile sludge with hydrothermal carbonization treatment. *Journal of Hazardous Materials*, *402*, 123635. https://doi.org/10.1016/j.jhazmat.2020.123635

9 Abstracts: Materials engineering

9.1 A phase-field study of the energy and morphology of martensite–twinned martensite interface in CuAlNi shape memory alloy

Seyedshoja Amini*,1, Mohsen Razaee-Hajidehi[1], Stanisław Stupkiewicz[1]

1. Institute of Fundamental Technological Research (IPPT), Polish Academy of Sciences, Warsaw, Poland

e-mail: samini@ippt.pan.pl

KEYWORDS: *microstructure, martensitic phase transformation, transition layer, phase-field method, size effects*

When a single-crystal bar of CuAlNi shape memory alloy (SMA) is under the temperature gradient, a special microstructure (known as λ-microstructure) is observed (Figure 9.1.1(a, b)). This microstructure involves two macroscopic interfaces between austenite and twinned martensite and two between martensite and twinned martensite. At the micro scale of martensite–twinned martensite interface, needle-like twins are revealed as depicted in Figure 9.1.1.(c)[1].

This study[2] aims to conduct a numerical investigation employing phase-field approach, with a primary focus on simulating the morphology of the transition layer and analyzing its energy measures. More specifically, the effects of twin spacing and twin volume fraction on the morphology of transition layer, elastic strain and interfacial energy quantities are considered. Our simulation results demonstrate the tapering and bending in the needle-shaped microstructures which are qualitatively in agreement with literature[1]. Moreover, in certain twin volume fractions, twin branched morphology occurring as a result of minimize the total free energy stored in the microstructure.

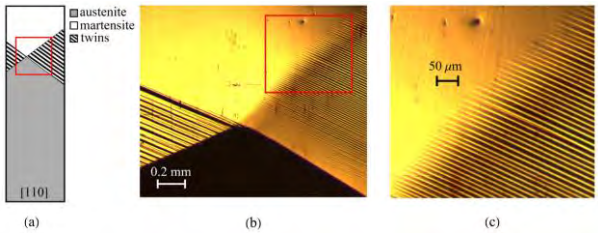

Figure 9.1.1. (a) Schematic of λ-microstructure on a [110] plane in single-crystal bar of CuAlNi, (b) close-up view of the λ-microstructure, (c) magnified view of needle shaped microstructure at the martensite–twinned martensite interface[1]

9.2 Continuum model of twin branching in shape memory alloys

Seyedshoja Amini*,1, Mohsen Razaee-Hajidehi[1], Stanisław Stupkiewicz[1]

1. Institute of Fundamental Technological Research (IPPT), Polish Academy of Sciences, Warsaw, Poland

e-mail: samini@ippt.pan.pl

KEYWORDS: *shape memory alloys, branched microstructures, free energy, continuum model*

The presence of a branched microstructure or the refinement of twin spacing near the macroscopic austenite-twinned martensite (A-MM) interface in shape memory alloys has been observed in numerous experiments[3]. This morphology forms as a means to reduce the elastic strain energy localized at macroscopic A-MM interface at the cost of increasing the interfacial energy. Recently, Seiner et al.[4] introduced a discrete model of branching, focusing on estimating the elastic strain energy and interfacial energy of each branched microstructure.

The main objective of the present study is to introduce a simplified continuous energy formulation based on the model proposed by Seiner et al.[4]. Our findings reveal that the results of our model are in quantitative agreement with the literature over a wide range of input parameters[4].

[1] H. Seiner, O. Glatz, M. Landa, A finite element analysis of the morphology of the twinned-to- detwinned interface observed in microstructure of the Cu–Al–Ni shape memory alloy, Int. J. Solids Struct. 48 (2011) 2005–2014

[2] S. Amini, M. Rezaee-Hajidehi, S. Stupkiewicz, Energy and morphology of martensite–twinned martensite interface in CuAlNi shape memory alloy: A phase-field study, Computational Materials Science 230 (2023) 112472

[3] C. Zhang, G. Qin, S. Zhang, X. Chen, Y. He, Hysteresis effect on austenite-martensite interface in Ni-Mn-Ga single crystal, Scripta Materialia 222 (2023) 115029

[4] H. Seiner, P. Plucinsky, V. Dabade, B. Benesova, R. D. James, Branching of twins in shape memory alloys revisited, J. Mech. Phys. Solids 141 (2020) 103961

9.3 Use of used cooking oil as a modifier of road bitumen

Ivan Danylevich*,1, Yuriy Hrynchuk1, Volodymyr Reutskyy1, Volodymyr Gunka1, Olha Poliak1

1. Lviv Polytechnic National University, Lviv, Ukraine
e-mail: ivan.danylevych.kht.2021@lpnu.ua

KEYWORDS: *bitumen, modification, epoxying, road, used oil*

Road pavements tend to deteriorate and wear out over time. As one of the key elements of the road surface, bitumen often does not meet modern requirements, which is why modifying additives for road bitumen are being developed to improve the characteristics of both the bitumen itself and the road surface as a whole. Another problem is the insufficient utilization or use of used cooking oil. It is used in the production of biodiesel.

By combining these two aspects, we propose a joint solution - using food waste as a modifying additive to road bitumen. The idea is to use recycled cooking oil (used oil) as a modifier to improve the properties of road bitumen, thereby solving the environmental problem associated with industrial waste.

To do this, we first epoxidize the used oil. The procedure involves mixing the used oil in a 3-liter round-bottomed three-neck flask equipped with a stirrer, reflux condenser, thermocouple, and drip funnel with a mixture of hydrogen peroxide (60%) and formic acid. The next step is amidation of the resulting product. The amidation was carried out at 70 °C, the process duration was 4 hours, and monoethanolamine was used as the amidating agent.

The resulting product was further studied as a modifying additive for petroleum bitumen. The modification was carried out according to the following parameters: temperature - 180 °C, mixing speed – 600 rpm, modification time - 180 minutes. The additive content is 3% by weight of bitumen.

After the bitumen was modified, the bitumen characteristics were analysed, including softening point (°C), adhesion to glass (points), and penetration (0.1 mm). The results of the analysis are presented:

- The softening point (°C) of BND70/100+EURO-A is 46.6 and that of BND70/100+EURO-B is 49.4.
- Adhesion (point) of BND70/100+EURO-A is 4.0, but that of BND70/100+EURO-B is 4.5.
- Penetration at 25 °C, ($m \times 10^{-4}$ (0.1 mm)) BND70/100+EURO-A is 62 but BND70/100+EURO-B is 47.

It is important to note that a change in the method of manufacturing a bitumen modifier based on epoxy oil of the EURO-B type has a positive effect on the result. The successful approach allows us to preserve both amine and epoxy groups. Experimentally, it was confirmed that the characteristics of the resulting product exceed not only the original ones but also the indicators of EURO-A, which were included in the modified bitumen.

9.4 Influences of temperature and extractions duration on the chemical composition of digestate extracts

Eglė Didžiulyte*,1, Rasa Šlinkšienė1

1. Department of Physical and Inorganic Chemistry, Kaunas University of Technology, Kaunas, Lithuania
e-mail: egle.didziulyte@ktu.lt

KEYWORDS: *digestate, organic farming, organic carbon*

About 40% of the land area is used for agricultural activities. Extremely intensive and chemicalized agriculture severely damages the naturally formed ecosystem. This problem causes concern about soil conservation, improving its quality, human health, and environmental protection and it encourages the search for alternative methods of agriculture. One such method is organic farming in which mineral fertilizers are not used, and nutrients needed by plants are provided using biological substances of organic origin. One such waste is digestate.

Most of the digestate is directly used as fertilizer. Digestate regulates soil structure because it is rich in organic matter. Scientific studies confirm that biogas digestate is used as a soil fertilizer, as a biological product in the fight against diseases and pests, and as a substrate in hydroponics. Because the digestate is rich in organic matter, during the study when three different digestates were used (Agaro riešutas (Biržai), Tvari energija (Vievis), and Kurana (Pasvalys)), firstly the organic carbon content was determined. The tests were carried out on dried digestates, which were of two types: whole and chopped. It was found that the content of organic carbon is higher in whole samples, about 50.0%, and in chopped – 40%. In order to obtain the maximum concentration of organic carbon from the used digestates, extracts were produced based on water (plants absorb water-soluble carbon more easily), by applying different production conditions. The samples were kept for 3-9 days at room temperature and for 3-9 hours at different temperatures, mixed with a mechanical stirrer and in an ultrasonic bath. Also, the samples were heated at temperatures of 50-90 °C. It has been found that the amount of organic carbon produced by different extraction methods is similar.

The highest concentration of organic carbon is obtained when the extracts are prepared for 9 hours and exposed to a temperature of 90 °C. Also water-soluble total nitrogen has been found to range from 0.81% to 10.78%; water-soluble phosphorus (P_2O_5) 0.69-1.60%, water-soluble potassium (K_2O) 0.69-0.75%.

9.5 Valence and coordination states of Co transition metal ions in a view of the borate bioactive glass structure

Patrycja Gaćkowska*,1, Michał Dziadek[1], Wojciech Błachucki[2], Katarzyna Cholewa-Kowalska[1]

1. Department of Glass Technology and Amorphous Coatings, AGH University of Krakow, Krakow, Poland
2. Institute of Nuclear Physics Polish Academy of Sciences, Cracow, Poland

e-mail: pgackowska@agh.edu.pl

KEYWORDS: *bioactive borate glass, transition metal ions, cobalt ions, valence state*

Bioactive glasses containing B_2O_3 are intriguing amorphous materials with distinctive structure and physical characteristics. Transition metal ions, crucial in tissue engineering, play a major role in stimulating diverse biological processes. For instance, cobalt ions promote angiogenesis both *in vitro* and *in vivo*. The properties of these glasses heavily rely on the proportion of different valence states and coordination of transition metal ions within the glassy matrix.

This study aims to evaluate the influence of the synthesis method on valence state and coordination of the transition metal (Co) ions. Cobalt-doped BBGs were obtained using traditional melting and the sol-gel method with various organic boron precursors (triethyl borate – TEB, tributhyl borate – TBB, trimethyl borate – TMB, trimethoxyboroxine – TMBx). The glass composition was $40B_2O_3$-(54-x)CaO-$6P_2O_5$-xCoO %mol, where x was 0 and 5. X-ray diffraction (XRD) determined the phase composition and crystallization tendency, while infrared spectroscopy (FTIR) provided insights into structural characteristics. The oxidation state and coordination of cobalt were investigated through UV-Vis spectroscopy. X-ray absorption spectroscopy (XAS) determined the concentration of transition metal ions (Co) at each oxidation state in molten glass and glass obtained by sol-gel method using TMBx as boron precursor.

The obtained BBGs exhibited diverse colours, attributed to the presence of cobalt ions at different oxidation states and/or in various coordination within the glass matrix. XRD analysis proved the amorphous nature of all samples (except melt-derived). The molten glass contains Co^{2+} ions both in octahedral and in tetrahedral coordination, while the glasses obtained by the sol-gel method contains Co^{2+} ions only in tetrahedral coordination. XAS spectra proved presence of metallic cobalt and Co^{2+} ions in both samples, while Co^{3+} ions are present only in molten glass. The study's analysis revealed that both the glass synthesis method and the environment of transition metal ions significantly influence the oxidation state and coordination of cobalt ions in BBGs.

Acknowledgements

This work was supported by the program „Excellence initiative – research university" for the AGH University of Krakow.

9.6 Sol-gel synthesis of metal-ion modified preceramic polymers for DLP 3D printing

Justyna Grygierek*,1, Jakub Marchewka[1], Patryk Bezkosty[1], Maciej Sitarz[1]

1. Faculty of Material Science and Ceramics, AGH University of Krakow, Krakow, Poland

e-mail: jgrygierek@student.agh.edu.pl

KEYWORDS: *additive manufacturing, DLP, sol-gel*

Silicon oxycarbide materials, so-called black-glasses, are characterised by an amorphous silica structure in which carbon ions are introduced by substitution of some of oxygen atoms. This results in a local increase in bond density thereby strengthening the structure of the glass network. By the phase separation, carbon can form a free phase, which gives characteristic colour of these materials. Its total content and the ratio between the amounts introduced into the structure and as a separate phase, determines the properties of black glasses. The amount of carbon can be controlled by using specific organosilicon compounds as substrates in the synthesis.

In this study, sol-gel synthesis of ladder-like polysilsesquioxanes was performed using 3-(trimethoxysilyl)propyl methacrylate (TMSPMA) and dimethyldiethoxysilane (DMDES) as substrates. The precursors have been appropriately selected to enable the processing of the material by Digital Light Processing (DLP) 3D printing. Modifications with specific ions (e.g. copper(II) and calcium cations) were introduced by adding an appropriate amount of hydrated nitrate(V) of a given metal into the reaction mixture in order to provide desired properties of the final product (e.g. catalytic).

The obtained materials were subjected to detailed microstructural (SEM analysis) and structural (FT-IR and Raman spectroscopy) characterisation. Through utilising the DLP method, it was demonstrated that the material could be prepared with a defined geometry. Additionally, SEM analysis indicated that an appropriate addition of metal cations allows for the microstructure to be tailored for catalytic reactions.

Acknowledgements

This research was funded by the National Science Centre, Poland, grant no. 2019/35/B/ST5/00338 and supported by the program „Excellence initiative – research university" for the AGH University of Krakow.

9.7 Electrospinning as an innovative method to improve the mechanical properties of eco-friendly and fully biodegradable food packaging

Justyna Jakubska*,1, Gabriela Dudek1

1. Department of Physical Chemistry and Technology of Polymers, Gliwice, Poland
e-mail: jl309041@student.polsl.pl

KEYWORDS: *electrospinning, nanofibers, biodegradable films, eco-friendly food packaging, polysaccharides*

Considering growing public awareness and the European Union policy on the need to care for the environment, it is important to enhance the use of naturally derived substances instead of commonly used plastics to produce food packaging materials. For daily use, films based on biodegradable polymers have already appeared. However, chitosan or sodium alginate have not been applied on an industrial scale until now, mainly due to the significantly weaker mechanical properties obtained materials compared to traditional food packaging. To prevent this issue, natural polymers are subjected to various modifications. In this case, the formation of multilayer films with electrospinning nanofibres is created.

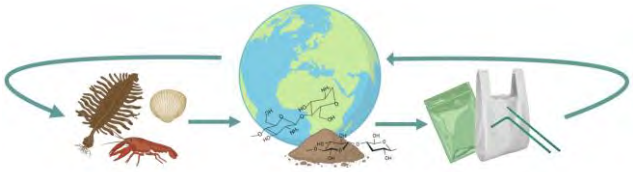

Figure 9.7.1. The closed loop diagram of produced food packaging films.

The obtained materials were characterised by mechanical, barrier (oxygen, carbon dioxide and water vapour), hydrophilic and antimicrobial properties. Furthermore, the structures of the investigated materials were examined. The results showed that the addition of an electrospinning layer to the sheet of chitosan and alginate material significantly improve the mechanical properties of considered films. Moreover, connection of two different layers also impacts on the other film properties, making them better for use as biodegradable packaging films.

Acknowledgements

This research was co-financed by the Ministry of Education and Science of Poland under grant SKN/SP/535370/2022 and Silesian University of Technology under project 31/010/SDU20/0006-10.

9.8 Improving the efficiency of ethanol dehydration via pervaporation using magnetite and molecular magnet combination as a filler for alginate membranes - analysis of the synergistic effect

Łukasz Jakubski*,1, Gabriela Dudek1

1. Department of Physical Chemistry and Technology of Polymers, Gliwice, Poland
e-mail: lukajak378@student.polsl.pl

KEYWORDS: *synergistic effect, single-molecule magnet, magnetite, sodium alginate, hybrid membrane, pervaporation, ethanol dehydration*

The alginate membranes filled with various proportions of mixed magnetite and molecular magnet[$Fe_4(acac)_6(Br\text{-}mp)_2$] (MM) were investigated to improve the process of ethanol dehydration via pervaporation. The results show that the synergistic effect of combining these two fillers strongly improves the efficiency of the process.

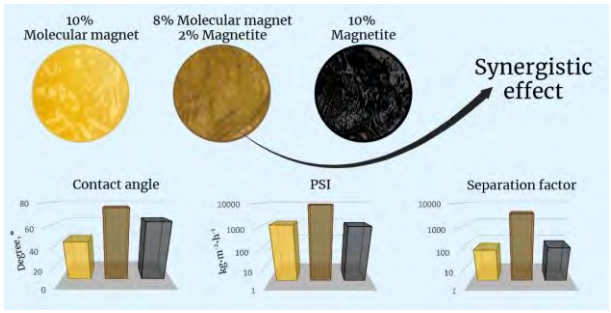

Figure 9.8.1. The comparison of results obtained for membranes containing magnetite and mm alone as filler of membrane and for their combination of 2% magnetite and 8% molecular magnet in the membrane.

MMs represent a new class of magnetic materials. The powder shows paramagnetic properties and the ability for excellent dispersion in the polymer matrix. On the other hand, magnetite exhibits ferromagnetic properties but does not show good dispersion in the membrane. The favourable synergistic effect was achieved by combining a substance with strong magnetic properties and a substance with excellent dispersion. It contributes to the homogeneous dispersion of mm and magnetite particles in the polymer matrix. As a result, the molecules of fillers do not form clusters in the membrane. They are present in the membrane throughout the volume, allowing them to interact freely with water molecules permeating the membrane. In the case of magnetite alone, such a strong interaction between the magnetic field and water molecules does not occur, which results in lower ethanol dehydration efficiency.

The efficiency varied depending on the percentage of powders. The best results were obtained for an alginate membrane filled with 2 wt% magnetite and 8 wt% molecular magnet, for which the PSI was 8438.9 $kg \cdot m^{-2} \cdot h^{-1}$, and the separation factor was 3425.5.

Acknowledgements

This research was co-financed by the Silesian University of Technology under project 31/010/SDU20/0006-10.

9.9 (Meth)acrylate-based copolymers for potential use as hydrophobic and self-healable coatings

Katarzyna Kisiel[1], Izabela Zaborniak[1], Arkadiusz Zych[2], Paweł Chmielarz[*,1]

1. Department of Physical Chemistry, Faculty of Chemistry, Rzeszow University of Technology, Rzeszow, Poland
2. Smart Materials, Italian Institute of Technology, Genova, Italy

e-mail: p_chmiel@prz.edu.pl

KEYWORDS: *vitrimers, self-healing, poly(meth)acrylates, SARA ATRP*

One of the outstanding features that render vitrimers highly appealing for industrial applications is their ability to undergo self-repair under mild conditions. Coatings formulated from these materials possess the potential to significantly enhance the products durability. Hence, it's crucial to develop new techniques to prepare vitrimers.

In this research, we employed supplemental activation and reducing agent atom transfer radical polymerization (SARA ATRP) of tert-butyl acrylate (tBA), n-butyl acrylate (nBA), 2,3-dihydroxypropyl methacrylate (DHPMA) and diboronic ester dimethacrylate (DBEDMA) – cross-linker enabling dynamic bond exchange in the resulting polymer, using ppm amounts of catalyst. Additionally, we conducted two separate polymerizations to illustrate the influence of different conditions on the characteristics of the final polymers. One procedure was executed without the cross-linker, while the other utilized divinylbenzene (DVB) as a substitute for DBEDMA, forming a crosslinked polymer without the potential for dynamic bond exchange.

We demonstrated the successful application of SARA ATRP in the preparation of vitrimers. Final polymers exhibited precisely controlled copolymer structure. The prepared materials hold promise for application as coatings in divergent materials such as textiles, wood or glass. This involves the process of bromination followed by functionalization with vitrimers, imparting hydrophobic and self-healing properties to the materials.

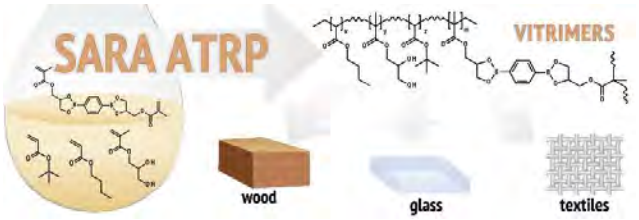

Figure 9.9.1. Synthesis of vitrimers and their potential use for the functionalization of surfaces.

Acknowledgements

Financial support from Ministry of Education and Science under the program "Students Research Clubs creates innovations" (Contract no: SKN/SP/569572/2023) and from National Science Centre in Poland as a part of the SONATA BIS 10 project (2020/38/E/ST4/00046).

9.10 MTMS aerogel-based ssPCM – morphology effect and sorption method investigation

Monika Klimek[*,1], Ewelina Radomska[2], Kinga Pielichowska[3], Bartosz Nowak[1]

1. Faculty of Chemical and Process Engineering, Warsaw University of Technology, Warsaw, Poland
2. Faculty of Energy and Fuels, AGH University of Cracow, Cracow, Poland
3. Faculty of Materials Science and Ceramics, AGH University of Krakow, Krakow, Poland

e-mail: monika.klimek3.stud@pw.edu.pl

KEYWORDS: *ssPCM, paraffins, aerogel, MTMS, spatial stabilisation*

Phase change materials (PCMs) allow heat storage as latent heat due to the phase transition, most often solid-liquid. Unfortunately, these materials cannot be used as independent heat storage media due to the possible leakage of the liquid phase during the phase change, leading to loss of material and corresponding environmental contamination. This issue can be overcome by the spatial stabilisation of PCMs utilising a matrix, providing the highest possible heat transfer with the lowest possible leakage. The organosilica aerogels exhibit high porosity, mechanical strength and flexibility, with good affinity to paraffin and hydrophobicity, thus making them suitable for shape-stabilized PCM (ssPCM) matrix.

This research investigated the effect of the methyltrimethoxysilane (MTMS)-based aerogel morphology and the stabilisation method of an organic phase change material – paraffin wax – on the PCM loading and the leakage during phase transition cycles. Aerogels with different internal structures (nanoporous, co-continuous and microporous) were used as matrix for PCM stabilization. Stabilisation was carried out using two methods: a dry method (sorption of PCM into a dry aerogel) and a wet method (sorption of PCM into a wet gel with simultaneous solvent removal). In addition, the effect of sorption temperature on aerogels' sorption capacity was investigated. Research was supported with wettability investigation, FT-IR and DSC tests of aerogel with and without PCM.

In the study, the inertial structure of the aerogel was proven to have a significant effect on stabilising the PCM and minimalizing leakage during phase change cycles. Smaller pore size, due to high capillary pressure, ensured good retention of the PCM. On the other hand, larger pore size resulted in easier sorption of paraffin and less susceptibility to damage when the PCM volume changed during the phase transformation. It was noted that the wet sorption method was more efficient due to lower aerogel volume shrinkage which translated directly into higher PCM loading.

Acknowledgements

This work was supported by The National Science Centre, Poland - project "Organosilica aerogel shape-stabilized phase-change materials for solar distillation system enhancement" PRELUDIUM-20 (2021/41/N/ST8/02690).

9.11 Printing parameter optimization to achieve high-resolution objects for the dentistry

Karolina Kozanecka*,1, Monika Topa-Skwarczyńska[1], Katarzyna Starzak[1], Andrzej Świeży[1,2], Joanna Ortyl[1,2,3]

1. Laboratory of Photochemistry and Optical Spectroscopy, Faculty of Chemical Engineering and Technology, Cracow University of Technology, Cracow, Poland
2. Photo4Chem sp. z o.o., Cracow, Poland
3. Photo HiTech sp. z o.o., Cracow, Poland

e-mail: k.kozanecka@onet.eu

KEYWORDS: *3D printing, photopolymerization, dental materials*

Liquid, light-curable resins, or photopolymers are the main components used in photopolymerization processes. The majority of photopolymers respond to light with wavelengths in the ultraviolet (UV) region. These materials go through a chemical reaction that solidifies them when exposed to radiation. This process, known as photopolymerization, usually involves a large number of both chemical and physical transformations and is quite complex[5].

Rapid prototyping, also referred to as additive manufacturing or 3D printing, is a manufacturing technique that uses powdered metal, plastic, photosensitive resin, and other materials to create objects layer-by-layer using the digital design of the desired 3D object[6]. Light curing has fundamentally altered the field of dentistry. Apart from bonding to tooth structure, maybe no other breakthrough has increased dentistry's ease of use, productivity, efficiency, and success in such a way[7]. Compared to conventional production techniques, photocurable polymer materials in dental 3D printing provide a number of benefits. These include shorter production times, more flexible designs, less material waste, and better mechanical properties in the finished dental restorations[8].

This paper presents the possible use of compositions incorporating the new photoinitiators for broad-spectrum dental applications in 3D printing, along with optimization strategies for 3D printing conditions.

Acknowledgements

This research was funded by National Centre for Research and Development in Poland under the Lider Program, grant number LIDER13/0156/2022.

[5] Gibson, I., Rosen, D., Stucker, B. (2010). Photopolymerization Processes. In: Additive Manufacturing Technologies. Springer, Boston, MA. https://doi.org/10.1007/978-1-4419-1120- 9_4

[6] H. Ren, J. Yang, L. I. Chaolin, H. Liu, X. Zhang, J. Chengdu Technol. Univ. 2018, 21, 30

9.12 Synthesis of Silver-Modified Halloysite – a material with antibacterial properties

Karolina Kryszczyńska*,1, Michał Stor[1], Andrzej Krasiński[1]

1. Faculty of Chemical and Process Engineering, Warsaw University of Technology, Warsaw, Poland

e-mail: karolina.kryszczynska.stud@pw.edu.pl

KEYWORDS: *modified halloysite, antibacterial material, bacteriostatic additives, Escherichia coli*

Various types of water pollution are currently among the most serious threats to aquatic ecosystems and human health. One of these pollutants is microbiological contamination, such as bacteria, viruses, and protozoa. The quest for new methods to remove them is crucial to ensure access to clean water. Materials with antibacterial properties can serve this purpose. One such material is a composite based on a natural mineral, halloysite, modified with silver. This material can be used as an antibacterial agent in water filters. The primary aim of the research is to optimize the synthesis process of the composite and the composite integrated into polymer structures for industrial applications.

A series of composite syntheses with different parameters were conducted during the research. The material was synthesized using sulfuric acid-treated halloysite obtained from the Polish "Dunino" mine, KH-792 trimethoxysilane, silver nitrate, and a $NaBH_4$(aq) solution. Each synthesis differed in the concentrations of these reagents and the separation method. Among the prepared materials, one exhibiting the greatest durability and antibacterial properties was chosen. This sample was then embedded into the structure of polymer fibers. The antibacterial properties of the prepared composite and the composite within the polymer structure were examined through a bacteriostatic plate-based *in vitro* test. The bacteria, which was selected for the test was *Escherichia coli* (*E. coli*), one of the most common indicators of microbiological contamination.

The research results confirmed the antibacterial properties of the composite. The plate-based *in vitro* test showed inhibition of *E. coli* growth around the applied material. Furthermore, the composite's thermal resistance up to 300 °C was demonstrated, which is crucial for manufacturing polymer fibers with the composite using the melt-blown method. The composite constitutes approximately 0.5-1% of the liquid filter's polymer structure. The antibacterial nature of such a filter structure was observed, forming the basis for further research in a flow system.

Acknowledgements

The research was supported by the Polish National Centre for Research and Development, grant no. TECHMATSTRATEG-III/0005/2019-00"

[7] Rueggeberg, Frederick A. "State-of-the-art: dental photocuring—a review." Dental Materials 27.1 (2011): 39-52

[8] Noworyta, M.; Topa-Skwarczyńska, M.; Jamróz, P.; Oksiuta, D.; Tyszka-Czochara, M.; Trembecka-Wójciga, K.; Ortyl, J. Influence of the Type of Nanofillers on the Properties of Composites Used in Dentistry and 3D Printing. Int. J. Mol. Sci. 2023, 24, 10549

9.13 Structural analysis of polymer-derived SiCN with tuneable carbon content

Zofia Kucia*,1, Maciej Bik[1], Piotr Jeleń[1], Daria Pakuła[2], Robert Przekop[3], Maciej Sitarz[1]

1. Faculty of Materials Science and Ceramics, AGH University of Krakow, Krakow, Poland
2. Faculty of Chemistry, Adam Mickiewicz University in Poznan, Poznan, Poland
3. Centre for Advanced Technologies, Adam Mickiewicz University in Poznan, Poznan, Poland

e-mail: zofiakucia@agh.edu.pl

KEYWORDS: *polymer-derived ceramics, silicon carbonitride, spectroscopy*

Polymer-derived ceramics (PDCs) is a group of advanced ceramic materials with easily tuneable properties, which makes them applicable in different fields. One member of the PDCs group is silicon carbonitride (SiCN), a material which can simultaneously contain covalent Si-N and Si-C bonds as well as the free carbon phase (sp^2-hybridized carbon nanodomains). The presence of the former ensures that the material exhibits good resistance to high-temperature oxidation, and the latter provides electrical conductivity.

In this study, SiCN with tuneable carbon content was obtained from polysilazanes synthesized by hydrosilylation of Si-H containing silazane monomers and vinyl-group-containing crosslinkers. Two monomers were chosen: 1,1,3,3-tetramethyldisilazane and 1,2,3,4,5,6,7,8-octamethyltetracyclosilazane, and three crosslinkers: 1,7-octadiene, divinylbenzene and 1,3,5-trivinyl-1,3,5-tri-methylcyclotrisilazane. In total, 6 polysilazanes were synthesized. The crosslinkers contain a different number of carbon atoms, therefore the polysilazanes, and hence the SiCN ceramics, also contain a different amount of carbon. The polysilazanes were pyrolyzed in pure argon and in argon-hydrogen atmosphere at two temperatures: 800 and 1000 °C, to form amorphous SiCN with a varying carbon content. The materials before and after pyrolysis were characterized by FTIR, Raman and ^{29}Si and ^{13}C MAS NMR spectroscopy, XRD, TGA, XRF, combustion elemental ana-lysis, and SEM.

The results confirm that the obtained ceramic materials contain Si-N and Si-C bonds as well as the free carbon phase, therefore, SiCN was formed. According to elemental combustion analysis, the samples contain a varying carbon content. However, unfortunately, the presence of oxygen in the material was also confirmed.

Acknowledgements

This work has been supported by the Polish National Science Centre project No 2019/35/B/ST5/00338: "New biocompatible coatings on metallic substrates based on materials from the Si-O-C system". We kindly acknowledge Prof. Magdalena Szumera (Faculty of Materials Science and Ceramics, AGH University of Krakow) for TGA measurements, Ph.D. Zbigniew Olejniczak (Institute of Nuclear Physics, Polish Academy of Sciences) for NMR measurements, Ph.D. Michał Kubecki (Łukasiewicz Research Network-Institute for Ferrous Metallurgy) for the combustion analysis, and MSc. Eng. Patryk Szymczak (Faculty of Materials Science and Ceramics, AGH University of Krakow) for XRD and XRF measurements.

9.14 Experimental research on rheological and tribological properties of oil suspensions with the addition of MoS_2/CNTs hybrid nanostructures

Weronika Ługowska*,1, Wojciech Orciuch[1], Zuzanna Bojarska[1], Łukasz Makowski[1]

1. Faculty of Chemical and Process Engineering, Warsaw University of Technology, Warsaw, Poland

e-mail: weronika.lugowska.stud@pw.edu.pl

KEYWORDS: *oil additives, hybrid materials, tribological properties, MoS_2/CNTs nanoparticles, viscosity distribution*

In the twenty-first century, studies are focusing on the responsible use of energy and raw materials. Car industries also began to search for a method to prolong a car's engine life. The engine operates in high temperatures. This and the influence of friction causes damage and wearing down of gears. To prevent those, one should use highperformance lubricants. They help to reduce the power loss caused by friction both in engine start and its operating phases in high temperatures. Lubricants consist of the base oil to which one adds additives to improve their properties and efficiency. Recent studies show that nanomate-rials as an additive in lubricants significantly reduce the friction between gears.

This work examined the tribological and rheological properties of oil suspensions with the addition of nanostructures based on molybdenum disulfide and carbon nanotubes (MoS_2/CNTs) and surfactant in order to decrease friction coefficient. Molybdenum disulfide creates layers consisting of covalently connected S-Mo-S molecules. Additionally, individual layers are connected to each other by weak Van der Waals bonds, thanks to which they can move freely in relation to each other. This feature means that MoS_2 has low coefficient of friction and is an effective lubricant additive. Additionally, its effects is enhanced by the addition of carbon nanotubes. Thanks to their uncial shape, are also characterized by a low coefficient of friction. To prevent the sedimentation of these hybrid nanoparticles the surfactant was added. The base oil used during the tests was oil 10W-40 by *Liqui-Moly*. Various concentrations of nano-additives as well as various surfactants were tested to find the best oil composition. The samples were tribologically tested at the following temperatures: -10 °C, 0 °C, 25 °C, 75 °C, 100 °C. The examination was carried out on a modern multifunctional measuring device *Anton Paar*.

Conducted tests proved, that hybrid nanostructures MoS_2/CNTs significantly decreased friction. The results show that the most effective surfactant concentration in terms of performance is 70%$_{wt.}$. With this quantity the value of the coefficient of friction at 75 °C is 18% lower than for the oil with the addition of 0.5%$_{wt.}$ MoS_2/CNTs.

Acknowledgements

This study was funded by the National Science Centre through the project No 2021/41/N/ST8/03764

9.15 Cationic modifications of black glasses – preparation and properties

Klaudia Łyszczarz*,[1], Piotr Jeleń[1], Magdalena Szumera[1], Magdalena Gawęda[2], Maciej Sitarz[1]

1. AGH University of Krakow, Krakow, Poland
2. NOMATEN CoE, NOMATEN MAB, National Centre for Nuclear Research, Otwock-Swierk, Poland

e-mail: lyszczar@agh.edu.pl

KEYWORDS: *black glasses, FT-IR, PDC*

Black glasses are ceramic materials typically obtained through the pyrolysis process of organosilicon compounds. Of particular interest is the possibility of easily modifying the properties of SiOC materials by introducing various cations into their structure. This allows for the design of materials with desired properties. The aim of the research was to obtain boron-modified black glasses (SiOCB). Preparation of these materials was carried out in stages.

First, pre-ceramic precursors were obtained through hydrolytic polycondensation (sol-gel) carried out in a controlled atmosphere of oxygen and argon. Boron atoms were introduced by adding trimethyl borate to the structure of ladder-like silsesquioxanes. The introduction of these ions, which are in a +3 oxidation state, brings a series of benefits in case of material properties. Furthermore, they significantly increase the thermochemical stability of black glasses obtained through their pyrolysis. The pyrolysis process of modified compounds will take place within a selected temperature range based on TG/DSC studies, in a controlled atmosphere of argon using an alumina tube furnace. This will ensure stability and repeatability of the conducted ceramization process.

Structural analysis of prepared sols using spectroscopic methods (infrared spectroscopy, FT-IR) was used in order to confirm the successful introduction of boron into black glass ladder precursors. Final samples were subjected to structural tests (FT-IR, Raman spectroscopy), thermal research (thermogravimetry (TGA) and differential scanning calorimetry (DSC)) as well as laser-induced breakdown spectroscopy (LIBS) in order to check the concentration of major elements.

To conclude, cation-modified black glasses are possible to obtain by hydrolytic polycondensation method and then the process of pyrolysis. The conducted research showed that the materials obtained from the SiOC system containing boron were successfully obtained.

Acknowledgements

Scientific work was funded by the state budget within the program of the Minister of Education and Science of Poland under the name "Perły Nauki I" project number PN/01/0134/2022 funding amount 240 000 PLN, total project value 240 000 PLN.

9.16 Cost-effective electroconductive sodium lignosulfonate/carbon nanotube composite coating for paper electronics

Anna Martin*,[1], Damian Łukawski[1], Alina Dudkowiak[1]

1. Faculty of Materials Engineering and Technical Physics, Poznan University of Technology, Poznan, Poland

e-mail: anna.martin@doctorate.put.poznan.pl

KEYWORDS: *carbon nanotube, coating, paper, sodium lignosulfonate, cellulose*

In the era of continuous scientific and technological progress, nanomaterials, especially carbon nanotubes (CNTs), play a crucial role in modern technologies. Their exceptional properties, such as excellent electrical conductivity and chemical activity, make CNTs increasingly used in the production of thin-film electronic components. Both the scientific and technological fields are particularly interested in aqueous suspensions of CNTs and biopolymers, such as sodium lignosulfonate (SLS), a derivative of lignin. SLS, due to its dispersing properties, has found applications in dispersing dyes, pesticides, and carbon nanomaterials.

This work presents research on electroconductive coatings containing CNT and SLS, obtained using an automatic paint applicator. The stability of CNT/SLS suspensions, dependence of coating resistance on ultrasonic homogenization time, and hygroscopic properties were investigated. The wetting angle for different CNT concentrations and sensitivity tests of the SLS/CNT composite to water exposure were determined. Additionally, the mechanical strength of the obtained coatings was assessed with a perspective on potential applications in organic printed electronics. The research results indicate that SLS is an effective agent for creating aqueous suspensions of CNT, and the resulting electroconductive coatings are flexible, resistant to bending, and exhibit resilience to annealing. Exposure of samples to water and water vapor influences the electrical conductivity of the composite while maintaining the integrity of the layer.

The SLS/CNT composite possesses low surface resistance, enabling its application in various sensors and heaters. Moreover, the production costs of the coating are relatively low, making it an attractive material for a wide range of applications. Despite promising results, there is potential for further research, such as the application of protective layers, or the addition of graphene or other carbon nanotubes to improve electrical conductivity.

Acknowledgements

The authors would like to thank the Ministry of Education and Science of Poland. This work was financially supported by The National Centre for Research and Development as part of the project TANGO-IV-A/0014/2019-00.

9.17 The effect of water on electroconductive carbon composite coatings containing sodium carboxymethylcellulose

Anna Martin*,1, Damian Łukawski[1], Alina Dudkowiak[1]

1. Faculty of Materials Engineering and Technical Physics, Poznan University of Technology, Poznan, Poland

e-mail: anna.martin@doctorate.put.poznan.pl

KEYWORDS: *carbon nanotube, coating, sodium carboxymethylcellulose, cellulose*

In recent years, carbon nanomaterials, such as carbon nanotubes (CNTs), have facilitated the fabrication of numerous types of thin-film, flexible electrical and electronic components, including conductive paths, transistors, sensors, and heating surfaces. Electroconductive coatings are produced through techniques like printing, spraying, or coating layers of CNTs from aqueous suspensions. Due to the thermal stability of CNTs at high temperatures and their hydrophobicity, it can be inferred that the dispersing substance plays a crucial role in modifying the conductivity of carbon coatings in the presence of environmental factors. Some commonly used stabilizing biopolymers exhibit lower resistance to environmental conditions, affecting the electrical conductivity of the coating. Changes in the resistance of carbon coatings due to external factors are utilized in monitoring devices, such as humidity, pressure, or temperature sensors.

One of the biopolymers used for aqueous dispersions of CNTs is sodium carboxymethylcellulose (CMC), a derivative of cellulose, one of the most abundant biopolymers in nature. Apart from its dispersing properties, CMC demonstrates hygroscopic characteristics used for thickening and stabilizing prepared suspensions. This study presents research results on electroconductive coatings containing CNTs and CMC. To achieve thin layers, the suspension was spread on a cellulose substrate using an automatic paint applicator, resulting in a wet layer thickness of 107 µm. Electrical studies established the percolation threshold in the CNT/CMC composite on the cellulose surface. Using the sessile drop method, wetting angle measurements analysed the hydrophilic properties of the coatings depending on the CNT concentration in the polymer matrix. The resistance of carbon coatings was examined under varying relative humidity conditions, and changes in resistance were determined during partial and complete water flooding of conductive surfaces.

Research on CMC/SLS composites opens perspectives for cost-effective and scalable production of electronics on various materials and surfaces.

Acknowledgements

The authors would like to thank the Ministry of Education and Science of Poland. This work was financially supported by The National Centre for Research and Development as part of the project TANGO-IV-A/0014/2019-00.

9.18 Investigation of vulcanization and drying method influence on the mechanical properties of the VTMS-based aerogels

Aleksandra M. Pisarek*,1, Bartosz Nowak[1], Max Zinke[2], Kai Steffens[2,3], Danny Bialuschewski[2,3], Barbara Milow[2,3], Jakub M. Gac[1]

1. Faculty of Chemical and Process Engineering, Warsaw University of Technology, Warsaw, Poland
2. Institute of Materials Research, German Aerospace Center (DLR), Cologne, Germany
3. Institute of Inorganic Chemistry, University of Cologne, Cologne, Germany

e-mail: aleksandra.pisarek2.dokt@pw.edu.pl

KEYWORDS: *organosilica aerogel, VTMS, double-crosslinking, mechanical properties*

Aerogel production is often energy-consuming due to its brittle nature, necessitating supercritical drying (SCD). Double-crosslinking represents a novel paradigm in enhancing the mechanical properties of aerogels. This method combines polycondensation with the polymerization of vinyl functional groups (vulcanisation). Structure reinforcement enables the preservation of the mesoporous structure, which is crucial for maintaining the unique features of these materials, allows for a more cost-effective and scalable drying method, such as ambient pressure drying (APD), and simultaneously broadens the potential applications of aerogel.

This research aimed to examine the impact of polymerization on the mechanical properties of APD and SCD aerogels. To achieve the research goal, four types of vinyltrimethoxysialne(VTMS)-based samples obtained from three different formulations were compared: vulcanized and non-vulcanized, dried using APD and SCD methods. Volumetric shrinkage, porosity and density were determined for all samples. The structure was also examined using SEM, Helium pycnometry, and ASAP. The influence of particle sizes and their distribution on the properties of the produced aerogels were examined along with the chemical structure and drying method. Mechanical properties were assessed through uniaxial compression tests, including measurements up to sample destruction and determination of loading and unloading hysteresis. Analysis of the obtained mechanical results included the determination of Young's modulus, the range of non-plastic areas and the maximum stress.

Tested samples showed the same volume shrinkage and, therefore, similar density/porosity, which allowed a thorough analysis of the impact of the vulcanization and drying methods. It was noticed that vulcanization increases Young's modulus while reducing the material's elastic range. AP-dried aerogels – due to the spring-back effect and related stresses – showed a higher Young's modulus. Specific boundary layer effects occurred depending on the formulation and drying methods used. The ana-lysis of these effects has been a topic neglected in the literature.

Acknowledgements

This work was supported by The National Science Centre, Poland - project "Super-flexible double-crosslinked organosilica aerogels dried via cheap and scalable ambient pressure method" PRELUDIUM BIS and COST Action AERoGELS CA18125 (Advanced Engineering and Research of aeroGels for Environment and Life Sciences), supported by COST (European Cooperation in Science and Technology).

9.19 Precipitation of doped hydroxyapatite nanoparticles in a continuous reactor

Miłosz Podsiadły[1], Kornel Prystupiuk[*,1], Artur Małolepszy[1], Michał Wojasiński[1], Paweł Sobieszuk[1]

1. Faculty of Chemical and Process Engineering, Warsaw University of Technology, Warsaw, Poland

e-mail: kornel.prystupiuk.dokt@pw.edu.pl

KEYWORDS: *hydroxyapatite nanoparticles, doped hydroxyapatite, continuous precipitation, continuous reactor, modification, doping*

Hydroxyapatite (HAp) is one of the most widely studied forms of calcium phosphate. It has been found in human bones and teeth, among others. HAp has the lowest solubility in aqueous media of all forms of calcium phosphate. More-over, it has many properties as a promising biomaterial, which can be extended by incorporating ions of other elements into its structure. There are many methods for HAp synthesis, but precipitation is the most popular and straightforward method.

This study presents a method for the formation of doped nHAp in a continuous reactor. For this purpose was carried out the wet precipitation in a flow microreactor of nHAp from calcium and phosphate salts with magnesium, zinc, cobalt, strontium or copper salts for sphere-shaped nHAp doped production, previously using ammonia water to set the pH of the reactants at 10.

The product quality was determined by Fourier-transform infrared spectroscopy (FTIR) and X-ray fluorescence spectrometry (XRF), the morphology of the particles was studied by scanning electron microscopy (SEM), and the particle size distribution was determined by dynamic light scattering (DLS). The tendency of the nanoparticles to agglomerate was also estimated by zeta potential measurements.

X-ray fluorescence spectrometry showed that the synthesis was successful, and the metal ions were incorporated into the nHAp structure; however, their content depended on the metal used. Fourier transform infrared spectroscopy indicated that the doped nHAps obtained by continuous synthesis had hydroxyapatite-specific bonds in their structures. The SEM images showed that the resulting particles retained their spherical form. Their diameters ranged from 40 to 130 nm, but they were unstable and agglomerated because the zeta potential of all samples tested ranged from -30 to 30 mV.

The results showed that a simple continuous process for the precipitation of doped nHAp was successful. This indicates that the presented technology can be applied on a larger scale to produce a viable product for bone tissue regeneration.

9.20 The influence of strontium- and zinc-doped borate bioactive glasses on the chitosan-based injectable hydrogels

Szymon Salagierski[*,1], Michał Dziadek[1], Patrycja Domalik-Pyzik[2], Weronika Gura[1], Katarzyna Cholewa-Kowalska[1]

1. Department of Glass Technology and Amorphous Coatings, Faculty of Materials Science and Ceramics, AGH University of Krakow, Krakow, Poland
2. Department of Biomaterials and Composites, Faculty of Materials Science and Ceramics, AGH University of Krakow, Krakow, Poland

e-mail: salagier@agh.edu.pl

KEYWORDS: *hydrogel, borate bioactive glass, strontium, zinc*

Hydrogels based on biopolymers are extremely attractive group of biomaterials for tissue engineering due to their beneficial properties such as high porous three-dimensional structure, large water content, great swelling and biocompatibility. Especially hydrogels based on dynamic covalent bonding have gained huge attention in recent years due to their great rheological properties and self-healing ability, what lets them to be used as injectable materials with high surgical handiness, ideal for minimally invasive surgery.

The subject of this research are dynamic covalent chitosan-based injectable hydrogels crosslinked with dextran dialdehyde with the addition of borate bioactive glasses (BBGs) doped with zinc and strontium. Sol-gel BBGs such as A_2B_{40} (40 %mol B_2O_3, 54 %mol CaO, 6 %mol P_2O_5), zinc-doped $A_2B_{40}Zn_5$ (40 %mol B_2O_3, 49 %mol CaO, 6 %mol P_2O_5, 5 %mol ZnO) and strontium-doped $A_2B_{40}Sr_5$ (40 %mol B_2O_3, 49 %mol CaO, 6 %mol P_2O_5, 5 %mol SrO) play a dual role in the obtained hydrogels – they serve a functional component, modifying hydrogel properties, and provide additional multi-level crosslinking mechanisms.

The aim of this research was to obtain injectable chitosan-based hydrogels and evaluate the impact of different BBGs on the crosslinking process, physicochemical and rheological properties of materials. After the materials were freeze-dried their microstructure, porosity and mineralization was assessed by SEM/EDX and ATR-FTIR. Additionally, mechanical, rheological, self-healing properties and injectability were investigated.

Obtained results showed that the presence of BBGs influenced the properties of chitosan-based hydrogel materials. Borate bioactive glasses improved the crosslinking process by the release of boron and calcium ions providing dynamic covalent ester bonds and imine bonds with the NH_3^+ groups of chitosan respectively. BBGs also significantly improved stiffness, compressive strength, viscoelastic characteristics of hydrogels, and self-healing properties as well as greatly reduced crosslinking time.

Acknowledgements

This work was supported by the program „Excellence initiative – research university" for the AGH University of Krakow.

9.21 Spectroscopic and kinetic studies of new fluorophores derived from citric acid as component in a photoinitiating systems for the obtaining the hydrogel materials in 3D printing processes

Katarzyna Starzak*[,1], Wiktor Kasprzyk[1], Joanna Ortyl[1,2,3]

1. Laboratory of Photochemistry and Optical Spectroscopy, Faculty of Chemical Engineering and Technology, Cracow University of Technology, Cracow, Poland
2. Photo4Chem sp. z o.o., Cracow, Poland
3. Photo HiTech sp. z o.o., Cracow, Poland

e-mail: katarzynastarzak1998@gmail.com

KEYWORDS: *spectroscopy, fluorophores, hydrogel materials, 3D printing*

Photopolymerization is a process in which monomers and/or oligomers polymerize when exposed to light. This process takes place using photoinitiators that absorb light and generate reactive molecules or free radicals, which are responsible for the initiation step of the polymerization process. In radical photopolymerization, photoinitiators act by generating reactive radicals, which are highly reactive and initiate polymerization reactions, combining with monomers to form polymer chains.

Currently, photopolymerization processes are widely used in industry, including the production of protective coatings, paints, adhesives or printing toners. However, nowadays the photopolymerization processes are widely used in 3D printing technology, where light is directed at specific areas to cure layers of polymer material and create 3D objects. Work continues extensively on biosources, such as oils, plant oils, lignin derivatives and terpenes, for the development of renewable photopolymers. In contrast, less attention has been paid to the sustainable development of systems of photoinitiators. While natural or naturally derived compounds have been used in photopolymerization, their application in light-based 3D printing has not yet received as much attention yet. Natural dyes, however, have several advantages: they are bio-based, abundant and less toxic compared to conventional photoinitiating systems. The use of light to polymerize or cure biomaterials in vivo has already been adopted clinically. In addition, custom 3D devices can be created using spatial and temporal control of the photoinitiation process and automated stereolithography (SLA) solutions.

The purpose of this study was to carry out spectroscopic and electrochemical analysis, as well as kinetics studies of the photopolymerization process using initiating systems based on citric acid fluorophores in the role of photosensitizers, and to prepare 3D print-outs of hydrogel materials from the examined compositions.

Acknowledgements

This research was funded by the NCN project OPUS ("Emerging strategy approaches for the design and functionalization of carbon dots as multifunctional, dynamic, green systems photoinitiators and photocatalysts involved in photopolymerisation processes"), Grant No. UMO-2021/41/B/ST5/04533.

9.22 Investigating the spectroscopic properties and kinetics of photopolymerization processes based on new photoinitiators dedicated to dental applications

Katarzyna Starzak*[,1], Monika Topa-Skwarczyńska[1], Andrzej Świeży[1,2], Karolina Kozanecka[1], Joanna Ortyl[1,2,3]

1. Laboratory of Photochemistry and Optical Spectroscopy, Faculty of Chemical Engineering and Technology, Cracow University of Technology, Cracow, Poland
2. Photo4Chem sp. z o.o., Cracow, Poland
3. Photo HiTech sp. z o.o., Cracow, Poland

e-mail: katarzynastarzak1998@gmail.com

KEYWORDS: *spectroscopy, photopolymerization kinetics, photoinitiators, dental materials*

In the case of photopolymerization, there are two basic types of photo-curable resins, that is, intermediates used to obtain cross-linked polymers via photochemical processes. The main difference in this case is the mechanism of polymerization. Therefore, we distinguish: radical photoinitiated polymerization and cationic photoinitiated polymerization. Photopolymerization is characterized by fast curing times, which allows for fast production processes. It is also a process that is easy to control, as the curing time can be adjusted by controlling the parameters of the light sources used, such as light intensity, wavelength and exposure time.

The dental care industry may be one of the most important uses for photopolymerization. Photopolymerizable resin-based products, such as adhesive systems, resin cements, pit and fissure sealants, and composite resins, include some of the examples of possible use. These materials are often made using a basic monomer combination of BisGMA or UDMA, which is diluted with another low-viscous monomer such as TEGDMA. The use of a suitable, high-efficiency photoinitiating system is crucial in photopolymerization processes and the optimization of their conditions. The rapid and successful photopolymerization of dental resins with little light exposure is a critical aspect of clinical use of dental adhesives, composites, and sealants. Furthermore, optimized cure is one of the most important parameters that governs the long-term performance of polymeric materials, influencing mechanical properties, as well as biocompatibility while possibly cytotoxic materials escape from the cured polymers.

The initial research on novel initiator systems and their applicability for initiating cationic and radical photopolymerization processes is presented in this paper. The possible use of compositions containing novel photoinitiators in 3D printing of materials for application in the dental industry has also been examined.

Acknowledgements

This research was funded by National Centre for Research and Development in Poland under the Lider Program, grant number LIDER13/0156/2022.

9.23 Rosemary - a natural way to improve the properties of polymeric materials

Karol Tutek*,1, Anna Masek1

1. Institute of Polymer and Dye Technology, Faculty of Chemistry, Lodz University of Technology, Lodz, Poland

e-mail: karol.tutek@dokt.p.lodz.pl

KEYWORDS: *rosemary, polymer, stabilizer, indicator, aging*

The use of naturally derived, renewable, and ecological additives to polymer materials is becoming increasingly important due to climate change, plastic waste management challenges, and new legislation. Among the most promising multifunctional additives are rosemary derivatives, rich in polyphenolic substances with antioxidant properties.

This study investigated the effects of adding dried ground rosemary (RE_D), a supercritical fluid extraction (RE_SFE) extract, and a Soxhlet extraction (RE_SE) extract to an ethylene-norbornene copolymer (EN) matrix. Additives were introduced at 2.5 and 5 phr, and the finished materials were subjected to weathering for 300 and 600 h under exposure to water, light, air, and temperature. The samples were then evaluated for colour change, static mechanical properties, thermal properties, oxidation induction time, and migration.

The results indicate that rosemary derivatives enhance the material's resistance to degradation factors, extending its useful life. Extracts outperform dried rosemary as additives. SFE extracts improved mechanical properties more effectively, while SE extracts better limited oxygen's effects. This study demonstrates the potential of rosemary derivatives as sustainable additives for improving the resistance of polymeric materials.

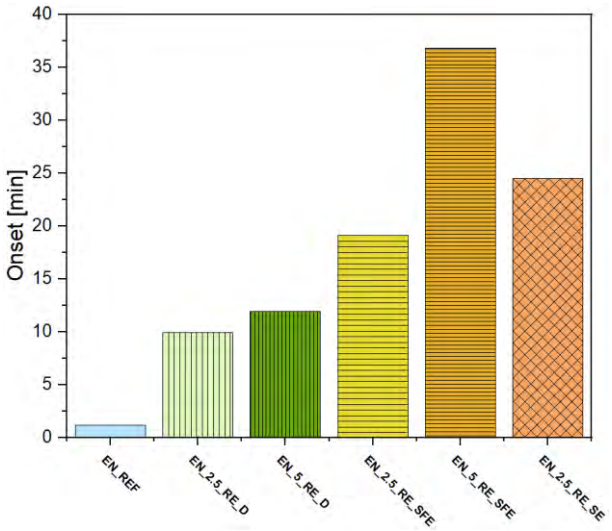

Figure 9.23.1. Graph of the variation of OIT depending on the type and amount of rosemary-derived additive (RE_D-Dried, RE_SFE- Supercritical Fuild Extraction, RE_SE- Soxhlet Extract).

9.24 Rowanberry - a natural alternative to synthetic additives for polymeric materials

Karol Tutek*,1, Anna Masek1

1. Institute of Polymer and Dye Technology, Faculty of Chemistry, Lodz University of Technology, Lodz, Poland

e-mail: karol.tutek@dokt.p.lodz.pl

KEYWORDS: *rowanberry, polymer, stabilizer, indicator, aging*

The incorporation of plant-derived substances has gained prominence in the development of modern polymer materials. Ensuring their degradation resistance is crucial, and polyphenolic compounds, abundant in rowan berries, are often employed for this purpose.

This study delves into the effectiveness of dried and ground rowan berries (RB_D) and their extract (RB_SE) as multifunctional polymer additives. These natural additives were introduced into the ethylene-norbornene copolymer (EN) at varying concentrations: 2.5-15 phr for RB_D and 2.5-5 phr for RB_SE. The resulting materials underwent weathering for periods of 300 and 600 hours. Subsequently, the samples were evaluated for static mechanical properties, spectrocolorimetric properties, thermal properties, migration, and oxidation induction time.

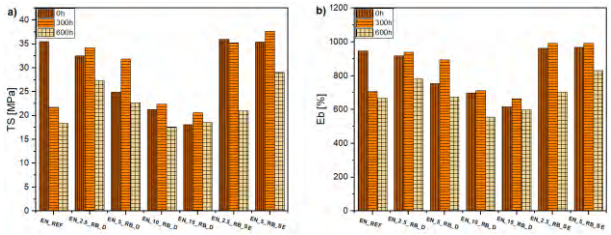

Figure 9.24.1. Effect of Additive Type, Quantity, and Weathering Time on Mechanical Properties: a) Tensile Strength, b) Elongation at Break

The results revealed a more pronounced effect from the extract. Notably, the addition of 5 phr rowan extract enhanced mechanical properties, yielding a 58% increase in TS and a 25% increase in Eb after 600 hours of weather aging compared to the reference sample. These findings support the validity of rowan extract as a blend of anti-aging substances in polymeric materials.

9.25 Inverse-opal titania films for photocatalytic activity enhancement

Lei Wang*[,1,2], Ewa Kowalska[1,2]

1. Institute for Catalysis, Hokkaido University, Sapporo, Japan
2. Faculty of Chemistry, Jagiellonian University, Cracow, Poland

e-mail: lei.wang@uj.edu.pl

KEYWORDS: *photocatalysis, photonic crystals, slow photon effect, titania*

Novel materials with a periodic structure, named as photonic crystals, have recently been intensively studied for possible photocatalytic applications, due to their characteristic feature, i.e., photonic band gap (PBG) and slow photon effect. It should be pointed out that the light of wavelength approaching the PBG wavelength cannot travel through the material while the light of shorter or longer wavelengths than PBG one might propagate, but with reduced group velocity, i.e., slow photon effect. Here, inverse opal titania (IOT) films have been investigated for possible enhancement of photocatalytic activity.

The IOT films (on a glass sample) were prepared from silica and polystyrene (PS) opals by sandwich-vacuum--assisted infiltration and co-assembly methods, respectively. The reference sample was prepared by co-assembly method but with disordered PS array, and thus without photonic feature. The modification of preparation conditions was investigated to prepare the films with a high quality and different photonic properties, i.e., photonic bandgap (PBG) and slow photons' wavelengths. The morphology and optical properties were characterized by scanning electron microscopy (SEM) and UV/vis spectroscopy, respectively. The photocatalytic activity was evaluated (also in dependence on the irradiation angle) for oxidative decomposition of acetaldehyde gas under irradiation with blue LED by measuring the rate of evolved carbon dioxide.

The highest activity (more than two-fold enhancement in the comparison to the reference) has been achieved for the IOT sample of 226 nm void diameter and PBG wavelength at 403 nm. Interestingly, significant decrease in activity (five times lower than reference) has been obtained for the IOT with 195 nm voids (green in Figure 9.25.1), and thus PBG at 375 nm (prohibited light). Accordingly, it has been proposed that the perfect tunning of photonic properties (here the blue-edge slow-photon effect) with bandgap energy of photocatalyst (e.g., absorption of anatase) results in the improved photocatalytic performance due to efficient light harvesting ability owing to the slow photon effect.

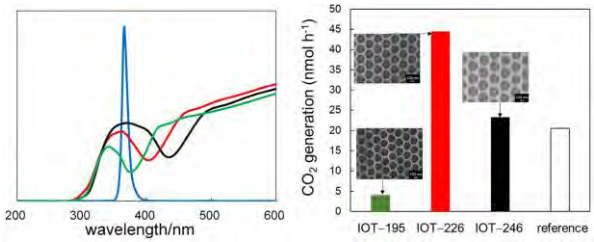

Figure 9.25.1. (left) Transmittance spectra of IOT samples and irradiation source (blue), (right) The photo-catalytic activity of IOT (with SEM images) and reference (no PC) samples.

Acknowledgements

The project is co-financed by the Polish National Agency for Academic (BPN/PPO/2021/1/00037) and the National Science Centre (2022/01/1/ST4/00026).

9.26 Extensional flow of mixed surfactant CAPB/SDBS solutions with the addition of metal ions

Ewelina Warmbier*[,1], Jacek Różański[1], Sylwia Różańska[1], Patrycja Wagner[1]

1. Division of Chemical Engineering and Equipment, Faculty of Chemical Technology, Poznan University of Technology, Poznan, Poland

e-mail: ewelina.warmbier@doctorate.put.poznan.pl

KEYWORDS: *rheology, extensional viscosity, surfactants*

Cocamidopropyl betaine (CAPB) is a zwitterionic surfactant with versatile applications in the production of cosmetics and household chemicals, influencing the rheological properties of shampoos, body wash gels, or liquid soaps. CAPB demonstrates synergy with anionic surfactants in aqueous solutions, resulting in the formation of viscoelastic fluids. Viscoelastic properties are commonly observed in surfactant solutions where wormlike micelles or networked micelles have been formed. The transformation from spherical micelles to wormlike micelles can be induced by the addition of simple salts or cosurfactants. As this surfactant plays a significant role in the cosmetic and household chemical industry, the outcomes of such studies hold practical importance. The presented research aimed to determine the influence of salts on the viscoelastic properties of solutions obtained at various molar ratios of surfactants and different total concentrations.

The objective of the presented research was to determine the rheological properties in the extensional flow of aqueous solutions containing a mixture of the anionic surfactant sodium dodecylbenzenesulfonate (SDBS) and the zwitterionic surfactant cocamidopropyl betaine (CAPB). Based on the obtained profiles of changes in the middle fiber diameter D_{min} over time t, the extensional relaxation time λ_E was determined. Following measurements in shear flow, it was established that for both molar ratios of CAPB/SDBS, there is a maximum of zero viscosity for different NaCl salt contents. The occurrence of a zero viscosity maximum indicates the transformation of entangled wormlike micelle networks into networked micelles. Based on longitudinal flow measurements, a characteristic cylindrical shape of the fiber was observed, indicating that the rheo-capillary thinning range of CAPB/SDBS mixture solutions can be described using a viscoelastic fluid model. The extensional relaxation time increases with the growth of the system's zero viscosity.

Acknowledgements

This research was supported by the Ministry of Education and Science of Poland through grant 0912/SBAD/2302.

9.27 Composite Ni/SiO_2 scaffolds obtained by DIW 3D printing

Łukasz Wilk*,1, Jakub Marchewka1, Maciej Sitarz1

1. Faculty of Material Science and Ceramics, AGH University of Krakow, Krakow, Poland
e-mail: luwilk@agh.edu.pl

KEYWORDS: *3D printing, DIW method, composite scaffolds, catalysis*

Fossil fuels are now the dominant source of energy for humanity, and their combustion produces a large amount of carbon dioxide. Excessive CO_2 emissions in recent decades caused a number of environmental problems, such as global warming, sea acidification and extreme climate change. Capture and catalytic conversion of CO_2 into fuels or chemical compounds useful for industry (e.g. methane, methanol, ethanol, formic acid) are currently arousing great interest among scientists. Currently designing an efficient heterogeneous catalyst with a high degree of conversion in the CO_2 methanation reaction that will operate at relatively low temperatures remains a big challenge. Transition metals such as Ru, Rh, Pd and Ni are proved to be active in this reaction. Among them, nickel catalysts attract special attention because of their good catalytic properties and low price of the material.

The research involved the development of new procedure for the preparation of 3D silica-nickel heterogenous catalyst using Direct Ink Writing 3D printing. This included the following steps:

- Optimalization of the starting material including selection of appropriate proportions of the components and additives influencing rheology.
- Optimization of the 3D printing process using F-NIS 23151 (Sygnis, Poland), especially the selection of appropriate pressure and printing speed.
- Thermal processing of the printed samples to obtain the 3D structures with given microstructural properties such as specific surface area.
- Characterization of the microstructure (BET analysis, scanning electron microscopy) and structure (FT-IR and Raman spectroscopy).

The optimum rheological properties of the paste were achieved through the selection of appropriate components, resulting in high dimensional accuracy of samples compared to 3D computer model. Thorough analysis of the thermal, structural and microstructural properties provides a comprehensive characterization of the properties of the samples. In order to obtain efficient heterogeneous Sabatier reaction catalysts useful in industry, modification of the surface was carried out by means of the EPD method.

Acknowledgements

This research was funded by the National Science Centre, Poland, grant No. 2020/37/B/ST8/02859 and supported by the program „Excellence initiative - research university" for the AGH University of Krakow.

9.28 Development of new materials based on ZnO and MoS_2 for photo(electro)--catalytic oxygen evolution reaction

Jakub Zabrzycki*,1, Zuzanna Bojarska1, Marta Mazurkiewicz-Pawlicka1

1. Faculty of Chemical and Process Engineering, Warsaw University of Technology, Warsaw, Poland
e-mail: jakub.zabrzycki.dokt@pw.edu.pl

KEYWORDS: *OER, photo(electro)catalysis, zinc oxide, molybdenum disulfide, carbon nanotube*

Oxygen evolution reaction (OER) is an essential process in energy industry, since it is one of the reactions occurring during water splitting, hence associated with hydrogen production. It is known that OER is a sluggish reaction, so to efficiently accelerate its kinetics, effective catalysts are needed. In OER catalysis, photo(electro)catalysts are especially promising, as they use solar radiation to improve the reaction's efficiency. One of the materials showing photocatalytic activity in OER is zinc oxide (ZnO). This material, combined with another semiconductor such as molybdenum disulfide (MoS_2), may become an efficient OER photo(electro)catalyst.

The aim of the research was to develop a new method of obtaining active OER photo(electro)catalysts based on ZnO, MoS_2, and functionalized carbon nanotubes (N-CNTs). During the experiments, two methods were examined: the sonochemical method (US) and microwave-assisted solvothermal synthesis (MSS). These methods consisted of direct precipitation of ZnO on the MoS_2 and N-CNTs-based heterostructure. For the preparation, different ZnO mass content was used: 10, 50, and 90%. After successful synthesis, the obtained samples were examined in terms of their composition (X-ray diffractometry - XRD, thermogravimetric analysis - TGA), as well as their morphology and size (scanning transmission electron microscopy - STEM). Chronoamperometry measurements were performed in order to determine the samples' photo(electro)catalytic activity, measured as their capability to increase the intensity of oxygen production under the influence of the catalysts' irradiation by ultraviolet light.

The results indicate that both US and MSS methods allow for successful deposition of ZnO in wurtzite form on MoS_2/N-CNTs heterostructure. As the experiments showed, the MSS method allows for obtaining more active OER photo(electro)catalysts than the US method. Furthermore, the mass content of ZnO showing the highest catalytic activity turned out to be 90%. Analysis of the results showed that high catalytic activity of the materials is probably achieved due to the distinctive structure of ZnO and mutual band structure of ZnO and MoS_2.

Acknowledgements

This work was supported by the National Centre for Research and Development [PL-TW/VIII/2020/9].

9.29 Investigation of coatings based on carbon-rich SiOC glasses

Patryk Zając*,[1], Maciej Bik[1], Maciej Sitarz[1]

1. Faculty of Materials Science and Ceramics, AGH University of Krakow, Krakow, Poland
e-mail: patrykza@agh.edu.pl

KEYWORDS: *silicon oxycarbide, protective layer, sol-gel, dip-coating*

Silicon oxycarbide (SiOC) is an amorphous polymer-derived ceramics material that thanks to its low density, high strength and resistance to oxidation at high temperatures can be considered in terms of applications in high-temperature environments. Its thermomechanical resistance and electrical conductivity make it suitable for applications as protective-conductive layers for interconnects in solid oxide fuel cells (SOFCs).

In this investigation, Crofer 22 APU, a commonly utilized alloy for SOFC interconnects was used as the metallic substrate. The preceramic polymer was synthesized via sol-gel method. Organic precursors containing phenyl groups were selected to increase the carbon content in the final material to influence its conductivity. Optimal coating thickness was obtained by adjusting the appropriate withdrawal speed during the dip-coating technique. Such obtained samples were subjected to a two step thermal treatment yielding the formation of ceramic coatings. The sample of the most promising properties has been tested under conditions imitating the operation of the interconnect in the cathode space (800 °C and air atmosphere) for 250 hours . SEM imaging has revealed coating and scale microstructure, and possible cracks formation. For the purpose of structure analysis, infrared and Raman spectroscopies, GIXRD, and EDS were used.

Oxidation resistance testing through thermogravimetry (TG) demonstrated that the parabolic oxidation constant of coatings is lower compared to the majority of coatings reported in the literature. However, it also revealed that the samples began to oxidize at a faster rate between 100 and 150 hour of testing that can be linked to Cr_2O_3 and Mn-Cr spinel crystals forming on the top of the layer that diminish layers protective properties. ASR examination revealed an unsatisfactory level of conductivity that resulted from probable carbon oxidation during oxidation tests.

Acknowledgements

This work has been supported by the Polish National Science Centre project No 2019/35/B/ST5/00338: “New biocompatible coatings on metallic substrates based on materials from the Si-O-C system“.

10 Abstracts: Bioengineering, biotechnology, biomedical engineering

10.1 Effect of electrospun fiber morphology on microbial properties of fiber membranes

Paulina Armatys*[,1], Aleksandra Laber[1], Ewa Stodolak-Zych[1]

1. Faculty of Materials Science and Ceramics, AGH University of Krakow, Krakow, Poland

e-mail: parmatys@agh.edu.pl

KEYWORDS: *fiber, microbial properties, electrospinning, membranes, morphology*

Fiber membranes are used in fields such as medicine and environmental protection. With time of use, hypertrophic layers develop on the surface of membranes, on which bacterial biofilm development can be observed. Attempts to reduce the biofilm are associated with modification of membrane surfaces. One of them is a method that allows the production of fibers of varying morphology on a nano- and micrometer scale. The method used to produce this type of material is electrospinning.

The aim of this work was to obtain fibrous membranes at the pre- and post-spinning stages of processing, which would differ significantly in the morphology of the elementary fiber. Using a commercial synthetic polymer poly(ε-caprolactone) (PCL, Sigma-Aldrich) and a pre-selected solvent system of dichloromethane (DCM, Avantor SA) and N,N-dimethylformamide (DMF, Avantor SA), a series of fibrous membranes with a random arrangement of fibers were produced by electrospinning from solution. The random fibers were modified by post-processing homoepitaxial growth to give them a collar structure (shish-kebab, SK). Nonwoven fabrics with bead-on-string (BOS) morphologies were fabricated in a prespinning process by coaxial electrospinning of two PCL polymer solutions of different concentrations.

The fiber morphologies were observed using an SEM electron microscope (Scios 2 DualBeam, ThermoFisher Scientific). Analysis of the size distribution of the fibers showed that the random fibers taken as reference are characterized by diameters in the range of 0.6-1.5 μm while the fibers subjected to modification show a size of 0.14±0.07 μm (BOS), with an equivalent bead diameter of 3.30±1.12 μm, respectively, while the shish-kebab fibers show 1.31±0.42 μm with an average flange size of 0.16±0.07 μm. The hierarchical fiber morphology is responsible for the high hydrophobicity of the membranes, which reaches a value of 140° (DSA 25 Kruss). On the other hand, the value of surface free energy for the tested nonwovens was, respectively: random: 45.51 $mN \cdot m^{-1}$, BOS: 52.59 $mN \cdot m^{-1}$, and shish-kebab 29.78 $mN \cdot m^{-1}$. The obtained materials were also subjected to microbiological testing using commercial bacterial strains of *E. coli* (ATCC 8739, Biomaxima) and *S. aureus* (ATCC 6538P, Biomaxima).

Studies have shown that fiber morphology significantly affects the surface properties of fiber membranes and the ability to model the microbial response.

Acknowledgements

Research project supported by program IDUB "Excellence initiative – research university" for the AGH University of Krakow". Project ID 4204

10.2 Polyesters of azelaic acid and selected short-chain dihydroxy alcohols for the preparation of cell scaffolds

Aleksandra Bandzerewicz*[,1], Kamil Wierzchowski[2], Piotr Denis[3], Maciej Pilarek[2], Agnieszka Gadomska-Gajadhur[1]

1. Faculty of Chemistry, Warsaw University of Technology, Warsaw, Poland
2. Faculty of Chemical and Process Engineering, Warsaw University of Technology, Warsaw, Poland
3. Laboratory of Polymers and Biomaterials, Institute of Fundamental Technological Research Polish Academy of Sciences, Warsaw, Poland

e-mail: 01132383@pw.edu.pl

KEYWORDS: *azelaic acid, polyazelate, biomaterials, cell scaffolds, electrospinning*

Azelaic acid is a dicarboxylic acid of plant origin with numerous applications in dermatology. Pharmacological applications of azelaic acid have been studied since the 1980s. Its anti-inflammatory and antioxidant properties are believed to determine its efficacy in the treatment of rosacea and acne vulgaris, among others. Both dihydroxy alcohols, 1,3-propanediol and 1,5-pentanediol, have cosmetic applications. 1,3-propanediol shows moisturising properties and can be used as a humectant in skin and hair products. Studies on selected dihydroxy alcohols have shown that their antifungal activity increases with carbon chain length, with the use of 1,5-pentanediol allowing up to a 10-fold increase in efficacy compared to shorter diols.

The work focuses on synthesising polyesters of azelaic acid and chosen dihydroxy alcohols: 1,3-propanediol and 1,5-pentanediol. The intended use of the materials obtained is the production of biodegradable and bioresorbable scaffolds for skin cell culture.

Polymer syntheses were carried out, varying in temperature and reaction time. The products were characterised by their molecular weight, degree of acid group conversion and thermal properties. The chosen materials were used to produce cell culture scaffolds by electrospinning. The fibre-forming potential of poly(azelate diols) were asses-sed. The applicability of the obtained fibres was determined based on mechanical and surface properties and their internal morphology. Resistance to radiation sterilisation was determined. An essential part of the project were cytotoxicity tests on extracts.

Acknowledgements

Research was funded by the Warsaw University of Technology within the Excellence Initiative: Research University (IDUB) programme.

10.3 The effect of chitosan molecule mass on naphthoquinone secretion and proliferation of *Rindera graeca* transgenic roots cultured on PLA-chitozan hybrid scaffolds

Szymon Bober[1], Kamil Wierzchowski[*,1], Aleksandra Bandzerewicz[2], Mateusz Kawka[3], Agnieszka Gadomska-Gajadhur[2], Katarzyna Sykłowska-Baranek[3], Maciej Pilarek[1]

1. Faculty of Chemical and Process Engineering, Warsaw University of Technology, Warsaw, Poland
2. Faculty of Chemistry, Warsaw University of Technology, Warsaw, Poland
3. Faculty of Pharmacy, Medical University of Warsaw, Warsaw, Poland

e-mail: kamil.wierzchowski@pw.edu.pl

KEYWORDS: *transgenic (hairy) roots, plant secondary metabolites, biomass immobilization, chitosan, PLA biomaterials*

For centuries, plants have been well-known for their medical applications. Nowadays, plant biomass is recognized as the greatest source of anticancer drugs all over the world. The *in vitro* plant tissue cultures allow to exceed the productivity of secondary metabolites observed in wild plants, which makes plant biomass an increasingly attractive source of pharmaceutical agents. Furthermore, different *in vitro* techniques can be used to maximize biomass proliferation and secretion of the desired metabolites. Biomass immobilization is a very effective way to increase plant biomass proliferation and secretion of secondary metabolites. The polymeric-based scaffolds are a useful and cheap bioengineering tool applied for *in vitro* cultures. The combination of polymer scaffolds and elicitors, i.e., chitosan, can efficiently increase the production of secondary plant metabolites.

The aim of the study was to evaluate the influence of chitosan molecule mass on naphthoquinones derivatives secretion and biomass proliferation of *Rindera graeca* transgenic roots. The plant biomass was cultured on scaffolds made of certified polylactic acid (PLA) blended with chitosan. The polysaccharides used in this study came from squids and fungi. In the case of fungal chitosan, three chitosan molecule masses, i.e., 30 kDa, 300 kDa and 3000 kDa, were used. The average concentration of elicitor in polymeric-chitosan hybrid scaffolds was around 25%$_{m/m}$. As the control group was used, hairy roots were immobilized on PLA scaffolds without chitosan. The increase of the fresh biomass and the amount of secreted secondary metabolites in *Rindera graeca* transgenic root cultures were determined quantitatively.

The increase of the *Rindera graeca* transgenic root proliferation was noticed with the chitosan molecule mass increase. Unlike the biomass proliferation, the secretion of naphthoquinone derivatives decreased with increasing chitosan molecule mass. The chitosan from the fungi shows a slightly greater impact on hairy root proliferation in comparison to the squid chitosan. The difference in the secretion of secondary metabolites was also noticeable. In the cultures with fungi, more naphthoquinone derivatives were observed than in the squid chitosan cultures.

Acknowledgements

This research was funded by the National Science Centre (NCN), Poland, grant no. 2021/41/N/ST8/00958.

10.4 Methods for Assessing the Metabolic Activity of Plant Cells

Maria Bobrova[1], Kamil Wierzchowski[*,1],Mateusz Bartczak[1], Mateusz Kawka[2], Katarzyna Sykłowska-Baranek[2], Maciej Pilarek[1]

1. Faculty of Chemical and Process Engineering, Warsaw University of Technology, Warsaw, Poland
2. Faculty of Pharmacy, Medical University of Warsaw, Warsaw, Poland

e-mail: kamil.wierzchowski@pw.edu.pl

KEYWORDS: *BY-2 cells, single-use bioreactors, wave-type agitation, bioprocess intensification*

The study of *Nicotiana tabacum* BY-2 cell line is important in biotechnological research, particularly in pharmaceuticals where these cells excel in producing valuable compounds like recombinant proteins and vaccines. Beyond pharmaceuticals, they are instrumental in understanding plant cell functions and responses to stress or pathogens. This investigation aims to explore the metabolic processes of these cells using innovative methodologies, potentially advancing biotechnology and pharmaceutical applications.

The study focuses on the development of methods for evaluating the metabolic activity of plant cells. The first method of assessing metabolic activity involves using the Presto Blue reagent, commonly used in studies involving animal cells. The second method entails spectrophotometric measurement of the activity of lactate dehydrogenase (LDH). The research was conducted using *Nicotiana tabacum* BY-2 line cell.

Method 1: Determining metabolic activity using Presto Blue Reagent.

This technique relies on the ability of active mitochondrial dehydrogenases to reduce resazurin to resorufin. Cells of the tobacco BY-2 line, appropriately prepared and mixed with Presto Blue reagent, were incubated at the suitable temperature. After an experimentally determined incubation period, fluorescence intensity was measured using a spectrofluorometer. The level of metabolic activity of the examined cells was determined based on the results.

Method 2: LDH Activity Measurement Using Spectrophotometry.

This method is based on measuring the amount of NADH, a product of the reaction catalysed by lactate dehydrogenase (LDH). It is a technique for evaluating metabolic activity, allowing for an accurate assessment of enzyme activity. The measurement was carried out using spectrophotometry.

The developed techniques can be employed for determining the metabolic activity of plant cells, potentially impacting advancements in biotechnological analyses.

Acknowledgements

The research was funded by the Warsaw University of Technology within the Excellence Initiative: Research University (IDUB) programme.

10.5 Novel 3D printed culture flasks for transgenic root culture under wave-type agitation conditions

Rafał Czajka[1], Kamil Wierzchowski[*,1], Mateusz Bartczak[1], Katarzyna Sykłowska-Baranek[2], Maciej Pilarek[1]

1. Faculty of Chemical and Process Engineering, Warsaw University of Technology, Warsaw, Poland
2. Faculty of Pharmacy, Medical University of Warsaw, Warsaw, Poland

e-mail: kamil.wierzchowski@pw.edu.pl

KEYWORDS: *transgenic (hairy) roots, biomass immobilization, 3D printing, polylactic acid, wave-type agitation*

Transgenic root cultures can be used as a vital source of various secondary plant metabolites, which are widely used in the pharmaceutical industry as active drug agents. In vitro culture systems based on hairy roots allow exceeding production of secondary metabolites observed in wild plants owing to the many possibilities for bioprocess parameters optimization. 3D printing technology provides a favourable condition for rapid prototyping and testing of new culture vessels. The wide range of biocompatible 3D printing filaments available on the market allows to match the culture flask material to the desired application.

The aim of this study was to develop and test novel 3D-printed culture flasks for transgenic root culture under wave-type agitation conditions. The study can be divided into two main stages: (i) designing and printing of culture vessels and (ii) cultures of transgenic roots in developed flasks under wave-type agitation conditions. In the first stage, four different geometries were designed using FDM (fused deposition modeling) and printed by PRUSA i3 MK3 3D printer. PLA (polylactic acid) was used as the filament due to its biocompatibility. Additionally, before the transgenic root cultures, the degradation rate of rectangular samples of PLA 3D prints in culture conditions was determined. In the case of the second stage, 3D printed vessels were used for the 28-day cultures of *Rindera graeca* transgenic roots at 24 °C in darkness. The morphology of hairy roots and the fresh biomass increases were determined to evaluate the effect of vessel geometry on cultured biomass.

The degradation rate testes showed no loss of sample weight over 6 weeks, which indicates the lack of degradation of 3D prints during the study period. In the case of *Rindera graeca* transgenic root cultures, vessel geometry significantly impacted the morphology of transgenic roots and the fresh biomass increase. Geometries with conical tabs at the bottom of the culture vessel allowed for immobilization of the hairy root biomass. In these systems, the morphology of transgenic roots was highly ramified, and the fresh biomass increase was higher than in systems with a flat bottom.

Acknowledgements

This research was funded by the National Science Centre (NCN), Poland, grant no. 2021/41/N/ST8/00958.

10.6 Piezoelectric materials as scaffolds for tissue regeneration

Barbara Guzdek[*,1], Jagoda Tylisz[1], Dominik Matyszok[1], Zofia Zakrzewska[2], Beniamin Kopiec[2], Ziemowit Ostrowski[1], Katarzyna Krukiewicz[1]

1. Silesian University of Technology, Gliwice, Poland
2. Academic High School, Gliwice, Poland

e-mail: barbara.guzdek@gmail.com

KEYWORDS: *piezoelectric materials, nanocellulose, poly(vinylidene) fluoride, poly(glycerol sebacate urethane), poly(vinyl alcohol)*

It is a well-known fact that all living organisms produce bioelectricity. Therefore, it is an intuitive approach to apply external electric stimulation as a way to treat several disfunctions and facilitate the regeneration of tissues. Several studies have shown the advantageous effects of electrical stimulation on the blood vessel regeneration[1], however, this treatment is highly limited by the need to implant a stimulatory device equipped with a power source and wiring. An emerging alternative is to use materials able to generate electricity as a response to naturally occurring loads, i.e. piezoelectric materials.

The aim of our research is to design a biocompatible piezoelectric material that could act as a scaffold facilitating the regeneration of blood vessels in response to pulsatile blood flow. An ultimate goal is to form a material that will disintegrate after a certain period of time and will not have any negative effects on the patient's health. Therefore, we have examined several biocompatible polymers: poly(vinylidene) fluoride, poly(glycerol sebacate urethane), poly(vinyl alcohol), and fillers: fibrous nanocellulose and crystalline nanocellulose, to form membranes that were further assessed in terms of piezoelectric properties and biocompatibility. Simultaneously, numerical modelling of the materials was developed to check how the electrical field is generated during the conditions mimicking vessel distortion due to pulsatile blood flow. The final stage was to produce materials with the right dimensions (housed in a blood vessel) in order to simulate the effects in the human body.

[1] Cheng et al. Electronic Blood Vessel. Matter 3 (2020) 1664–1684

10.7 The upcycling of spent coffee grounds and their application in the immobilization of microbial lipases

Karina Jasińska*,1, Agata Fabiszewska[1], Bartłomiej Zieniuk[1]

1. Department of Chemistry, Institute of Food Sciences, Warsaw University of Life Sciences, Warsaw, Poland

e-mail: karina_jasinska@sggw.edu.pl

KEYWORDS: *spent coffee grounds, immobilization, lipases, carrier*

Due to the popularity of coffee, the amount of waste generated during the preparation of this beverage is steadily increasing around the world. For this reason, the interest in reusing spent coffee grounds (SCGs) - lignocellulosic residues is growing. In this study spent coffee grounds were used as supports in the immobilization process of lipases synthesized by mold species *Aspergillus oryzae*, *Thermomyces lanuginosus* and *Rhizomucor miehei*. Synthetic macroporous resin (Lewatit VP OC 1600) was used as a reference carrier. SCGs were subjected to four different pretreatment procedures resulting in various purity of carrier materials. Immobilized enzymes were characterized in terms of surface structure, stability under various conditions and their reusability.

The aim of the research was to obtain new biocatalysts and the experiments succeeded in obtaining immobilized enzyme preparations that were more active in both hydrolysis and synthesis reactions compared to biocatalysts immobilized on a synthetic carrier. The study confirmed that the immobilization process increased the lipolytic activity of enzymes relative to free lipase.

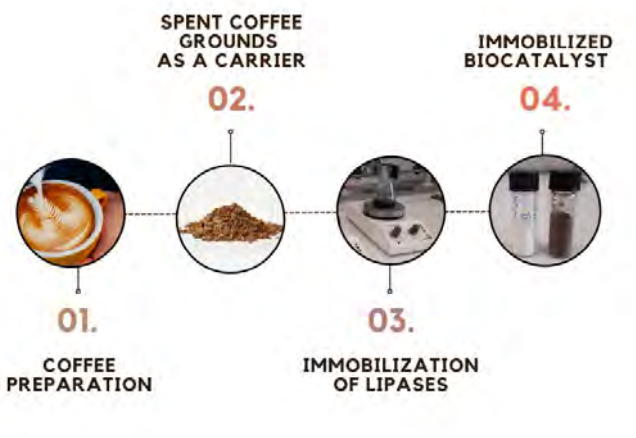

Figure 10.7.1. Graphical abstract presenting methodology of the conducted research.

Acknowledgements

The samples of spent coffee grounds with different type of pretreatment were kindly received from Ecobean (Warsaw, Poland). As a reference the synthetic carrier – Lewatit VP OC 1600 was gifted from Lanxess (Cologne, Germany). The enzymes were kindly gifted from Novozyme (Bagsvaerd, Denmark).

10.8 Development of chokeberry and apple pomace as matrices for immobilization of microbial lipases

Karina Jasińska*,1, Maksym Nowosad[2], Aleksander Perzyna[2], Andrzej Bielacki[2], Stanisław Dziwiński[2], Agata Fabiszewska[1]

1. Department of Chemistry, Institute of Food Sciences, Warsaw University of Life Sciences, Warsaw, Poland
2. Faculty of Biology and Biotechnology, Warsaw University of Life Sciences, Warsaw, Poland

e-mail: karina_jasinska@sggw.edu.pl

KEYWORDS: *immobilization, lipases, fruit pomace, carrier*

Fruit pomace is a waste product in juice production. Still, this raw material is rich in biologically active compounds, but usually is discarded, when it could otherwise be recycled and valorised with a new use. In the present study apple and chokeberry pomaces were applied as matrices for immobilization of lipases of microbial origin derived from fungi *Rhizomucor miehei*.

The aim of the study was to obtain an immobilized biocatalyst characterized with hydrolytic and synthetic activities. The measurement of hydrolytic activity was based on hydrolysis of *p*-nitrophenyl laurate and synthetic activity was performed using transesterification of *n*-butanol with vinyl acetate. Lipases were attached on pomaces with different degrees of purification to compare the effect of the pretreatment methodology on biocatalyst activity. Appropriately selected parameters of the immobilization process allowed obtaining lipolytically active enzyme preparations. Biocatalysts showed activity, both in hydrolysis and synthesis reactions. The best results were achieved for preparations that were immobilized on the native form of apple and chokeberry pomaces, i.e. not pretreated. In the case of chokeberries, the removal of selected functional groups led to a significant reduction in the activity of the obtained preparations.

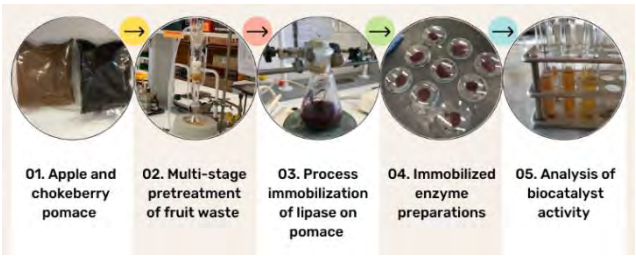

Figure 10.8.1. Graphic abstract of the conducted research.

Acknowledgements

The enzymes were kindly gifted from Novozyme (Bagsvaerd, Denmark).

10.9 The new approach of cardiovascular diagnostic using CFD simulations

Krystian Jędrzejczak*,1, Wojciech Orciuch1, Piotr Piasecki2, Łukasz Makowski1

1. Faculty of Chemical and Process Engineering, Warsaw University of Technology, Warsaw, Poland
2. Interventional Radiology Department, Military Institute of Medicine-National Research Institute, Warsaw, Poland

e-mail: krystian.jedrzejczak.dokt@pw.edu.pl

KEYWORDS: *cRR, CFD, digital twins, artery, stenosis*

Cardiovascular diseases are one of the leading causes of death nowadays. With the growing number of patients with atherosclerosis, there is a growing need to increase the pace of patient diagnostics to start treatment as soon as possible. Currently, the leading method for diagnosing atherosclerotic stenosis is the invasive method of measuring the pressure before and after stenosis. The research aims to develop a quick and universal method for diagnosing atherosclerotic stenosis using non-invasive imaging methods and computer simulations. The study is focused on developing a numerical procedure for virtual segmenting the geometry of blood vessels to obtain results similar to experimental measurements. It was decided to measure the cRR (constant Resistance Ratio) parameter to simplify calculations for flow analysis at a constant blood flow corresponding to constant hydraulic resistance during wave-free period. The obtained pressure distribution results allowed the calculation of the cRR parameter to classify the patient's disease state. The conducted research can be adapted into clinical practise in the future, supporting the daily work of cardiologist and interventional radiologists.

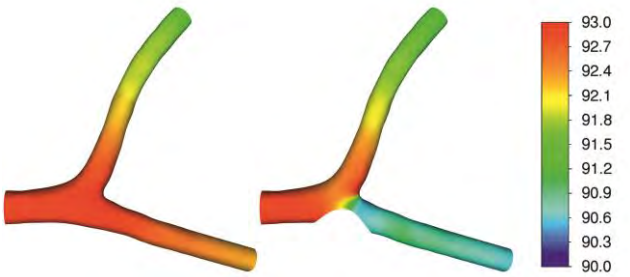

Figure 10.9.1. Pressure distribution [mmHg] in the left coronary artery at rest (left) in a heathy one (right) with LAD stenosis.

Acknowledgements

This research was supported by the PW YOUNG project, granted by the Warsaw University of Technology under the Excellence Initiative: research University program.

10.10 Cultivation of transfected *Nicotiana tabacum* BY-2 cells in a rocking disposable bioreactor

Grzegorz Karpiński1, Kamil Wierzchowski*,1, Mateusz Bartczak1, Mateusz Kawka2, Katarzyna Sykłowska-Baranek2, Maciej Pilarek1

1. Faculty of Chemical and Process Engineering, Warsaw University of Technology, Warsaw, Poland
2. Faculty of Pharmacy, Medical University of Warsaw, Warsaw, Poland

e-mail: kamil.wierzchowski@pw.edu.pl

KEYWORDS: *BY-2 cells, single-use bioreactors, wave-type agitation, bioprocess intensification*

Plant biotechnology has been in development for centuries, providing the scientific world with new possibilities and challenges. One of many aspects which caused a growing interest in plant cell biotechnology is their ability to produce callous – unorganised parenchyma cells, which can differentiate and heal wounded plant tissues and restore entire plants from a single callous cell. *Nicotiana tabacum Bright Yellow-2* (BY-2) is one of the most meticulously researched plant callous lines. Cells of this line are easily synchronised and have a satisfying growth rate and homogeneity of culture. One of the most important features of BY-2 cells is their ability to synthesise mammalian proteins after genetic modification. Therefore, they are likely to become increasingly attractive for biosimilar particle manufacturing.

However, due to the high sensitivity of BY-2 cells to shear stress and the high density and viscosity of BY-2 cell cultures, large-scale cultures of *N. tabacum* cells require specific conditions for cultivation. Rocking disposable bioreactors are characterised by satisfactory mass transfer conditions with simultaneously low shear stress values. Wave-type agitation and bubble-free aeration, which occur in these bioreactors, provide favourable conditions for BY-2 cell cultivation.

In our study, we focused on the influence of wave-type agitation conditions on *N. tabacum* BY-2 cell line cultures. In this case, we used a *ReadyToProcess* WAVE 25 bioreactor equipped with a 2 L culture vessel. The effect of the angle (α) and the frequency (ω) of oscillations on BY-2 cell proliferation and biosynthesis of protein bioproducts was determined.

During the cultivation of BY-2 cells, the density and viscosity of the culture broth increased significantly. Due to this, the wave-type agitation parameters were increased during cultures. The highest proliferation of BY-2 cells and the highest activity of protein bioproducts was observed for cultures performed at the following WAVE 25 bioreactor conditions: 0–2 days at $\alpha = 6^\circ$ and $\omega = 20$ min^{-1}, 3–5 days at $\alpha = 8^\circ$ and $\omega = 26$ min^{-1}, and 6–10 days at $\alpha = 12^\circ$ and $\omega = 30$ min^{-1}.

Acknowledgements

The research was funded by the Warsaw University of Technology within the Excellence Initiative: Research University (IDUB) programme.

10.11 Polydopamine as a possible binding agent for antithrombotic coating for small-diameter artificial vascular grafts

Jakub Knap-Kowalski*,1, Beata Butruk-Raszeja2

1. Faculty of Chemical and Process Engineering, Warsaw University of Technology, Warsaw, Poland
2. Laboratory of Biomedical Engineering, Department of Biotechnology and Bioprocess Engineering, Faculty of Chemical and Process Engineering, Warsaw University of Technology, Warsaw, Poland

e-mail: jakubkarolkowalski@gmail.com

KEYWORDS: p*olydopamine, small-diameter vascular grafts, artificial grafts, surface modification*

Currently one of the main issues halting the wide-spread application of vascular artificial grafts for human implantation is a high risk of thrombosis. Highlighted problem is especially prominent in small-diameter (<6mm) grafts. One of currently used methods of improving hemocompatibility of surfaces designed for extended exposure to blood is applying a coating layer consisting of antithrombotic agents. However, oftentimes the adhesion of agent to modified surface is not strong enough to be effective in long-term implantation.

This work examines the impact of polydopamine on wettability, and human blood platelets adhesion to polyurethane surfaces. Furthermore, the properties of surfaces modified in two-step procedure were examined. The two-step procedure consisted of primer coating using polydopamine as a binding agent and then applying the secondary coating of antithrombotic agent. During the experiment albumin or taurine were used as a secondary coating agent. Properties of single and double coated surfaces have been compared to uncoated surfaces and samples exposed to only antithrombotic agents. For assessing the wettability of potential grafts, the contact angle of water droplet was measured. Antithrombotic effect of applied coatings was estimated as a fraction of occupied surface area by adhered platelets aggregates to examined surface, which was observed using scanning electron microscopy.

Concluded study suggests that polydopamine coating highly increases the wettability of polyurethane surfaces and increases the adhesion of platelets, comparing to unmodified samples. After applying the secondary coating, the fraction of surface area occupied by platelets, was greatly reduced in both examined variants (albumin or taurine). The wettability of surfaces subjected to secondary coating was moderately lowered.

Surfaces modified with polydopamine, and albumin presented the lowest platelets adhesion of all proposed modification procedures. Percentage of surface occupied by platelets in double coated samples was significantly lower than in samples exposed only to high concentrations of albumin. This could suggest that polydopamine is a viable candidate for further studies concentrating on researching binding agents for multi-layered antithrombotic coatings.

Acknowledgements

This work was supported by The National Science Centre, Poland, grant number: UMO 2020/39/I/ST5/01131.

10.12 Exploring the potential of poly(glycerol itaconate) gels: innovative nonwovens for possible biomedical applications

Krzysztof Kolankowski[1], Magdalena Miętus[1], Piotr Denis[2], Aleksandra Bandzerewicz[1], Agnieszka Gadomska-Gajadhur*,1

1. Faculty of Chemistry, Warsaw University of Technology, Warsaw, Poland
2. Laboratory of Polymers and Biomaterials, Institute of Fundamental Technological Research, Polish Academy of Sciences, Warsaw, Poland

e-mail: agnieszka.gajadhur@pw.edu.pl

KEYWORDS: *biomaterials, nonwovens, poly(glycerol itaconate)*

Electrospinning is a process that has received a lot of attention in recent years. The fibers produced mimic the extracellular matrix well, so the possibility of using nonwovens as cellular scaffolds is being tested. The electrospinning technique is widely used in areas such as engineering bone tissue, cartilage tissue, skin tissue, the nervous system and the cardiovascular system.

The aim of the present study was to synthesize a new polymer – poly(glycerol itaconate) and then produce nonwoven fabrics with the addition of polylactide. The use of a mixture of polymers has allowed to obtain a material with different properties than in the case of stand-alone polyesters. The produced nonwovens were examined for potential use in tissue engineering - SEM image analysis, cytotoxicity, surface character determination were performed.

All the produced nonwovens were characterized as hydrophilic. It is beneficial to crosslink the nonwovens to prolong their degradation time. Further cytotoxicity studies on cell lines and mechanical tests are needed. In the future, it will be beneficial to conduct cytotoxicity studies of UV-crosslinked nonwovens to rearrange C=C bonds.

The studies conducted have provided a preliminary indication of the potential use of PGItc+PLA nonwovens as subcutaneous tissue fillers or drug delivery systems.

Acknowledgements

This scientific research was financed by the National Centre for Research and Development as a research project “Lider 11” (LIDER/4/0010/L-11/19/NCBR/2020) titled “Porous, biodegradable implants for the regeneration of spongy bone”.

10.13 Gel-derived bioactive glass nanoparticles

Katarzyna Kozubal*,[1], Michał Dziadek[1], Katarzyna Cholewa-Kowalska[1]

1. Department of Glass Technology and Amorphous Coatings, Faculty of Materials Science and Ceramics, AGH University of Krakow, Krakow, Poland

e-mail: kozubal@agh.edu.pl

KEYWORDS: *bioactive glass, nanoparticles, sol-gel method*

Bioactive glasses are widely used in bone tissue regeneration. They facilitate the formation of apatite, a crucial component of the extracellular matrix of bone tissue, so the reconstruction of bone defects can occur faster, allowing for an earlier return to health, reducing hospitalization time, and minimising complications. Special interest have been made to bioactive glass nanoparticles due to their potential as novel therapeutic and regenerative agents. However, designing and obtaining desired nano-bioglass may present various challenges. Choosing the appropriate composition and manufacturing methods allows for controlling the dissolution kinetics of nanoparticles, enabling the customization of the biomaterial for individual patients. The significantly expanded surface area of nanoparticles enhances the interaction area, while their small size influences a less invasive method of delivering materials into the body.

This study focused on nanoscale materials with bioactive properties (SiO_2-CaO-P_2O_5 ternary glasses) such as A2 (40%$_{mol}$ SiO_2, 54%$_{mol}$ CaO, 6%$_{mol}$ P_2O_5) and S2 (80%$_{mol}$ SiO_2, 16%$_{mol}$ CaO, 4%$_{mol}$ P_2O_5) bioactive glasses. The primary research goal was to optimize the sol-gel method of obtaining bioglass nanoparticles, involving the determination of the process course, synthesis time, selection of suitable catalysts, and precursors, with special attempts to get nanoparticles with nominal compositions. Structural analysis (FTIR, XRD) and morphology assessment (SEM) were conducted, along with an examination of the materials' ability to form an apatite layer (SEM, FTIR, XRD, ICP-OES).

The obtained nanoparticles exhibit a uniform shape and size for selected materials. The changes introduced in the synthesis process not only yielded bioactive glass with a composition that meets the nominal composition, but also revealed limitations of controlling the particle size and agglomeration tendency in regard to chemical composition. Samples with high SiO2 content were amorphous (S2) while A2 materials demonstrate glass-crystalline nature. The formation of the biological apatite phase served as an indicator of bioactive glass behaviour in a simulated body fluid was evaluated for selected materials and demonstrated high bioactive potential, including both glass nanoparticles from the S2 and A2 groups.

Acknowledgements

This work was supported by the program „Excellence initiative – research university" for the AGH University of Krakow.

10.14 The impact of proton radiation on osteoblasts

Magdalena Król*,[1], Barbara Zagrajczuk[2], Zuzanna Piątek[3], Elżbieta Menaszek[3], Renata Szymańska[1]

1. Department of Applied Nuclear Physics, Faculty of Physics and Applied Computer Science, AGH University of Cracow, Cracow, Poland
2. Department of Silicate Chemistry and Macromolecular Compounds, Faculty of Materials Science and Ceramics, AGH University of Krakow, Krakow, Poland
3. Department of Cytobiology, Faculty of Pharmacy, Jagiellonian University, Cracow, Poland

e-mail: krolmagda@student.agh.edu.pl

KEYWORDS: *radiation, osteoblasts, proton beam, tumor osteoblast-like cells, molecular biology*

Tumour treatment heavily relies on high-dose radiation, a potent tool in eliminating pathological cells. However, this approach presents challenges, particularly adverse effects on bones, such as osteopenia and osteoporosis. Cancer patients undergoing radiotherapy often experience complications like radiation-induced bone necrosis and frequent fractures. This concern extends beyond terrestrial treatments; it reaches into space travel, where astronauts face bone mass loss due to both cosmic radiation exposure and prolonged microgravity conditions.

In the pursuit of understanding the intricate effects of high-energy proton radiation on cellular systems, this research focused on two cell lines, NHOst (Normal Human osteoblast) and MG63 (human osteoblast-like cells derived from bone tumor). A 225 MeV proton accelerator was utilized, employing an entrance dose that contributed to a reduction in uncertainties associated with the delivered dose. Varied doses of radiation were used: 0.5 Gy, 2 Gy and 10 Gy. The experiment aimed to investigate the immediate and lasting impacts of radiation, exploring viability, repair mechanisms, and potential functional implications. In addition to standard viability assessments, complementary assays were conducted to gain a comprehensive understanding of the cellular responses. The PrestoBlue test was used to assess cell viability and metabolic activity and the ToxiLight assay was instrumental in evaluating the toxicity levels associated with the experimental conditions. Furthermore, the incorporation of Enzyme-Linked Immunosorbent Assay (ELISA) for GADD45 expanded the investigation into the molecular realm.

NHOst cells exhibited an immediate decline in viability, correlating with increasing radiation doses. The initial measurement highlighted immediate radiation effects on cell viability. Extended incubation revealed a significant increase in cell activity associated with repair attempts after radiation exposure. This observation suggested that cells initiate complex repair mechanisms in response to radiation-induced stress. Despite initial impact, irradiated cells tended to return to values comparable to control cells over time, indicating efficient repair mechanisms mitigating prolonged damage. In MG63 cells, a 10 Gy dose led to a substantial viability decrease, confirming a lasting impact on cell survival. Unlike previous cell lines showing some improvement in viability, cells exposed to a 10 Gy dose maintained low viability even two days post-irradiation, suggesting sustained and lasting effects, involving significant damage or disruption of repair processes hindering cell regeneration.

Acknowledgements

I would like to express my sincere gratitude to Prof. Justyna Miszczyk for her invaluable assistance in irradiating cells and coordinating the entire undertaking at CCB IFJ. I appreciate the unwavering support and dedication throughout the process.

The project was financed by AGH University of Krakow as part of a grant obtained through the activities of the scientific club SKNF Bozon.

10.15 Selection of conditions for obtaining fibrous substrates with variable wettability intended for soft tissue restoration

Anna Marszałek*[,1], Roksana Kurpanik[1], Ewa Stodolak-Zych[1]

1. Department of Biomaterials and Composites, Faculty of Ceramics and Materials Science, AGH University of Krakow, Krakow, Poland

e-mail: amarszalek@agh.edu.pl

KEYWORDS: *polycaprolactone, polyvinylidene fluoride, concurrent electrospinning, sequential electrospinning, wettability*

Polymeric fibrous materials are used in many fields. One of them is regenerative medicine, where they are a promising choice for stimulating hard and soft tissues to autoregenerate. Such materials can be used as extracellular substrates or scaffolds to enable proliferation and differentiation of cells in damaged tissue. It is very important to choose the right manufacturing conditions, as they translate directly into the properties of the material, such as morphology or wettability, affecting the quality of the cellular response.

The aim of the study was to obtain two types of polymer fibers, from which, using sequential and competitive electrodeposition, fibrous substrates differing in wettability and surface energy can be obtained. Two commercial polymer: polycaprolactone (PCL, Sigma-Aldrich, M_w~80 kDa) and polyvinylidene (PVDF, Sigma-Aldrich, M_w~275 kDa) were used. The research began with the development of viscosity-stable polymer solutions. They were prepared using different system of solvent: for PCL dichlorometane (DCM, POCH) and dimethylformamide (DMF, POCH), for PVDF dimethylacetamide (DMAc, Sigma-Aldrich) and acetone (Ac, Sigma-Aldrich) respectively. First, the viscosity of polymer solutions of different concentrations was tested using a rheometer (Modular Compact Rheometer MCR 302, Anton Paar). Then four types of nonwovens were produced: PCL or PVDF fibers only, PCL/PVDF fibers using sequential electrospinning, and PCL/PVDF fibers using concurrent electrospinning. An electrospinning machine able to stabilize humidity and temperature was used to obtain the fibers. Selected pro-perties of the materials obtained in this way were examined. Wettability and surface free energy were measured using goniometer (DSA 25 KRÜSS). The materials showed different wettability depending on the composition, PVDF being more hydrophobic than PCL. Microstructure of fibrous materials was observed with scanning electron microscope (Apreo 2 SEM, ThermoFisher Scientific). The distribution of the fiber thickness was unimodal for both polymers. Average fiber thickness for PCL was around 1 µm, while PVDF fibers were thicker, around 1.5 µm.

The obtained results show the relationship between the manufacture conditions and material features such as morphology and wettability. However, in order to choose the most optimal arrangement of PCL/PVDF fibers, it is necessary to study cells-materials interaction.

Acknowledgements

Research project supported by program IDUB "Excellence initiative – research university" for the AGH University of Krakow". Project ID 4204

10.16 Aspects to consider during aza--Michael addition reactions of itaconic compounds

Magdalena Miętus[1], Krzysztof Kolankowski[1], Paweł Ruśkowski[1], Agnieszka Gadomska-Gajadhur*[,1]

1. Faculty of Chemistry, Warsaw University of Technology, Warsaw, Poland

e-mail: agnieszka.gajadhur@pw.edu.pl

KEYWORDS: *aza-Michael addition reaction, itaconic adducts, undesirable reactions, unsaturated electrophiles, PPM*

In the structure of itaconic acid, fumaric acid, and maleic acid, a C=C multiple bond is present. Its presence allows to perform post-polymerization reactions such as aza-Michael additions.

Aza-Michael reactions are practically irreversible, but the use of elevated temperature can reverse the addition of a nucleophile. The main advantage of aza-Michael addition is its possibility to occur at temperatures close to the room temperature. It also does not require the use of a catalyst and solvent. In this reaction, itaconic compounds act as an electrophile (Michael acceptor). The role of the nucleophile (Michael donor) can be performed by primary and secondary aliphatic or aromatic amines, azides, carbamates, and amides. Because of the presence of the C=C bond in the side chain of the itaconic compound, the aza-Michael addition reaction occurs preferably on the side of the carbon atom at the β position in the C=C bond.

While conducting the aza-Michael addition reaction of itaconic compounds, there are several important aspects to consider. Itaconic compounds can isomerize to mesaconic and citraconic ones. They are less or not reactive towards the nucleophile during the addition reaction. It is due to the presence of a methyl group in the neighbourhood of the C=C bond. By carrying out the aza-Michael addition reaction, the used nucleophile can act as a catalyst for the isomerization reaction. It reduces the efficiency of the addition reaction. To prevent this, it is beneficial to use the nucleophile in excess. While using a primary amine as a nucleophile, there is a possibility of an undesired lactamization reaction. Despite this, primary amines are frequently used in the aza-Michael addition reaction, since secondary amines suffer from the problem of a higher steric crowding. Although the aza-Michael addition reaction can proceed without a catalyst and solvent, their presence can be advantageous. There is a reduction in the proportion of isomerization reactions, leading to the increased efficiency of the addition reaction.

Despite some of the problems that can occur while conducting aza-Michael addition, it is a high-potential post-polymerization reaction – for instance in medicine.

Acknowledgements

This scientific research was financed by the National Centre for Research and Development as a research project, "Lider 11" (LIDER/4/0010/L-11/19/NCBR/2020), titled "Porous, biodegradable implants for the regeneration of spongy bone".

10.17 Aza-Michael addition reactions of itaconic compounds

Magdalena Miętus[1], Krzysztof Kolankowski[1], Paweł Ruśkowski[1], Agnieszka Gadomska-Gajadhur[*,1]

1. Faculty of Chemistry, Warsaw University of Technology, Warsaw, Poland

e-mail: agnieszka.gajadhur@pw.edu.pl

KEYWORDS: *unsaturated itaconic compounds, aza-Michael addition, post-polymerisation modification*

In the structure of the itaconic compounds, a multiple bond is present in their side chain. It makes post-polymerization reactions possible - thermal and photoinduced crosslinking reactions, and addition reactions. Among the most popular addition reactions there are the aza-, thio-, and oxo-Michael addition reactions.

The aza-Michael addition reaction has many advantages. By all means, it can occur at temperatures close to T_{room}. It does not require the use of any solvent or a catalyst. It is also characterized by a wide choice of substrates. What is crucial, the only product of the reaction is most often the addition product.

To perform the aza-Michael addition reaction, the used electrophile (a chemical compound with an α, β-unsaturated bond) should have good solubility and should not be isomerized. Itaconic compounds can isomerize to less reactive compounds - mesaconic and citraconic ones. According to the literature reports, they are not reactive toward nucleophiles in the aza-Michael addition reaction. For this reason, while conducting the aza-Michael addition reaction, it is necessary to minimize their content as much as possible - for instance, by using a suitable attacking nucleophile (an aliphatic/aromatic primary/secondary amine, for example).

While carrying out the aza-Michael addition reaction of itaconic compounds, it is necessary to pay attention to the chosen substrates and their molar ratio. Particular focus should be given to the structure of the used amine (primary/secondary amine). It is also necessary to consider the temperature and time of the conducted aza-Michael addition reaction. It can affect the yield of the adduct.

Taking into account the above aspects, it is possible to carry out an efficient post-polymerization reaction, which is the aza-Michael addition reaction.

Acknowledgements

This scientific research was financed by the National Centre for Research and Development as a research project, "Lider 11" (LIDER/4/0010/L-11/19/NCBR/2020), titled "Porous, biodegradable implants for the regeneration of spongy bone".

10.18 3D printing of thermosensitive hydrogel with antimicrobial properties

Martyna Niziół[*,1], Justyna Paleczny[2], Adam Junka[2], Amin Shavandi[3], Anna Dawiec-Liśniewska[1], Daria Podstawczyk[1]

1. Wroclaw University of Science and Technology, Wroclaw, Poland
2. Wroclaw Medical University, Wroclaw, Poland
3. Univesité Libre de Bruxelles, Brussels, Belgium

e-mail: martyna.niziol@pwr.edu.pl

KEYWORDS: *stimuli-responsive, wound patch, biocompatible, 3D printing*

Skin wounds are a growing healthcare problem worldwide as a result of an aging population coupled with an increasing incidence of diabetes, obesity and cancer. The healing process of such wounds can take several years, while failure to heal leads to amputation - diabetic ulceration accounts for 80% of all lower extremity amputations. To this purpose, new functional materials are being explored that could contribute to the development of personalized wound dressings.

The focus has been on hydrogels, which, due to their ability to hold large amounts of water and biological fluids, are excellent materials for chronic wound care applications. An alginate-based hydrogel (Alg) was created that is biocompatible and has low cytotoxicity but poor printability. To improve viscosity and printability, methylcellulose (MC) was added. Octenisept® antiseptic (OCT) was also suspended in the material to provide antimicrobial protection. To achieve the shape effect (Figure 10.18.1), p(N-isopropylacrylamide) was added to the hydrogel matrix.

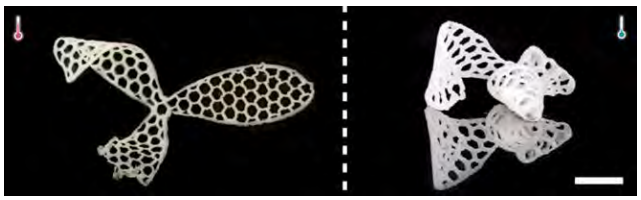

Figure 10.18.1. Temperature behaviour of the printed hydrogel.

A well-printable hydrogel with temperature-dependent swelling, shape variation and release of active compounds was developed. The performed studies (rheology, SEM, drug release profile, swelling and biological activity) proved the multifunctionality of the hydrogel and confirmed that the material can be used as a wound dressing

Acknowledgements

I would like to acknowledge the Wroclaw University of Science and Technology for use of their lab facilities.

10.19 Optimization of the 3D printing process of gelatin methacryloyl bioink

Agnieszka Piontek*[,1], Jadwiga Laska[2]

3. Faculty of Electrical Engineering, Automatics, Computer Science and Biomedical Engineering, AGH University of Krakow, Krakow, Poland
4. Faculty of Materials Engineering and Ceramics, AGH University of Krakow, Krakow, Poland

e-mail: piontek@student.agh.edu.pl

KEYWORDS: *bioink, hydrogels, gelatin methacryloyl, 3D bioprinting, tissue engineering*

3D bioprinting is an innovative tissue engineering technique that ensures an even distribution of cells in the manufactured construct and precise deposition of material, which allows imitation of the native tissue. Effective bioprinting requires fitting the material properties and printing method to the cells contained in the bioink. In our research, a prototype of bioink based on gelatin modified with methacrylic anhydride (GelMA) was produced for printing tissue substitutes using the extrusion method. The primary advantage of GelMA is its high biocompatibility with various types of cells. The main challenge was to optimize the material composition and its physical and rheological properties. The properties of hydrogel can be controlled in a wide range by adjusting the degree of substitution of amino groups in the gelatin protein chain. The potential use of an innovative crosslinking agent in the form of ammonium persulfate was tested as a cheaper alternative to the commonly used photoinitiator Irgacure 2959. The properties of GelMA with various methacrylation degrees were compared to those of unmodified gelatin. Printing parameters in terms of bioink initial temperature, nozzle diameter and shape, pressure, and printing speed were optimized. The following research focuses on currently challenging aspects of effective bioprinting.

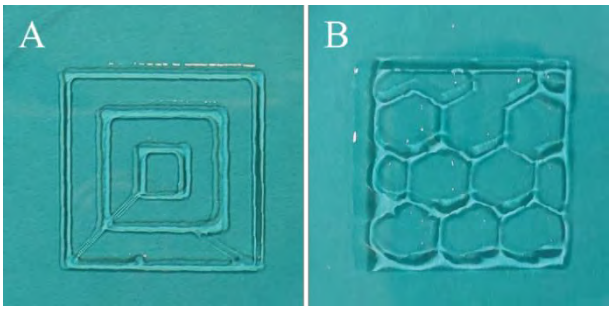

Figure 10.19.1. GelMA 3D-printouts obtained during the optimization process to produce scaffolds in the form of: A. coaxial squares, B. honeycomb.

Acknowledgements

The research was financially supported by AGH University of Krakow, Faculty of Materials Science and Ceramics, grant No. 16.16.160.557.

10.20 Personalized 3D printing in skin cancer brachytherapy: development, implementation, clinical applications, and treatment assessment

Michał Półtorak*[,1], Paweł Banatkiewicz[1], Łukasz Półtorak[2], Piotr Sobolewski[1,4], Damian Zimoń[1,4], Maciej Szwast[3], Irena Walecka[1,4]

1. The National Institute of Medicine of the Ministry of the Interior and Administration, Warsaw, Poland
2. Electrochemistry@Soft Interfaces Team, Department of Inorganic and Analytical Chemistry, Faculty of Chemistry, University of Lodz, Lodz, Poland
3. Department of Chemical and Process Engineering, Warsaw University of Technology, Warsaw, Poland
4. Department of Dermatology, Centre of Postgraduate Medical Education, Warsaw, Poland

e-mail: Krzysztof.Truchel.dokt@pw.edu.pl

KEYWORDS: *superficial brachytherapy, 3D printing, fused deposition modeling, skin cancer, individual applicator*

This study delves into the widespread use of brachytherapy for skin cancer treatment, emphasizing the crucial role of personalized applicator fabrication for effective treatment delivery. It highlights the utilization of adaptable devices tailored to individual patient anatomy, made possible by advancements in 3D printing technology (Figure 10.20.1). Patients with inoperable tumor lesions in various anatomical locations were enrolled in the study. Customized applicators were 3D printed for each patient. Throughout and post-radiotherapy, patient assessments included evaluations using the RTOG scale and reflectance confocal microscopy. The applicators were fabricated using fused deposition modelling technology, with careful optimization of printing parameters to ensure precise control over shape, directly impacting treatment efficacy. The study demonstrated diverse treatment responses, with complete remission achieved in all cases. Additionally, air gap pockets between the skin and applicator were examined on computed tomography scans. These findings underscore the potential of 3D-printed applicators to enhance brachytherapy outcomes in skin cancer management. The study concludes by emphasizing the effectiveness of 3D-printed applicators in treating inoperable skin cancer lesions with precision, minimizing treatment-related side effects, and improving overall patient outcomes. It suggests a promising future for 3D printing in skin cancer therapy, stressing the importance of further research and clinical validation to establish it as a standard practice.

Figure 10.20.1 3D-printed applicator with two catheters used in High Dose Rate (HDR) brachytherapy for skin cancer.

10.21 Simplification of the ventricular model in the CFD analysis of hemolysis in mitral paravalvular leak pathology

Krzysztof Truchel*,1, Krzysztof Wojtas1, Michał Kozłowski2, Wojciech Orciuch1, Łukasz Makowski1

1. Faculty of Chemical and Process Engineering, Warsaw University of Technology, Warsaw, Poland
2. Department of Cardiology and Structural Heart Diseases, Medical University of Silesia, Katowice, Poland

e-mail: Krzysztof.Truchel.dokt@pw.edu.pl

KEYWORDS: *paravalvular leak, hemolysis, computational fluid dynamics, dynamic mesh, large deformation diffeomorphic metric mapping*

This paper presents four alternatives for hemodynamics modeling of cardiac contraction affected by the mitral paravalvular leak. Using computational fluid dynamics and large deformation diffeomorphic metric mapping, simulations were performed in which the motion of the ventricle was represented in four different ways.

Based on the results of the computed tomography, a model of the heart was created that represented the real heart structure. This model most accurately describes the hemodynamics of cardiac contraction, but due to the long preparation time and the difficulty of geometry preprocessing, an application of this model in everyday diagnostics is not feasible. Therefore, two possible simplifications of the geometry have been proposed: the static mesh and the universal ventricular geometry. Simulation results for the most complex variant (real model, dynamic mesh) were compared with simplified variants: 1) real model, static mesh; 2) universal model, dynamic mesh; 3) universal model, static mesh. Simulations were performed for unsteady flow during the entire ventricular contraction using the non-Newtonian Carreau-Yasuda blood rheological model.

The hemodynamic conditions, as well as the values of the parameters based on the hemolysis criterion (shear stresses greater than 300 Pa), did not indicate significant differences between the compared models. This proves that the approach to the analysis of the phenomenon of hemolysis in cases of mitral leaks can be simplified to a variant where the motion of the ventricle is replaced by appropriate boundary conditions, and the geometry of the ventricle can be described by simple shapes and does not have to be based on medical imaging of the patient's ventricle. In such a case, it is only necessary to accurately map the geometry and location of the leak. This approach significantly reduces the time to prepare the geometry and perform the calculations, thus making it feasible for day-to-day medical diagnostics.

Acknowledgements

This study was funded by the BIOTECHMED-3 project granted by the Warsaw University of Technology under the program, Excellence Initiative: Research University.

10.22 3D-Printed Anatomy Models: Enhancing FEA Results Visualization

Wiktoria Wojnarowska*,1

1. Department of Physics and Medical Engineering, Faculty of Mathematics and Applied Physics, Rzeszow University of Technology, Poland

e-mail: wwojnarowska@prz.edu.pl

KEYWORDS: *patient-specific models, simulation results, biomechanics, additive manufacturing, finite element method*

Finite element analysis (FEA) can be crucial in surgical planning and rehabilitation. However, the presentation of FEA results in 2D images is often not detailed enough to provide comprehensive diagnostic insight and can be difficult for physicians without engineering expertise to interpret. This study aims to overcome these limitations and create an accessible form of visualizing FEA results by using anatomical models produced using additive manufacturing (AM) processes.

The methodology involves two main parts. The first is the preparation of a colour digital model, which included geometric modeling, FEA analysis and integration of the results with a colour contour map. The second part encompasses a comprehensive AM process, utilizing Fused Deposition Modeling (FDM) for cost-effective multi-coloured models and PolyJet for high-resolution, intricate details.

The study demonstrates the potential of 3D-printed models in conveying FEA results, providing quantitative representations of anatomical structures and stress distribution. This enhances diagnostics, treatment planning, and communication for medical professionals and engineers. The choice between FDM and PolyJet depends on project specifics and budget considerations. This work establishes the effectiveness of 3D-printed models for visualizing FEA results in medical applications.

Acknowledgements

This research was conducted as part of the project "Wieloobiektowe spersonalizowane modele medyczne ze strukturą wewnętrzną oraz metoda ich wytwarzania," supported by Podkarpackie Centrum Innowacji Sp. z o.o. under the "Podkarpackie Centrum Innowacji" project, a component of the Regional Operational Programme for the Podkarpackie Voivodeship 2014-2020, Priority Axis I: Competitive and Innovative Economy, Measure: R&D Projects Competition, Call III.

10.23 An integrative biomechanical approach to developing a patient-specific numerical model of the pelvic bones

Wiktoria Wojnarowska*,1

1. Department of Physics and Medical Engineering, Faculty of Mathematics and Applied Physics, Rzeszow University of Technology, Poland

e-mail: wwojnarowska@prz.edu.pl

KEYWORDS: *patient-specific model, biomechanics, finite element method, physiological boundary conditions, simulation*

An integrative biomechanical approach, utilizing specific patient data collected through various measurement techniques, is gaining popularity in developing finite element method (FEM) models of anatomical structures. This study aims to contribute to this growing trend by applying this approach to develop a numerical model of the pelvic bones.

To create a numerical model, input data, including material properties, boundary conditions, loads, and geometry, were identified. To employ the integrative biomechanical approach, the geometry was create from DICOM data obtained through medical imaging, and loads were computed using kinematic data recorded via an inertial Motion Capture system (Figure 10.23.1).

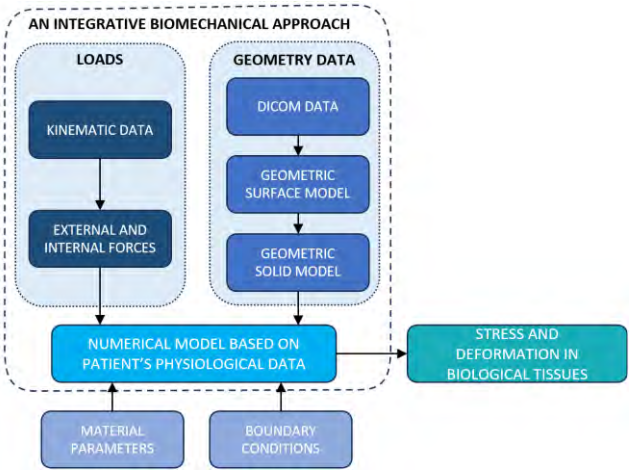

Figure 10.23.1. The integrative biomechanical approach used to develop personalized FEM model of pelvic bones.

This integrative biomechanical methodology successfully yielded a patient-specific model of the pelvic bone. The utilization of CT scans and gait analysis provided precise information crucial for numerical calculations. Consequently, this approach enables the creation of personalized models that accurately capture unique body characteristics. The model holds promise in assisting surgical planning, optimizing implants, and evaluating treatment outcomes. Furthermore, the methodology developed for the pelvic model shows adaptability to other anatomical structures. In conclusion, the resulting model is a potentially effective tool for various medical applications.

10.24 Optimisation of the measurement procedure for the colourimetric method adaptation in wave-mixed single-use bioreactors

Tuğba Yılmaz*,1, Mateusz Bartczak1, Kamil Wierzchowski1, Maciej Pilarek1

1. Faculty of Chemical and Process Engineering, Warsaw University of Technology, Warsaw, Poland

e-mail: tugba.yilmaz.stud@pw.edu.pl

KEYWORDS: *single-use bioreactors, mixing time, colourimetric method, optimisation, design of experiment (DoE)*

The term "disposable" bioreactor means that the cultivation container is made of FDA-approved plastics (e.g., PE, EVA, PC, PS) and is designed to be used only once. The container is typically shipped sterile and pre-assembled to be used directly without further preparation. Wave-mixed disposable bioreactors are commonly used in biotechnology processes where shear stress sensitive cell cultures are used. This type of bioreactor uses oscillatory movements to ensure homogeneous mixing of the culture medium through characteristic "wave" liquid flow. With this mechanism, the biomass is enabled to access nutrients effectively and produce valuable bioproducts.

In wave-mixed bioreactors, mixing time is a critical factor for effective biological processes and increasing product efficiency. Mixing time refers to the time it takes to mix the liquid to a set level of homogeneity. Mixing with appropriate efficiency allows nutrients, microorganisms or cell cultures to interact with each other and for reactions to occur under optimal conditions, ensuring the desired properties of the bioproducts.

The goal of our study was to optimise the measurement procedure of the colourimetric method adaptation for mixing time determination in a wave-mixed bioreactor. In our case, we used a ReadyToProcess WAVE™ 25 bioreactor with a Cellbag™ 10 L vessel. The colourimetric method is based on observing the colour change of an indicator dissolved in the bulk mixture after adding a small portion of tracer solution, which triggers an acid-base neutralisation reaction. The impact of three independent parameters: volume of tracer related to the bulk liquid volume (V_{tracer}/V_{bulk}), the molar ratio of reagents (n_{tracer}/n_{bulk}), and the composition of the two solutions (acid in bulk + base in tracer; base in bulk + acid in tracer) has been determined under constant wave agitation parameters ($\alpha = 2°$, $\omega = 21$ rpm, $V_{bulk} = 2.75$ L). The best combination of parameters, pre-selected using DoE methodology, was determined based on the repeatability and deviation between mixing time values obtained under the same conditions.

Acknowledgements

The research was funded by the Warsaw University of Technology within the Excellence Initiative: Research University (IDUB) programme.

11 Abstracts: Process equipment & environmental protection

11.1 The effect of 1,4-butanediol on the efficiency of CO_2 absorption and inhibition of NH_3 escape during the mineral carbonation of gypsum

Temesgen Abeto Amibo[*,1,2], Donata Konopacka-Łyskawa[1]

3. Gdansk University of Technology, Gdansk, Poland
4. Jimma University, Jimma, Ethiopia

e-mail: temesgen.amibo@pg.edu.pl

KEYWORDS: *mineral carbonation, butanediol, CO_2 capture, gypsum, ammonia desorption*

Effectively and affordably advancing methodology for selectively capturing and storing CO_2 from diverse sources is one of the central challenges in addressing climate change. Ammonia solutions, highly valued for advantages like improved absorption efficiency and reduced regeneration energy needs, face a problem due to ammonia's high volatility, causing desorption during gas flow. Nevertheless, ammonia solutions as the CO_2 absorption solvent are proposed for reasons of cost-effectiveness, high capacity, and versatility. Various studies employ inorganic, organic, and nanoparticles as additives to tackle this issue. In this particular study, different concentrations of 1,4-butanediol were utilized to counteract ammonia escape and enhance CO_2 absorption.

This study aimed to explore the optimal concentration of 1,4-butanediol for maximizing CO_2 absorption and minimizing ammonia desorption. Physicochemical properties of the liquid phase, including density, viscosity, and surface tension were determined. Mineral carbonation of gypsum slurry was carried out in a bubble reactor with a magnetic stirrer maintaining constant speed for 1 hour. The gas introduced to the reactor was a mixture of CO_2 and air. The gas flow was controlled by the mass controllers. Gas sensors were used to determine the concentration of CO_2 and NH3 in the outlet gas. The initial and final pH values were measured. The liquid phase was ammonia solutions at a concentration of 1.69 mol.dm^{-3} with the addition of varying concentrations of 1,4-butanediol (ranging from 0.1 to 0.5 mol. dm^{-3}). The ratio of gypsum to liquid phase was maintained as 1:14 (kg. dm^{-3}). Based on measured CO_2 and NH3 concentrations, the efficiency of carbon dioxide absorption and the efficiency of ammonia escape inhibition were calculated.

Results demonstrated a direct correlation between increased additive weight, enhanced CO_2 absorption, and effective inhibition of ammonia escape. The addition of 1,4-butanediol enhances CO_2 dispersion within the solution, expanding the gas-solvent contact area and promoting a more effective absorption process. Therefore, it effectively inhibits the escape of ammonia during reactions by temporarily binding free ammonia in the solution. The application of 1,4-butanediol emerges as a promising strategy for optimizing the overall efficiency and performance of the studied processes.

11.2 A project of demonstration installation for plant-based drink production

Grzegorz Bernacki[*,1,2], Andrzej Krasiński[1], Jakub Lewandowski[1,2]

1. Faculty of Chemical and Process Engineering, Warsaw University of Technology, Warsaw, Poland
2. Scientific Club of Chemical and Process Engineering "Venturi", Faculty of Chemical and Process Engineering, Warsaw University of Technology, Warsaw, Poland

e-mail: grzegorz.bernacki.stud@pw.edu.pl

KEYWORDS: *plant-based drinks, vegan, extraction*

Plant-based drinks have become increasingly popular in recent years. They are an alternative to or substitute for animal milk for people who cannot assimilate lactose or who, for various reasons, do not wish to consume animal products.

Before building the plant, recipes for a nut-based vegetable drink were reviewed. Then, experiments were carried out for selected procedure to determine the ratio of nuts: water, or the size of oil droplets dispersed in water.

Laboratory-scale tests allowed establishing the favourable process layout and set of design parameters for the installation. Various methods of grinding, extracting fat from the plant ingredient and the method of emulsifying and stabilizing the water-oil emulsion were considered. Then, the devices included in the system were selected. A system operation with recirculation of the liquid in the system was chosen. In the main tank, there is a sieve (wedge-wire filter basket), where the soaked and crushed nuts were fed. After extraction, the liquid from the tank enters a plate filter or heated pipeline loop. The filter removes fine solids for the circulation line (and from the product). Heating enhances the extraction efficiency of fats from the nuts into the water. The liquid circulates through the system entering the tank through a system of flow guiding nozzles,, which enables agitating the suspension, thus preventing solids from settling and improving extraction.

Launching the installation with cashew nuts showed that relatively stable emulsion with small drops of the oil phase was obtained. In future work, the addition of emulsifiers will be verified to improve the long-term stability, while maintaining the taste and extending the shelf-life of the product.

Acknowledgements

The project was carried out as part of a grant from the Rector of Warsaw University of Technology awarded to the Scientific Club of Chemical and Process Engineering "Venturi".

11.3 Struvite precipitation as a method of liquid preparation before purification of post-processing liquid derived from hydrothermal carbonization of sewage sludge using membrane techniques

Klaudia Czerwińska*,[1], Agnieszka Urbanowska[2], Maciej Śliz[1], Izabela Kalemba-Rec[3], Małgorzata Wilk[1]

1. Department of Heat Engineering and Environment Protection, Faculty of Metals Engineering and Industrial Computer Science, AGH University of Krakow, Krakow, Poland
2. Department of Environment Protection Engineering, Faculty of Environmental Engineering, Wroclaw University of Science and Technology, Wroclaw, Poland
3. Department of Surface Engineering & Materials Characterisation, Faculty of Metals Engineering and Industrial Computer Science, AGH University of Krakow, Krakow, Poland

e-mail: kczerwin@agh.edu.pl

KEYWORDS: *membrane treatment, struvite precipitation, hydrothermal carbonization, post-processing liquid*

One of the most promising alternatives of sewage sludge conversion is hydrothermal carbonization process. This process does not require energy-intensive drying and is carried out in an aqueous environment. Hydrochar, produced in the HTC process, may be used as a potential biofuel. The liquid phase, which is the main product of hydrothermal carbonization of sewage sludge, poses major problems due to toxic compounds that make disposal impossible without proper treatment.

Taking the above into account, the main goal of the work is to present new methods of postprocessing liquid purification. For this reason, a comparative analysis of membrane filtration and membrane filtration combined with the struvite precipitation process was carried out by using different polymer and ceramic membranes. The study compares the liquid efficiency of three types of ceramic. A physical and chemical analysis was performed for each of the resulting permeates the following parameters were determined: pH, conductivity, NH_4^+, PO_4-P, PO_4^{3-}, P_2O_5, COD, Mg, and N_{total}. Additionally, SEM analysis was performed for the obtained struvite and selected membranes surfaces. XRD analysis was also performed for struvite. Moreover, the influence of struvite precipitation on the properties of the membrane used and the so-called membrane fouling effect was examined. In this case, an important aspect was to determine the parameters membrane relative permeability, degree of recovery S, permeate flux for each of the processes.

It was found that the properties of the permeate are influenced by the type of membrane used. However, membranes made of polyethersulfone behave differently than membranes made of regenerated cellulose. In general, for HTCL it was observed that a lower membrane cut-off value usually resulted in lower contaminant content in the permeate, but significant contamination occurred significantly faster. However, in the case of membrane filtration of struvite precipitation liquids, lower values of impurities and a smaller fouling effect were found.

Acknowledgements

This research was funded by the National Science Centre, Poland, under project no. 2021/41/B/ST8/01815 [OPUS21].

11.4 Influence of plant extracts on the fibering process and properties of structures obtained from PLA solution blow spinning

Radosław Gernaszewski*,[1], Agata Penconek[1], Arkadiusz Moskal[1]

1. Faculty of Chemical and Process Engineering, Warsaw University of Technology, Warsaw, Poland

e-mail: radek.gernaszewski@gmail.com

KEYWORDS: *polylactic acid, nanofibers, filter fabric, solution blow spinning, biostaticity*

The purpose of this research is to investigate how the rheological properties of a polymer solution have an influence on its solution blow spinning process. With the aim of doing that, a series of experiments were done to determine the rheological properties of polylactic acid solutions with additives, and the properties of the filter materials made from them were investigated. In addition, the biostaticity of the tested solutions and fibers was tested. The general idea of the research is to create relatively optimal biostatic easily biodegradable filter fabrics for air purification.

Literature on methods of producing polymer fibers and natural biocidal substances was used as a starting point. The properties and applications of the substances used in the study as solution additives are also described. Various methods of extracting these additives are also presented.

Further, the reagents and apparatus used were presented, as well as the research methodology. Solutions of polylactic acid with various vegetable additives and natural seasonings were used. Flow curves were determined using a rheometer. The filter fibers were then obtained using the solution blow spinning method, which were subjected to macroscopic and microscopic analysis. Based on fiber diameter measurements, diameter distributions were developed. Some additions of plant extracts provided both the solutions and the obtained fibers with biostatic properties on resident bacteria.

11.5 Benefits of frass in fertilizer production

Goda Gudinskaitė*,1, Rasa Paleckienė1

1. Department of Physical and Inorganic Chemistry, Kaunas University of Technology, Kaunas, Lithuania

e-mail: goda.gudinskaite@ktu.edu

KEYWORDS: *frass, fertilizer, Green Deal*

The current direction of development is the Green Deal, and its main goal is to create a sustainable, modern economy without harming the environment. In order to avoid the negative effects of intensive farming, various options for sustainable agriculture are often offered, such as partially replacing synthetic fertilizers, replacing chemical plant protection measures with biological ones. Due to the growing world population, the agricultural industry is challenged to produce the required amount of food. This is not possible without the use of fertilizers. In the fertilizer market, new products, which focus on the processes occurring naturally in the plant and the circular economy, are now appearing next to traditional fertilizers more frequently. The current trends in insect breeding, which are gaining wider applicability and legalization for use in the food industry, also create prerequisites for the development of possibilities for processing waste products.

Frass (Figure 11.5.1) is a by-product of insect breeding, the leftover substrate, which is composed of spent feedstock, insect feces, and cuticles. Recently, it has been evaluated as a potential fertilizer, in a circular economy perspective.

Figure 11.5.1. Samples of different frass forms

Under laboratory conditions, studies of frass were carried out by the company UAB "Divaks", concerning the suitability for fertilizer production, the chemical composition of frass and the composition of their extracts.

11.6 Enhancing Ammonia Oxidation (AOR) through Electrochemical Polarization: NiCu-S/NF Electrocatalyst

Afaq Hassan*,1, Justyna Łuczak1, Marek Lieder1

1. Department of Chemical Engineering, Gdansk University of Technology, Gdansk, Poland

e-mail: afaq.hassan@pg.edu.pl

KEYWORDS: *ammonia electrooxidation reaction (AOR), Mott-Schottky, electrochemical polarization, surface modification, heterojunction*

To produce high-purity hydrogen with less energy consumption ammonia oxidation reaction (AOR) has the ability to replace the oxygen evolution reaction (OER) in water splitting. AOR emerged as a potential technique due to its lower overpotential over OER, and preventing the mixing of hydrogen and oxygen. Transition metals-based anodes are one of the most effective and environmentally friendly for the AOR process.

Thus, we synthesized a highly efficient Ni0.5Cu1.5-S deposited on Nickel foam by sulphur doping and studied its AOR performance. The formed Ni0.5Cu1.5-S/NF Mott-Schottky heterojunction exhibits 287 $mA{\cdot}cm^{-2}$ current density at 1.69 V vs RHE and requires only 1.439 mV to obtain 50 $mA{\cdot}cm^{-2}$. Moreover, the electrode has a small Tafel slope of 90.72 $mV{\cdot}dec^{-1}$ and shows good stability for 24 hours.

Energy dispersion spectroscopy (EDS) shows that electrochemical polarization increases the oxygen content and reduces the sulphur content, indicating the transformation of metal sulphide to metal (hydroxyl) oxide. X-ray diffraction measurements demonstrated the existence of surface reconfiguration, which promotes the formation of true active species ($Ni_3O_{27}S_3H_{36}$, NiO_2, and Cu_2O). At 1.45 V vs RHE, 4320 ppm of N_2 were recorded after one hour. According to the experimental findings, we proposed a possible pathway for ammonia oxidation reaction based on the electrochemical polarization of the Ni0.5Cu1.5-S/NF. This study enriched the in-depth understanding of ammonia oxidation and provided a very promising way to produce hydrogen.

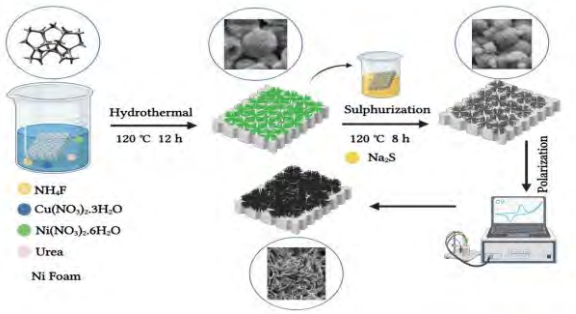

Figure 11.6.1. Schematic representation of the synthesis process of Ni0.5Cu1.5-S/NF CV-P

Acknowledgements

This work was fully funded by OPUS program of the National Science Centre, Poland (UMO-2021/41/B/ST4/03255) and experiments were carried out at Department of Process Engineering and Chemical Technology, Gdansk University of Technology, Gdansk, Poland.

11.7 3D-printing as the method for prototyping novel PEM electrolyzers

Maria Jarząbek-Karnas*,1, Zuzanna Bojarska1, Łukasz Makowski1

1. Faculty of Chemical and Process Engineering, Warsaw University of Technology, Poland
e-mail: maria.jarzabek.dokt@pw.edu.pl

KEYWORDS: *electrolysis, hydrogen production, 3D printing, green energy, sustainability*

Due to the climate change, the European Union (EU) emphasizes reducing greenhouse gas emissions and replacing conventional energy sources with alternative ones. The EU has a plan to achieve climate neutrality by 2050. Investments are being made in renewable energy sources (RES), energy efficiency, and other clean, low-emission technologies to achieve this goal. Hydrogen has been identified as a promising fuel of the future among RES technologies.

There are various methods for hydrogen production. Depending on the technologies used, hydrogen is classified by colors. The three main ones are grey, purple and green. Gray hydrogen is the most commonly obtained, which is produced from fossil fuels. The second group is purple hydrogen, produced by water electrolysis using electricity generated in nuclear power plants. The ideal solution for the environment is green hydrogen, which is produced by water electrolysis using renewable energy.

Purple and green hydrogen can be obtained through water electrolysis using a polymer electrolyte membrane (PEM) electrolyzers. Water electrolysis is a process that uses electricity to decompose water into hydrogen and oxygen. This technology allows for the production of pure hydrogen. In addition, if we use electricity from renewable sources to power the electrolyzer, we will be able to produce sustainable hydrogen.

My research focuses on the creation of a plant incorporating a PEM electrolyzer with critical features such as modularity, adaptability and testing of own materials. 3D-printing was used to develop the novel electrolyzer models. This technology allows for the creation of any housing and bipolar plate geometries to obtain optimal process conditions and high efficiency. This enables us to rapidly test different geometries and tailor them to the new electrolyzer's requirements.

We are currently in the initial construction phase. At this research stage, we have selected the housing geometry. Research on bipolar plate printing is ongoing, and we are also investigating catalysts based on molybdenum disulfide.

Our research may contribute to the widespread adoption of hydrogen on an industrial scale in the future. This would allow us to reduce fossil fuel consumption while increasing hydrogen production.

11.8 Antioxidant potential of fermented black chokeberry pomace

Sylwia Sady1, Patrycja Kawałek*,2, Adam Konopelski2, Zuzanna Płaczek2, Nikola Dłużniewska2, Karolina Pakuła2, Aleksandra Kaczmarek3

1. Department of Natural Science and Quality Assurance, Institute of Quality Science, Poznan University of Economics and Business, Poznan, Poland
2. Student Scientific Association NEXUS, Department of Natural Science and Quality Assurance, Institute of Quality Science, Poznan University of Economics and Business, Poznan, Poland
3. WSB Merito University, Poznan, Poland
e-mail: patkowa012@gmail.com

KEYWORDS: *chokeberry, pomace, antioxidant potential, sustainable fermented product*

In recent years, there has been a growing interest in the by-products of fruit processing, consisting of seeds, pulp residue and peel, due to their high content of nutritionally valuable components and their importance in the prevention of many diseases. In the food industry, chokeberry pomace can be a valuable secondary raw material due to its use in the production of, among other things, anthocyanin pigments, innovative additives to enrich food products or ingredients for dietary supplements. However, fermented products, especially those based on vegetables or fruit, are becoming increasingly popular among consumers. Many studies have confirmed that the fermentation process can increase the antioxidant activity of plant extracts. Metabolic hydrolysis has been suggested to increase phenolic compounds. Moreover, during the fermentation process, the walls of plant cells are broken down, resulting in the release or synthesis of biologically active compounds, including those with antioxidant activity.

The aim of this study was to evaluate the antioxidant potential of fermented pomace of black chokeberry in the context of their potential use in the food industry. For the determination, lyophilised black chokeberry pomace was fermented using reference strains of *Lactobacillus* and *Lactococcus* bacteria and *Saccharomyces* yeast. The content of total polyphenols was determined by spectrophotometric method with the Folin-Ciocalteu reagent, the reducing properties were assessed by the FRAP test, and the antiradical properties by the DPPH (2,2-diphenyl-1-picrylhydrazyl) radical test.

Acknowledgements

The study was conducted within the research project 'TEAcycle – innovative functional teas based on fruit by-products', financed by Student Scientific Association Create Innovations' programme of the Minister of Science and Higher Education of Poland grant no. SKN/SP/569242/2023.

11.9 Development of a liquid-splitting system for a laboratory- scale additively manufactured dividing wall column (DWC)

Chiara Lukas*,1

1. Institute of Chemical Engineering, Ulm University, Ulm, Germany
e-mail: chiara.lukas@uni-ulm.de

KEYWORDS: *dividing wall column (DWC), additive manufacturing, liquid split*

With increasing need for energy efficient technologies, the replacement of conventional distillation sequences with dividing wall columns (DWC) is a promising approach. As there are more degrees of freedom as in conventional distillation, the design and operation of such columns is challenging. Therefore, validation experiments to ensure feasibility and scalability of the process must be conducted. This is usually done in pilot scale DWCs, which are typically expensive and inflexible. Thus, the general DWC development process is only possible under high investment costs. To address this problem, a novel modular 3D-printed DWC on a laboratory scale should be developed to make DWC development economically feasible. For the realization of such a setup, it is necessary to develop special components of the DWC. The focus of this work is the development of a liquid splitting system, with which liquid streams within the column can be divided into two individual streams.

A multifunctional liquid splitter (MFLS) was developed which integrates the functionalities of liquid collection, splitting and distribution. For the liquid splitting, two different methods were investigated. The first MFLS operates with a swinging funnel, the second one with a pneumatic cylinder. The design of the MFLS was realized in a CAD model, which was later manufactured additively with SLS. The liquid split was experimentally investigated for both operation principles with different liquid loads and switching frequencies. For that purpose, a control was implemented in LabView.

In general, the results of the MFLS operated with the swinging funnel were closer to the desired liquid split compared to pneumatic operation. For both splitting mechanisms the results were not fully reproducible. An improvement of the liquid split towards the desired value was achieved with the pneumatically operated MFLS by adjusting the durations of retracted and extended state of the cylinder. In future work, the improvement of reproducibility must be addressed. So far, only liquid flow has been evaluated. To apply the MFLS within a DWC, it is necessary to also consider the countercurrent vapor flow. Further, tightness of all individually 3D printed parts regarding vapor and liquid must be evaluated.

11.10 Photocatalytic Potential of MOF-808 for photoconversion of CO_2 into valuable products

Seyed Soroush Mousavi Khadem*,1, Malwina Kroczewska[1], Mateusz Adam Balu[1], Szymon Zdybel[2], Aleksandra Pieczyńska[2], Paweł Mazierski[2], Adriana Zaleska-Medynska[2], Justyna Łuczak[1]

1. Department of Process Engineering and Chemical Technology, Faculty of Chemistry, Gdansk University of Technology, Gdansk, Poland
2. Department of Environmental Technology, Faculty of Chemistry, University of Gdansk, Gdansk, Poland
e-mail: Seyed.Soroush.Mousavi.Khadem@pg.edu.pl

KEYWORDS: *metal-organic framework, formic acid, photoconversion, photocatalyst, CO_2 reduction*

This study investigates the photoconversion of carbon dioxide (CO_2) to formic acid using MOF-808 as a promising photocatalyst. Formic acid, a valuable chemical with applications in various industries, can be synthesized through sustainable means, and MOF-808 emerges as an excellent candidate for this photocatalytic process. A comprehensive characterization approach, encompassing X-ray diffraction (XRD), Brunauer-Emmett-Teller (BET) surface area analysis, scanning electron microscopy (SEM), UV-Vis spectroscopy, and CO_2 sorption measurements, is employed to unravel the intrinsic properties of MOF-808 that contribute to its efficacy in formic acid production.

XRD analysis reveals the crystalline nature of MOF-808, providing crucial insights into its structural integrity and confirming its suitability as a photocatalyst. BET surface area analysis elucidates the material's porosity, indicating a substantial surface for CO_2 adsorption, a pivotal step in the formic acid synthesis process. SEM imaging further unveils the morphology of MOF-808, showcasing its intricate structure and emphasizing the importance of surface features in catalytic activity. UV-Vis spectroscopy is employed for band gap measurement, showcasing MOF-808's commendable light absorption properties within the visible spectrum. These characteristic positions MOF-808 as a highly efficient catalyst for solar-driven photocatalysis, crucial for the conversion of CO_2 to formic acid. Concurrently, CO_2 sorption measurements provide valuable data on MOF-808's capacity to adsorb and interact with CO_2 molecules during the photoconversion process, underscoring its role in facilitating the overall reaction. In addition, diffuse reflectance infrared Fourier transform spectroscopy (DRIFTS) employed for demonstration the incorporation of CO_2 within the structure of the MOF.

In conclusion, this research utilizes a comprehensive suite of characterization techniques to underscore MOF-808's potential as a photocatalyst for the sustainable photoconversion of CO_2 into formic acid. The amalgamation of structural, morphological, and optical analyses collectively highlights MOF-808's suitability for efficient and environmentally benign CO_2 photoconversion, paving the way for advancements in sustainable chemical conversion of CO_2.

Acknowledgements

This research was supported by the Polish National Science Center under the grant 2021/41/B/ST4/00849.

11.11 Influence of Hydrothermal Carbonization process on elimination of selected organic and inorganic compounds from sewage sludge

Zuzanna Prus*[,1], Katarzyna Styszko[2], Małgorzata Wilk[1]

1. Department of Heat Engineering & Environment Protection, Faculty of Metals Engineering and Industrial Computer Science, AGH University of Krakow, Krakow, Poland
2. Department of Coal Chemistry and Environmental Sciences, Faculty of Energy and Fuels, AGH University of Krakow, Krakow, Poland

e-mail: zprus@agh.edu.pl

KEYWORDS: *hydrothermal carbonization, sewage sludge, biomarkers*

In recent years, the use of hydrochar (HC), a solid by-product of hydrothermal carbonization (HTC) of biomass as organic soil fertilizers, has become more popular. As a result of HTC process, organic waste such as sewage sludge (SS) from wastewater treatment plants (WWTPs) can be converted into bio-fuel and used as bio-based products in many applications.

Studies on thermal processes of biomass have focused mainly on the fuel properties of the solid products so far. However, some recent research indicates the potential of the HTC reaction to remove many organic and inorganic compounds that are toxic to environment.

The study reviews briefly the HTC process as a promising method to reduce the content of selected representatives of compounds, such as heavy metals (HMs) and polycyclic aromatic hydrocarbons (PAHs) from SS.

Acknowledgements

The research was funded by the Ministry of Science and Higher Education [AGH University grant no. 16.16.110.663 and no. 16.16.210.476]

11.12 Halloysite applied in various water treatment processes

Michał Stor*[,1], Karolina Kryszczyńska[1], Andrzej Krasiński[1]

1. Faculty of Chemical and Process Engineering, Warsaw University of Technology, Warsaw, Poland

e-mail: michal.stor.dokt@pw.edu.pl

KEYWORDS: *halloysite, water treatment, sorption, pharmaceuticals, bacteriostatic properties*

The scope of interest in recent years in the field of water treatment technologies is focused on universal materials, which can be used in various purification processes. The requirements to be accepted in the industry for this type of novelty is cheap, sustainable and available material, which leads to natural media i.e. biowastes and minerals. The high potential of silicate called halloysite was recognized during the last decade due to its good mechanical strength, large pore volumes, relatively high surface area, and chemical inertness. These properties are typical for the kaolin group minerals. Uniqueness of halloysite is its tendency to roll in the form of multilayer halloysite nanotubes (HNTs). Properly treated material can undergo delamination, thus creating access to a high specific surface area, which is available for sorption.

The aim of this research was to determine applications of halloysite as sorbent in terms of removal of various water contaminations i.e. heavy metal ions, organic substances, identifying bacteriostatic properties and application as a base platform for photocatalytic composite.

The adsorption properties of the raw and chemically etched halloysite particles were evaluated in a batch stationary system. The initial concentration of removed compounds, the mass of sorbent per water volume, and process time were determined based on the preliminary research. Various analytical techniques were used to determine the concentration of contaminant in the water: UV-Vis spectrophotometry, HPLC with UV-Vis detector for organic substances and AAS for analysis of heavy metal ions.

The experimental results confirmed a high potential of halloysite to remove the heavy metal ions and the organic compounds. In the research, various composites based on halloysite have been developed. One of them is halloysite dopped with silver nanoparticles, which exhibits strong bacteriostatic properties. Both qualitative and quantitative tests confirmed the inhibition of bacteria proliferation. the application of this composite as an additive to polymer filters structures used for the water cleaning extended the filter operation time.

As presented in the above-described examples, the material creates a good base for various modifications, including the preparation of photocatalytic or bacteriostatic composites, where these features coupled with the high sorption potential of halloysite can be integrated into a single process.

Acknowledgements

The research was supported by the Polish National Centre for Research and Development, grant no. TECHMATSTRATEG-III/0005/2019-00

11.13 Reduction of heat losses in lab-scale distillation columns and its consequences for scale-up

Dennis Stucke*,1, Mohamed Adel Ashour[1], Johannes Neukäufer[1], Thomas Grützner[1]

1. Institute of Chemical Engineering, Ulm University, Ulm, Germany
e-mail: dennis.stucke@uni-ulm.de

KEYWORDS: *heat loss, heat loss reduction, distillation, scale-up, additive manufacturing*

The design of production scale distillation columns is often done based on data obtained by experiments in laboratory scale. The standard diameter for these laboratory columns in industry is 50 mm. With the drive towards more cost efficient workflows, the reduction of the column diameter in laboratory distillation test rigs is tackled as this results in lower equipment and energy costs, lower consumption of costly novel chemicals and moderate safety and environmental demands in presence of hazardous substances. Therefore, the aim is to reduce the size to a target diameter of 20 mm.

This reduction in diameter raises several problems. These problems are related to the increasing wall-to-core ratio. The first impact is the maldistribution of liquid especially the tendency of liquid to collect at the wall. This issue can be addressed by the packing design and has been investigated by the authors in several publications. The second drawback of the smaller diameter is the increased impact of heat lost through the column wall. This problem was investigated and the results are presented in the following.

For the quantification, a batch distillation test rig is used that can measure the separation efficiency as well as the heat losses in the packed section for diameters from 20 mm to 50 mm. Initially, the heat losses of an uninsulated column are determined and in successive steps reduced by the application of different insulation materials and concepts. The insulation materials are Armaflex® HT and Armagel® HT. Additionally, an active insulation system has been developed using silicone heaters to heat the surrounding to the same temperature as the column and thereby diminish the driving force for heat transfer.

At the beginning, it could be proved that insulation is mandatory at small diameters. Application of insulation materials with lower heat conductivity and larger thickness showed the expected reduction in heat losses but didn't eliminate heat losses. With the actively heated column, it could be shown that the heat losses can be reduced significantly. Additionally, the implementation of an offset in the heater temperature compared to the column temperature allowed for complete prevention of heat losses in the actively insulated sections.

11.14 Experimental method of CO_2 bubble trajectories determination in direct formic acid fuel cell

Zofia Szewczyk*,1, Monika Jałowiecka[1], Łukasz Makowski[1]

1. Faculty of Chemical and Process Engineering, Warsaw University of Technology, Warsaw, Poland
e-mail: zofia.szewczyk.stud@pw.edu.pl

KEYWORDS: *direct formic acid fuel cell, efficiency enhancement, interconnector geometry*

A direct formic acid fuel cell (DFAFC) requires a fuel pump to function efficiently and reliably, similar to a combustion engine but with higher efficiencies. However, in the DFAFC, CO_2 bubbles are produced as a result of an electrochemical reaction at the anode side. These bubbles pose extra resistance for the flow, leading to increased pressure drop in the DFAFC system, which necessitates a more powerful pump. Furthermore, the bubbles reduce the contact between the formic acid molecules and the catalytic area, resulting in a voltage drop.

This study is focused on determining the trajectories of CO_2 bubbles to understand their impact on the efficiency of DFAFC. In order to evaluate the impact of CO_2 bubbles, a comparison of the pressure drop of the fuel cell while it is working and not working was conducted for a specific interconnector geometry. During the test, photos were taken to determine the CO_2 bubble trajectories, enabling the following:

- evaluation of bubble diameter and its potential alteration over distance covered in the flow field,
- observation of the rate of bubble coalescence resulting in elongated slugs,
- verification of the validity of DFAFC work duration as a contributing factor.

This study is made possible due to the design of a transparent housing for the DFAFC using the SLA 3D printing method.

The experimental research conducted provides detailed insights into the response of the DFAFC to bubbles in the fuel flow field plate. The outcome of the research not only highlights the impact of bubbles on the fuel cell's performance but also identifies the type of bubble dispersion that causes the most significant pressure drops. This information is valuable for optimizing the fuel cell's design and improving its efficiency.

11.15 Development of a Bioreactor with Continuous Supernatant Harvesting and Uninterrupted Bioprocessing

Adam Tymoszewski*[,1,2], Karolina Drężek[1], Jolanta Mierzejewska[1]

1. Faculty of Chemistry, Warsaw University of Technology, Warsaw, Poland
2. Pro-mill s.c. Warsaw, Poland

e-mail: adam.tymoszewski.dokt@pw.edu.pl

KEYWORDS: *membrane bioreactor, continuous cultivation, 2-phenylethanol production, ethanol production*

Continuous cultivation allows for the production of larger quantities of the desired product, in comparison with conventional periodic cultivation, by maintaining microorganisms in the desired growth phase. However, this bioprocessing type is relatively uncommon due to the lack of universal technological solutions. The poster clarifies the differences between periodic and membrane bioreactors and describes development of a membrane bioreactor with continuous nutrient supply and uninterrupted bioprocessing.

The prototype membrane bioreactor was designed and constructed at the Pro-mill company. The technical challenges faced during the project implementation have been overcome resulting in the development of a unique system with constant filtration efficiency throughout the entire cultivation. Importantly, the possibilities of an automatic membrane regeneration and device sterilization have been created. Moreover, the device has been equipped with advanced features to regulate the amount of dissolved oxygen, crucial parameter for aerobic processes, by adjusting the amount of dosed air and the agitation speed.

The successful development of membrane bioreactor was confirmed in two processes. The first one was a two-stage periodic production of 2-phenylethanol and ethanol. The second one was a continuous production of ethanol with uninterrupted nutrient dosing and product removal. The device offers new possibilities for cultivation while operating similarly to periodic bioreactors.

Figure 11.15.1. Bioreactor with continuous nutrient supply for microorganisms and uninterrupted bioprocessing.

11.16 Poly(ethylene terephthalate) utilization by production of plasticizers for poly(vinyl chloride)

Mateusz Zygadło*[,1], Marcin Muszyński[2,3], Agata Krasuska[2], Gabriela Dudek[4], Janusz Nowicki[2]

1. Chemistry Students Research Society, Faculty of Chemistry, Silesian University of Technology, Gliwice, Poland
2. Łukasiewicz Research Network, Institute of Heavy Organic Synthesis "Blachownia", Kedzierzyn-Kozle, Poland
3. Department of Physical Chemistry and Technology of Polymers, PhD School, Silesian University of Technology, Gliwice, Poland
4. Department of Physical Chemistry and Technology of Polymers, Faculty of Chemistry, Silesian University of Technology, Gliwice, Poland

e-mail: matezyg797@student.polsl.pl

KEYWORDS: *poly(ethylene terephthalate), chemical recycling, plasticizers*

Plastic find applications in every field, from packaging to space missions. It would be hard to imagine the modern world without plastic. However, its mass production generates a massive amount of waste in the form of used packaging such as boxes or bottles. The statistical data show, that only 40% of plastic wastes were recycled. This means that over 220 million tons annually contaminates every spot of our planet. Remaining 60% is the reason for an increasing push for waste segregation in society and the development of technologies to process them.

There are many methods for disposing of waste poly(ethylene terephthalate) (PET), which can be assigned to one of two main categories: thermo-mechanical recycling or chemical utilization. First method includes processes like melting and reusing the material, for example, in the production of polyester fibers. However, this method damages the polymer chains. Chemical utilization, allows to break the polymer chain in the process of the depolymerization. One of the derivative of mentioned process is alcoholysis, that is the main scope of the work. This process involves the transesterification reaction of PET with the chosen alcohol. That allows to reduce a consumption of pure TPA in plasticizer production.

The aim of the research was the selection of the most efficient catalytic system for the synthesis of plasticizers for poly(vinyl chloride) (PVC) in the PET alcoholysis reaction. Processes were performed with alcohols consist of 8, 9 and 10 carbon atoms in a molecule chain. The investigated catalysts origin from the groups of organometallic compounds, super bases, and ionic liquids. The efficiency of plasticizers synthesis was determined using gas chromatography. For each applied alcohol, the most efficient catalyst was identified. Obtained plasticizers with chosen catalysts were compared with commercially available plasticizers. The results show, that the synthetized compounds have similar plasticization properties in comparison with commercial plasticizers.

Acknowledgements

This research was co-financed by the Ministry of Education and Science of Poland under grants DWD/5/0567/2021, SKN/SP/535370/2022 and Silesian University of Technology under grant 31/010/SDU20/0006-10.

12 Abstracts: Mathematical modelling, simulations & optimalization

12.1 A coupled CFD-PBE model of particle breakage during grinding in a horizontal stirred media mill

Julia Chaładej*,1, Radosław Krzosa[1], Wojciech Orciuch[1], Łukasz Makowski[1]

1. Faculty of Chemical and Process Engineering, Warsaw University of Technology, Warsaw, Poland
e-mail: julia.chaladej.stud@pw.edu.pl

KEYWORDS: *stirred media milling, population balance equations, CFD*

The population balance equation allows to model processes in systems consisting of a continuous phase and a dispersed phase in the form of solid or fluid particle populations. The particles are characterized by distributions of individual physical quantities such as size, composition, porosity or chemical activity evolving alongside the particles number in the course of a process. The changes are driven by the mass, momentum and energy transport processes described by the convection and diffusion terms and the birth and death of the particles due to chemical reaction, phase transition or interparticle interactions all captured by the source terms in the population balance equations. The coupling with Computational Fluid Dynamics (CFD) simulations enables to determine the underlying hydrodynamic conditions for example viscosity.

Stirred media milling is a method to produce sub-micron- and nanosized particles with applications in industrial fields. To improve the power efficiency of the process an understanding of physical mechanisms governing the fragmentation and the investigation of their results depending on operating conditions and milled material properties are required. This study provides a coupled CFD-population balance model that accounts for empirically proven comminution mechanisms of intensity determined by the hydrodynamics of multiphase flow of the ground suspension and milling medium in a horizontal stirred media mill. The milled material in our investigation is an industrial titanium dioxide powder spread in demineralized water. The motion of the suspension-milling balls mixture is modelled using the Eulerian multi-phase approach. The population balance equations include theoretically derived kernels of breakage events due to mechanical stresses exerted on particles. The equations are solved using the quadrature method of moments. It allows to track the change of the average characteristic size of suspension particles over the grinding time.

The obtained resulted of dynamics of the size change was compared with experimentally measured particle breakage kinetics. The calculated coefficients of milling medium collisions efficacy properly predict contribution of each breakage mechanisms. Therefore the minimum achievable size of the particles for particular process conditions can be predicted using proposed model. Also developed model can be used in optimization of production of powders with controlled particle size distributions.

12.2 Hydrodynamics of barley brewer's spent grain filtration drying

Roman Chyzhovych*,1, Oleksandr Ivashchuk[1], Volodymyr Atamanyuk[1], Serhii Barabakh[1], Vladyslava Manastyrska[1]

1. Department of Chemical Engineering, Lviv Polytechnic National University, Lviv, Ukraine
e-mail: roman.a.chyzhovych@lpnu.ua

KEYWORDS: *biomass, brewer's spent grain, filtration drying, hydrodynamics, CFD*

The secondary use of plant biomass is one of the most important areas of research, not only to find new ways to use it but also to improve and optimize the existing ones. One of the plant-based wastes that requires attention is barley brewer's spent grain, that is a by-product of the industrial beer production process. This material is characterized by high moisture content (~70% wt.), and needs to be previously dried to increase its shelf life and being used in a secondary way[1]. The hydrodynamics of thermal agent movement through a dispersed layer of dried brewer's spent grain study is important for the definition of the optimal drying parameters, the dependence of the fictitious velocity w_0 on the resistance of the material layer ΔP was researched. Based on the obtained experimental data on the hydrodynamics of thermal agent movement through a stationary layer of dispersed material, the coefficients of viscous $1/\alpha$ and inertial C2 resistances were determined, which were used to carry out computer modeling of the considered process in the ANSYS Fluent 2022 R2 software package. The maximal relative simulation error is 5.03%, the average simulation error is 2.91% (Figure 12.2.1).

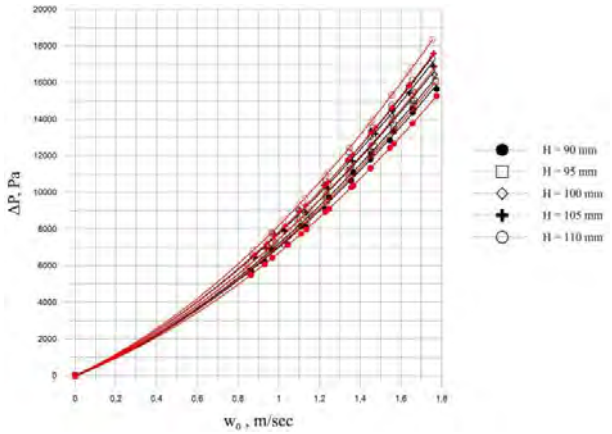

Figure 12.2.1. Graphical comparison of the obtained modeling values (––– red lines) of the hydraulic resistance of the dried coffee production waste stationary layer with the experimental data (––– black lines) (T=17°C, H=90÷110 mm, w_0 = 0,83÷1,78 m·s^{-1})

[1] Chyzhovych, R. A., Ivashchuk, O. S., Atamanyuk, V. M. (2023). CFD-Modeling of Thermal Agent Flow Through a Layer of Barley Brewer's Spent Grain. 4th International Scientific Conference "Chemical Technology and Engineering": Proceedings, 31-37. https://doi.org/10.23939/cte2023.031

12.3 Semi-empirical model of vapour transportation through alginate membranes filled with MQFP hard magnet

Paweł Grzybek*,1, Gabriela Dudek1

1. Department of Physical Chemistry and Technology of Polymers, Silesian University of Technology, Gliwice, Poland
e-mail: pawegrz205@student.polsl.pl

KEYWORDS: *pervaporation, alginate, magnetic membranes, diffusion*

The aim of the work is to present the semi-empirical model of water transportation through alginate composite membrane filled with hard neodymium magnet MQFP with four different size of grains (2, 5, 15 and 25 μm).

The magnetic membranes were prepared using a solvent evaporation method. The MQFP neodymium powder was added as a filler of investigated materials. The membranes were investigated in the process of ethanol dehydration via pervaporation and characterized in terms of the magnetic properties and transport ones. On the basis of the first Fick's law, some deviations between ratio of diffusion coefficient (D) to flux for pure alginate membrane and filled with magnetic powder ones were noticed. This situation was a result of aninaccurate calculation of D caused by not taking into account effect of magnetism in the standard time-lag method. Therefore, in order to obtain a more precise D values, the semi-empirical model was proposed. The influence of magnetism has been included in a coefficient of diffusion corelation in magnetic field presented in Figure 12.3.1.

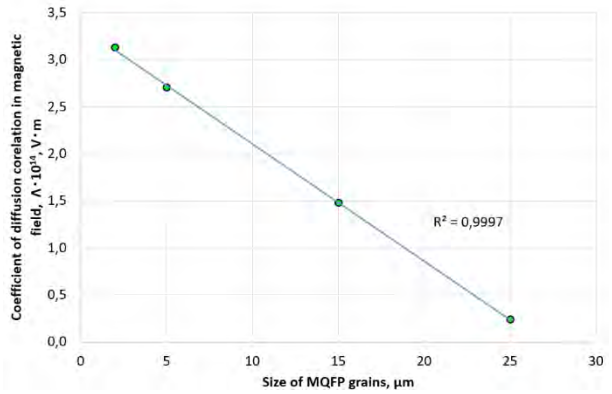

Figure 12.3.1. Effect of magnet size on the diffusion rate of water

Figure 12.3.1 showed that the influence of magnetic forces on diffusion rate was strongly dependent of size of MQFP grain.

The presented model can be useful for describing the diffusion of selected molecules in the presence of magnetic field, making it possible to predict the diffusion rate depending on the intensity of magnetic filler embedded in membrane.

Acknowledgements

"This research was funded in whole or in part by National Science Centre, Poland 04/040/PBU23/0269. For the purpose of Open Access, the author has applied a CC-BY public copyright licence to any Author Accepted Manuscript (AAM) version arising from this submission."

12.4 CFD modeling of multiphase flow in direct formic acid fuel cell

Monika Jałowiecka*,1, Łukasz Makowski1

1. Faculty of Chemical and Process Engineering, Warsaw University of Technology, Warsaw, Poland
e-mail: monika.jalowiecka.dokt@pw.edu.pl

KEYWORDS: *fuel cell, VOF model, multiphase flow, CO2 bubbles*

Direct formic acid fuel cells are electrochemical devices generating electricity within a one-step energy conversion process. They are a subtype of proton exchange membrane fuel cells, distinguished by the liquid fuel supplied to the anode. The fuel is formic acid, an environmentally friendly compound that can be implemented into the existing fuel infrastructure. This provides an opportunity for earlier deployment of fuel cell technology to areas where hydrogen storage and refueling is difficult or would pose additional risk. On the other hand, formic acid is a fuel with a higher volumetric energy density than hydrogen and, hence, a safe and convenient alternative.

The key difference in direct formic acid fuel cells compared to hydrogen-fueled cells is the presence of two-phase flow on both sides of the membrane, not only on the cathode side in the form of water droplets but also in the form of carbon dioxide bubbles produced during the reaction on the anode side. Critical to the efficient operation of the fuel cell is the removal of the dispersed phase from the reaction zone so that it does not block the access of the reactants to the catalyst. In the present study, numerical analysis of the two-phase flow at the anode side was conducted to evaluate the effectiveness of the designed interconnector geometry in uniform reactant distribution and carbon dioxide bubble removal.

Simulations revealed a significant problem with the adhesion of carbon dioxide bubbles to the interfacial boundary between the electrode and the fluid. Therefore, it is beneficial to introduce turbulizing elements to the channel geometry to detach the bubbles from the electrode surface. Solving this problem will not only help increase the maximum power density of direct liquid fuel cells but also contribute to the development of electrolyzer technology, in which the problem of two-phase flow with gas bubbles occurs on both sides of the membrane.

Acknowledgements

Research was funded by the Warsaw University of Technology within the Excellence Initiative: Research University (IDUB) program.

12.5 Chaotic advection in twisted bend mixer - flow visualization and CFD study

Janusz Kopytowski*,1, Antoni Rożeń1

1. Faculty of Chemical and Process Engineering, Warsaw University of Technology, Warsaw, Poland

e-mail: kopytowski@gmail.com

KEYWORDS: *chaotic advection, laminar mixing, CFD, visualization*

Twisted bend mixers, often called "chaotic", are designed to work efficiently in a laminar regime. Chaotic mixers take advantage of pipe curvature to create Dean's vortices as secondary flow and use a rapid change of bend curvature plane to reorient and reverse rotation of Dean's vortices. Two vortex flow patterns and their periodic change enhance the generation of the new intermaterial surface area and, consequently, mixing in the laminar flow regime.

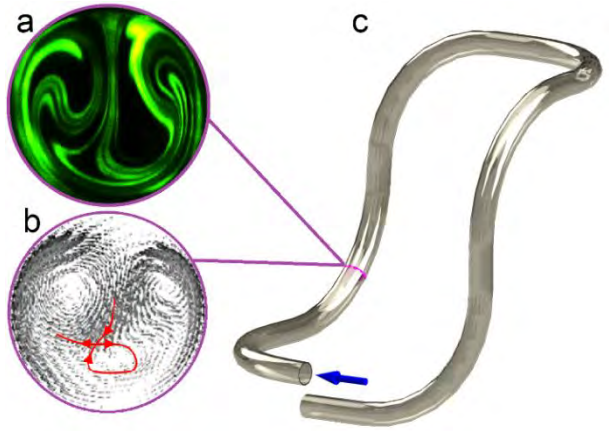

Figure 12.5.1 . a) specific deformations b) homoclinic connection (orbit) – red line c) twisted bend mixer.

To correctly identify fully developed chaotic mixing, three signatures of chaos must appear in the flow:

1. homoclinic and/or heteroclinic orbits,
2. specific deformations – e.g., "Smale horseshoe", baker transformation,
3. system sensitivity to minor changes presented by a positive Lyapunov exponent.

Chaos signatures can appear in flow at various distances from the inlet for different Reynolds numbers (Re); for low Re, chaos could not be fully induced, as not all signatures manifest themselves.

The PLIF method was used to identify the appearance of specific deformations, revealing the horseshoe structures. Identification of homoclinic/heteroclinic orbits and calculation of the Lyapunov exponent was accomplished with CFD methods.

Determination of the Reynolds number for which all three chaos signatures are present and finding a distance from the inlet at which chaos signatures appear can help optimize mixer operation conditions, especially when mixing viscous liquids or when other processes accompanying mixing are relatively slow.

12.6 Mathematical modeling of particle breakage in high energy industrial ball mill

Radosław Krzosa*,1, Łukasz Makowski1, Wojciech Orciuch1, Radosław Adamek2

1. Faculty of Chemical and Process Engineering, Warsaw University of Technology, Warsaw, Poland
2. ICHEMAD Profarb sp. z o. o., Gliwice, Poland

e-mail: radoslaw.krzosa.dokt@pw.edu.pl

KEYWORDS: *paint, coating, CFD, population balance, titanium dioxide*

Reduction of particle size is a crucial process in many brand of industry, especially in the paint and coating industry. This process allows to obtain desirable particle properties, as refractive index, viscosity of a suspension and a cover factor. Investigation of those parameters is necessary to keep the same properties of the final product in a production line. Various type of devices are used in this process. Mixers equipped with high shear impeller and rotor-stator systems are used in first stages of particle processing to uniformly disperse the solvent. Rollers and ball mills are used to break the solid particles and aggregates of primary particles. Those devices generate high enough values of stresses to break the particles. Ball mills are frequently used due to high performance and large energies generated in those devices.

Application of computational fluid dynamics (CFD) methods to investigate the particle breakage process let us better understand this process and create the modifications, that improve it. In a ball mills internal shaft cause the movement of the filling beads. Collisions between the beads cause the stresses that rupture the particles suspended in the solvent. This system consist of three phases: beads, broken particles and the solvent. Particles suspended in solvent can be described as a homogenous fluid with shear thinning rheology. To include presence of beads in the system Eulerian multiphase model is applied.

To investigate the particle size change In the system population balance method was applied. Population balance equation is complex and can be solved implicit only in simple systems. To solve this equation in a particle breakage process Quadrature Method of Moments (QMOM) was applied. Based on the CFD simulation values of generated stresses were found and applied in those equations. Experiments carried out on a titanium dioxide powders allowed to find the breakage mechanism, and this mechanism were also include in this method to investigate the particle size change and compare effectiveness of different devices.

12.7 Experimental and numerical investigation of residence time distribution in a fuel cell

Jakub Lewandowski*,1, Monika Jałowiecka1, Łukasz Makowski1

1. Faculty of Chemical and Process Engineering, Warsaw University of Technology, Warsaw, Poland
e-mail: jakub.lewandowski9.stud@pw.edu.pl

KEYWORDS: *direct formic acid fuel cell, interconnector design, residence time distribution, CFD*

Direct formic acid fuel cells, abbreviated as DFAFCs, are electrochemical reactors used for converting formic acid into electricity. Used as a hydrogen carrier, formic acid has higher volumetric energy density than hydrogen stored at 70 MPa[2]. It is also easier to convert current fueling stations for storage and distribution of formic acid than hydrogen.

In fuel cells fed by liquid fuels such as formic acid, hydrodynamic conditions play an important role. The prevailing laminar flow regime significantly slows down the mass transfer, which has a large impact on reactor efficiency under higher current loads. Channel geometry is a decisive factor in ensuring that enough fuel is delivered to the catalyst interface to undergo the reaction and providing stable working conditions for the device. This study focuses on the investigation of the residence time distribution, abbreviated as RTD, in a fuel cell. Determining RTD provides an opportunity to derive hold-back and segregation parameters of the interconnector channels. These parameters describe deviation from the plug flow model in the case of hold-back and the ideal mixing model in the case of segregation. In literature[3], RTD is usually obtained through numerical simulation. In this research, the experimental method of determining RTD has been developed. The comparison between the CFD results and the experimental data allowed for the validation and further analysis of hydrodynamic conditions in the interconnector geometry. The RTD was determined by measuring step tracer response curve. Sodium chloride was chosen as the tracer. The step function and the response curve can be acquired by measuring the conductivity of the solution before and after the examined system. To realize aforementioned procedure a specialized testing system has been created using 3D printing. Benefits of creating custom parts are: increased repeatability and accuracy of the experiments.

Therefore, the purpose of this research was to develop an experimental method of determining RDT in fuel cells fed by liquid fuel. Obtained experimental results were compared with numerical simulations. This helped further the knowledge about the mixing conditions inside the fuel cell and will facilitate the development of new geometries that provide better conditions for the ongoing reaction.

Acknowledgements

Research was funded by the Warsaw University of Technology within the Excellence Initiative: Research University (IDUB) program.

[2] J. Eppinger, K.W. Huang, ACS Energy Lett. 2 (2017) 188–195

12.8 Numerical Simulations of The Heat Transfer In A Stirred Tank

Kleopatra Majewska*,1, Anna Story1

1. Faculty of Chemical and Process Engineering, West Pomeranian University of Technology in Szczecin, Szczecin, Poland
e-mail: mk50097@zut.edu.pl

KEYWORDS: *CFD, heat transfer, jacket, coil, mechanical impeller*

Many operations that take place in stirred tanks involve heat transfer in order to achieve the required conditions for the chemical reaction, to reach the melting point of one of the components, or to enable further processing. The process of heating or cooling in the stirred tank is mostly provided by a heating jacket or coil. The choice between them is based on a number of considerations. In this work, numerical simulations were performed to determine which of these two methods of heating in stirred tanks is more effective.

The aim of the study was to perform unsteady numerical simulations (ANSYS Fluent) for two flat-bottomed stirred tanks with a diameter of D = 0.190 m, equipped with four symmetrically placed standard baffles and a Rushton turbine with a diameter of d = 0.074 m. The impeller was placed centrally at a height of z = 1/3 D and rotated with constant impeller speed n = 5 s^{-1}.The stirred tanks differed in heating method: one was equipped with a heating jacket, the other with a coil. Both heating systems had approximately the same heat exchange surface area.

Each stirred tank was filled with water to the level of H = D. The temperature of the water inside the tank was 10 °C, while the temperature of the heat exchange surface for both heating systems was 50 °C. Based on transient numerical simulations, the temperature distributions in the tank mid-plane and the average temperature of the water (Figure 12.8.1) were investigated for increasing mixing times, up to 300 s.

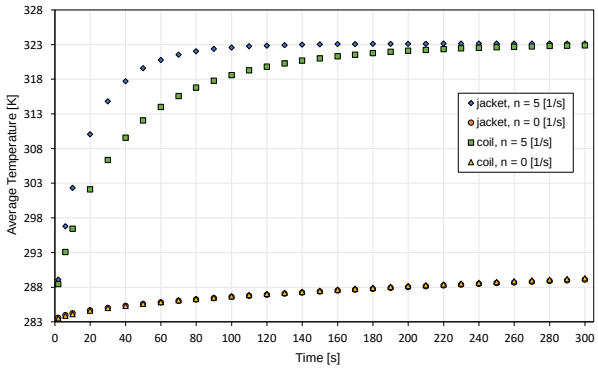

Figure 12.8.1. Average temperature of the water for increasing mixing times

[3] M. Jałowiecka et al., Chem. Eng.i J.(2023), 451, Part 1, 138474

13 Abstracts: Kinetics & thermodynamics

13.1 Investigations of reaction kinetics using thermogravimetric analysis integrated with gas chromatography

Stanisław Murgrabia*,1, Tomasz Kotkowski1, Eugeniusz Molga1, Andrzej Stankiewicz1, Robert Cherbański1

1. Faculty of Chemical and Process Engineering, Warsaw University of Technology, Warsaw, Poland
e-mail: stanislaw.murgrabia.dokt@pw.edu.pl

KEYWORDS: *thermogravimetric analysis, gas chromatography, reaction kinetics*

Reducing the carbon footprint is one of the challenges facing the industry today. One way to combat the carbon footprint is to electrify chemical processes. Microwave heating is one of the unconventional methods based on electricity use. It is distinguished primarily by its remote, selective and volumetric heating. However, a material (e.g. catalyst) used in a given process must be appropriately selected to take full advantage of this method.

This work presents kinetic studies of methane pyrolysis on a carbon-coated iron catalyst. Due to its specific dielectric properties, this catalyst is suitable for microwave-assisted reactors.

A method combining two different techniques, TGA and GC, was employed. Methane pyrolysis on the Fe/C catalyst was investigated at different temperatures and methane concentrations. While mass gains were examined in a thermobalance (TG), the inlet and outlet gas concentrations were tested by GC. The consistency of both methods was checked, showing the same reaction order with respect to methane. Taking advantage of both methods, the reaction order for the catalytic decomposition of methane was calculated.

The obtained results agree with previous literature data published for various carbon-based catalysts.

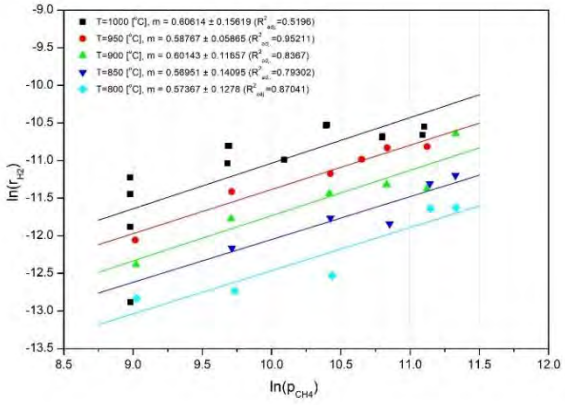

Figure 13.1.1. Determination of the reaction order with respect to methane in the methane pyrolysis reaction.

Acknowledgements

Funded by the European Union. Views and opinions expressed are however those of the authors only and do not necessarily reflect those of the European Union or the European Climate, Infrastructure and Environment Executive Agency (CINEA). Neither the European Union nor the granting authority can be held responsible for them.

13.2 Mechanism studies of new initiating systems for 3D printing of crowns and bridges

Małgorzata Noworyta1, Katarzyna Starzak1, Jakub Pietraszewski1, Martyna Sitko1, Monika Topa-Skwarczyńska1, Andrzej Świeży1,2, Filip Petko1,2, Joanna Ortyl*,1,2,3

1. Faculty of Chemical Engineering and Technology, Cracow University of Technology, Cracow, Poland
2. Photo HiTech Ltd., Cracow, Poland
3. Photo4Chem Ltd., Cracow, Poland
e-mail: jortyl@pk.edu.pl

KEYWORDS: *photopolymerization, dentistry, 3D printing, polymer materials, photoinitiators*

Photopolymerisation, due to its advantages, such as occurring at room temperature, which entails energy savings due to the lack of need to heat the reaction system, is used in many industries. Photopolymerisation is used in the coating industry, the furniture industry, the printing industry and the cosmetics industry to obtain light-curing hybrid varnishes. Photopolymerisation is also currently used particularly in dentistry, for the 3D printing of dentures or dental braces ideally suited to the palate of the individual consumer, as well as for obtaining bone fillings and in dentistry for curing dental fillings directly in the patient's mouth with light from the visible range.

The photopolymerization aspect of the dental industry is extremely important and evolving, as there is a constant search for suitable initiator systems adapted to new monomers and patient needs. It is important to ensure the safety of the systems used and eliminate potential risks in terms of, for example, mutagenicity or cytotoxicity. Accurate printing is also desirable in this type of industry, as it ensures patient comfort.

In this study, a basic spectroscopic study of the photoinitiators used in the systems and the chain conveyor additive was conducted. The polymerization kinetics of the produced compositions were investigated, including determination of the final conversion factors and induction times of the polymerizing systems, the disappearance of the bond vibration bands characteristic of the monomers in question was monitored directly during the real-time measurement . In this study, new systems were proposed to initiate the photopolymerization process in combination with monomers commonly used in dentistry, excluding Bis-GMA monomer with potentially harmful effects on the human body. An attempt was made to make 3D prints from the developed compositions.

Acknowledgements

This research was funded by National Centre for Research and Development in Poland under the Lider Program, grant number LIDER13/0156/2022.

13.3 Two-component photoinitiating systems as an alternative to commercially available photoinitiators for photopolymerization processes

Małgorzata Noworyta[1], Dominika Krok-Janiszewska[1], Joanna Ortyl[*,1,2,3]

1. Faculty of Chemical Engineering and Technology, Cracow University of Technology, Cracow, Poland
2. Photo HiTech Ltd., Cracow, Poland
3. Photo4Chem Ltd., Cracow, Poland

e-mail: jortyl@pk.edu.pl

KEYWORDS: *photopolymerization, photoinitiators, sensibilizer, photoinitiating systems*

Photopolymerization processes are widely used in many industries such as printing and furniture making. Nowadays, however, in some areas the use of UV light is often abandoned, and visible light is used, which is related to cost savings and safety. Increasingly popular and even used for educational purposes 3D printing, which is based on photopolymerization processes, uses visible light for resin curing. Commercially available photoinitiators often efficiently initiate photopolymerization processes only with light in the ultraviolet range, which is related to their chemical and absorption characteristics.

The solution to this problem in the field of photopolymerization is the use of two-component initiator systems characterized by the presence in the system of a photoinitiator and a sensitizer which first absorbs a quantum of energy and transfers it to the photoinitiator molecule. Thanks to this process, it is possible to initiate the photopolymerization process of many systems composed of various monomers and often their mixtures extremely efficiently. With such two-component initiating systems, a situation arises in which the commonly used light in 3D printers at 405 nm is easily able to initiate a system composed of a photoinitiator whose absorption bandwidth without the addition of a sensitizer does not reach a given wavelength.

The work presents basic spectroscopic studies such as absorbance, photolysis, emission and excitation measurements of various chemical compounds acting as sensitizers and quenching of sensitizer-photoinitiator binary systems. The Real Time FT-IR method was used to study the kinetics of compositions composed of the author's binary initiator systems and acrylate, vinyl or epoxy monomers. By monitoring the disappearance of the intensity of the characteristic bonds in the given monomers, the final conversion rates for individual compositions and the photopolymerization induction times were determined.

Acknowledgements

The presented research was carried out within the framework of the project "New possibilities for the development of strategies for the design and functionalization of carbon dots as multifunctional, dynamic, green photoinitiating systems and photocatalysts used in photopolymerization processes" contract number 2021/41/B/ST5/04533 in the OPUS 21 Program funded by the National Science Center.

14 Abstracts: Analytical chemistry & nanotechnology

14.1 Advanced analytical techniques to assess the stability of emulsions containing functionalized organosilicon compounds

Anna Łapeta[*,1,2], Anna Olejnik[1,2]

1. Adam Mickiewicz University, Poznan, Poland
2. Centre for Advanced Technologies, Poznan, Poland

e-mail: annlap1@st.amu.edu.pl

KEYWORDS: *multiple light scattering, laser diffraction, flocculation, colloids*

Emulsions are used in a variety of branches such as the cosmetic, pharmaceutical, or food industries. Stability assessment is crucial to ensure the required standards for a final product. An essential part of emulsions' stability is that properties must be maintained for a over prolonged storage periods at different temperature conditions. Commonly, thermal and centrifugation tests are applied to determine emulsions' stability. However, recently advanced analytical techniques have been employed in order to shorten the time of analysis in comparison to conventional techniques.

In this study, advanced analytical methods such as multiple light scattering and laser diffraction were used to assess the stability of emulsions containing functionalized organosilicon compounds. In addition, zeta potential measurements were performed to estimate shelf-life of a final cosmetic product. Multiple light scattering enabled the evaluation of processes occurring in the colloidal system, for instance flocculation, creaming, sedimentation, much faster than traditional methods. This method allows computing a stability index to enable comparison of emulsion stability for a wide selection of formulations. Furthermore, the laser diffraction method can be used to measure the size distribution of droplets in emulsions, which is a key factor in examining their stability.

The prepared emulsions containing modified organosilicon compounds demonstrated stability at different temperatures (4, 25, 45 °C) over a 2-month period. The most effective approach for assessing emulsion stability is multiple light scattering, as it eliminates sample dilution and provides the most reliable results.

Acknowledgements

This research was financially supported by The National Centre for Research and Development (Poland), grant number LIDER/5/0036/L-12/20/NCBR/2021 "Technology of obtaining high molecular weight UVA/UVB filters for modern cosmetic formulations".

14.2 Determination of Per- and Poly-Fluorinated compounds in the Hungarian Section of the Danube River

Esther Orenibi[1,2,3], Illés Ádám[2,3], Záray Gyula[*,2,3,4]

1. Eötvös Loránd University, Doctoral School of Environmental Science, Budapest, Hungary
2. Ecological Research Center, Institute of Aquatic Ecology, Budapest, Hungary
3. National Laboratory of Water Science and Water, Budapest, Hungary
4. Eötvös Loránd University, Institute of Chemistry, Budapest, Hungary

e-mail: gyula.zaray@ttk.elte.hu

KEYWORDS: *PFAS, bioaccumulation, Danube, solid-phase extraction, HPLC-Q-TOF-MS*

Per- and polyfluorinated alkyl substances (PFAS) garnered increasing attention in recent years due to their persistence in the environment and potential bio-accumulative adverse effects on the ecosystems and human health. Their main sources are sewage treatment plants and landfills. These compounds exhibit both hydrophobic and hydrophilic properties and possess high stability, making them extensively utilized by firefighting facilities, lithium-ion batteries, and paper factories.

PFAS compounds, specifically perfluorooctanoic acid (PFOA) and perfluorooctanesulfonic acid (PFOS), have been detected in various European rivers. A comprehensive study conducted along the entire length of the Danube in 2015 revealed PFOA and PFOS concentrations in the range of 5-40 and 5-30 $ng \cdot L^{-1}$, respectively, with measurements in the Hungarian section ranging from 5-20 and 5-15 $ng \cdot L^{-1}$.

This study focuses on assessing the presence, distribution, and potential risks associated with PFASs in the Hungarian section of the Danube at twelve sampling points. Specifically, the investigation includes areas near the battery factory in Komárom, and the river sections upstream and downstream the paper mill in Dunaújváros, as well as Budapest.

In addition to determining these PFAS compounds, samples collected from these strategic locations were accessed to enable a comparative examination of the Inorganic Fluoride (IF), Extractable Organic Fluoride (EOF), and Adsorbable Organic Fluoride (AOF) content using the Combustion Ion Chromatography (C-IC). The IF concentration was relatively stable, ranging from 30-50 $\mu g \cdot L^{-1}$. The AOF and EOF content were typically 3-5% of the total fluoride.

Following water phase filtration, samples were enriched through solid-phase extraction (SPE) using 500 mg Strata X-AW cartridges in the presence of isotope-labelled internal standards and standard solution comprising ten selected PFAS compounds. The enriched samples were analysed using the HPLC-Q-TOF-MS technique, with a targeted detection limit of 5-10 $ng \cdot L^{-1}$.

15 Abstracts: Other

15.1 Synthesis and application of cinchona-based organocatalyst

Dóra Erdélyi[1], Gyula Dargó[1], Dóra Richter[1], József Kupai*[,1]

1. Department of Organic Chemistry and Technology, Budapest University of Technology and Economics, Budapest, Hungary

e-mail: kupai.jozsef@vbk.bme.hu

KEYWORDS: *organocatalyst, cinchona derivatives, asymmetric synthesis, amine catalysis*

Enantioselective reactions play a crucial role in the pharmaceutical industry. Enantiomers of a chiral molecule could have different, in some cases even toxic, biological effects. This is one of the reasons why enantiomerically pure drug forms came to the fore in the last few decades. Using chiral organocatalysts is a possible solution to produce the preferred enantiomer.

During my work, I aimed to synthesise two new, cinchona squaramide-based organocatalysts (SQ1 and SQ2). The catalysts could be used to produce the anticoagulant warfarin in the one-step Michael addition of 4-hydroxycoumarin (1) to benzylideneacetone (2). Moreover, the catalytic activity of the two catalysts is aimed to be compared in terms of yield and enantiomeric excess (**Figure 1.3.1**). To improve these values, investigation of the reaction parameters (solvent, temperature, amount of catalyst, etc.) is essential.

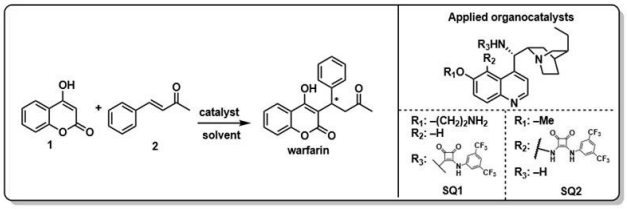

Figure 15.1.1. Synthesis of warfarin by using chiral cinchona-based organocatalysts

Acknowledgements

This work was supported by the National Research, Development, and Innovation Office (grant number FK138037), Gedeon Richter Centennial Foundation and Gedeon Richter Talentum Foundation (Gedeon Richter Plc.). Moreover, it was supported by the ÚNKP-23-2-I-BME-159 New National Excellence Program of the Ministry for Culture and Innovation from the source of the National Research, Development and Innovation Fund, and the National Research, Development and Innovation Fund. Project no. RRF-2.3.1-21-2022-00015.

15.2 Development of photocatalytic systems for C–C bond formation reactions

Gergő Gémes[1], Dóra Richter[1], Péter Kisszékelyi[2], József Kupai*[,1]

1. Department of Organic Chemistry and Technology, Budapest University of Technology and Economics, Budapest, Hungary
2. Department of Organic Chemistry, Comenius University Bratislava, Bratislava, Slovakia

e-mail: kupai.jozsef@vbk.bme.hu

KEYWORDS: *photocatalysis, visible light, C–C bond formation, 3D printing*

During the last century it was discovered that chemical reactions can be accomplished by light irradiation. Today photocatalysis is having a renaissance since it allows us to carry out reactions in exceptionally mild conditions. This is particularly useful in the late-stage functionalization of pharmaceuticals.

Our goal was to develop a photocatalytic system for conducting C–C bond formation reactions (**Figure 15.2.1**). We started with previously published reactions to validate our setup. With the coupling reaction between dimethyl malonate and 1,1-diphenylethylene up to 69% yield was achieved (**Figure 15.2.1 b)**). With the setup sorted out, we proceeded to expand the substrate scope. We executed an open-source 3D printed photoreactor plan as well. It provides fine control over the reaction parameters and has the possibility of flow chemical implementation.

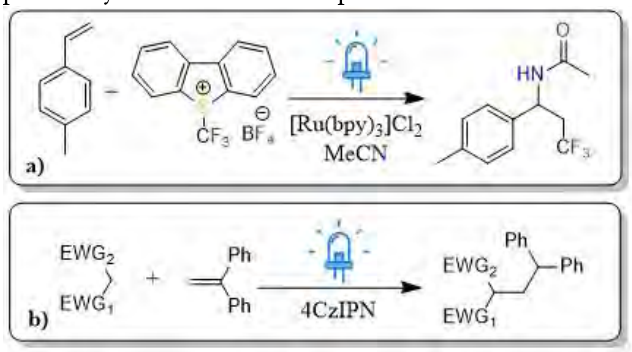

Figure 15.2.1. a) Trifluoromethylation of 4-methylstyrene b) Alkylation of CH-acidic compounds

Acknowledgements

This work was supported by the National Research, Development, and Innovation Office (grant number FK138037), and the Richter Talentum Excellence PhD Scholarship, and the National Research, Development and Innovation Fund. Project no. RRF-2.3.1-21-2022-00015.

15.3 Bio-based substitutes of polar aprotic solvents as reaction environment for ATRP

Katarzyna Kisiel[1], Izabela Zaborniak[1,2], Małgorzata Sroka[1,3], Cicely M. Warne[4,5], Alessandro Pellis[6], Krzysztof Matyjaszewski[2], Paweł Chmielarz[*,1,2]

1. Department of Physical Chemistry, Faculty of Chemistry, Rzeszow University of Technology, Rzeszow, Poland
2. Department of Chemistry, Carnegie Mellon University, Pittsburgh, Pennsylvania, United States
3. Doctoral School of the Rzeszow University of Technology, Rzeszow, Poland
4. Department for Agrobiotechnology, Institute for Environmental Biotechnology, University of Natural Resources and Life Sciences, Tulln an der Donau, Austria
5. ACIB GmbH, Tulln an der Donau, Austria
6. Department of Chemistry and Industrial Chemistry, University of Genova, Genova, Italy

e-mail: p_chmiel@prz.edu.pl

KEYWORDS: *bio-based solvents, cyrene, SARA ATRP*

The advancement of atom transfer radical polymerization (ATRP) relies on the adoption of bio-based reagents to mitigate the environmental risks associated with hazardous waste. Among several eco-friendly alternative solvents, dihydrolevoglucosenone (Cyrene™) stands out as one of the most promising. It is derived from cellulose and offers a bio-based alternative to toxic aprotic dipolar solvents such as dimethylformamide (DMF) usually employed in ATRP.

In this study, Cyrene™ was employed in the polymerization of acrylates via supplemental activation and reducing agent atom transfer radical polymerization (SARA ATRP). Copper wire served as the reducing agent, along with trace amounts of the catalyst. Results were compared to the polymerization in conventional solvent (DMF) under similar conditions.

Effective control of the polymerization was confirmed by low dispersity of the final polymers. Cyrene™ showed minimal adverse effects on the polymerization. Therefore, the replacement of DMF with Cyrene™ can be performed efficiently, without any risk of losing control over the reaction, which holds great significance in the future development of ATRP.

Figure 15.3.1. Comparing the characteristics of harmful and bio-based solvents used in ATRP.

Acknowledgements

Financial support from Ministry of Education and Science of Poland under the program "Student science clubs creates innovations" (SKN/SP/569572/2023) and from National Science Centre in Poland (SONATA BIS 10, 2020/38/E/ST4/00046).

15.4 Sonogashira reactions in MeSesamol, a new bio-based solvent

Dávid Kis[1], Gyula Dargó[1], József Kupai[*,1]

1. Department of Organic Chemistry and Technology, Budapest University of Technology and Economics, Budapest, Hungary

e-mail: kupai.jozsef@vbk.bme.hu

KEYWORDS: *bio-based solvents, carbon–carbon coupling, Sonogashira reaction, Cacchi reaction, alternative solvent*

With the tightening of the environmental regulations, alternative solvents are getting greater attention, which may be capable of replacing the traditional, environmentally harmful solvents. These solvents have lower tension, are non-toxic, and often derived from bio-based materials.

In my research, MeSesamol, a new bio-based solvent was used as a solvent in palladium-catalyzed Sonogashira and Cacchi reactions (Figure 15.4.1). The Sonogashira reaction can be used for the synthesis of compounds with an alkyne unit, while the Cacchi reaction is capable of synthesizing molecules with a benzofuran or an indole unit. It was examined whether different reaction conditions or the substituents have an effect on the achievable yield of the reaction.

MeSesamol worked as a good solvent for the mentioned reactions. A good yield was achived with a wide range of substrates, and it was clear how the halogen atom has an effect on the yield of the reaction.

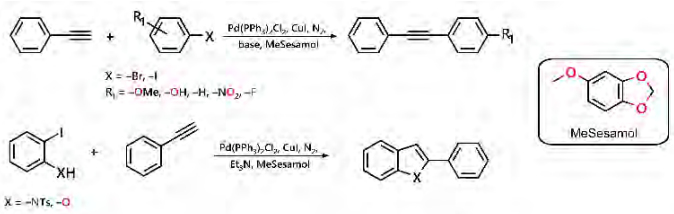

Figure 15.4.1. The reactions in MeSesamol

Acknowledgements

This work was supported by the National Research Development and Innovation Office (grant number OTKA-FK138037), the Richter Gedeon Talentum Foundation, Richter Gedeon Plc, the National Research, Development and Innovation Fund. Project no. RRF-2.3.1-21-2022-00015 and by the ÚNKP-23-2-I-BME-377 New National Excellence Program of the Ministry for Culture and Innovation from the source of the National Research, Development and Innovation Fund.

15.5 Modified oorganosilicon compounds as next-generation UV filters for sun protection

Anna Łapeta*[,1,2], Miłosz Frydrych[2], Bogna Sztorch[2], Robert Przekop[2], Anna Olejnik[1,2]

1. Adam Mickiewicz University, Poznan, Poland
2. Centre for Advanced Technologies, Poznan, Poland

e-mail: annlap1@st.amu.edu.pl

KEYWORDS: *emulsion, sunscreens, oxybenzone, broad spectrum protection*

Thousands of deaths occur annually worldwide due to melanoma caused by solar radiation exposure. Widespread sunscreen use is therefore recommended to prevent additional skin damage and mitigate skin cancer risk. However, recently it has been reported that commonly-used UV filters may penetrate skin and degrade due to sunlight, potentially provoking allergic and toxic reactions. Benzophenone-3 known also as oxybenzone demonstrated substantial permeability across the epidermis to then enter systemic circulation. As a result, benzophenone-3 has been under suspicion regarding potential endocrine disruptive activities. Thus, the aim of this study is to develop next generation UV filters offering improved safety profile considering permeation though the skin compared to existing solutions.

Organosilicon compounds modified with benzophenone-3 and polyethylene glycols were obtained via hydrosilylation reaction and then introduced to the emulsions. The stability of the sunscreens was characterized using multiple light scattering, and droplet sizes were assessed through laser diffraction and optical microscopy. In the final step, the permeation of the next generation UV filters was determined through skin-mimicking membranes by using a Franz diffusional cell. It was proved that newly modified organosilicon compounds are not permeable due to their high molecular weight. Therefore, they can replace commonly-used oxybenzone, which permeated the skin.

Acknowledgements

This research was financially supported by The National Centre for Research and Development (Poland), grant number LIDER/5/0036/L-12/20/NCBR/2021 "Technology of obtaining high molecular weight UVA/UVB filters for modern cosmetic formulations".

15.6 Influence of power supply on gliding discharge plasma-catalytic ammonia decomposition

Michalina Perron*[,1,2], Michał Młotek[1], Krzysztof Krawczyk[1]

1. Faculty of Chemisty, Warsaw University of Technology, Warsaw, Poland
2. Trumpf Heuttinger, Zielonka, Poland

e-mail: michalina.perron.dokt@pw.edu.pl

KEYWORDS: *ammonia decomposition, hydrogen, plasma-catalytic procces, gliding discharge*

Hydrogen can be one of the emission-free energy sources. The use of hydrogen as an energy carrier is difficult due to problems associated with its transportation and storage. Chemically bonding hydrogen to ammonia may be one of the solutions to solve this problem. To use ammonia for transport or storage of hydrogen, an effective method of its decomposition must be developed.

The decomposition of NH_3 was carried out in a plasma-catalytic system using a gliding discharge and cobalt catalysts: cobalt on alumina support and cobalt on cerium oxide support promoted by barium. Measurements were conducted in the range of initial ammonia concentrations of 50-90% by volume in nitrogen and a discharge power of 200-600 W. Two types of power supply were used: the first one with a frequency of 50 Hz and power regulation by a thyristor. The second was commercial Bipolar HV by Trumpf Heutinger power supply with a frequency of 20 kHz.

The aim of this study was to investigate the influence of the type of power supply on the plasma-catalytic process of ammonia decomposition.

The highest ammonia conversion was achieved using a Bipolar HV power supply and cobalt-cerium catalyst promoted with barium.

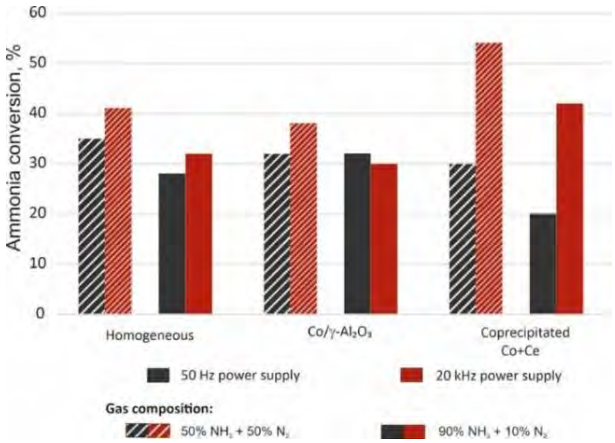

Figure 15.6.1. Influence of catalysts and kind of power supply on ammonia conversion.

Acknowledgements

This work was supported by the Warsaw University of Technology, Faculty of Chemistry, ul. Noakowskiego 3, 00-664 Warszawa, Poland.

15.7 Synthesis of layered double hydroxides and their enhanced catalytic activity for ammonia electrooxidation reaction (AOR)

Sara Sumbal*,1, Justyna Łuczak1, Marek Lieder1

1. Gdansk University of Technology, Gdansk, Poland
e-mail: sara.sumbal@pg.edu.pl

KEYWORDS: *ammonia electrooxidation reaction (AOR), layered double hydroxides (LDH), nickle hydroxides, NiCu-LDH/NF*

Ammonia is a carbon-free small molecule favored for energy conversion and storage through electrochemical oxidation reaction. However, the slow kinetics of the ammonia electrochemical reaction, as well as the high cost and poisoning of platinum-based catalysts still remain challenges. Ni based catalysts (Ni^{2+}/Ni^{3+}) were found to be catalytically active for AOR. Subsequently, Cu was found to be only metal in the examined first-row transition elements that can significantly increase the activity of $Ni(OH)_2$ for ammonia electrooxidation reaction (AOR).

In this work, we present novel monometallic Ni-LDH and bimetallic NiCu-LDH directly grown over nickle foam (NF) via typical solvothermal synthesis route for AOR. NiCu-LDH catalyst achieves a current density of 55 mA· cm^{-2} at 1.55 V vs. RHE, which is higher than that of monometallic catalyst (37 mA·cm^{-2}). Moreover, NiCu-LDH exhibits an excellent durability and stability (24 hr) for AOR. This is due to abundant active sites and a synergistic effect between Ni and Cu. Meanwhile, the ultrathin strucutre and plentiful interfaces of Mott–Schottky heterojunction of NiCu-LDH facilitate mass transfer and provide numerous channels for charge transfer.

It was discovered that this bimetallic NiCu-LDH nanosheet catalyst is a promising, stable, low-cost catalyst for ammonia electrooxidation. This study will also open new patways of developing more non-noble metal based catalysts for electrooxidation reactions.

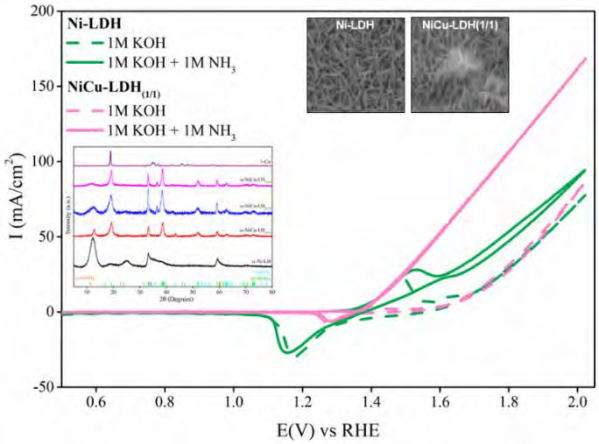

Figure 15.7.1. Cyclic voltammograms (CVs) performed in 1M KOH (dashed lines) and 1M KOH + 1M NH3 (solid lines) solution along with insets of XRD patterns and SEM images of Ni-LDH and NiCu-LDH, respectively.

Acknowledgements

This work was fully funded by OPUS program of the National Science Centre, Poland (UMO-2021/41/B/ST4/03255) and experiments were carried out at Department of Process Engineering and Chemical Technology, Gdansk University of Technology, Gdansk, Poland.

15.8 Carbon dots as photocatalysts in photoinitiating systems for photopolymerization processes in 3D printing application

Agnieszka Sysło*,1, Dominika Krok1, Wiktor Kasprzyk1, Joanna Ortyl1,2,3

1. Cracow University of Technology, Cracow, Poland
2. Photo HiTech Ltd., Cracow, Poland
3. Photo4Chem, Cracow, Poland
e-mail: agnieszka.syslo1@gmail.com

KEYWORDS: *carbon dots, 3D printing, photoinitiating systems*

A promising technique for producing highly personalized and structurally complex objects is a method based on additive manufacturing, also known as 3D printing. The advantages of this technique are primarily the flexibility to create individualized designs of complex construction along with the possibility of rapid prototyping while minimizing waste production. 3D printing is widely used in electronics, robotics and military industries, among others, as well as in many areas of tissue engineering and medicine.

Carbon dots, due to their small size, good biocompatibility, low toxicity and low preparation cost are finding increasing applications in biomedicine and many fields of technology. Photostability and the ability to modify photoluminescent properties make carbon dots potentially usable as photocatalysts in photopolymerization processes in 3D printing. Modification of the surface of carbon dots by doping them with selected heteroatoms leads to their potential use as photosensitizers of iodonium salts in cationic polymerization processes. The research carried out in the present study was focused on characterizing the properties of the obtained polymer compositions using carbon dots in 3D printing. For this purpose, a one-pot, solvent-free synthesis of citric acid-based carbon dots was conducted, which were then purified to eliminate impurities and fluorophores. Spectroscopic and kinetics studies of the photopolymerization process were performed to determine the effect of the presence of carbon dots in the composition on the ongoing process and properties of the obtained material.

The conducted studies indicate interesting characteristics of the obtained carbon dot materials. The presented properties of the developed materials suggest their potential use in photopolymerization processes in 3D printing and can significantly advance the knowledge of the use of carbon sources in photoinitiating systems.

Acknowledgements

This research was funded by the NCN project OPUS ("Emerging strategy approaches for the design and functionalization of carbon dots as multifunctional, dynamic, green systems photoinitiators and photocatalysts involved in photopolymerisation processes"), Grant No. UMO-2021/41/B/ST5/04533

15.9 Synthesis, purification and characterization of carbon dots for application in cationic and free-radical photopolymerization processes

Agnieszka Sysło*[,1], Dominika Krok[1], Wiktor Kasprzyk[1], Joanna Ortyl[1,2,3]

1. Cracow University of Technology, Cracow, Polan
2. Photo HiTech Ltd., Cracow, Poland
3. Photo4Chem, Cracow, Poland

e-mail: agnieszka.syslo1@gmail.com

KEYWORDS: *carbon dots, 3D printing, photoinitiating systems*

Photopolymerization is a technology used extensively both for the production of printing materials, coatings and in the field of 3D printing. Depending on the type of material being photocured and the type of active centers formed that are responsible for initiating the polyreaction, the reaction follows a cationic or radical mechanism. Cationic photopolymerization does not require an inert environment, as it is not inhibited by oxygen, and once initiated the reaction does not require the constant presence of a light source, which distinguishes it from free radical photopolymerization. Free radicals are formed in such systems only in the constant presence of a light source, which, in turn, allows for increased control of the conducted photocuring process.

Chemically stable carbon dots are characterized by a variety of properties that lead to their potential use in cationic and free radical photopolymerization processes. Substrates for the synthesis of carbon dots can be a wide range of carbon sources, thus making the conducted synthesis non-toxic. Synthesis based on green substrates is more desirable due to the simplicity of the procedure, low cost and its negligible environmental impact. However, there is still a need to develop a replicable and scalable synthesis and carry out an efficient purification process for the obtained products. In the work presented here, a one-pot, solvent-free synthesis of carbon dots from citric acid was carried out. The obtained products were purified to remove present impurities and fluorophores. Then the properties of the obtained citric acid-based carbon dots were characterized by spectroscopic and kinetic studies.

Presented studies indicate the great potential of the obtained carbon dots as components of photoinitiating systems used in 3D printing. The steps taken to develop an efficient method for obtaining and synthesizing carbon dots based on citric acid will certainly contribute to the development of related topics.

Acknowledgements

This research was funded by the NCN project OPUS ("Emerging strategy approaches for the design and functionalization of carbon dots as multifunctional, dynamic, green systems photoinitiators and photocatalysts involved in photopolymerisation processes"), Grant No. UMO-2021/41/B/ST5/04533

15.10 Characterization of micellar networks in selected nonionic/ionic surfactant mixtures

Ewelina Warmbier*[,1], Ali Altaee[2], Jacek Różański[1], Sylwia Różańska[1], Patrycja Wagner[1]

1. Division of Chemical Engineering and Equipment, Faculty of Chemical Technology, Poznan University of Technology, Poznan, Poland
2. School of Civil and Environmental Engineering, University of Technology Sydney, Sydney, Australia

e-mail: ewelina.warmbier@doctorate.put.poznan.pl

KEYWORDS: *surfactants, wormlike micelles, viscoelasticity, rheology*

One method to control the rheological properties of cosmetics and household chemical products involves using surfactants, which in aqueous solutions can form elongated micellar structures known as wormlike or threadlike micelles. Similar to aqueous polymer solutions, these micelles display viscoelastic properties quantified by the Maxwell model. Unlike polymer chains, wormlike micelles continuously disintegrate and recombine within a solution over a characteristic breaking time. For these reasons, they are often referred to as living polymers.

The objective of this study was to assess the micellar network parameters in specific aqueous solutions, varying the molar ratios of surfactants and total concentrations. The solutions comprised a mixture of the anionic surfactant sodium cholate (NaC) and the nonionic surfactant (BrijL4). Furthermore, the study investigated the impact of salt and temperature on the rheological properties of the examined solutions. Rheological measurements in shear flow were conducted using the MCR302 rheometer (Anton Paar).

The findings revealed the potential for obtaining viscoelastic fluids with the BrijL4/NaC mixture. The stability of viscoelastic NaC/BrijL4 solutions was demonstrated across a broad range of temperature variations (from 5°C to 80°C) and pH levels (from 1.5 to 8). Utilizing the results from oscillatory studies and Cates' theory, micelle breakup time and reptation time were determined, allowing for the calculation of the average size of the micellar network mesh. This correlation facilitated an understanding of observed changes in the macroscopic properties of the solutions in relation to alterations in their microstructure. These findings suggest a synergy between NaC and BrijL4 surfactants in aqueous solutions.

Acknowledgements

This research was supported by the Ministry of Education and Science of Poland through grant 0912/SBAD/2302 and by the ERASMUS+ Programme of the European Union.

15.11 Synthesis and structural characterization of PDCs layers based on iron-dopped silicon oxycarbide

Wojciech Wieczorek*,[1], Piotr Jeleń[1], Maciej Bik[1], Jakub Marchewka[1], Zofia Kucia[1], Maciej Sitarz[1]

1. Faculty of Material Science and Ceramics, AGH University of Krakow, Krakow, Poland
e-mail: wwieczor@student.agh.edu.pl

KEYWORDS: *sol-gel synthesis, polymer dericed ceramics, spectroscopy, silicon oxycarbide*

Sol-gel process allows the formation of solid materials from solutions of precursors.

A network of solid material is formed by hydrolysis of precursors and subsequent condensation of the reaction products to form macromolecules and their networks. The properties of materials obtained by sol-gel process depend on the type and concentration of precursors, type and concentration of catalysts, amount of added water, order in which the reactants are added, time of mixing, temperature, and humidity. One group of the very interesting materials, produced frequently by means of sol-gel method are Polymer Derived Ceramics. Their intriguing properties are strictly dependent on the veryeach level of the material's formation process. One of them include so-called cationic substitution of basic Si^{4+} cations present in the glassy network with different ones i.e. Al^{3+}, Ni^{2+}.

The aim of this study was to obtain SiOC layers glasses doped with Fe^{3+} cations and analyse the obtained materials structurally. Fe^{3+} cations were introduced by dissolving iron (III) acetylacetonate [$Fe(C_5H_7O_2)_3$] in the synthesised sol. After synthesis and deposition by dip coating method, the material was subjected to a two-step heat treatment process: drying at 70 °C for 7 days and annealing in argon atmosphere at 800 °C. For materials after both heat-treatment processes, structural analysis was carried out, which included the following methods: X-ray diffraction (XRD), Middle Infrared spectroscopy (MIR), Raman spectroscopy, and SEM microscopy with EDS.

Structural and microstructural characterization indicated the presence of a double layers consisted of SiFeOC and $MnCr_2O_4$ interlayer. SEM/EDS imaging pointed to incompatibilities between applied withdrawn speed and Landau-Levich's model which theoretically describes the dip-coating method. However, the successful incorporation of Fe^{3+} in silicon oxycarbide structure allows the use of these materials as protective coatings for fuel cell interconnectors.

Acknowledgements

This research was funded by the National Science Centre, Poland, grant no. 2019/35/B/ST5/00338 and supported by the program „Excellence initiative – research university" for the AGH University of Krakow.

Index of Authors

Index of Keywords

Cover design
Monika Klimek, klimek.monika2000@gmail.com

Paper review team
Lead by Michał Stor
Radosław Krzosa, Mateusz Młynek

Typesetting team
Layout and formatting by Grzegorz Bernacki
Izabela Kazimierczak, Monika Klimek, Iga Komar,
Zuzanna Kupniewska, Jakub Lewandowski, Kamila Matysiak,
Adam Romanowicz, Bartosz Sobolewski

Typeset using Libertinus font family, distributed under SIL Open Font Licence 1.1

12TH EYEC

Special Guests

assoc. Prof Ameya Rege

Dagmara Chmielewska-Śmietanko, PhD

Francisco Fernandes, PhD

Alvaro Garcia, PhD

Grzegorz Izydorczyk, PhD

Scientific Commission

assoc. Prof. Nadia Shardt

Zuzanna Bojarska, PhD

Grzegorz Cieślak, PhD

Grzegorz Izydorczyk, PhD

Rasa Keruckienė, PhD

Bartosz Nowak, PhD

Paulina Trzaskowska, PhD

Karol Ulatowski, PhD

ISBN 978-83-953822-2-2